

UNIVERSITY OF OKLAHOMA

GRADUATE COLLEGE

STRUCTURAL ANALYSIS OF THE WICHITA UPLIFT AND STRUCTURES IN THE
SOUTHEAST ANADARKO BASIN, SOUTHERN OKLAHOMA

A DISSERTATION

SUBMITTED TO THE GRADUATE FACULTY

in partial fulfillment of the requirements for the

Degree of

DOCTOR OF PHILOSOPHY

By

MOLLY TURKO
Norman, Oklahoma
2019

STRUCTURAL ANALYSIS OF THE WICHITA UPLIFT AND STRUCTURES IN THE
SOUTHEAST ANADARKO BASIN, SOUTHERN OKLAHOMA

A DISSERTATION APPROVED FOR THE
SCHOOL OF GEOSCIENCES

BY THE COMMITTEE CONSISTING OF

Dr. Shankar Mitra, Chair

Dr. Kurt Marfurt

Dr. Matthew Pranter

Dr. Deepak Devegowda

Dr. Bryan Tapp

© Copyright by MOLLY TURKO 2019
All Rights Reserved.

Dedication

This dissertation is dedicated to my family, my grandma, and to the men and women who've written so many classic papers on southern Oklahoma geology.

To my beautiful 2-year-old son Bo Brooks, I love you more than I've ever loved. Thank you for being a light in my life, maybe just maybe, you'll be a geologist to someday!

To my husband Richard, thank you for being such a wonderful husband and awesome Daddy! Now that I'll have more free time, we should go on a family adventure!

To my grandma Molly Waldren, you taught me determination, and although some might call it stubbornness, it is because of this quality that pushed me to finish. So many times, when life got hard, or busy, or overwhelming, all I wanted to do was drop out. But it was your determination that kept me going and pushing forward. I love you and I miss you dearly, but I know we'll meet again someday!

To the men and women who've contributed invaluable information to southern Oklahoma geology, thank you! Your names are forever embedded in my head, and I enjoyed all the classic research. You all are superstars to me!

Acknowledgments

This dissertation would not be possible without the support of so many people. First, I would like to thank my advisor Dr. Mitra for bearing with me over the past 8 years as I worked full time while completing this research. His knowledge, guidance, and assistance taught me so much and helped make this dissertation exceptional. I'd also like to personally thank Dr. Bryan Tapp who taught me so much in my younger years as an undergraduate and while I completed my master's thesis. He's the one who sparked a passion in me for southern Oklahoma geology and all that it had to offer! And a special thank you to rest of my committee, Dr. Kurt Marfurt, Dr. Matthew Pranter, and Dr. Deepak Devegowda. This journey would not have been possible without support from Chesapeake Energy, my employer for almost 9 years now. They have been gracious to allow me to use their datasets along with software support. I'm especially thankful for the seismic vendors who allowed me to use and publish vital datasets for this project. I am forever indebted to SEI, Seitel, and MIDCON along with Chesapeake Energy for all their support. Throughout the years many people from Chesapeake and elsewhere have helped me, whether by geologic conversations, data support, or permissions/approvals. Although I may not remember everyone, I would like to personally thank a few; Mark Falk, John Kapchinske, Frank Gagliardi, Frank Patterson, Robin Pearson, Micaela McFarland, Lindsay Gowan, Steve Knowles, Bob Pope, Lans Taylor, Fola Kolawole, Jerry McCaskill, and Chris Saxon. I am grateful for all their support and contributions to this research! And most importantly, I'd like to thank God for carrying me through this journey and blessing me with wisdom, passion, and perseverance. Without Him I wouldn't have been able to achieve this major milestone!

Table of Contents

Acknowledgments.....	v
List of Figures.....	viii
Abstract.....	xv
Chapter 1: Introduction.....	1
Chapter 2: Structural Styles in the Wichita Uplift and Anadarko Basin, Southern Oklahoma.....	2
Abstract.....	2
1. Introduction.....	3
2. Regional Tectonics.....	5
3. Previous Studies.....	8
4. Data and Methods.....	13
5. Stratigraphy.....	16
6. Structure Map.....	18
7. Structural Cross Sections.....	21
7.1 Cross section A: Wichita Front - Carter-Knox.....	21
7.2 Cross section B.....	28
7.3 Cross section C: Wichita Front (Slick Hills) - Cement.....	30
7.4 Cross sections D and E: Slick Hills.....	40
7.5 Cross section F: Western Wichita Front.....	44
7.6 Cross section G, H, and I: Southern Wichita Uplift.....	46
8. Discussion.....	51
9. Conclusions.....	58
References.....	60
Appendix 2.1 Well Information from Cross Sections.....	69
Appendix 2.2 Additional Cross Sections.....	72
Chapter 3: Macroscopic Structural Styles in the Southeastern Anadarko Basin, Southern Oklahoma.....	76
Abstract.....	76
1. Introduction.....	76
2. Geologic Background.....	79
3. Stratigraphy.....	80
4. Previous Studies.....	82
4.1 Carter-Knox Anticline.....	82

4.2 Cruce Anticline	83
4.3 Chickasha Anticline	84
4.4 Cement Fault Zone and Anticline	84
5. Data and Methods	85
6. Results	88
6.1 Structure Map.....	88
6.2 Carter-Knox Structure.....	91
6.3 Cruce Structure	100
6.4 Chickasha Structure	106
6.5 Cement Structure and Fault	112
7. Discussion and Conclusions	126
References	128
Appendix 3.1 Well Information from Cross Sections	132
Chapter 4: Structural Geometry and Evolution of the Carter-Knox Structure, Anadarko Basin, Oklahoma.....	136
Abstract	136
1. Introduction.....	137
2. Regional Structure and Stratigraphy	137
2.1 Basin History	137
2.2 Regional Structure	138
2.3 Stratigraphy.....	141
3. Previous Studies.....	143
4. Structural Interpretation and Approach	146
5. Structural Maps.....	146
6. Structural Cross Sections	150
7. Kinematic Reconstruction and Structural Evolution	160
8. Regional Structural Evolution.....	167
9. Conclusions.....	169
References.....	171

List of Figures

Figure 2.1 Regional map showing faults mapped at the Arbuckle level (black), and at the basement where Arbuckle is eroded on the Wichita Uplift (bold gray). The Mountain View Fault is highlighted in blue; Washita Valley Fault in green; Cement Fault in purple; and Wichita Mountain Fault in red. Pre-Pennsylvanian surface geology is derived from the USGS (Heran et al., 2003). Significant uplifts, basins, fields and structures are labeled with a key on the map. Cross section locations are shown in blue. 4

Figure 2.2 Aeromagnetic data processed by Chase (2019), data courtesy of Shah and Finn (2018). Cross section locations are shown in blue. Regional fault map from Figure 2.1 overlays the aeromagnetic data. (A) Total magnetic intensity (B) First derivative of total magnetic intensity..... 15

Figure 2.3 Modified from Granath (1989). Color of top refers to horizons interpreted in the cross sections. Lithologies include an igneous basement, followed by clastic, carbonate, and shale units. Detachment levels are shown by black arrows. 17

Figure 2.4 Subsea structure map on the Arbuckle formation, contour interval is 1,000 feet. Where Arbuckle becomes eroded faults are at the basement level (bold gray). Pre-Pennsylvanian surface geology is from USGS (Heran et al., 2003). Cross sections locations are shown and labeled in blue..... 20

Figure 2.5 Regional cross section A. (A) Interpreted seismic section in time. Time scale has been removed for proprietary data. Horizon colors are shown in Figure 2.3. (B) Depth cross section. Well information is listed in appendix 1. Well tops (colored circles), dip data (brown check mark), and fault picks (red x) are shown where available. Dashed well is projected from 9 miles. Seismic Data Courtesy of Chesapeake Energy & SEI, Interpretation is that of Molly Turko. 26

Figure 2.6 Restoration of cross section A. Evolution is discussed in the text. 27

Figure 2.7 Cross section B. (A) Interpreted seismic section in time. Time scale has been removed for proprietary data. Horizon colors are shown in Figure 2.3. (B) Depth cross section. Well information is listed in appendix 1. Well tops (colored circles), dip data (brown check mark), and fault picks (red x) are shown where available. Seismic Data Courtesy of SEI, Interpretation is that of Molly Turko 29

Figure 2.8 Cross section C. (A) Interpreted seismic section in time. Time scale has been removed for proprietary data. Horizon colors are shown in Figure 2.3. (B) Depth cross section. (C) Alternative interpretation of the Cement structure. Well information is listed in appendix 1. Well tops (colored circles), dip data (brown check mark), and fault picks (red x) are shown where available. Seismic Data Courtesy of SEI & Seitel, Interpretation is that of Molly Turko. 33

Figure 2.9 (A) Missourian age Hoxbar subsea structure map over the Cement-Chickasha structure. Contour interval is 500 feet. Part of the Hoxbar is eroded on the Chickasha structure in gray. (B) Shallow time slice over the Cement-Chickasha trend. Green arrows indicate the main thrust fault cutting the slice. Yellow arrows indicate normal faults oriented NE-SW. Red arrows show where the Cement normal/strike-slip fault cuts the slice. Blue arrows show the continuation of that fault trend east of the main structure. Seismic data courtesy of Chesapeake Energy. 34

Figure 2.10 Cross section 1. (A) Location map of Cement-Chickasha cross sections (B) Interpreted seismic section in time. Horizon colors are shown in Figure 2.3. (C) Depth cross section. Well information is listed in appendix 1. Well tops (colored circles), dip data (brown check mark), and fault picks (red x) are shown where available. Seismic Data Courtesy of CHK, Interpretation is that of Molly Turko 35

Figure 2.11. (A) Cross section 2 interpreted seismic section in time and depth. (B) Cross section 3 interpreted seismic section in time and depth. Horizon colors are shown in Figure 2.3. Well information is listed in appendix 1. Well tops (colored circles), dip data (brown check mark), and fault picks (red x) are shown where available. Locations shown in Figure 2.10A . Seismic Data Courtesy of CHK, Interpretation is that of Molly Turko 36

Figure 2.12 Restoration of cross section C. Evolution is discussed in the text. 39

Figure 2.13 Cross section D. (A) Interpreted seismic section in time. Horizon colors are shown in Figure 2.3. (B) Depth cross section. Well #1 is the Kimbell Ranch 32-1 mentioned in the text, other well information is listed in appendix 1. Well tops (colored circles), dip data (brown check mark), and fault picks (red x) are shown where available. Seismic Data Courtesy of MIDCON, Interpretation is that of Molly Turko. 42

Figure 2.14 Cross section E. (A) Interpreted seismic section in time. Time scale has been removed for proprietary data. Horizon colors are shown in Figure 2.3. (B) Depth cross section. Well information is listed in appendix 1. Well tops (colored circles), dip data (brown check mark), and fault picks (red x) are shown where available. Seismic Data Courtesy of SEI, Interpretation is that of Molly Turko 43

Figure 2.15 Cross section F. (A) Interpreted seismic section in time. Horizon colors are shown in Figure 2.3. (B) Depth cross section. Well information is listed in appendix 1. Well tops (colored circles), dip data (brown check mark), and fault picks (red x) are shown where available. Seismic Data Courtesy of Seitel, Interpretation is that of Molly Turko..... 45

Figure 2.16 Cross section G. (A) Interpreted seismic section in time. Time scale has been removed for proprietary data. Horizon colors are shown in Figure 2.3. (B) Depth cross section. Well information is listed in appendix 1. Well tops (colored circles), dip data (brown check mark), and fault picks (red x) are shown where available. Seismic Data Courtesy of SEI, Interpretation is that of Molly Turko. 48

Figure 2.17 Cross section H. (A) Interpreted seismic section in time. Horizon colors are shown in Figure 2.3. (B) Depth cross section. Well information is listed in appendix 1. Well tops (colored circles), dip data (brown check mark), and fault picks (red x) are shown where available. Seismic Data Courtesy of MIDCON, Interpretation is that of Molly Turko.... 49

Figure 2.18 Cross section I. (A) Interpreted seismic section in time. Horizon colors are shown in Figure 2.3. (B) Depth cross section. Well information is listed in appendix 1. Well tops (colored circles), dip data (brown check mark), and fault picks (red x) are shown where available. Seismic Data Courtesy of MIDCON, Interpretation is that of Molly Turko..... 50

Figure 2.19 Diagram illustrating the structural styles that develop based on the angle between pre-existing faults and the angle of convergence. SHmax is the maximum horizontal stress orientation (A) Scenerio for Morrowan-Atokan, SHmax is N45°E and at high angles to pre-existing faults, thrust faulting occurs. (B) Scenerio for Virgilain, SHmax rotated to N75°E, where the angle of convergence is high thrust faulting occurs, where it is low strike-slip faulting occurs. 53

Figure 2.20 (A) Location map of regional cross section J and outline of the block diagram. (B) Cross section J, constructed using sections D and I (C) Restored to show early contraction in the

Late Mississippian/Early Permian prior to major fault offset (D) Restored to the end of the Cambrian-Ordovician showing hypothetical rift fault geometry. 56

Figure 2.21 Schematic block diagram at the basement level. Red arrows represent stress orientations. (A) End of the rifting stage where extension was oriented N-S. (B) Contraction at the end of the Atokan, maximum horizontal stress is oriented NE-SW. (C) Contraction at the end of the Virgilain accompanied by strike-slip faulting along WNW-ESE faults, maximum horizontal stress has rotated to a ENE-WSW orientation. 57

Figure 2.22 Location map for supplementary cross sections 4 and 5 (in red) superimposed on a cropped version of the regional fault map from Figure 2.1. The trace of the Washita Valley Fault is highlighted in green. ER is the Eola-Robberson Field just east of the cross sections. See Figure 2.1 for legend and key to named structures. 73

Figure 2.23 Cross section 4. (A) Interpreted seismic section in time. Time scale has been removed for proprietary data. Horizon colors are shown in Figure 2.3. (B) Depth cross section. Well information is listed in appendix 1. Well tops (colored circles), dip data (brown check mark), and fault picks (red x) are shown where available. Seismic Data Courtesy of SEI, Interpretation is that of Molly Turko. 74

Figure 2.24 Cross section 5. (A) Interpreted seismic section in time. Time scale has been removed for proprietary data. Horizon colors are shown in Figure 2.3. (B) Depth cross section. Thrust fault cutting the Arbuckle-Sycamore is shown out-of-the-plane movement. Well information is listed in appendix 1. Well tops (colored circles), dip data (brown check mark), and fault picks (red x) are shown where available. Seismic Data Courtesy of SEI, Interpretation is that of Molly Turko. 75

Figure 3.1 Regional map showing faults mapped at the Arbuckle level (black), and at the basement where Arbuckle is eroded on the Wichita Uplift (bold gray). The Mountain View Fault is highlighted in blue; Washita Valley Fault in green; Cement Fault in purple; and Wichita Mountain Fault in red. The study area is within the red rectangle. Pre-Pennsylvanian surface geology is derived from USGS (Heran et al., 2003). Significant uplifts, basins, fields and structures are labeled with a key on the map. 78

Figure 3.2 Modified from Granath (1989). Color of top refers to horizons interpreted in the cross sections. Dashed lines represent the top of an age, which in some parts of the cross sections represents an unconformity. The solid lines represent a marker within the different ages to help constrain structure in the cross sections. 81

Figure 3.3 Map showing locations of cross sections (red), field names (green), and approximate outline of 3D seismic coverage (blue dashed line). Trace of the Washita Valley Fault is highlighted in green, Cement Fault in purple, Mountain View Fault in blue, and Wichita Mountain Fault in red. Faults are mapped at the Arbuckle level, except a small part of the Wichita Mountain Fault is mapped on the basement near the Slick Hills where the Arbuckle is eroded. Pre-Pennsylvanian surface geology on the southeast end of the Wichita Uplift is from USGS (Heran et al., 2003). 87

Figure 3.4 Subsea structure map on top of the Mississippian Sycamore Formation, contour interval is 1,000 feet. Cross section locations are shown in red. Faults on the Wichita Uplift shown in bold gray are at the basement level. Sycamore is eroded off of the Pauls Valley Uplift in the east. Pre-Pennsylvanian surface geology on uplifts is from USGS (Heran et al., 2003). 90

Figure 3.5 Regional cross section A. (A) Interpreted seismic section in time. Time scale removed from proprietary data. Horizon colors are shown in Figure 3.2. (B) Depth cross section. Well

information is listed in appendix 1. Well tops (colored circles), dip data (brown check mark), and fault picks (red x) are shown where available. Dashed well is projected 9 miles. Seismic Data Courtesy of Chesapeake Energy & SEI. 93

Figure 3.6 Cross section CK1 over the Carter-Knox structure (A) Interpreted seismic section in time. Horizon colors are shown in Figure 3.2. (B) Depth cross section. Well information is listed in appendix 1. Well tops (colored circles), dip data (brown check mark), and fault picks (red x) are shown where available. Seismic Data Courtesy of Chesapeake Energy. 96

Figure 3.7 Kinematic reconstruction and structural evolution of section CK1 (A) Depth cross section. (B) Faulting is restored and dashed to illustrate fold geometries. (C) Structure is restored to Missourian time with the Hoxbar horizon flattened. (D) Morrow and older units are restored to their undeformed state. Initial dips of these units are not known, so units are shown as horizontal. 97

Figure 3.8 Method of area restoration applied to the units between the Springer detachment and the top of the Morrow/Springer Formation. (A) Final cross section. (B) Line-length restoration showing a wedge-shaped geometry resulting from differential strain of individual units. (C). Restoration with the area balanced into a rectangle shape. The height of the rectangle is determined by the average thickness (t), and the average restored length (l_0) is determined by dividing the area (A) by t 98

Figure 3.9 Cross section CK1 over the Carter-Knox structure (A) Interpreted seismic section in time. Horizon colors are shown in Figure 3.2. (B) Depth cross section. Well information is listed in appendix 1. Well tops (colored circles), dip data (brown check mark), and fault picks (red x) are shown where available. Seismic Data Courtesy of Chesapeake Energy. 99

Figure 3.10 Cross section CR1 over the Cruce structure (A) Interpreted seismic section in time. Time scale removed from proprietary data. Horizon colors are shown in Figure 3.2. (B) Depth cross section. Well information is listed in appendix 1. Well tops (colored circles), dip data (brown check mark), and fault picks (red x) are shown where available. Seismic Data Courtesy of SEI. 103

Figure 3.11 Cross section CR2 over the Cruce structure (A) Interpreted seismic section in time. Time scale removed from proprietary data. Horizon colors are shown in Figure 3.2. (B) Depth cross section. Well information is listed in appendix 1. Well tops (colored circles), dip data (brown check mark), and fault picks (red x) are shown where available. Seismic Data Courtesy of SEI. 104

Figure 3.12 Kinematic reconstruction and structural evolution of section CR1 (A) Depth cross section. (B) Faulting is restored and dashed to illustrate fold geometries. (C) Structure is restored to Missourian time with the Hoxbar horizon flattened. (D) Springer and older units are restored to their undeformed state. Initial dips of these units are not known, so units are shown as horizontal. 105

Figure 3.13 Missourian age Hoxbar subsea structure map over the Cement-Chickasha structure. Contour interval is 500 feet. West Cement, East Cement, and Chickasha Fields are labeled. Part of the Hoxbar is eroded on the Chickasha structure in gray. Cement-Chickasha cross section locations are shown in red. 108

Figure 3.14 Cross section CM4 over the Chickasha structure (A) Interpreted seismic section in time. Horizon colors are shown in Figure 3.2. (B) Depth cross section. Well information is listed in appendix 1. Well tops (colored circles), dip data (brown check mark), and fault picks (red x) are shown where available. Seismic Data Courtesy of Chesapeake Energy. 109

Figure 3.15 Cross section CM5 over the Chickasha structure (A) Interpreted seismic section in time. Horizon colors are shown in Figure 3.2. (B) Depth cross section. Well information is listed in appendix 1. Well tops (colored circles), dip data (brown check mark), and fault picks (red x) are shown where available. Seismic Data Courtesy of Chesapeake Energy. 110

Figure 3.16 Kinematic reconstruction and structural evolution of section CM4 (A) Depth cross section. (B) Faulting is restored and dashed to illustrate fold geometries. (C) Structure is restored to Missourian time with the Hoxbar horizon flattened. (D) Morrow and older units are restored to their undeformed state. Initial dips of these units are not known, so units are shown as horizontal. 111

Figure 3.17 Regional cross section B. (A) Interpreted seismic section in time. Time scale removed from proprietary data. Horizon colors are shown in Figure 3.2. (B) Depth cross section. (C) Alternative interpretation of the Cement structure. Well information is listed in appendix 1. Well tops (colored circles), dip data (brown check mark), and fault picks (red x) are shown where available. Dashed well is projected from 1.5 miles. Seismic Data Courtesy of SEI & Seitel. 114

Figure 3.18 Block diagram of the Cement structure looking east. (A) Configuration prior to strike-slip movement. (B) Left-lateral strike-slip occurs along a pre-existing basement fault. A small amount of normal slip on the Springer detachment allows for the normal fault to cut the crest of the structure. (C) Alternative interpretation, left-lateral strike-slip occurs along the Springer detachment, a small amount of normal slip allows for the normal fault to cut the crest of the structure. 115

Figure 3.19 Cross section CM1 over the Cement structure (A) Interpreted seismic section in time. Horizon colors are shown in Figure 3.2. (B) Depth cross section. (C) Alternative seismic interpretation in time. (D) Alternative interpretation of depth cross section. Well information is listed in appendix 1. Well tops (colored circles), dip data (brown check mark), and fault picks (red x) are shown where available. Seismic Data Courtesy of Chesapeake Energy..... 117

Figure 3.20 Shallow time slice over the Cement-Chickasha trend. Green arrows indicate the main thrust fault cutting the slice. Yellow arrows indicate normal faults oriented NE-SW. Red arrows show where the Cement normal/strike-slip fault cuts the slice. Blue arrows show the continuation of that fault trend east of the main structure. Seismic data courtesy of Chesapeake Energy. 120

Figure 3.21 Cross section CM2 over the Cement-Chickasha transition (A) Interpreted seismic section in time. Horizon colors are shown in Figure 3.2. (B) Depth cross section. (C) Alternative seismic interpretation in time. (D) Alternative interpretation of depth cross section. Well information is listed in appendix 1. Well tops (colored circles), dip data (brown check mark), and fault picks (red x) are shown where available. Seismic Data Courtesy of Chesapeake Energy. 122

Figure 3.22 Cross section CM3 over the Cement-Chickasha transition (A) Interpreted seismic section in time. Horizon colors are shown in Figure 3.2. (B) Depth cross section. Well information is listed in appendix 1. Well tops (colored circles), dip data (brown check mark), and fault picks (red x) are shown where available. Seismic Data Courtesy of Chesapeake Energy. 123

Figure 3.23 Cross section CM6 over the Cement Fault zone (A) Interpreted seismic section in time. Horizon colors are shown in Figure 3.2. (B) Depth cross section. Well information is listed in appendix 1. Well tops (colored circles), dip data (brown check mark), and fault picks (red x) are shown where available. Seismic Data Courtesy of Chesapeake Energy. 125

Figure 4.1 Regional map showing uplifts, basins, and regional fault trends. Pre-Pennsylvanian surface geology is shown in uplifted areas. Red triangle is the location of the 3D seismic study area. Carter-Knox Field is the green polygon. Uplifted areas are highlighted in light red. AA = Arbuckle Anticline; AB = Ardmore Basin; CF = Cement Fault; CHF = Chickasha Fault; CU = Criner Hills Uplift; GT = Golden Trend; MAF = Madill-Aylesworth Fault; MF = Meers Fault; MVF = Mountain View Fault; OF = Ouachita Frontal Thrust Fault; TU = Tishomingo Uplift; WMF = Wichita Mtn Fault. Faults are modified from Marsh and Holland, 2015, Axtmann 1985, and proprietary data. Surface data and Carter-Knox Field outline are from USGS and Oklahoma Geological Survey (Boyd, 2002; Heran et al., 2003)..... 140

Figure 4.2 Stratigraphic Chart for the Carter-Knox Field modified from Reedy and Sykes, 1958. Tectonic History is modified from Granath (1989). Legend shows colors for tops of formations. Black arrows represent detachment locations near basal Springer and basal Arbuckle/Reagan ss. 142

Figure 4.3 Cross sections showing previous interpretations of the Carter-Knox structure. (A) Cross section modified from Reedy and Sykes (1959) showing three to four thrust faults and two shallower normal faults. (B) Cross section from Petersen (1983), showing detachment surface within Middle Arbuckle (C) Cross section from Saxon (1998), showing triangle zone in core of fold (D) Cross section modified from Perkins (1997) showing near vertical strike-slip faults. 145

Figure 4.4. Map of the study area showing data used. Area of 3D seismic is located in red rectangle. Surface locations of selected wells are shown by black dots and deviated tracks. Wells with dipmeter data are shown by red triangles. Locations of cross sections are shown by blue lines. 148

Figure 4.5. Time structure maps on (A) Upper Dornick Hills (B) Primrose (C) Hunton. Cross sections are shown by blue lines. A portion of the Upper Dornick Hills and Primrose are truncated by the Permian Unconformity near the crest of the structure. Note the significant change in structure between the two shallower horizons (A) & (B), and the deeper Hunton horizon c. which are separated by the Springer detachment..... 149

Figure 4.6 Cross section AA' (A) Interpreted seismic section in time (B) Depth cross section (C) location map. Wells on sections are 1 = BERNARD 1-4; 2 = BRAY 1; 3 = BRAY 2-25; 4 = BRAY 1-25; 5 = FISHER 1-25; 6 = NEVIUS 1-25; 7 = CLEARY 1A. 153

Figure 4.7 Cross section BB' (A) Interpreted seismic section in time (B) Depth cross section (C) location map. Wells on sections are 1 = SIZEMORE-PHIPPS 1; 2 = LYNDELL 1-1; 3 = PRESIDIO 1-6; 4 = JOHNSON 1-6; 5 = PRESIDIO 2-6; 6 = HEFNER 1-6; 7 = BETSY RUTH 1-32 154

Figure 4.8 Cross section CC' (A) Interpreted seismic section in time (B) Depth cross section (C) location map. Wells on sections are 1 = MARY DAN 1-30; 2 = JAELYN 1; 3 = SIERRA K 4-20; 4 = PHILMORE 1-21; 5 = CAROLINE 1; 6 = BY 'G' MERCER 1-21; 7 = EASON-KNOX 1; 8 = SLEDGE DEEP 1; 9 = GOFF 1-16..... 155

Figure 4.9 Cross section DD' (A) Interpreted seismic section in time (B) Depth cross section (C) location map. Wells on sections are 1 = LEONA HAYES 1; 2 = KAYE J 2; 3 = JENNA NICOLE 1-28; 4 = W D HARRISON B 1; 5 = JULES 1-34; 6 = MONICA 1-28; 7 = MAGNOLIA 1-27; 8 = CUNNINGHAM 1-27; 9 = CUNNINGHAM 23-A..... 156

Figure 4.10 Cross section EE' (A) Interpreted seismic section in time (B) Depth cross section (C) location map. Wells on sections are 1 = BOYD 1-14; 2 = ROMAN 1-14; 3 = HPC 1-14; 4 =

ANDERSON 1-13; 5 = ARCANGUES 1-13; 6 = SNODGRASS 1-13; 7 = JO ANN 1H-18
..... 157

Figure 4.11 Cross section FF' (A) Interpreted seismic section in time (B) Depth cross section (C) location map. Wells on sections are 1 = DUNCAN 1-26; 2 = DAISY MCKINNEY 1; 3 = DIANE P 4; 4 = GRAHAM 1-19; 5 = FORREST 1-8H 158

Figure 4.12 Cross section GG' (A) Interpreted seismic section in time (B) Depth cross section (C) location map. Wells on sections are 1 = GRAHAM 1; 2 = DIANE P 3; 3 = GOODRICH 1-30; 4 = BRANCH 1H-16 159

Figure 4.13 Kinematic reconstruction and structural evolution of section AA' (A) Depth cross section. (B) Faulting is restored and dashed in red to illustrate fold geometries. (C) Structure is restored to Missourian time with the Hoxbar horizon flattened. (D) Primrose and older units are restored to their undeformed state. Initial dips of these units are not known, so units are shown as horizontal. 163

Figure 4.14 Method of area restoration applied to the units between the Springer detachment and the top of the Primrose Formation in all restorations. (A) Final cross section. (B) Line-length restoration showing a wedge-shaped geometry resulting from differential strain of individual units. (C) Restoration with the area balanced into a rectangle shape. The height of the rectangle is determined by the average thickness (t), and the average restored length (l_0) is determined by dividing the area (A) by t 164

Figure 4.15 Kinematic reconstruction and structural evolution of section DD'. (A) Depth cross section. (B) Faulting is restored and dashed in red to illustrate fold geometries. (C) Structure is restored to Missourian time with the Hoxbar horizon flattened. (D) Primrose and older units are restored to their undeformed state..... 165

Figure 4.16 Kinematic reconstruction and structural evolution of section FF'. (A) Depth section. (B) Faulting is restored and dashed in red to illustrate fold geometries. (C) Structure is restored to Missourian time with the Hoxbar horizon flattened. (D) Primrose and older units are restored to their undeformed state. 166

Figure 4.17. Regional section from the Wichita Uplift to the Carter-Knox structure showing the interpreted seismic interpretation in time, (B) and depth cross section (C). Location map and unconformity legend shown in (A). Faults related to the Wichita Mountain Fault (WMF) are labeled. Dashed lines represent unconformities. This section crosses a portion of the Washita Valley Fault where there may be some out-of-plane movement (black dashed fault). Wells on the depth section include 1 = S J PINSON 1; 2 = WOOLEVER GEORGE A 1 and is projected from 9 miles to the northwest, this well penetrates the Arbuckle, crosses the WMF and then goes into Mississippian and older units; 3 = HINES 1-9; 4 = HOWARD 1; 5 = DEBBY-SUE 1-36; 6 = SUMNER GARY 1; 7 = LAMAR 1-21; 8 = KILGO 3-21; 9 = LEONA HAYES 1; 10 = J KAYE 3-33; 11 = JULES 1-34; 12 = BLOCH 1-34; 13 = CALEB 1-271. Seismic Data Courtesy of Chesapeake Energy & SEI. Interpretation is that of Molly Turko. 169

Abstract

Regional structural transects across the Wichita Uplift and adjacent Anadarko Basin show the relationship between thick-skinned basement-involved structures and thin-skinned detached fold-thrust structures. Slip from the basement-involved structures in the Wichita Uplift is transferred along two major detachments into the Anadarko Basin. Along the southwestern margin of the Anadarko Basin, the Wichita Uplift is marked by a zone of frontal imbricates forming a triangular wedge with most of the slip dissipated along the Wichita front. Paleozoic units show tight folding with overturned beds in the frontal zone. The uplift is episodic as indicated by the truncation of major faults along unconformities and their subsequent reactivation.

In contrast, the southeast margin shows that a significant part of the slip is transferred into structures in the basin. These structures are tight faulted-detachment folds that formed above a major detachment within the Springer Shale, cored by broader structures detaching at the base of the Arbuckle Group. Examples include the Carter-Knox, Cement, Chickasha, and Cruce structures. The faulted-detachment folds formed within the thin-bedded Pennsylvanian-age clastic units while the broad structures formed in pre-Pennsylvanian units dominated by thick carbonate units. These two main structural packages underwent differential, but simultaneous, shortening due to a forward-shear along the frontal faults of the Wichita Uplift.

Pre-existing normal faults of Precambrian-Cambrian age were either reactivated along the Wichita Uplift, or controlled the location of the Pennsylvanian age structures in the Anadarko Basin. Progressive rotation of regional stresses from NE-SW to a more ENE-WSW direction during the Pennsylvanian uplift influenced the tectonic history of the area. As the regional stresses rotated to ENE-WSW, the more E-W oriented structures in the Anadarko Basin were cut

by strike-slip faults that linked down into the pre-existing normal faults. The strike-slip faults were accompanied by normal faulting with Virgilian-age sediments filling the accommodation space and indicating the timing of the strike-slip movement.

2D and 3D seismic, well log data, and surface geology were used to evaluate the structural styles of the Wichita Uplift and the Anadarko Basin, and allowed for an interpretation of the tectonic evolution of the region.

Chapter 1: Introduction

The dissertation is divided into three projects all related to southern Oklahoma geology. The first project, Chapter 2, looks at the regional structural styles over the Wichita Uplift and Anadarko Basin. Regional cross sections, and local supplementary cross sections, were constructed using seismic and well log data. Several of these cross sections were palinspastically restored to illustrate the tectonic evolution of the region. These cross sections were used to construct block diagrams of the basement that show a 3D model of the tectonic evolution of the study area.

The second project, Chapter 3, focuses on structures in the southeast Anadarko Basin that resulted from the Wichita Uplift. These structures include the Carter-Knox, Cruce, Chickasha, and Cement Anticlines. Structural cross sections, and accompanying restorations, look at the impact of thin-skin deformation that occurs along two detachment levels in the study area. Mechanical stratigraphy is a big factor on the types of structures that developed along with the orientation of pre-existing rift faults that likely localized these structures at either NW-SE or more E-W orientations.

The third project, Chapter 4, was a detailed structural analysis of the Carter-Knox Field. 3D seismic and well data were used to develop a model for the geometry and evolution of the structure. This structure is an analogue for the structures discussed in Chapter 3 and conveys details of a faulted-detachment fold that overlies a gentle faulted fold separated by a detachment. It discusses the episodic deformation, unconformities, and impact of mechanical stratigraphy on the structural styles.

Chapter 2: Structural Styles in the Wichita Uplift and Anadarko Basin, Southern Oklahoma

Abstract

Regional structural transects across the Wichita Uplift and adjacent Anadarko Basin show the relationship between thick-skinned basement-involved structures and thin-skinned detached fold-thrust structures. Slip from the basement-involved structures in the Wichita Uplift is transferred along two major detachments into the Anadarko Basin. Along the southwestern margin of the Anadarko Basin, the Wichita Uplift is marked by a zone of frontal imbricates forming a triangular wedge with most of the slip dissipated along the Wichita front. Paleozoic units show tight folding with overturned beds in the frontal zone. The uplift is episodic as indicated by the truncation of major faults along unconformities and their subsequent reactivation. In contrast, the southeast margin shows that a significant part of the slip is transferred into structures in the basin. These structures are tight faulted-detachment folds that formed above a major detachment within the Springer Shale, cored by broader structures detaching at the base of the Arbuckle Group. Examples include the Carter-Knox, Cement-Chickasha, and Cruce structures. Oblique faults with normal and strike-slip components cut some of these structures, resulting in more complex geometries. Pre-existing normal faults of Precambrian-Cambrian age were either reactivated along the Wichita Uplift, or controlled the location of the Pennsylvanian age structures in the Anadarko Basin. Progressive rotation of regional stresses from NE-SW to a more ENE-WSW direction during the Pennsylvanian uplift influenced the tectonic history of the area. 2D and 3D seismic, well log data, and surface geology were used to evaluate the structural styles of the Wichita Uplift and the Anadarko Basin.

1. Introduction

Southern Oklahoma is characterized by several uplifts including the Wichita, Arbuckle, and Ouachita Mountains. Adjacent to these uplifts are deep sedimentary basins containing prolific oil and gas fields. Both the surface and subsurface geology is complex, due to multiple tectonic events that shaped the region, including a failed rift and its subsequent inversion. By utilizing modern 2D and 3D seismic, well log data, and recently acquired high-resolution aeromagnetic data, a structural and tectonic model was developed for the region. It is proposed that Precambrian-Cambrian rift faults controlled the location of Pennsylvanian age structures, and that these structures developed under Early Pennsylvanian northeast directed contraction that rotated to east-northeast by the Late Pennsylvanian. Changes in mechanical stratigraphy from thick carbonate packages to thinly bedded clastics, along with two detachment levels, also impacted the structural styles that developed. Regional structural transects show a relationship between thick-skinned basement-involved structures along the Wichita Uplift and thin-skinned detached fold-thrust structures in the Anadarko Basin. Figure 2.1 shows the locations of the regional transects along with major uplifts, basins, and fault trends that traverse southern Oklahoma. Several major fault trends are highlighted on the map including the Wichita Mountain, Mountain View, Willow, Washita Valley, and Cement Faults. Several anticlines are also labeled which contain significant oil and gas fields including Cement, Chickasha, Carter-Knox and Cruce. The tectonic evolution of the region can be deciphered by studying the detailed geometry of the structures in the Wichita Uplift and Anadarko Basin and the relationship between them.

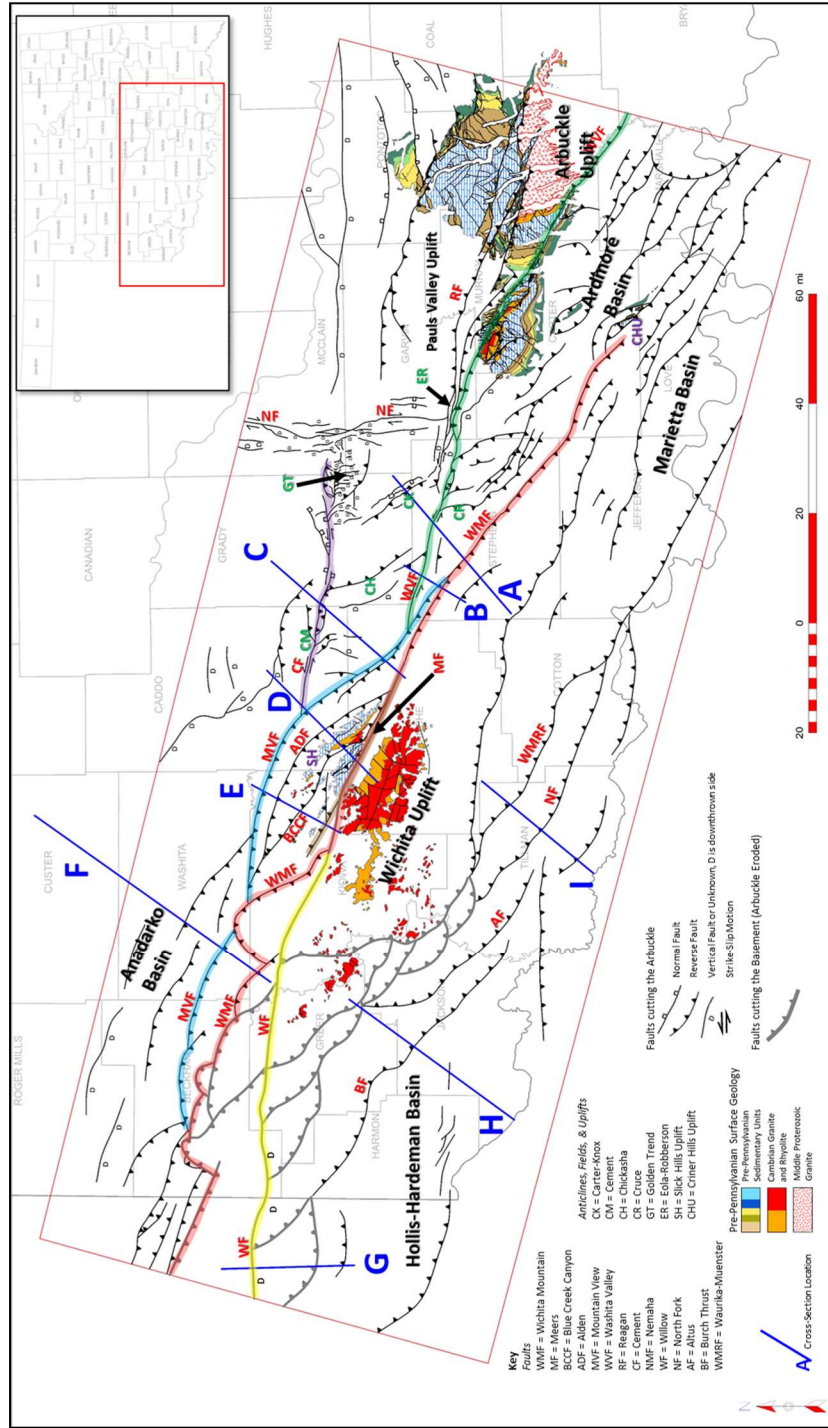


Figure 2.1 Regional map showing faults mapped at the Arbuckle level (black), and at the basement where Arbuckle is eroded on the Wichita Uplift (bold gray). The Mountain View Fault is highlighted in blue; Washita Valley Fault in green; Cement Fault in purple; and Wichita Mountain Fault in red. Pre-Pennsylvanian surface geology is derived from the USGS (Heran et al., 2003). Significant uplifts, basins, fields and structures are labeled with a key on the map. Cross section locations are shown in blue.

2. Regional Tectonics

The tectonic history of the region can be subdivided into three significant events: (1) the development of an aulacogen, or failed rift, that initiated in the Late Precambrian through the Middle Cambrian; (2) subsidence following the emplacement of the large igneous province in the early Paleozoic; and (3) the late Paleozoic Pennsylvanian Orogeny which uplifted the Wichita and Arbuckle Mountains and formed additional structures in the Anadarko and adjacent basins.

Rifting in the Late Precambrian to Cambrian resulted in a large igneous province in southern Oklahoma (Shatski, 1946; Hoffman et al., 1974; Walper, 1982; Perry, 1989; Keller and Stephenson, 2007; Keller, 2014). Some authors have proposed that instead of a failed rift, the NW-SE oriented large igneous province is the result of a left-lateral shear zone that developed into a large pull-apart (McBee, 1995), while others have suggested that it was a leaky continental transform fault (Skulski et al, 1991; 1992; Thomas, 2011;2014). Recent work, based on the igneous petrology of rocks from the Wichita Mountains, supports the hypothesis of a failed rift associated with the opening of the Iapetus Ocean (Hogan et al., 1995; Puckett, 2011; Hansen et al. 2012; Puckett et al., 2014; Brueseke et al. 2014). These igneous rocks consist of older intrusive basalts, gabbros, massive amounts of younger extrusive rhyolites and intrusive equivalents (Ham et al., 1964; Gilbert, 1983). The extrusive rhyolites are significant because it is believed they make up the floor of the Anadarko and Ardmore Basins (Ham et al., 1964; Denison, 1995). The Precambrian-Cambrian tectonic framework is important, since the type of faulting, whether strike-slip or normal, would influence the later Pennsylvanian deformation styles.

Subsidence due to cooling following the emplacement of the large igneous province began in the Middle Cambrian and continued through the end of the Ordovician (post-Hunton) (Feinstein, 1981; Perry, 1989). Feinstein demonstrated the concept of a thermally controlled isostatic subsidence. Subsidence curves from the Anadarko Basin show an exponential curve with initially higher subsidence rates that slow and nearly flatten in the Silurian through early Devonian (Hunton time). From the Silurian through the middle Mississippian the craton is considered relatively stable. Minor post-rift faulting likely occurred on pre-existing rift faults due to tectonic loading as the basin subsided, resulting in a significantly thickened Cambrian-Devonian section into the rift basin (Feinstein, 1981; Bott, 1979).

The onset of the Late Paleozoic Pennsylvanian Orogeny is documented by renewed subsidence in the Late Mississippian (Feinstein, 1981; Granath, 1989; Perry, 1989; Denison, 1989). The Pennsylvanian Orogeny is traditionally believed to be caused by the collision of North America with Africa/South America (Houseknecht, 1983; Kluth, 1986; Perry, 1989; Granath, 1989). This collision created the Appalachian and Ouachita-Marathon Fold and Thrust Belts and may have been responsible for uplift and inversion of the aulacogen as the fold and thrust belt wrapped around the southern margin of North America (Granath, 1989).

Another consideration is that the inversion of the aulacogen resulted from intraplate tectonics related to tectonic activity along the western (Nevada) and southwestern (Sonora) margins of North America. Some authors have suggested mechanisms for a NE-SW directed maximum horizontal stress orientation along the Sonora margin by either flat-slab subduction (Ye et al., 1996) or due to transpressional plate interactions between the Nevada, Sonora, and Ouachita Margins (Leary et al., 2017). This model is supported by the observation that the Ouachita Orogeny was relatively low energy and resulted in only thin-skinned deformation (Ye

at al., 1996; Keller and Stephenson, 2007). Domeier and Torsvik (2014) have used new geodynamic concepts (Torsvik et al., 2008) and analytical tools (www.geoplates.org), along with paleomagnetic data, to reconstruct plates and plate velocities back to the early Devonian (410 Ma). Leary et al. (2017) used this dataset to support the idea of a NE-SW directed stress field during the Pennsylvanian orogeny as a driving force. Understanding the paleostress orientations are important in considering which structural styles were dominant as the Pennsylvanian Orogeny progressed.

In southern Oklahoma the Pennsylvanian Orogeny has been divided into three tectonic events (Granath, 1989). The first and second Wichita Orogenies occurred during the Morrowan and Atokan when the Wichita Block underwent significant inversion and uplift. These Wichita Orogenies culminated in the early Atokan but uplift likely initiated in the Late Mississippian evident from onlapping of Chesterian age (Springer) units onto the Criner Uplift (Tomlinson and McBee, 1959; Granath, 1989; Perry, 1989; Cooper, 1995). Unconformities exist at the top of both the Morrowan and Atokan with as much as 8,000-13,000 feet of sediment eroded prior to the Desmoinesian time (Tomlinson and McBee, 1959). The third tectonic event is referred to as the Arbuckle Orogeny and occurred from the Late Desmoinesian through Virgilian (Granath, 1989). It was during this orogeny that the Arbuckle Mountains were uplifted as seen today. By the end of the Pennsylvanian, much of the major tectonic activity had ceased with only small amounts of rejuvenation in the Permian.

The structural styles that resulted from these orogenies have been variously attributed to simple compression (Taff, 1904; Dott, 1933; Brown, 1984; Naruk, 1994; Saxon, 1998), strike-slip (Ham, 1951; Tanner, 1963; Carter, 1979; Tomlinson and McBee, 1987) and/or transpression through inversion (Weldon, 1982; McCoss, 1986; Granath, 1989; Ferebee, 1991; Tapp, 1995;

Donovan et al., 1989; Donovan, 1995; Jones-Cecil, 1995). A possible reason for the different structural styles could be attributed to pre-existing rift-related basement faults and their orientation to Pennsylvanian stresses. Models of transpression show that the orientation of a pre-existing structure (fault) will determine whether that structure will be reactivated by strike-slip or compression, and to what degree, based on the angle of convergence (Sanderson and Marchini, 1984; McCoss, 1986; Richard and Krantz, 1991; Dewey et al., 1998; Casas et al., 2001). When the convergence angle is high, near perpendicular to the pre-existing fault, reactivation will be dominantly compressional. When the convergence angle is low, near parallel to the pre-existing fault, reactivation will be dominantly strike-slip. (Richard and Krantz, 1991; Casas et al., 2001). This could explain why some authors have recognized that E-W structures tend to have a stronger component of strike-slip, while NW-SE structures are dominantly compressional (Granath, 1989; Tripplehorn, 2014).

Adding to the complexity is a possible change in stress orientation during the Pennsylvanian. Perry (1989) proposed that maximum horizontal stress was likely oriented NE-SW in the Morrowan to Atokan but rotated toward ENE-WSW during the Desmoinesian to Virgilian based on cross-cutting relationships of faults and folds in the Arbuckle Mountains. A similar conclusion was reached by Ghosh (2017) looking at fracture trends in the Woodford. Cooper (1995) also suggested that early compressional structures were rejuvenated by later strike-slip deformation which could have been a result of a change in horizontal stress orientation.

3. Previous Studies

Some of the earliest literature on southern Oklahoma geology was derived prior to the concepts of plate tectonics resulting in models primarily driven by differential vertical uplift

(Saxon, 1998). Early cross sections across southern Oklahoma show high angle normal and reverse faults (Taff, 1904; Harlton, 1963). During the 1950's much of the surface geology was mapped out in southern Oklahoma. In the Arbuckle Mountains, several authors suggested one to three miles of left-lateral strike-slip along the Washita Valley Fault based on the offset of anticlinal axes as well as offset in Pennsylvanian age conglomerates (Ham, 1950; Dunham, 1955). Other authors have suggested much larger offsets based on isopach mapping (Tanner, 1967; Carter, 1979), secondary structures in the Arbuckle Mountains (Booth, 1982), and the offset of well log stratigraphy (McCaskill, 1998; 2015). These values range from 10-40 miles of left-lateral strike-slip. In contrast, others have proposed that no strike-slip has occurred, and that the lateral offset can be accounted for by unfolding the hanging-wall and foot-wall along the Arbuckle Thrust Fault (Brown, 1984; Saxon, 1994; Naruk, 1994). On a much larger scale, Budnick (1986) suggested more than 70 miles of left-lateral slip had occurred along the "Wichita Megashear" based on subcrop maps while McBee (1995) proposed 55 miles based on the offset of the Ouachita Fold and Thrust Belt near the southeast end of the Ardmore Basin.

Granath (1998) used a transpressional model developed by McCoss (1986) to describe structures in the Ardmore Basin. He suggested that structures oriented closer to E-W experienced a stronger degree of strike-slip while structures oriented NW-SE experienced more compression. Tapp (1995) agreed with the transpressional model and suggests the region is a partially inverted asymmetric half-graben. These two studies suggest that the relative orientations of pre-existing structures and Pennsylvanian-age stress orientations influence the structural styles that developed in the area.

The Slick Hills Block is part of the frontal Wichita Uplift that is bound between the Wichita Mountain Fault and Mountain View Fault. The Arbuckle Group is exposed at the

surface revealing complex Pennsylvanian age deformation. En echelon folding, reidel shears, shear zones, and fault orientations exposed in the surface geology support transpressive deformation (Weldon, 1982; Donovan et al., 1989; Donovan, 1995; Jones-Cecil, 1995). The Mountain View Fault is responsible for bringing up the Slick Hills Block with an estimated reverse-slip component up to ~23,700 feet while dipping 30°-40° to the south (Brewer, 1983; McConnell, 1989). The Mountain View Fault may also have a left-lateral strike-slip component of one to three miles (Axtmann, 1983) up to 7.5-14.5 miles (McConnell, 1989).

Other significant faults in the Slick Hills Block include the Alden, Blue Creek Canyon, and Meers Faults. The Alden Fault is not exposed at the surface but the named trace of it is shown on a map in Donovan (1995). Several others have interpreted it in their cross sections (McConnell, 1987; Saxon, 1998) where it could be described as a forward imbricate extending from the deeper Mountain View Fault. The Blue Creek Canyon Fault crops out in the Slick Hills and is traditionally mapped as a back-thrust fault extending from the Alden or Mountain View Fault (McConnell, 1987; Donovan et al., 1989; McConnell, 1989; Saxon, 1998). Donovan et al. (1989) describes this fault as having between 1,700-2,400 feet of throw by oblique reverse movement, and in his 1995 publication he discusses the fault kinematics as left-lateral reverse based on sigmoidal shear arrays and slickensides observed on the surface. He also mentions that although no single décollement is observed in the Slick Hills, it does appear that the lower thinly bedded parts of the Arbuckle Group (Signal Mountain and Mackenzie Hill Formations) are more susceptible to deformation by flexural slip. Flexural slip is a common deformation mechanism observed in southern Oklahoma, both in outcrop and subsurface data (Donovan et al., 1989; Tapp, 1995; Saxon, 1994; Saxon, 1998; Walker, 2006.)

The Meers Fault (Harlton, 1951; Miser, 1954) either runs parallel or is the same as the Wichita Mountain Fault along the southern boundary of the Slick Hills Block. Moody and Hill (1956) noticed quaternary displacement on this fault while both Gilbert (1983) and Donovan et al. (1983) brought attention to a modern seismic risk. Paleoseismology studies that followed determined that the fault has had at least four surface deforming episodes in the last 6,000 years (Ramelli and Slemmons, 1986; Streig et al., 2018) with magnitudes between M6.8-M7.1 (Baker and Holland, 2013). It is unknown if the Meers Fault is the surface expression of the basement-rooted south-dipping Wichita Mountain Fault (McConnel, 1987; Donovan et al., 1989; Saxon, 1998) or if it is a separate fault (Cullen, 2018). Several near-surface studies based on trenching, core, shallow magnetic data, and shallow seismic have suggested the surface expression of the Meers Fault dips to the north and has a left-lateral oblique reverse slip component (Crone and Luza, 1986; Miller et al., 1982; Cecil-Jones, 1990; Collins, 1992; Streig et al., 2018; Behm et al., 2018). However, studies have shown that shallow surface ruptures do not always represent the fault geometry at depth, particularly along a strike-slip fault (Hilley et al., 2001; Quigley et al., 2011; Meyers et al., 2012; Hornblow et al., 2014).

The Wichita Mountain Fault bounds the southern part of the Slick Hills but also makes up the northern boundary of the Wichita Uplift extending from southeastern Oklahoma to the Texas panhandle. Cross sections across this fault typically show it dipping between 30°-50° degrees to the south (McConnel, 1987; Brewer, 1983; Cooper, 1995; Saxon, 1998; Keller, 2012; Cullen, 2018). At the Slick Hills, Donovan (1989) suggested up to 10,000 feet of vertical throw on the Wichita Mountain Fault with decreasing offset to the southeast. He also suggested that a component of left-lateral strike-slip is probable for this fault based on left-lateral shears documented in the Slick Hills that subparallel this fault. Although the amount of strike-slip on

this fault is unknown due to a lack of piercing points, Granath (1989) used the geometrical transpression model from McCoss (1986) to estimate around six to nine miles of left-lateral slip near the Healdton Field which extends along the Wichita Mountain Fault in the Ardmore Basin.

In relation to transpression, several authors have suggested that the structures developed first by compression followed by strike-slip, or vice versa. Budnick (1986) concluded that strike-slip faulting occurred early in the Pennsylvanian followed by compression on the basis of en echelon Atokan-Desmoinesian age folding along the “Wichita Megashear” followed by Late Pennsylvanian folding and uplift of the Arbuckle Mountains. Alternatively, others have suggested that strike-slip faulting followed contractional deformation (Kluth and Coney, 1981; Brewer et al., 1983; Perry, 1989). Brewer et al. (1981) used deep seismic reflection data (COCORP) and determined that folding and thrusting along the Wichita Mountain Front was Morrowan and Atokan in age, but that Late Pennsylvanian strike-slip in the Arbuckle Mountains could be consistent with oblique slip along the Wichita Trend. Perry (1989) considered the orientation and age of significant structures in the region and concluded that Early Pennsylvanian compression (maximum horizontal stress) had to be oriented between 35°-60°, but then rotated to 70°-75° by Late Pennsylvanian to create the strike-slip structures observed in the Arbuckle Uplift.

In the Anadarko Basin along the mountain front, structures consist of tight faulted anticlines within Pennsylvanian stratigraphy that overlie gentle faulted folds within pre-Pennsylvanian stratigraphy (Reedy and Sykes, 1959; Harlton, 1960; Herrmann, 1961; Petersen, 1983; Saxon, 1998). These structures include the Carter-Knox, Cruce, Chickasha, and Cement Anticlines. These two levels of structures are separated by a detachment within the Springer Shale, while a second detachment has been observed near the base of the Arbuckle (Petersen,

1983; Saxon, 1998). These structures are synchronous with the Wichita Uplift and developed primarily from the Morrowan through Virgilian (Reedy and Sykes, 1959; Harlton, 1960; Herrmann, 1961; Jacobson, 1984; Saxon, 1998).

In summary, hypotheses on the structural styles and mechanisms that created the Wichita-Arbuckle trend have evolved over time. While some authors propose strike-slip as the main mechanism, the degree of strike-slip ranges as small as one mile (Ham, 1950; Dunham, 1955) up to 70 miles (Budnick, 1986). In contrast to strike-slip or wrench tectonics, several authors have suggested that these structures are derived solely from compression (Harlton, 1963; Brown, 1984; Naruk, 1994; Saxon, 1998), while others have proposed transpression as the main mechanism (Weldon, 1982; Granath, 1989; Donovan et al., 1989; Donovan, 1995; Jones-Cecil, 1995; Tapp, 1995; Carpenter and Tapp, 2014). In contrast to a single mechanism, some authors have proposed multiple mechanisms of deformation that progressed throughout the Pennsylvanian as a consequence of evolving continental-scale tectonics. This regional-scale study will address some of these structural styles and mechanisms to resolve some of the differences in previous interpretations and illustrate the tectonic history of southern Oklahoma.

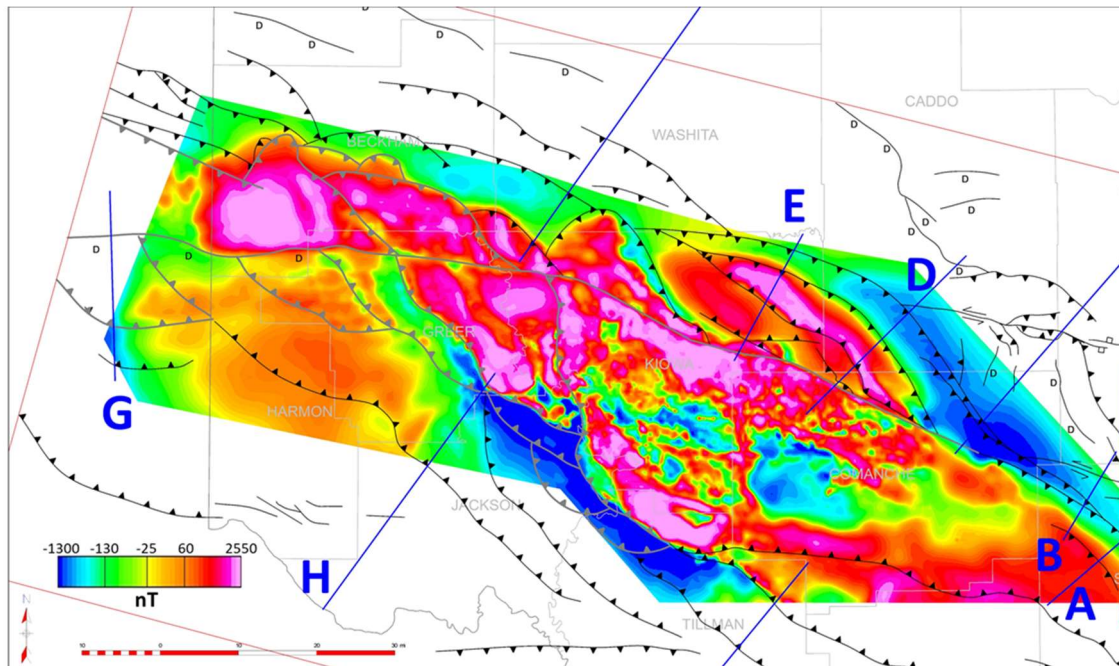
4. Data and Methods

The data used in the study include extensive 2D and 3D seismic and well data. Seismic interpretation of key regional and local lines was followed by the construction of structural cross sections. The cross sections were chosen in optimal locations to illustrate both structure and stratigraphy, including significant unconformities. Wells with sonic log data were used to create a time-depth chart and tied to the seismic data. Appropriate time-depth charts were used to tie wells without sonic data to the seismic data. These were used to convert the seismic time sections to structural sections in depth. Formation tops, faults, and unconformities were picked

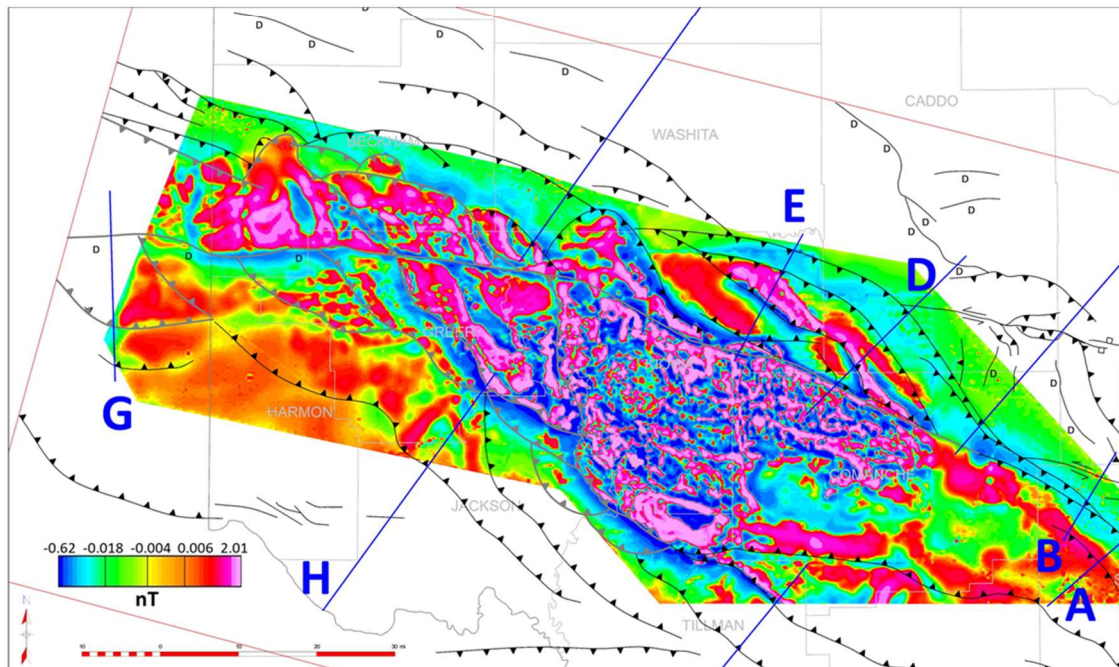
from well logs and projected onto the sections. Where available, surface dips from geologic maps and dip-meter data was also used. A number of regional sections were palinspastically restored to illustrate the structural evolution. The kinematic reconstructions involved multiple stages during key time intervals and used both line-length and area balancing.

A regional fault map was constructed for the area (Figure 2.1) using seismic, well log data, surface geologic maps, and gravity and magnetic data. The faults were mapped at the Arbuckle level, but where the Arbuckle is missing, the faults were mapped at the basement level. This occurs along the Wichita and Arbuckle Uplifts, and is evident on the pre-Pennsylvanian surface geology maps. By drawing them at the Arbuckle level, and not the basement level, the fault map is able to capture faults that cut the Arbuckle but sole out onto a detachment at the base of the Arbuckle (thin-skinned faults). Pre-Pennsylvanian surface geology from the Arbuckle and Wichita Uplifts show faults that have been mapped at the surface. These faults were extracted from the Oklahoma Geological Survey database (Marsh and Holland, 2015) and illustrate the fault architecture at the surface.

Gravity and aeromagnetic data were also incorporated into the project. In the western half of the Wichita Uplift, high resolution USGS aeromagnetic data acquired in 2017 (Shah and Finn, 2018) was used to map some of the major faults (Figure 2.2). This data shows potential faults and structures where seismic data is poorly imaged due to the proximity of basement rock near the surface. Derivative maps of the aeromagnetic data emphasized these structures as well. Derivative maps of the gravity data (both public domain and proprietary), helped to constrain areas of uplifts and determine where basement faults might transverse. Gravity, aeromagnetic and seismic data were integrated to construct the regional fault map.



A



B

Figure 2.2 Aeromagnetic data processed by Chase (2019), data courtesy of Shah and Finn (2018). Cross section locations are shown in blue. Regional fault map from Figure 2.1 overlays the aeromagnetic data. (A) Total magnetic intensity (B) First derivative of total magnetic intensity.

5. Stratigraphy

Figure 2.3 shows the stratigraphic column for the region. Dashed lines represent the top of a time unit, which in some parts of the cross sections represents an unconformity. The solid lines represent a marker within the different ages to help constrain structure in the cross sections. The stratigraphic chart can be divided into three mechanical stratigraphic packages; the igneous basement, a deeper carbonate section, and a shallower clastic section. The basement rock that underlies much of the study area includes both Precambrian basement and Cambrian layered rhyolite. Ordovician through mid-Mississippian age stratigraphy is dominated by a thick carbonate package including the Arbuckle, Viola, Hunton, and Sycamore Groups. Clastic units within the package include the Timbered Hills, Simpson, Sylvan, and Woodford. The Mississippian Caney shale and Early Pennsylvanian Springer Shale cap the deeper carbonate package. These shales are understood to act as a regional detachment surface and separate two mechanical units with different structural styles. The upper mechanical package includes Late Mississippian to Pennsylvanian units above the Springer detachment and consist dominantly of clastic sand/shale packages with some thin limestone intervals. The tectonic events listed to the right of the stratigraphic chart are adapted from Granath (1989). The events show which units are synchronous with the first and second Wichita Orogenies and the Arbuckle Orogeny. These formations are important in determining the timing of structures and can help decipher paleo-stress directions depending on the orientation of the structures that developed during each time period. The Permian Unconformity is nearly flat in the study area and indicates the region was relatively quiet post-Pennsylvanian.

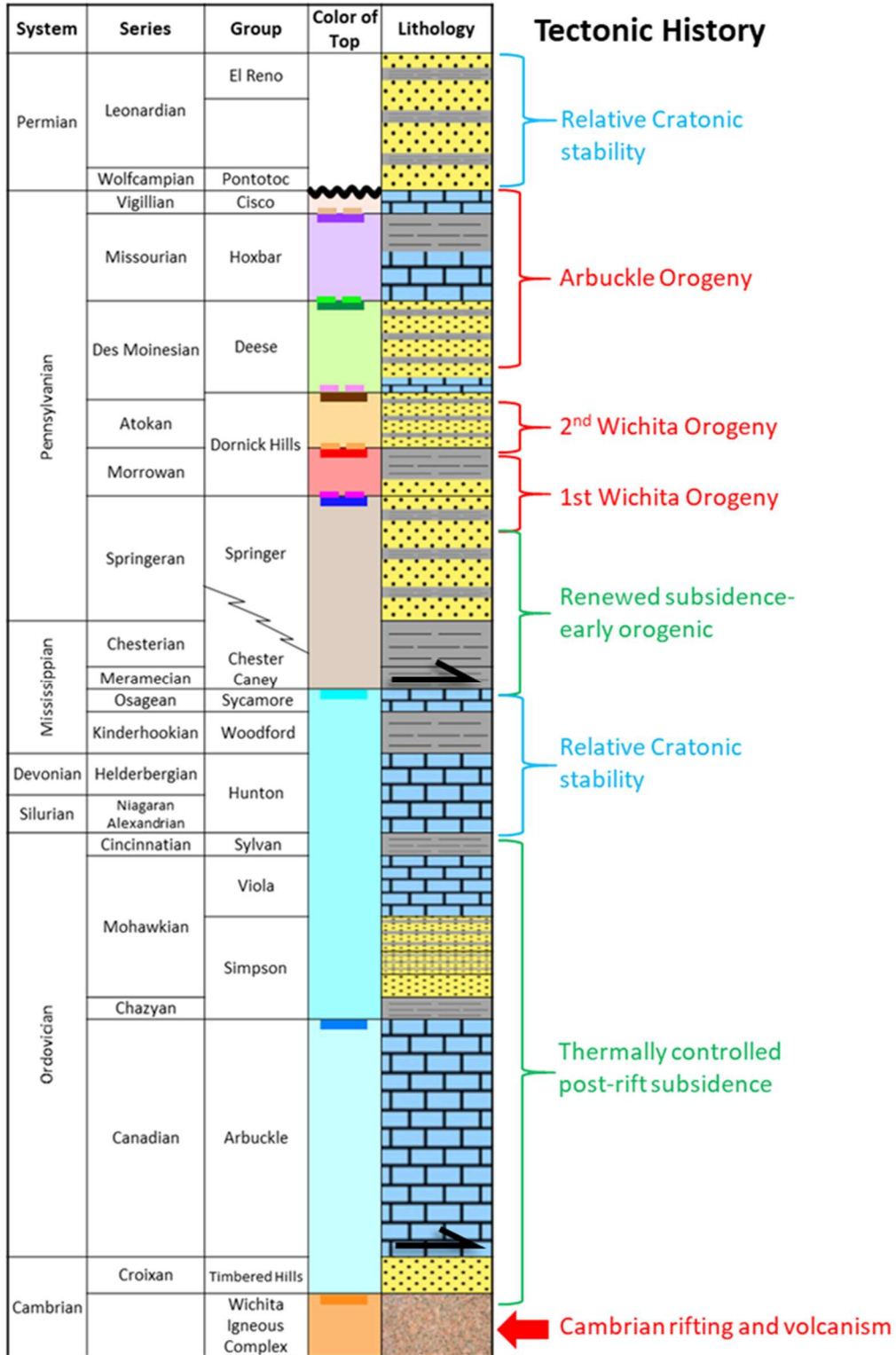


Figure 2.3 Modified from Granath (1989). Color of top refers to horizons interpreted in the cross sections. Lithologies include an igneous basement, followed by clastic, carbonate, and shale units. Detachment levels are shown by black arrows.

6. Structure Map

A regional structure map was constructed for the top of the Arbuckle Group using well tops and seismic data and is shown in Figure 2.4. Pre-Pennsylvanian surface geology is posted on the map in the Wichita, Arbuckle, and Criner Uplifts. The Wichita Uplift is a prominent structure that extends from the Texas Panhandle into southern Oklahoma and parts of northern Texas. It plunges southeast into the Marietta Basin. The southern margin of the Wichita Uplift consists of NW-SE oriented reverse faults that dip to the northeast. The northwest margin of the Wichita Uplift consists of south dipping reverse faults, many of which appear stacked.

The Wichita Mountain Fault is the main fault uplifting and exposing the Wichita Mountains. The trace of the Wichita Mountain Fault is relatively linear and trends WNW-ESE near the central and eastern parts of the Wichita Uplift, whereas in the western parts the fault is interpreted to consist of the multiple faults that form an imbricate thrust system (see Figure 2.1 for highlighted fault trace). It is likely that the Wichita Mountain Fault system and another major fault, the Mountain View Fault, merge at depth to the west.

The Slick Hills Block is located along the central part of the frontal Wichita Uplift. This block is brought up along the southwest-dipping Mountain View and Alden Fault systems exposing a number of faults cutting the Arbuckle Group. Two other faults, the Blue Creek Canyon Fault and an unnamed fault dip to the north. The Blue Creek Canyon Fault crops out at the surface exposing rhyolitic basement. The Slick Hills Block is bounded on the south by the Wichita Mountain Fault.

A prominent lineament observed in aeromagnetic data is the trace of the Willow Fault (Chase, 2019) which is likely the Cambridge Fault mentioned by Gay (2014) (see Figure 2.1 for

location). Both authors suggested left-lateral strike-slip based on the offset of aeromagnetic anomalies. However, the offset could be related to an eroded dip-slip component. The Arbuckle has been eroded over the trace of this fault in the western Wichita Uplift, but it is shown on the structure map as one of the faults that cuts the basement and appears to merge with the Wichita Mountain Fault towards the east.

Towards the east-southeast, the Wichita Mountain Fault extends to the Criner Hills Uplift, where the Arbuckle Group is exposed at the surface. The Marietta Basin is located south of the uplift. North of the Criner Hills Uplift is the Ardmore Basin as it plunges to the southeast under the Ouachita Fold and Thrust Belt. The Ardmore Basin is separated from another deep basin, the Anadarko Basin, by the Washita Valley Fault, which extends from the Arbuckle Anticline to the west where it terminates against the Mountain View Fault system. Several structures just south of the Washita Valley Fault and north of it in the southeastern Anadarko Basin are important for understanding the tectonic evolution of the region. These include the Cruce, Carter-Knox and Chickasha structures that all consist of NW-SE oriented thrust faults cutting the Arbuckle. The Nemaha Fault system is one of the only major N-S oriented fault trends and has historically been interpreted as a pre-existing structure reactivated in right-lateral strike-slip (Amsden, 1975; Budnik, 1986; McBee, 2003; Friess, 2005; Chopra et al., 2018).

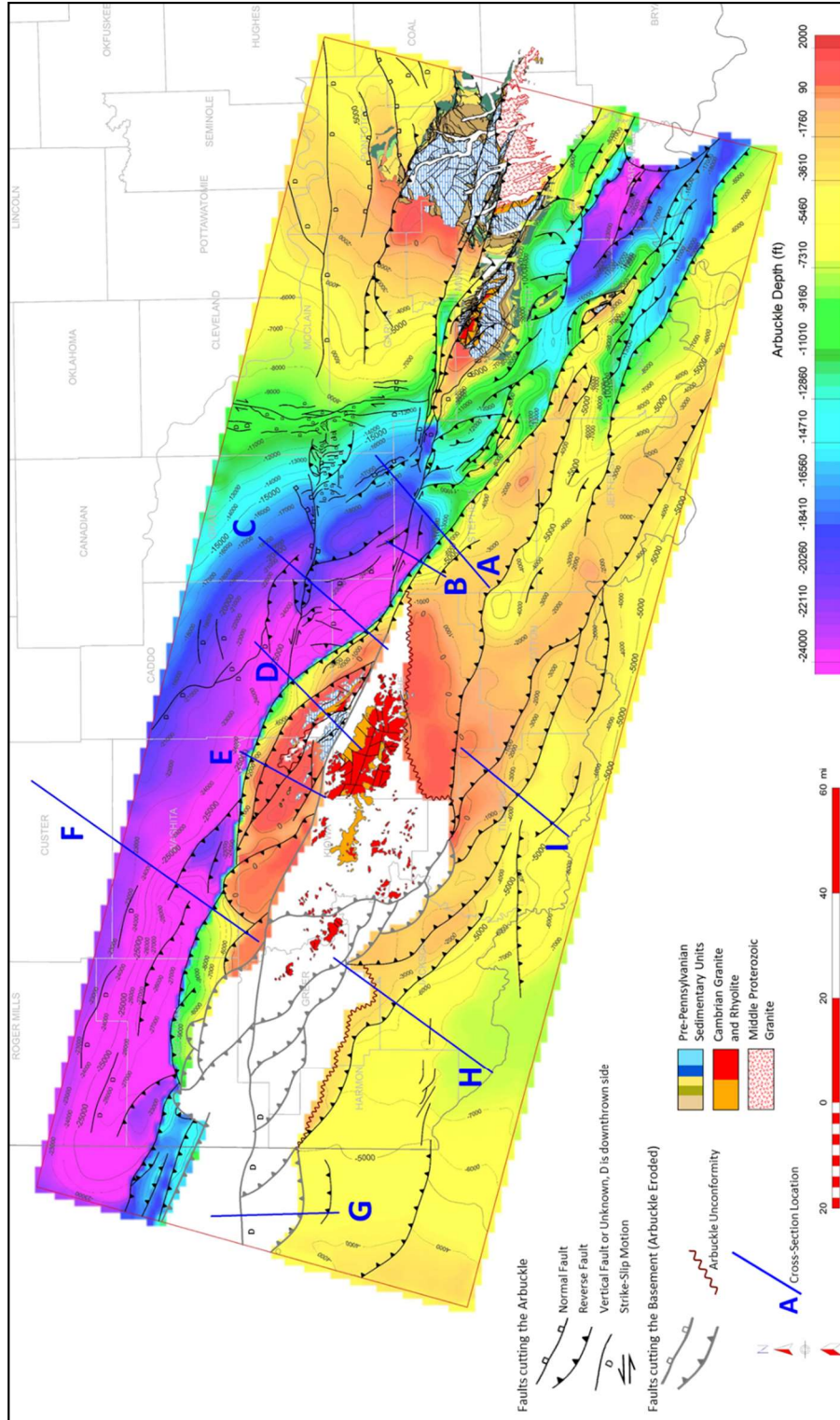


Figure 2.4 Subsea structure map on the Arbuckle formation, contour interval is 1,000 feet. Where Arbuckle becomes eroded faults are at the basement level (bold gray). Pre-Pennsylvanian surface geology is from USGS (Heran et al., 2003). Cross sections locations are shown and labeled in blue.

7. Structural Cross Sections

A series of five regional structural transects through the northeastern Wichita Mountain Front and the Anadarko Basin were constructed to show the regional structural styles and the relationship between the Wichita and Anadarko Basin structures. The regional cross sections are supplemented by shorter sections to show some of the details. Two of the regional lines are restored to show the tectonic evolution. Some of the details of the structural evolution are discussed in detail in the first cross section through the Wichita Mountains and the Carter- Knox structure. Subsequent cross sections are discussed in less detail, emphasizing the similarities and differences along trend.

Three additional sections through the simpler structures along the southwestern margin were also constructed. These were combined with the sections along the northeastern margin to develop a regional tectonic model for the area.

7.1 Cross section A: Wichita Front - Carter-Knox

Cross section A extends over the subsurface Wichita Uplift towards the northeast into the Carter-Knox Field showing the relationship between the Wichita Uplift and Anadarko Basin structures (Figure 2.5). This section shows the impact of mechanical stratigraphy on the structural styles and highlights multiple unconformities in the Pennsylvanian section.

Slip from the Wichita Mountain Fault causing the Wichita Uplift is transferred along two main detachments, one at the base of the Arbuckle Group, and the other within the Springer Shale. Slip on the Springer detachment is largely consumed along the ramp segment of the Wichita Mountain Fault, as it cuts through the Morrowan, Atokan, and shallower sections. Unconformities and onlapping relationships illustrate that movement on this and other faults was

episodic. The basement ramp in the Wichita Mountain Fault is also associated with a break-back imbricate as well as a backthrust. The Morrowan unconformity appears to onlap the hangingwall of the Wichita Mountain Fault suggesting uplift and erosion began just prior to Morrowan deposition. The seismic section may show a velocity pull-up below the hanging wall of the Wichita Mountain Fault which has been accounted for in the depth conversion.

In addition to the Wichita Mountain Fault, a number of faults are interpreted to propagate from the Springer detachment that are then truncated by the Morrowan unconformity. They appear to be reactivated and then truncated again by later unconformities including the Atokan and Desmoinesian unconformities.

Significant slip has also been transferred into the Carter-Knox structure, which is a tight faulted-detachment fold (Mitra, 2002), with several frontal imbricates and a steep to vertical front limb. The faulted-detachment fold occurs above the Springer detachment. Below this detachment is a gentle fold in the Mississippian through Cambrian units that resulted from slip along a detachment at the base of the Arbuckle. This deeper fold is cut by two forward imbricates with small offset. Two normal faults have been interpreted below the Carter-Knox structure, and may have acted as a buttress for the development of the structure. Morrowan units are relatively uniform over the structure with only minor thinning over the crest. Thickness changes that represent syn-depositional growth are more apparent in Atokan and younger units. Missourian age units onlap the Desmoinesian unconformity and the Virgilian units onlap the Missourian unconformity suggesting the structure experienced significant growth during these periods. Thickness changes in the Springer are due to flowage along the detachment. Minor folding of the Permian Unconformity over this structure suggests much of the growth had ceased by Permian time.

One or more footwall imbricates developed under the Wichita Mountain Fault zone. These footwall imbricate faults are responsible for transferring slip along a detachment at the base of the Arbuckle Group.

The Washita Valley Fault cuts through the center of the cross section. This fault has a component of strike-slip and appears to be most active from the Desmoinesian through Virgilian. Along this fault, the Morrowan and Atokan units are folded into an anticline from an earlier fold above the Springer detachment. The Desmoinesian units are also slightly folded but do not appear to have much vertical offset at this location. The Missourian and Virgilian units are cut by faults that splay off the Washita Valley Fault and appear to have a small normal sense of slip on them. Virgilian age units fill the small graben indicating timing of the normal faults. The Washita Valley Fault is therefore interpreted to have both dip-slip (normal) and strike-slip components.

The restoration and tectonic evolution of cross section A is shown in Figure 2.6. In the Early Mississippian the region was still relatively flat. Several normal faults have been interpreted in the basement as remnants of the Cambrian rifting. Brewer et al. (1983) has shown similar faults in his regional cross sections observed from deep seismic reflection data. By Late Mississippian post-Springer time, the Wichita Mountain Fault had become active with minor uplift and onlap of Springer units. Cooper (1995) observed Springer onlap in cross sections through the Criner Hills Uplift supporting initial uplift in the Late Mississippian. Several other workers (Tomlinson and McBee, 1959; Allen, 2000) also showed diagrammatic paleo-cross sections of post-Springer deposition with the Springer onlapping the Wichita Uplift in the southern Ardmore Basin. By the end of Springer deposition, an estimated 7,500 feet of offset had occurred along the Wichita Mountain Fault along this cross section.

Much of the Morrowan is eroded along this cross section therefore it has been restored to the Morrowan unconformity. By the end of the Morrowan, the offset on the Wichita Mountain Fault was close to 30,000 feet. The progressive increase in slip was largely accommodated by the forward propagation of several imbricate thrust faults rooting in the Springer detachment. A small amount of slip was likely transferred into the Carter-Knox structure during the Morrowan, both along the Springer and Arbuckle detachments. The observed basement normal fault acted as a buttress along the Arbuckle detachment resulting in the localization of the structure. Much of the pre-Pennsylvanian units were likely eroded off the uplift during this time and transferred into the Anadarko and Ardmore Basins.

Another 6,000 feet of offset occurred during the Atokan on the Wichita Mountain Fault along with continued slip along the Springer and Arbuckle detachments. Several thrust faults along the Springer detachment were reactivated while others became dormant. An additional 7,500 feet of slip occurred on the Wichita Mountain Fault during the Desmoinesian. Much of that slip was transferred along the Springer detachment into faulted-detachment folds near the future cut of the Washita Valley Fault and Carter-Knox structure. The southwest flank of the Carter-Knox structure was rotated along a flexural hinge in the basement due to sedimentary loading, resulting in thickening of growth units on this flank. By the end of the Virgilian, the Wichita Mountain Fault had close to 40,000 feet of offset. The evolving growth of this fault is captured by the onlap of the Morrowan, Atokan, Desmoinesian, and Missourian units.

The Virgilian units appear uncut by the Wichita Mountain Fault in this cross section, however they are cut by the Carter-Knox thrust fault. It's likely that any slip was transferred horizontally along the Springer detachment, and Arbuckle detachment, into the Carter-Knox structure during the Missourian through Virgilian resulting in continued growth of that structure.

The Virgilian units are cut by the Washita Valley Fault in the central part of the cross section. Much of the folding and thrust faulting across the Washita Valley Fault occurred prior to deposition of Missourian and Virgilian units which are relatively flat across this fault. However, both Missourian and Virgilian units are cut by the Washita Valley Fault, which is a steep to near-vertical fault with a small amount of normal displacement that is down to the south. This movement occurred late in the Pennsylvanian. Virgilian age movement on the Washita Valley Fault has also been documented in the Arbuckle Mountains to the east (Ham, 1950; Dunham, 1955; Carter, 1982; Allen, 2000). In summary, the NW-SE oriented structures maintained contractional deformation throughout their evolution. However, where the WNW-ESE oriented Washita Valley cuts this cross section, the structural style involved components of strike-slip and normal faulting, possibly related to changes in stress orientations. Restoration of the cross section shows that it has been shortened by 11.3 miles.

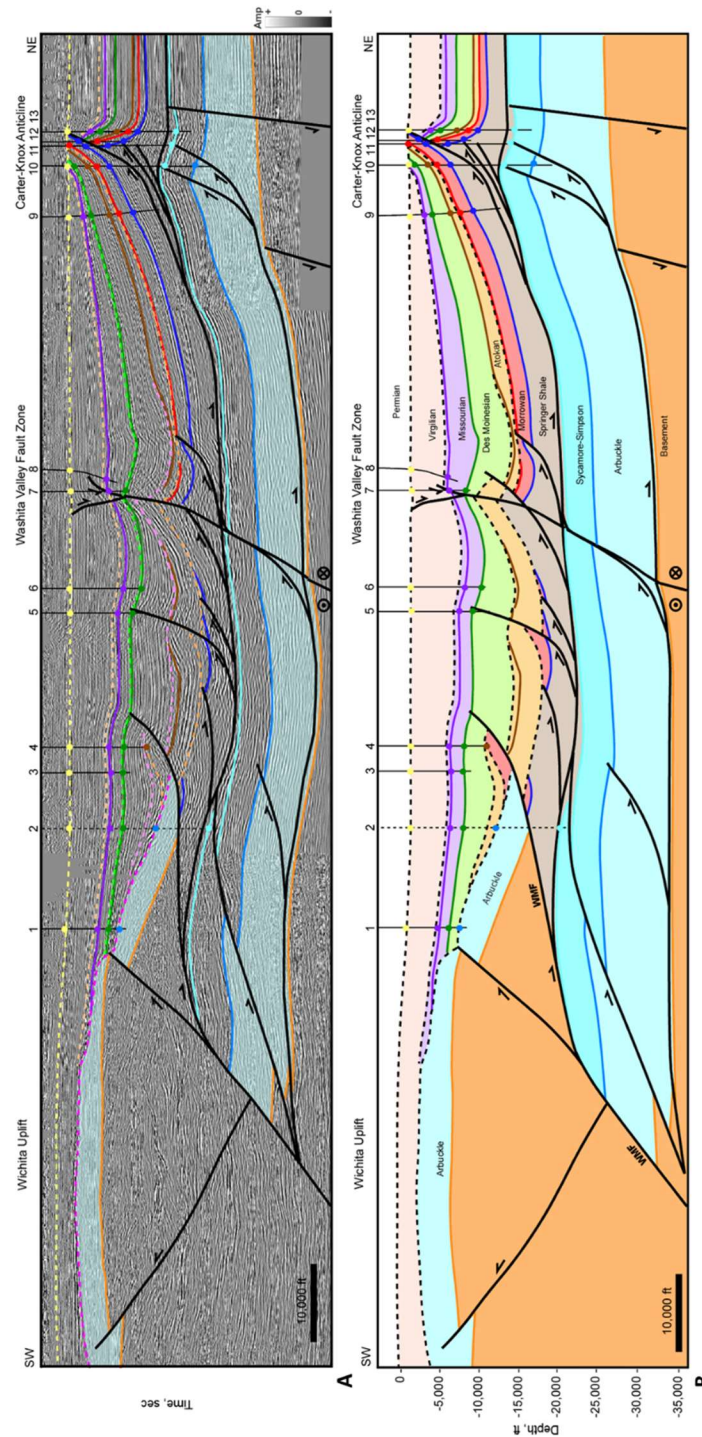


Figure 2.5 Regional cross section A. (A) Interpreted seismic section in time. Time scale has been removed for proprietary data. Horizon colors are shown in Figure 2.3. (B) Depth cross section. Well information is listed in appendix 1. Well tops (colored circles), dip data (brown check mark), and fault picks (red x) are shown where available. Dashed well is projected from 9 miles. Seismic Data Courtesy of Chesapeake Energy & SEI, Interpretation is that of Molly Turko.

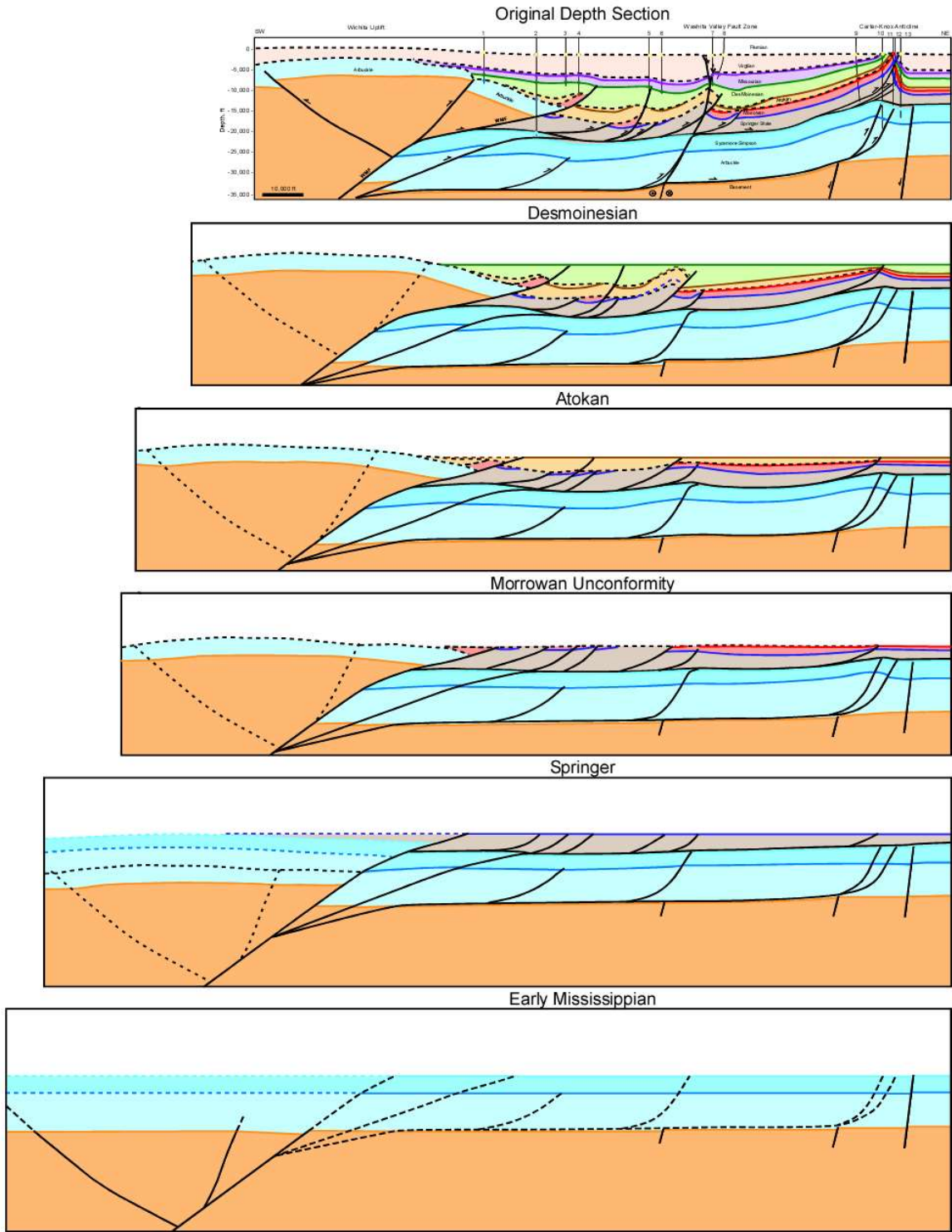


Figure 2.6 Restoration of cross section A. Evolution is discussed in the text.

7.2 Cross section B

Cross section B (Figure 2.7) is located six miles west of cross section A and illustrates some of the lateral changes in structure along trend of the Washita Valley Fault. In this section, the Wichita Uplift in the subsurface exhibits more relief so that the Arbuckle Group is almost completely eroded. In the previous section, the Missourian and Virgilian units were only gently folded over the tip of the Wichita Mountain Fault, but in this cross section those units are faulted, suggesting increasing offset on this fault towards the west. The two subthrust imbricates that flatten into the Arbuckle detachment have larger slip on this section, and eventually make up the Mountain View Fault system that uplifts the Slick Hills Block towards the west. The distance between the Wichita Mountain Fault and Washita Valley Fault has also decreased. As in the previous section, the Washita Valley Fault is a near vertical fault with a small amount of normal offset down to the south. Desmoinesian age units and older are all folded and faulted prior to being cut by the Washita Valley Fault, whereas the Missourian and Virgilian units are relatively flat, and show normal separation.

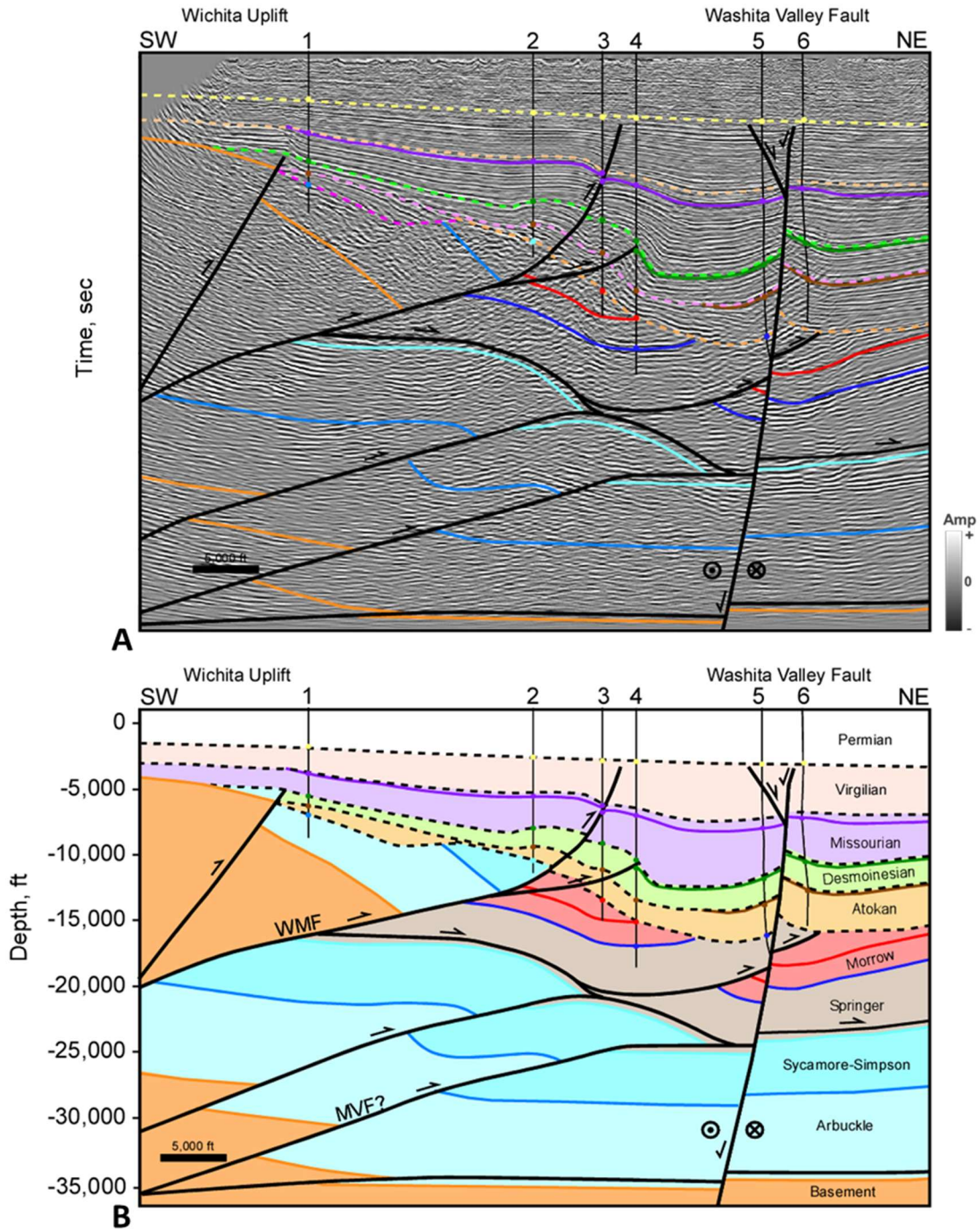


Figure 2.7 Cross section B. (A) Interpreted seismic section in time. Time scale has been removed for proprietary data. Horizon colors are shown in Figure 2.3. (B) Depth cross section. Well information is listed in appendix 1. Well tops (colored circles), dip data (brown check mark), and fault picks (red x) are shown where available. Seismic Data Courtesy of SEI, Interpretation is that of Molly Turko

7.3 Cross section C: Wichita Front (Slick Hills) - Cement

Cross section C (Figure 2.8) is a little over 20 miles to the northwest of cross section A. It covers a small part of both the Wichita Uplift and southeast Slick Hills Block before traversing the Cement Field in the Anadarko Basin. Much of the structure is similar to cross section A including detachments at the base of the Springer and the base of the Arbuckle that transfer slip into the basin from the Wichita Mountain Fault. The Wichita Mountain Fault, shown as two splays in this section, juxtaposes basement against the Permian Unconformity. Movement on the Mountain View Fault, and two other splays results in the exposure of the Slick Hills Block at the surface. This fault system has a tri-shear geometry (Erslev, 1991) and results in complex folding above the fault tips. These faults cut up through the Virgilian suggesting they were active until the Late Pennsylvanian.

The Cement Anticline is similar to the Carter-Knox Anticline where a deeper gentle faulted fold is overlain by a tight faulted-detachment fold. A major difference is that the Cement structure is cut by an E-W trending strike-slip/normal fault which roots into a pre-existing basement normal fault. This fault takes up at least part of the late-stage strike-slip/normal displacement, with the remaining displacement possibly transferred backwards along the Springer detachment. The normal faults that cut the top of the Cement structure contain Virgilian age syn-depositional fill suggesting that the normal/strike-slip fault system was active during the Virgilian.

An alternative interpretation is that the strike-slip faulting occurs above the Springer detachment (Figure 2.8C). This would suggest that displacement along the Springer detachment is initially transferred towards the north-northeast during much of the Pennsylvanian, but by the end of the Pennsylvanian the displacement direction becomes more east-northeast resulting in

oblique slip on the pre-existing thrust fault. In either case, the structure shows contractional deformation prior to the Missourian and oblique-slip along more E-W trending faults post-Missourian. This change in deformation style is possibly related to a rotation of the regional stress patterns, as will be discussed in a later section.

The Cement structure consists of two anticlinal structures making up the West Cement Field and the East Cement Field. To the east, it makes an abrupt bend to a more NW-SE trend forming the Chickasha structure, and hence the Chickasha Field. Figure 2.9A shows a structure map of the Missourian age Hoxbar Formation over the Cement-Chickasha trend. This structure map was constructed using a 3D seismic survey and was then converted to depth and tested against well data. Figure 2.9B shows a shallow time slice extending over the Cement-Chickasha structure. The purple trace is where the Hoxbar cuts the time slice.

A cross section through the Chickasha structure (Figure 2.10) shows that it is similar to both the Carter-Knox and Cement structures with a deeper gentle faulted fold overlain by an open faulted-detachment fold. In this cross section, the deeper fold is cut by a southwest verging thrust fault that soles out onto the Arbuckle detachment, whereas the shallow structure is cut by a thrust fault that soles out onto the Springer detachment. The normal and strike-slip faults that cut the Cement structure do not cut the Chickasha structure, but they do extend to the east of the anticlinal Cement structure as shown in the Hoxbar structure map (Figure 2.9A) and marked by the blue arrows on the time slice (Figure 2.9B). Cross sections 2 and 3 (Figure 2.11) show the architecture of the normal and strike-slip fault network that extends to the east beyond the anticlinal Cement structure. Cross section 2 shows two basement normal faults, one that is down to the south, and one that is down to the north. The basement fault that is down to the south is likely the same down-to-the-south normal fault observed in cross section C. However, this fault

likely dies out towards the east while the second normal fault, that is down-to-the-north, picks up displacement towards the east but does not extend very far towards the west. This second normal fault is observed on cross section 3 where it cuts the full stratigraphic section. The fault terminates within Virgilian sediments, establishing that it developed during the Virgilian. Cross sections 2 and 3 validate that the normal/strike-slip faulting event occurred late in the Pennsylvanian.

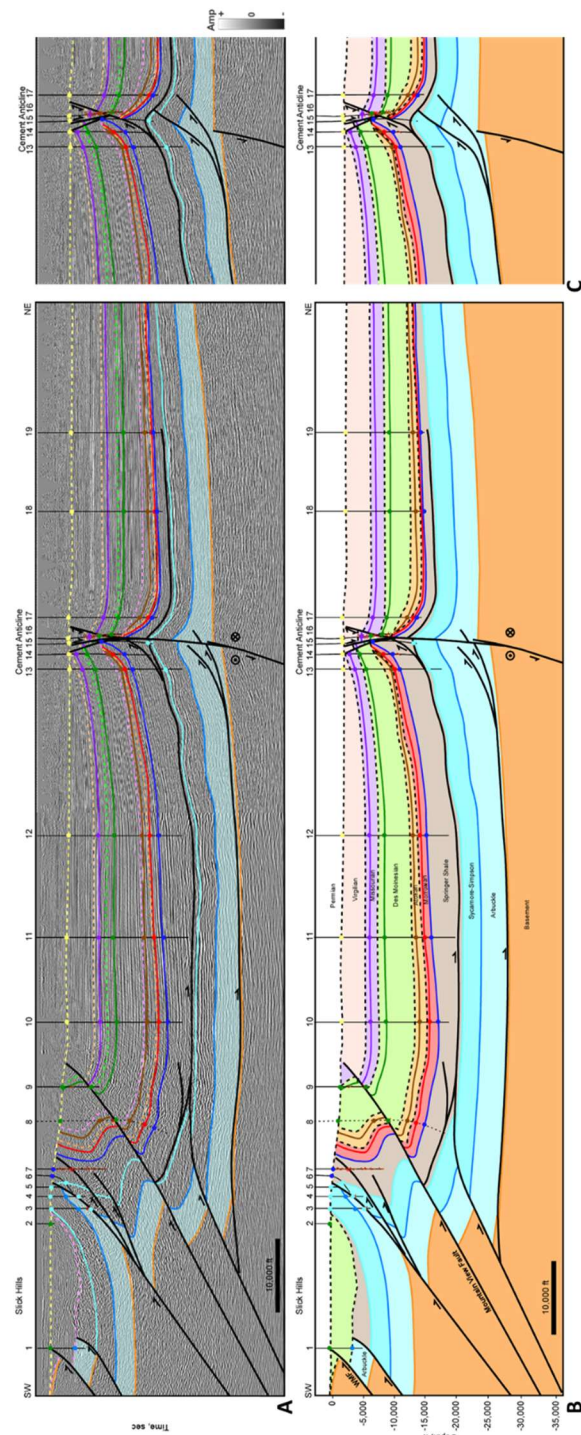


Figure 2.8 Cross section C. (A) Interpreted seismic section in time. Time scale has been removed for proprietary data. Horizon colors are shown in Figure 2.3. (B) Depth cross section. (C) Alternative interpretation of the Cement structure. Well information is listed in appendix 1. Well tops (colored circles), dip data (brown check mark), and fault picks (red x) are shown where available. Seismic Data Courtesy of SEI & Seitel, Interpretation is that of Molly Turko.

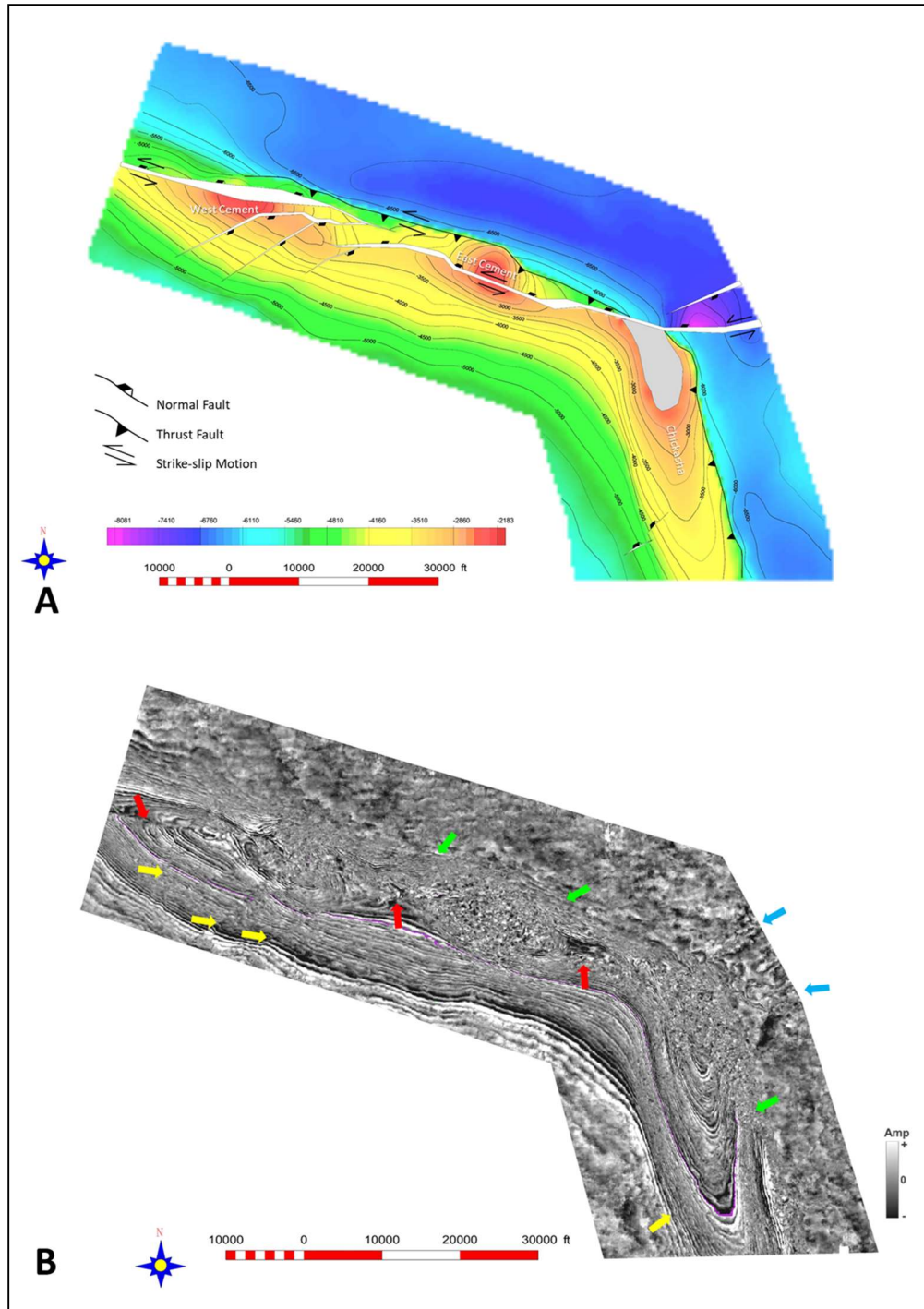


Figure 2.9 (A) Missourian age Hoxbar subsea structure map over the Cement-Chickasha structure. Contour interval is 500 feet. Part of the Hoxbar is eroded on the Chickasha structure in gray. (B) Shallow time slice over the Cement-Chickasha trend. Green arrows indicate the main thrust fault cutting the slice. Yellow arrows indicate normal faults oriented NE-SW. Red arrows show where the Cement normal/strike-slip fault cuts the slice. Blue arrows show the continuation of that fault trend east of the main structure. Seismic data courtesy of Chesapeake Energy.

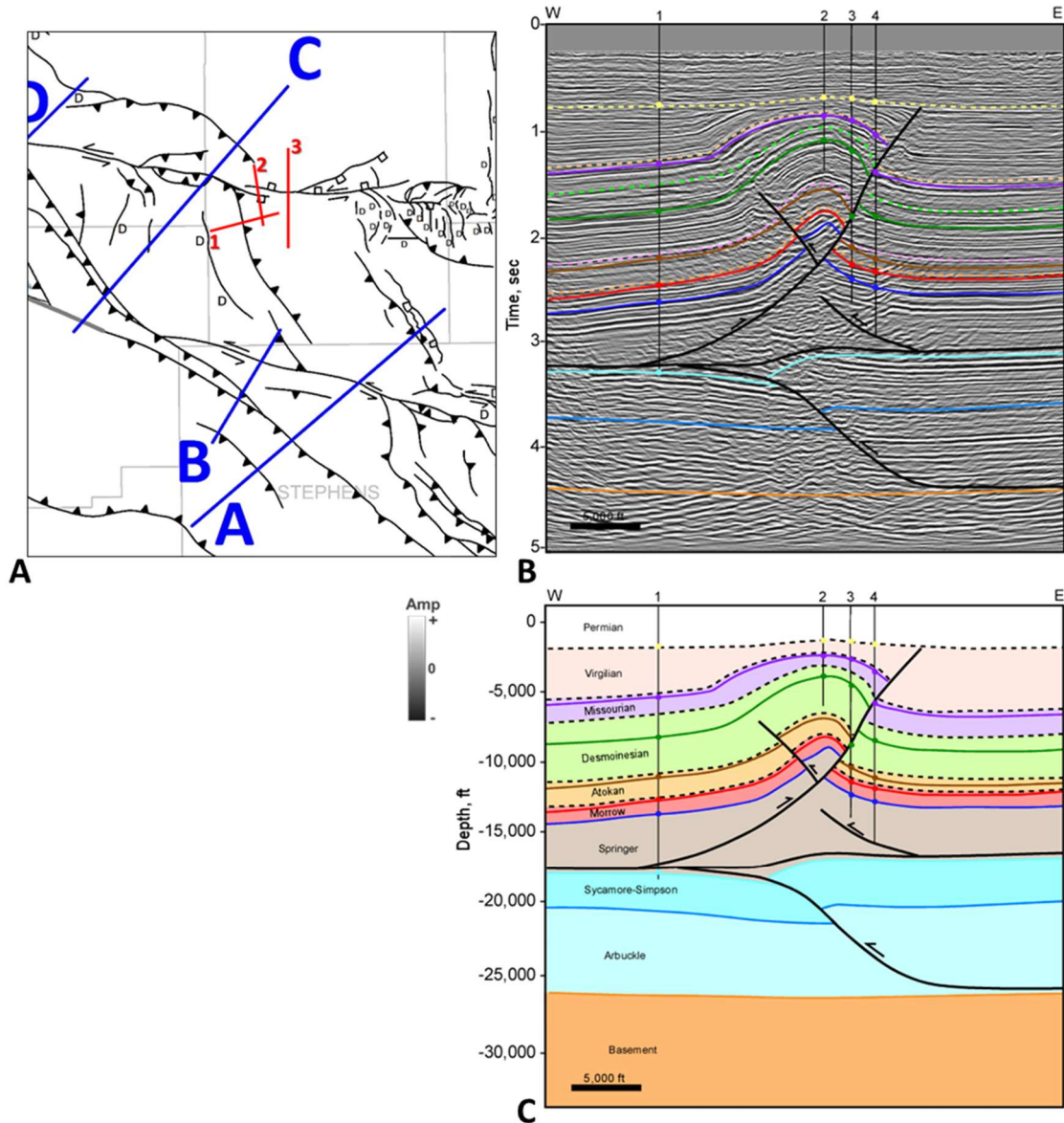


Figure 2.10 Cross section 1. (A) Location map of Cement-Chickasha cross sections (B) Interpreted seismic section in time. Horizon colors are shown in Figure 2.3. (C) Depth cross section. Well information is listed in appendix 1. Well tops (colored circles), dip data (brown check mark), and fault picks (red x) are shown where available. Seismic Data Courtesy of CHK, Interpretation is that of Molly Turko

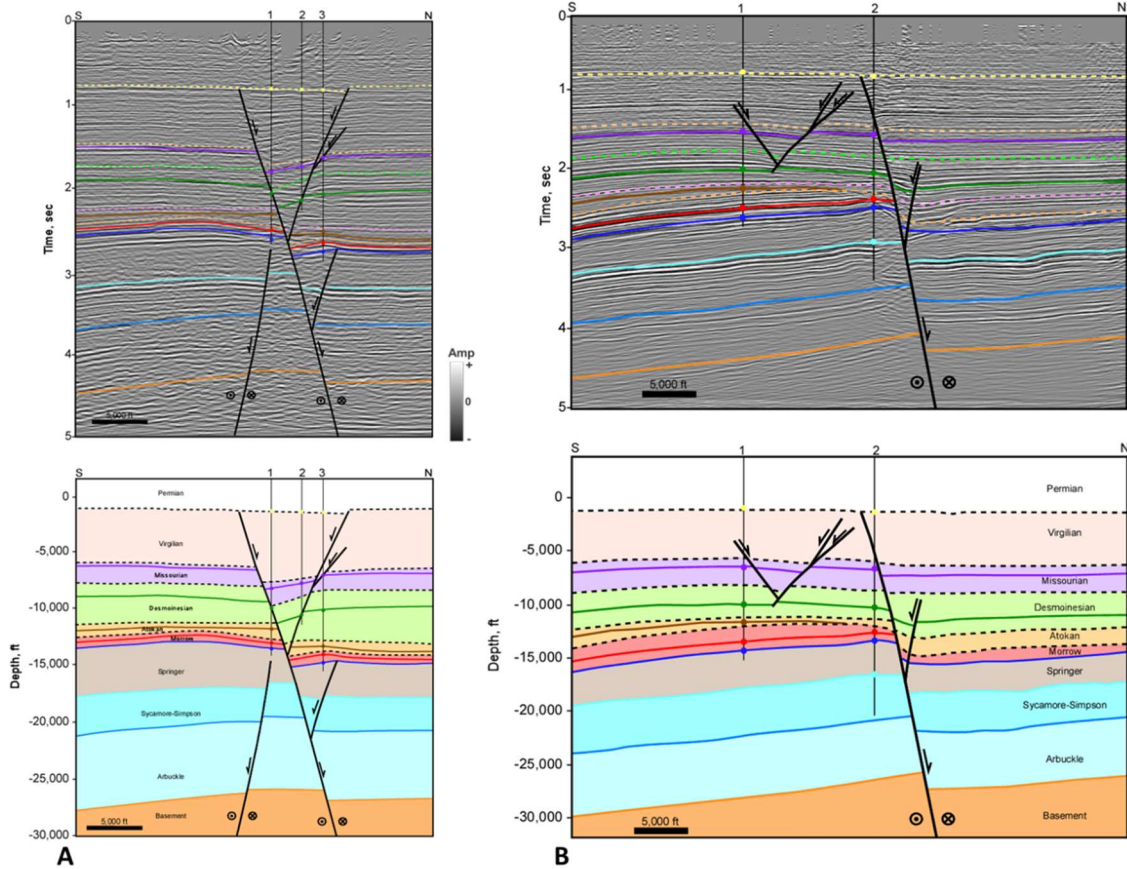


Figure 2.11. (A) Cross section 2 interpreted seismic section in time and depth. (B) Cross section 3 interpreted seismic section in time and depth. Horizon colors are shown in Figure 2.3. Well information is listed in appendix 1. Well tops (colored circles), dip data (brown check mark), and fault picks (red x) are shown where available. Locations shown in Figure 2.10A . Seismic Data Courtesy of CHK, Interpretation is that of Molly Turko

Figure 2.12 shows the palinspastic restoration of regional cross section C and illustrates the timing of events. During the Early Mississippian, the pre-Pennsylvanian stratigraphy is assumed to be relatively flat, with some basement normal faulting representing older rift faults. These normal faults were also interpreted in the restoration of cross section A. Just as in cross section A, the Springer is shown to onlap the Wichita Uplift as it has experienced a small amount of uplift during this time. Observations in well log data have shown that Springer facies change from clay-rich shale (deeper water) out in the basin, to a carbonate-rich facies on the Wichita Uplift where it is formally known as the Chester Limestone (McConnel, 1987; Saxon, 1998). This facies change validates that the Wichita Uplift likely initiated in the Late Mississippian. Slip along the Wichita Mountain Fault is estimated to be around 5,000 feet with an additional 2,500 feet on a secondary thrust or imbricate by Late Mississippian. These estimations were based off the restorations from cross section A where the top of basement was not affected by erosion.

The top of the Morrowan is relatively conformable with the Atokan, therefore the next stage in the restoration is the top of the Atokan unconformity. At this stage the Wichita Uplift and Slick Hills Block continued to grow, which also allowed slip to be transferred into the basin along the Springer and Arbuckle detachments resulting in early folding and faulting at the Cement structure.

The Slick Hills and Cement structures continued to develop through the Desmoinesian and Missourian. Desmoinesian age erosional unconformities are interpreted to cut the Wichita Uplift and southern part of the Slick Hills Block. A tri-shear geometry of the basement-rooted thrust faults allowed for intense folding and stretching of the deeper carbonate units in the Slick Hills. Basement offset along the three thrust faults that core the Slick Hills ranges from 6,500 to 7,000 feet each. The Cement structure continued to grow into the Early Virgilian as evident by

onlapping of the Virgilian units. At the Cement structure, offset of the Springer horizon is approximately 3,800 feet while offset of the Missourian is 2,900 feet indicating the progressive growth. The final cross section shows that the Cement Structure was cut by a strike-slip fault caused by reactivation of the pre-existing basement-rooted normal fault. This fault was reactivated by left-lateral shear with a component of dip-slip (normal) resulting in fault offsets of about 1,000 feet that cut the crest of the Cement structure. Virgilian age syn-depositional sediments filled the accommodation space along these normal faults indicating the timing of strike-slip movement. As mentioned previously, an alternative solution is that the strike-slip faulting occurred along the Springer detachment (Figure 2.8C), and that displacement due to normal faulting was transferred back along this pre-existing detachment. Shortening in this cross section is estimated to be 8.5 miles.

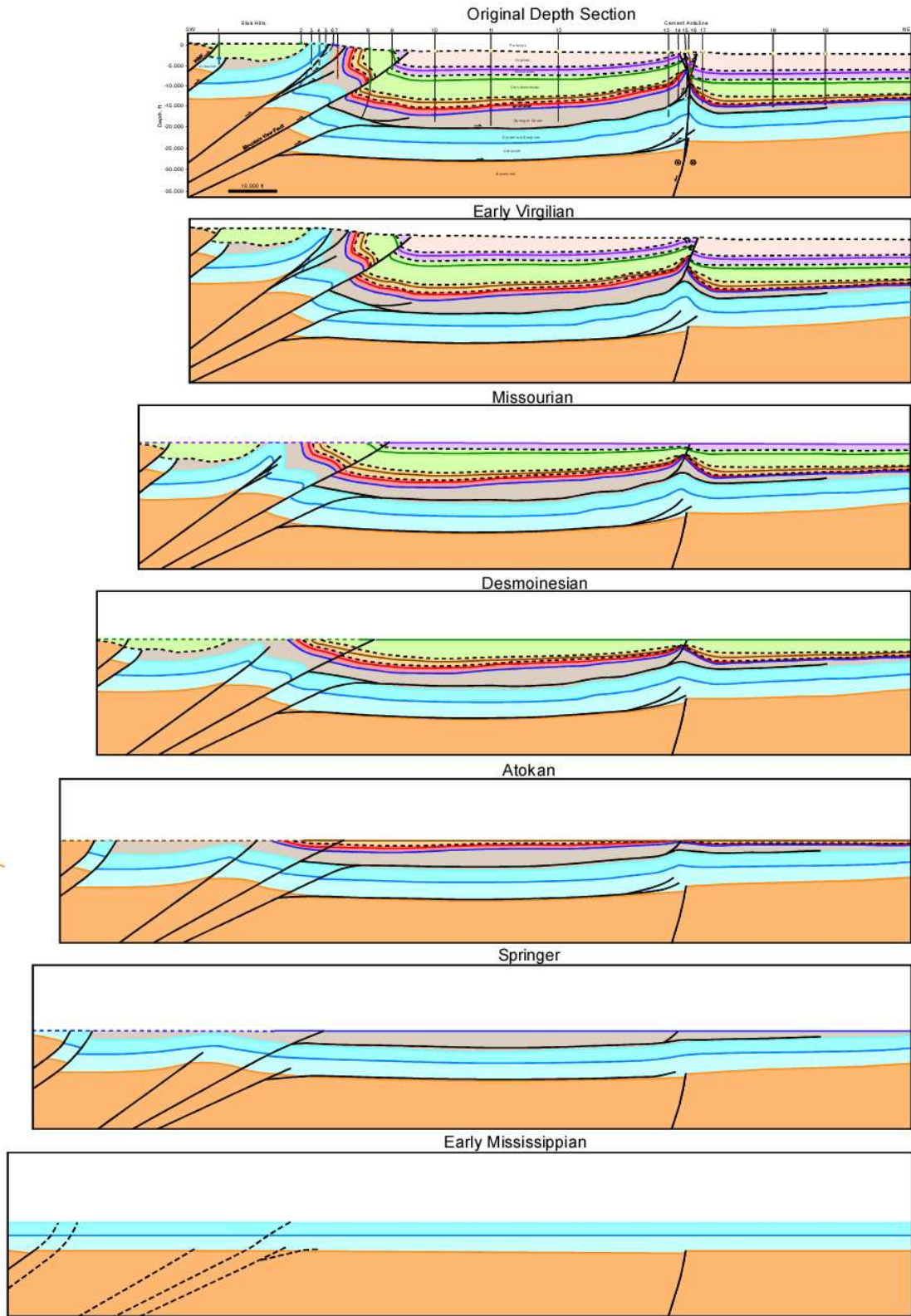


Figure 2.12 Restoration of cross section C. Evolution is discussed in the text.

7.4 Cross sections D and E: Slick Hills

Cross sections D (Figure 2.13) and E (Figure 2.14) both extend over the Slick Hills Block, where the Arbuckle Group is exposed at the surface. The Mountain View Fault system is responsible for bringing up this block along with the Alden Fault, which could simply be a forward imbricate off the Mountain View Fault system. Folding and faulting along these two fault systems are responsible for creating anticlinal structures representing historical oil fields including Fort Sill, Apache, Alden, and Carnegie along the northern boundary of the Slick Hills block. The Blue Creek Canyon Fault is interpreted as a backthrust off the Alden Fault. This fault is exposed near the southeast end of the Slick Hills where it brings the Carlton Rhyolite to the surface. Cecil-Jones (1995) observed folding in the Carlton Rhyolite and suggested it was not too rigid to fold. She described this fold as open, asymmetric, and plunging to the north. The Blue Creek Canyon Fault can be traced throughout the Slick Hills Block by studying the high-resolution aeromagnetic data (Figure 2.2). The crest of the anticline along the Blue Creek Canyon Fault shows up as a magnetic high trending NW-SE. It is unknown if the Blue Creek Canyon Fault is a single fault or made up of multiple splays. McConnell (1987) suggested that a single fault branches into multiple traces towards the northwest.

A second, and deeper, backthrust fault is interpreted to extend from the Alden Fault. This fault was discovered when the Kimbell Ranch 32-1 well was drilled in 2007 and cut a reverse fault in the basement repeating the Arbuckle, Reagan, and Basement sections (Cullen, 2019). Cullen (2016 & 2019) made a similar interpretation over the Slick Hills Block utilizing data from this key well.

Cross section E shows the cross-cutting relationship between the backthrust fault cut by the Kimbell Ranch 32-1 well and the Wichita Mountain Fault. It is interpreted that the Wichita

Mountain Fault cut this backthrust fault, as it was likely reactivated throughout the Pennsylvanian. Well number one on cross section E drilled through granite basement before entering subthrust Arbuckle, supporting the interpretation that the Wichita Mountain Fault would have cut the backthrust. Cross sections D and E illustrate the large-scale structures making up the core of the Slick Hills Block and show that low-angle basement-rooted thrust faults, the Mountain View and Alden Fault systems, are responsible for uplifting this prominent feature observed in surface geology and magnetic data.

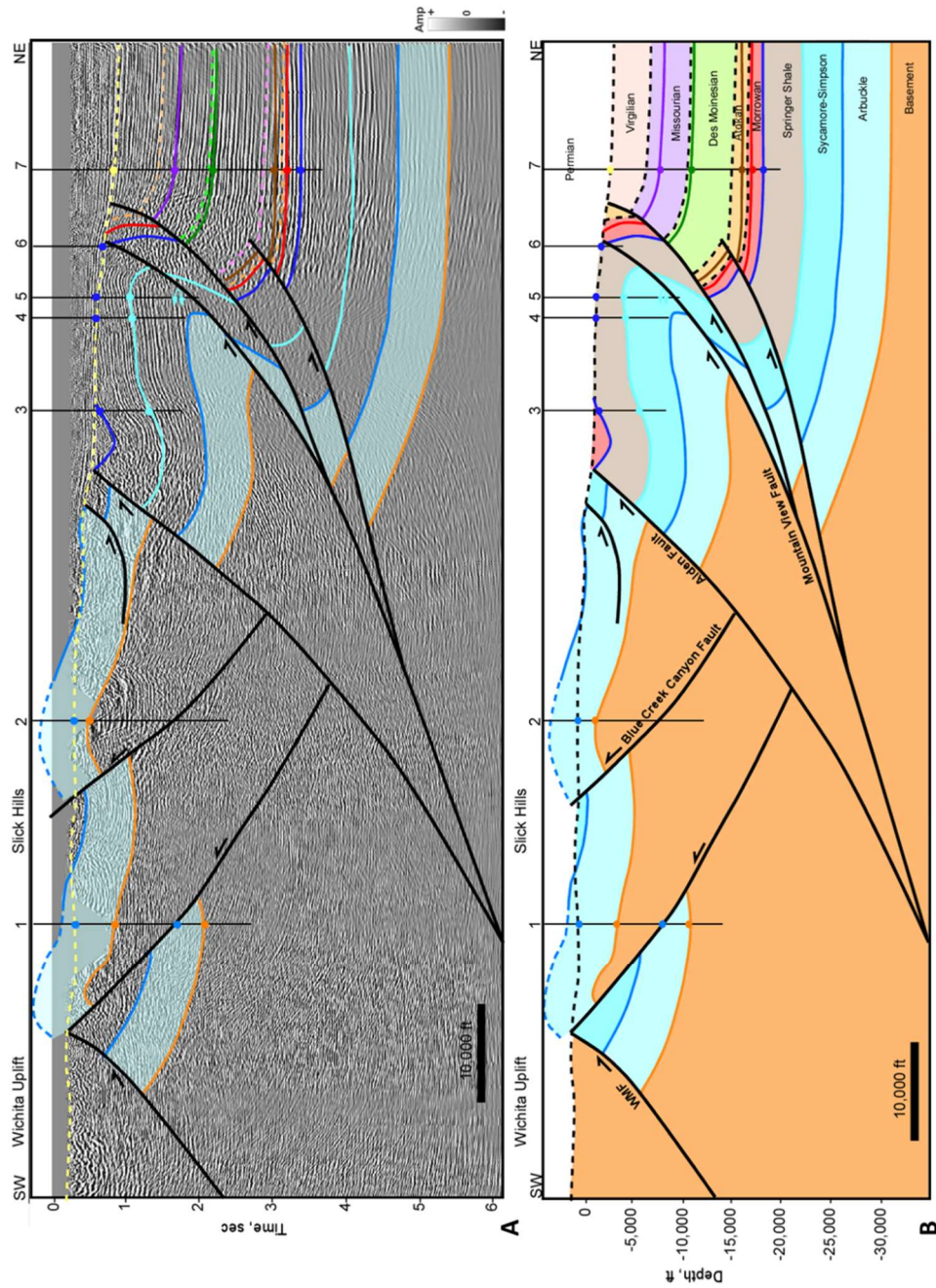


Figure 2.13 Cross section D. (A) Interpreted seismic section in time. Horizon colors are shown in Figure 2.3. (B) Depth cross section. Well #1 is the Kimbell Ranch 32-1 mentioned in the text, other well information is listed in appendix 1. Well tops (colored circles), dip data (brown check mark), and fault picks (red x) are shown where available. Seismic Data Courtesy of MIDCON, Interpretation is that of Molly Turko.

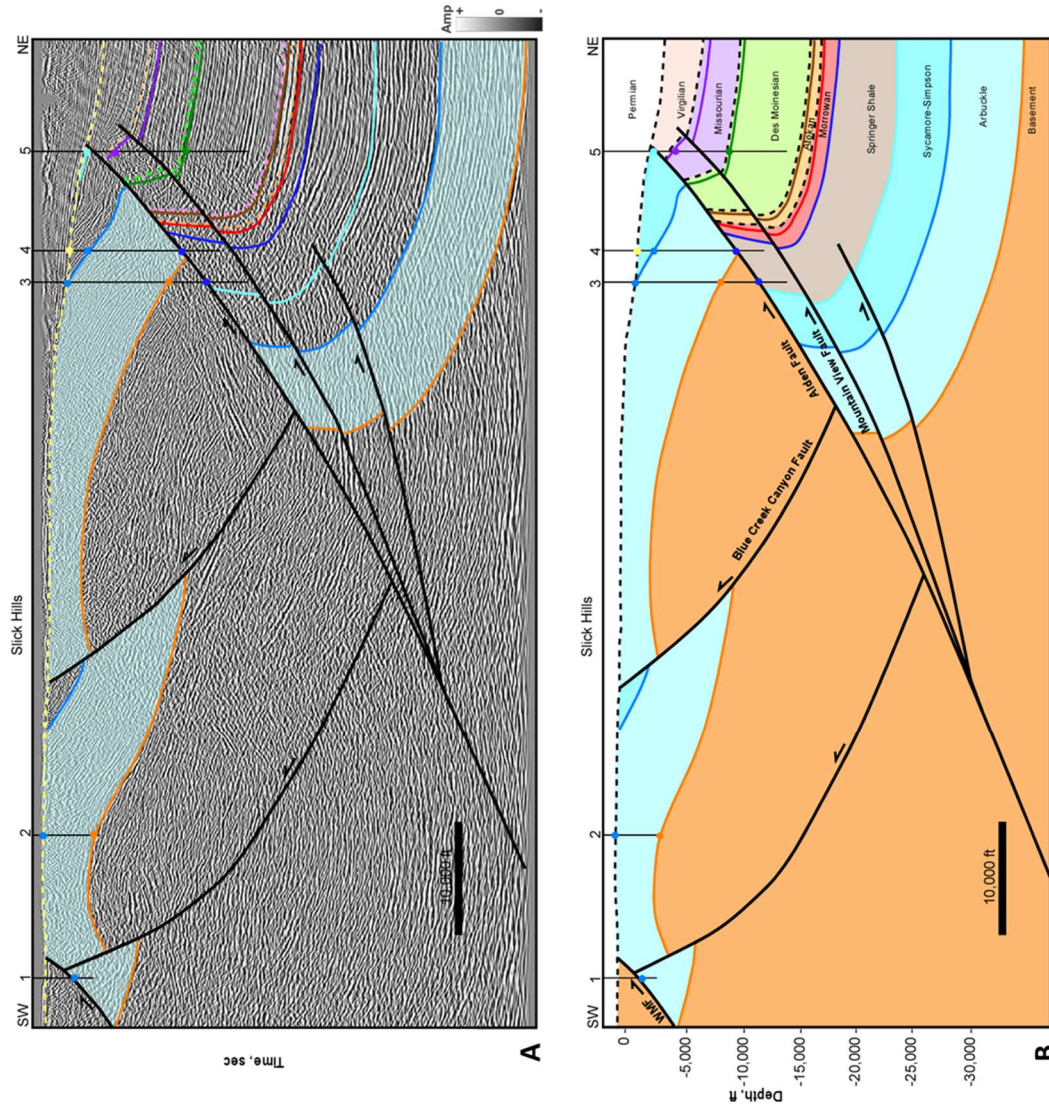


Figure 2.14 Cross section E. (A) Interpreted seismic section in time. Time scale has been removed for proprietary data. Horizon colors are shown in Figure 2.3. (B) Depth cross section. Well information is listed in appendix 1. Well tops (colored circles), dip data (brown check mark), and fault picks (red x) are shown where available. Seismic Data Courtesy of SEI, Interpretation is that of Molly Turko

7.5 Cross section F: Western Wichita Front

Cross section F (Figure 2.15) extends over the frontal part of the Wichita Uplift in western Oklahoma. Along this trend of the Wichita Uplift is where the Wichita Mountain Fault and Mountain View Fault systems merge to represent a tri-shear geometry along the frontal part of the uplift. The Wichita Mountain Fault is labeled as the southernmost fault and the Mountain View Fault is the main fault responsible for the Sentinel Anticline in cross section F. Sentinel Anticline is an overturned fold cut by multiple thrust faults. An out-of-syncline fold accommodation fault (Mitra, 2002) extends from the core of the footwall syncline. This anticline is truncated by the unconformity at the base of the Desmoinesian that onlaps the Wichita Uplift. The Missourian and Virgilian units both onlap the uplift, but then become cut by the Wichita Mountain Fault system showing late reactivation of that fault system.

Both the Springer detachment and Arbuckle detachment are observed in the basin extending into the northwest end of the Burns Flat anticline. The Burns Flat structure is similar to the Carter-Knox and Cement structures, except that it is associated with much less shortening above the Springer detachment along this section. It consists of a shallow faulted fold detaching along the base of the Springer that is cored by a deeper faulted fold that detaches at the base of the Arbuckle. This fault is also underlain by a basement-rooted normal fault that is likely a remnant of earlier rifting and controlled the location of this structure. Thickening of Early Pennsylvanian units are observed from the shelf margin into the basin showing the relationship between basin subsidence and the Wichita Uplift.

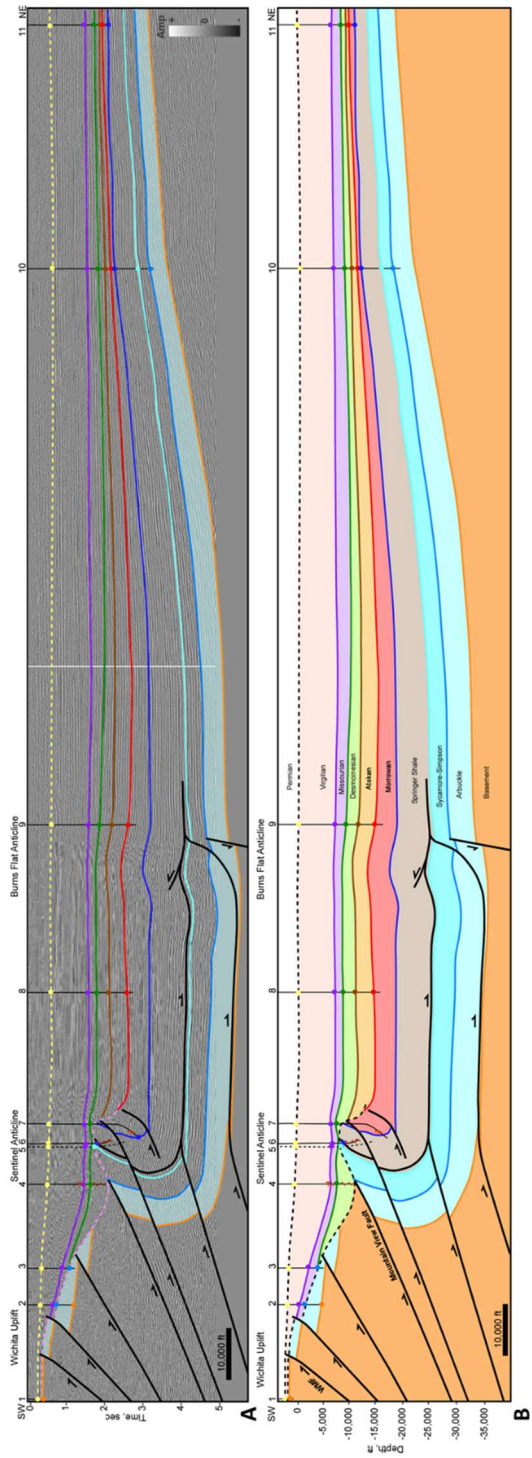


Figure 2.15 Cross section F. (A) Interpreted seismic section in time. Horizon colors are shown in Figure 2.3. (B) Depth cross section. Well information is listed in appendix 1. Well tops (colored circles), dip data (brown check mark), and fault picks (red x) are shown where available. Seismic Data Courtesy of Seitel, Interpretation is that of Molly Turko.

7.6 Cross section G, H, and I: Southern Wichita Uplift

Cross sections G, H, and I extend over the southern part of the Wichita Uplift into the Hollis-Hardeman Basin (Figures 2.16, 2.17, and 2.18). This region is characterized by high angle northeast-dipping reverse faults with small amounts of offset compared to the northern Wichita Uplift. In all cross sections, a significant unconformity exists cutting down into part of the Arbuckle Group. In cross section G, Virgilian units directly overlie the Arbuckle Group. The Virgilian is not cut by most of the high angle reverse faults, however they do appear to be cut by the Willow Fault. The Willow Fault is interpreted to be a near vertical left-lateral strike-slip fault, similar to what was interpreted by Chase (2019). Vertical offset on this fault is approximately 1,600 feet based on basement penetrations in wells 3 and 4, however this offset could be larger, considering that the top of basement is an erosional unconformity.

In cross section H, Desmoinesian units were deposited on top of the Arbuckle and onlap the Wichita Uplift along with Missourian and Virgilian units. The Burch Thrust Fault in the central part of the cross section does not cut through the unconformity at the base of the Desmoinesian, however faults closer to the core of the Wichita Uplift do cut higher in section, including the Virgilian, suggesting Late Pennsylvanian movement on that fault system. Some small normal faults were observed in the basin and are part of an en echelon fault system shown on the Oklahoma Fault Map from Marsh and Holland (2015).

Cross section I is similar to cross section H. High angle basement-rooted reverse faults cut through the Arbuckle but do not cut through the unconformity at the base of the Desmoinesian. Desmoinesian, Missourian, and Virgilian units all onlap the Wichita Uplift and are gently folded. At this location, the fault closest to the core of the Wichita Uplift, the Waurika-Muenster Fault, does not appear to cut the Virgilian. The unnamed fault between the

North Fork and Waurika-Muenster Faults appears to have a small amount of normal offset near the tip. This could indicate that these high angle reverse faults are slightly inverted rift faults, and that a small amount of normal faulting has been preserved on that fault. The reverse faults along the southern side of the Wichita Uplift dip approximately 60° , supporting the hypothesis that these faults are inverted normal faults.

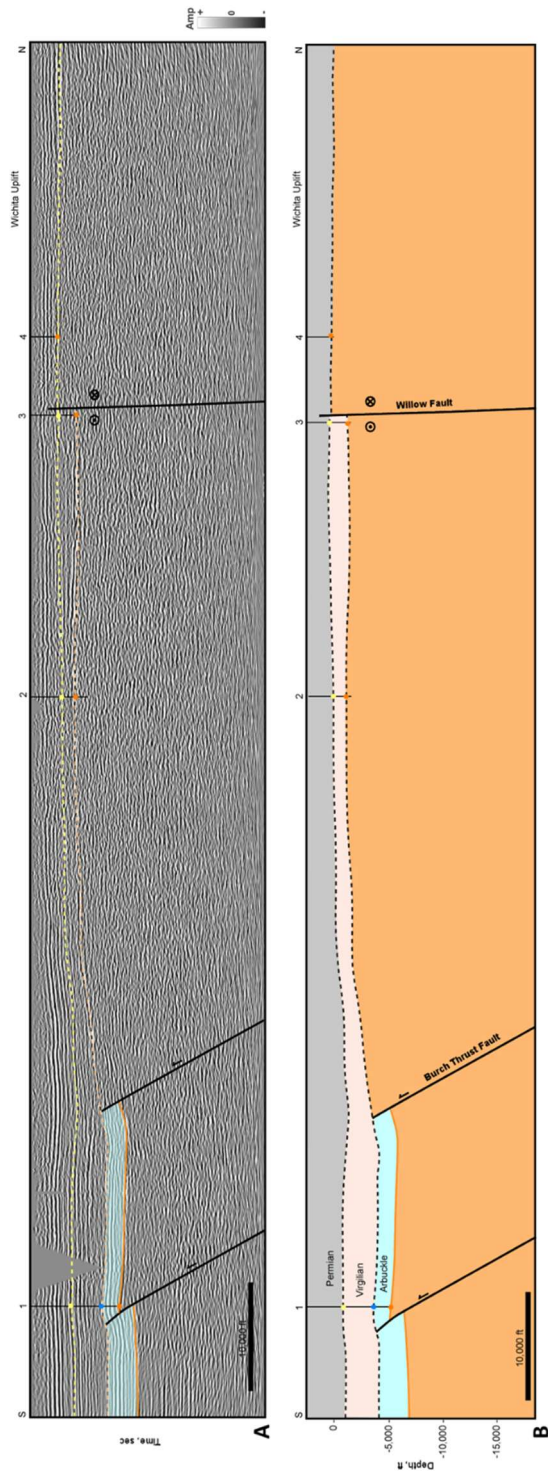


Figure 2.16 Cross section G. (A) Interpreted seismic section in time. Time scale has been removed for proprietary data. Horizon colors are shown in Figure 2.3. (B) Depth cross section. Well information is listed in appendix 1. Well tops (colored circles), dip data (brown check mark), and fault picks (red x) are shown where available. Seismic Data Courtesy of SEI, Interpretation is that of Molly Turko.

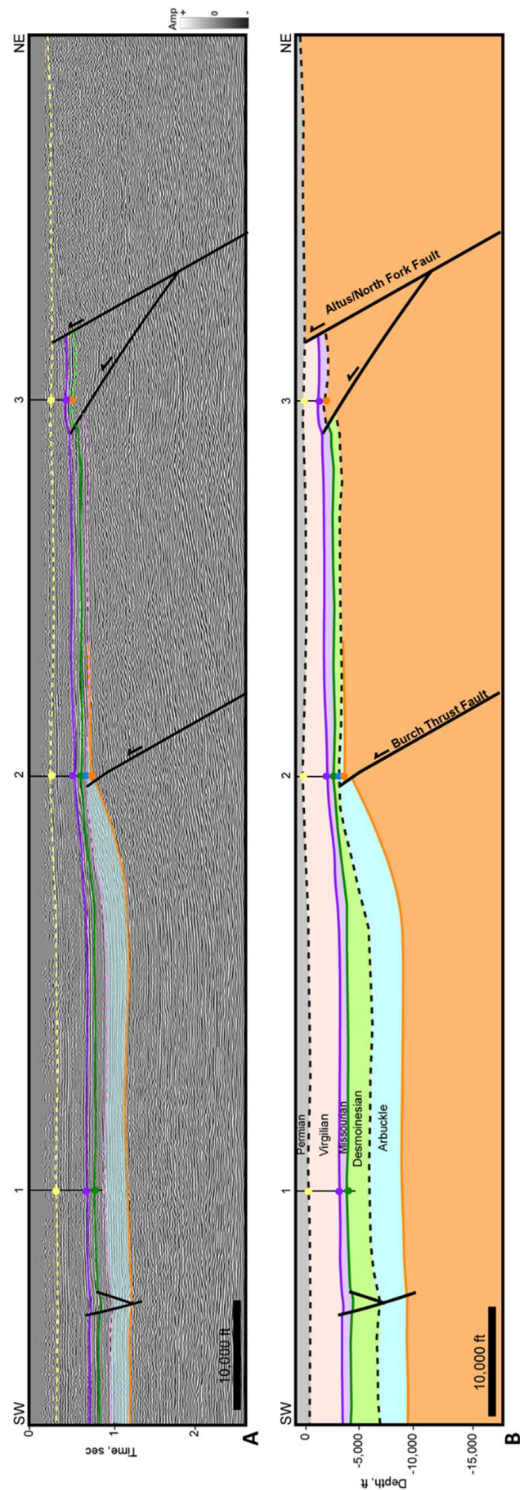


Figure 2.17 Cross section H. (A) Interpreted seismic section in time. Horizon colors are shown in Figure 2.3. (B) Depth cross section. Well information is listed in appendix 1. Well tops (colored circles), dip data (brown check mark), and fault picks (red x) are shown where available. Seismic Data Courtesy of MIDCON, Interpretation is that of Molly Turko.

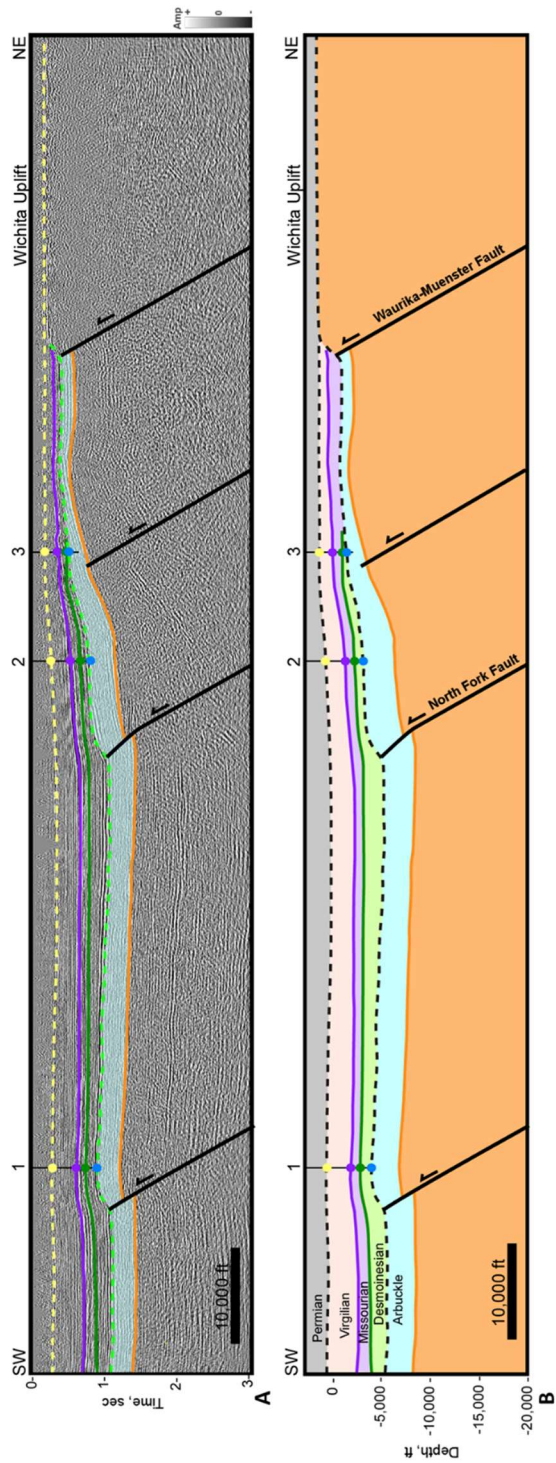


Figure 2.18 Cross section I. (A) Interpreted seismic section in time. Horizon colors are shown in Figure 2.3. (B) Depth cross section. Well information is listed in appendix 1. Well tops (colored circles), dip data (brown check mark), and fault picks (red x) are shown where available. Seismic Data Courtesy of MIDCON, Interpretation is that of Molly Turko.

8. Discussion

The southern part of the Wichita Uplift is characterized by high-angle reverse faults with small offsets whereas faults along the northern boundary are at a lower angle with large amounts of displacement. A detachment at the base of the Springer Shale transfers slip from the Wichita Uplift into the Anadarko Basin resulting in large faulted-detachment folds. These faulted-detachment folds are cored by more gentle folds cut by faults that sole into a detachment at the base of the Arbuckle Group. These structures form above basement-rooted normal faults that are likely a remnant of earlier rifting. The orientation and location of these pre-existing normal faults impacted the Pennsylvanian age structures.

The Wichita Uplift, along with most of the structures that developed in the basin, are oriented primarily NW-SE, although, several fault trends are oriented closer to WNW-ESE including the Washita Valley, Cement, and Willow Fault trends. In all the cross sections, strong contractional deformation was observed during the Morrowan and Atokan regardless of orientation. This contraction continued into the Desmoinesian and Missourian but is more apparent on structures oriented NW-SE and less apparent on WNW-ESE structures. During the Virgilian, NW-SE oriented structures, such as Carter-Knox and Chickasha, continued to undergo contractional deformation while the WNW-ESE faults, including Cement and the Washita Valley Fault, underwent strike-slip deformation with a component of normal slip. Additional cross sections across the Washita Valley Fault are shown in Appendix 2 illustrating the fault architecture and late timing of the strike-slip faulting.

The changes in structural styles, based on the age and orientation of structures, are indicative of a progressive rotation in the maximum horizontal stress direction. Maximum horizontal stress was oriented approximately NE-SW in the Early Pennsylvanian but rotated to

ENE-WSW by the Late Pennsylvanian. Early contractional deformation with a NE-SW maximum horizontal stress orientation, resulted in WNW-ESE and NW-SE contractional structures. However, rotation to a ENE-WSW maximum horizontal stress direction, resulted in partitioning of strain into contractional deformation on the NW-SE structures, and strike-slip deformation on the WNW-ESE faults, accompanied by normal faulting.

Several authors have shown that the angle of convergence to pre-existing structures will determine the degree of strike-slip versus compression (Richard and Krantz, 1991; Casas et al., 2001). The angle of convergence is the angle between the maximum horizontal stress direction and the orientation of a pre-existing structure, i.e. a fault plane, as seen in Figure 2.19 (Sanderson and Marchini, 1984; Tikoff and Teyssier, 1994; Dewey et al., 1998; Casas et al., 2001). Casas et al (2001) showed that convergence angles less than 15° reactivate pre-existing faults dominantly by strike-slip, but when the convergence angle is greater than 30° the faults become reactivated dominantly by thrusting. When the convergence angle is between 15° and 30° , high angle reverse faults developed at depth while structures above the fault included Reidel shears and Y faults typical of strike-slip faults (Casas et al., 2001). These studies support the idea that a rotation in stress orientation could result in a change in style of deformation.

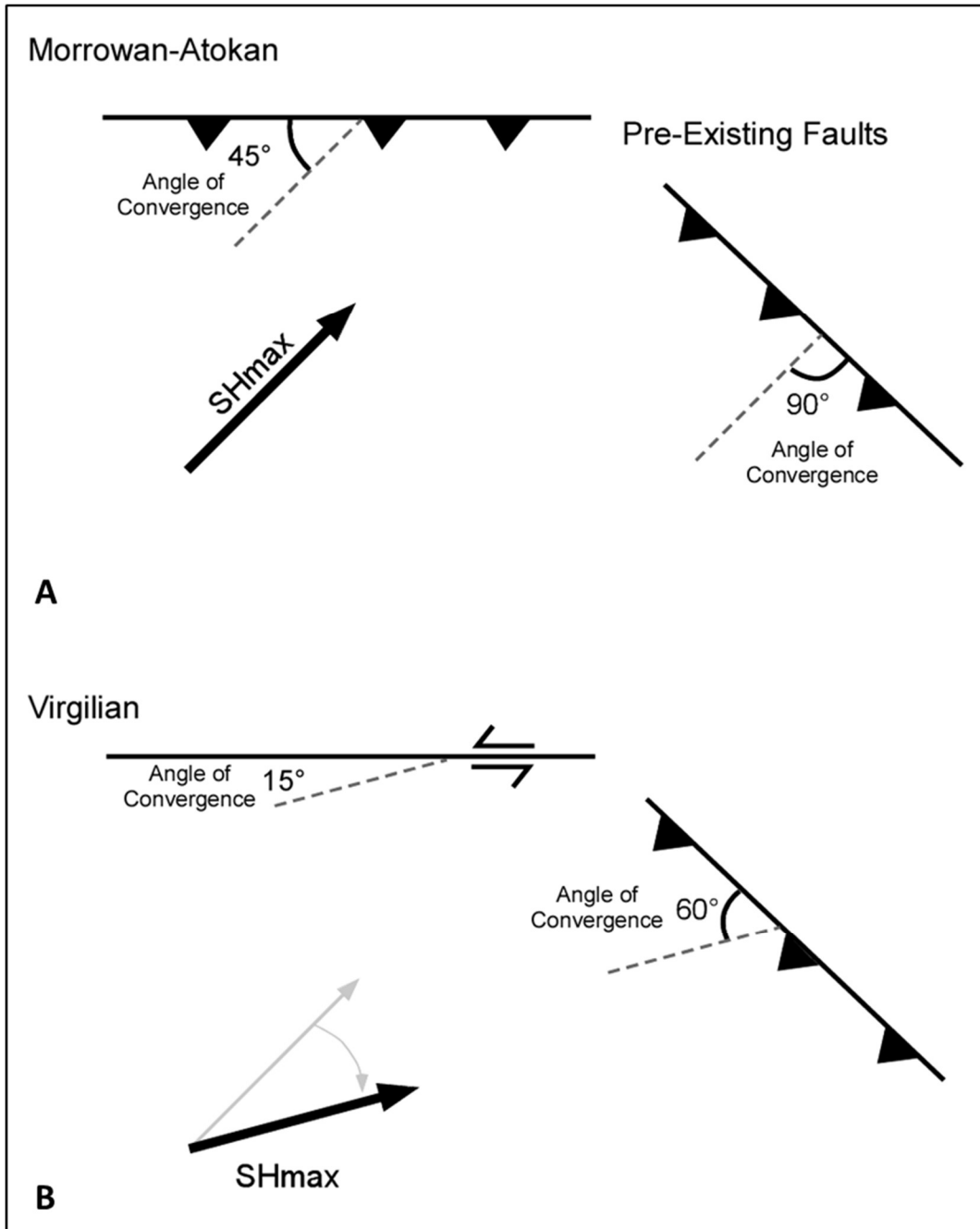


Figure 2.19 Diagram illustrating the structural styles that develop based on the angle between pre-existing faults and the angle of convergence. SH_{max} is the maximum horizontal stress orientation (A) Scenerio for Morrowan-Atokan, SH_{max} is $N45^\circ E$ and at high angles to pre-existing faults, thrust faulting occurs. (B) Scenerio for Virgilain, SH_{max} rotated to $N75^\circ E$, where the angle of convergence is high thrust faulting occurs, where it is low strike-slip faulting occurs.

A regional cross section and 3D block diagram illustrate the tectonic evolution of the central part of the Wichita Uplift and Anadarko Basin. Cross section J (Figure 2.20) extends over the southern Wichita Uplift and northward over the Slick Hills into the Anadarko Basin. Cross sections I and D were used to construct this cross section in its present form. The section was then restored to the Late Mississippian-Early Pennsylvanian where fault geometries are shown but without major reverse offset. The thickness of the Sycamore through Simpson is unknown so only the Arbuckle is shown over the Wichita Uplift for simplicity. The last step in the restoration was what the structures could have looked like at the end of the Cambrian into the Ordovician. The restorations suggest that normal faults representing an asymmetric failed rift were reactivated and/or influenced the localization and orientation of Pennsylvanian age structures.

The schematic block diagram in Figure 2.21A shows the orientation and location of probable rift faults based on observations in the seismic data. Faults in the block diagrams are shown at the basement level. Arrows in Figure 2.21A represent possible stress orientations for the development of the rift based on dikes trends documented in the Wichita Mountains by McLean and Stearns (1986) and Chase (2019). These dike trends show predominantly E-W and N-S orientations, which could indicate that the NW-SE oriented Wichita Uplift underwent oblique extension. Brune (2018) suggested that more than 70% of all rift segments exceeded an obliquity of 20° , therefore oblique extension of the Wichita trend is plausible and may have resulted in the sinusoidal-like fault trends. Figure 2.21B illustrates deformation at the end of the Atokan where many of the rift faults have been inverted through contraction or provided the buttress for the localization and orientation of the contractional structures in the basin. Inversion would have occurred while maximum horizontal stress was oriented approximately NE-SW.

The Nemaha Fault trend is oriented N-S and may have had a right-lateral sense of shear on it (Amsden, 1975; Budnik, 1986; McBee, 2003; Friess, 2005; Chopra et al., 2018).

Examination of seismic data over the Nemaha trend, shows that it was primarily active in the Morrowan and Atokan but became dormant post-Desmoinesian. If maximum horizontal stress was oriented NE-SW during the Morrowan and Atokan, then the N-S oriented Nemaha trend would be at an optimal orientation for right-lateral strike-slip movement. The rotation of the maximum horizontal stress to ENE-WSW by Late Pennsylvanian resulted in the fault becoming dormant at that time.

The structural geometry at the end of the Virgilian at the basement level is illustrated in Figure 2.21C. The maximum horizontal stress has rotated to ENE-WSW. This rotation caused a small amount of left-lateral shear to occur along the Wichita Uplift and the Anadarko Basin causing left-lateral strike-slip to develop along the WNW-ESE oriented Washita Valley and Cement Fault trends, while the NW-SE oriented structures continued to develop through contraction. Strike-slip movement is also evident in the Arbuckle Mountains where horizontal slickenlines have been observed along the Washita Valley Fault (Booth, 1982). The 3D block diagrams present a model representing the tectonic evolution of the region based on stress orientations and faulting at the basement level.

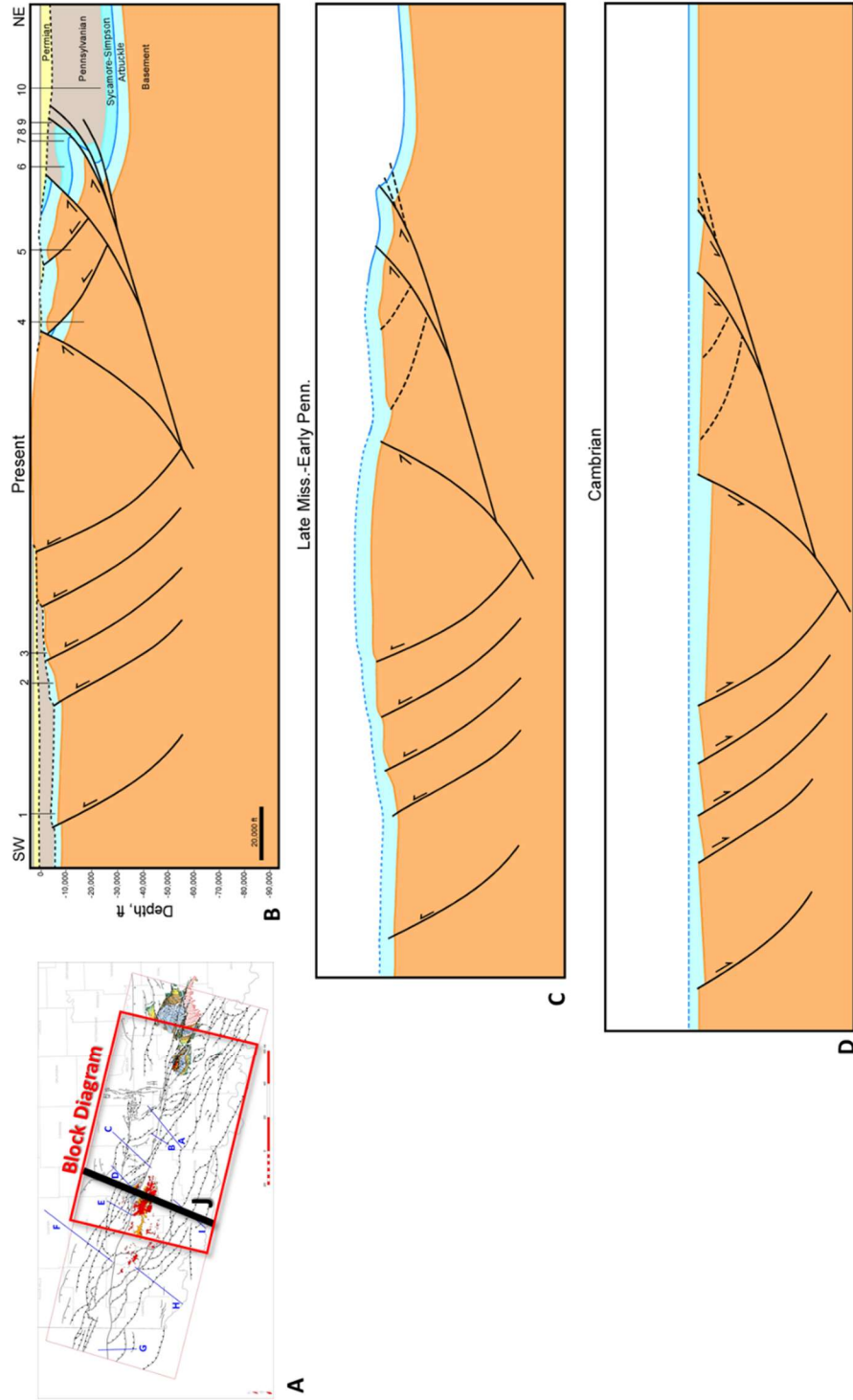


Figure 2.20 (A) Location map of regional cross section J and outline of the block diagram. (B) Cross section J, constructed using sections D and I (C) Restored to show early contraction in the Late Mississippian/Early Permian prior to major fault offset (D) Restored to the end of the Cambrian-Ordovician showing hypothetical rift fault geometry.

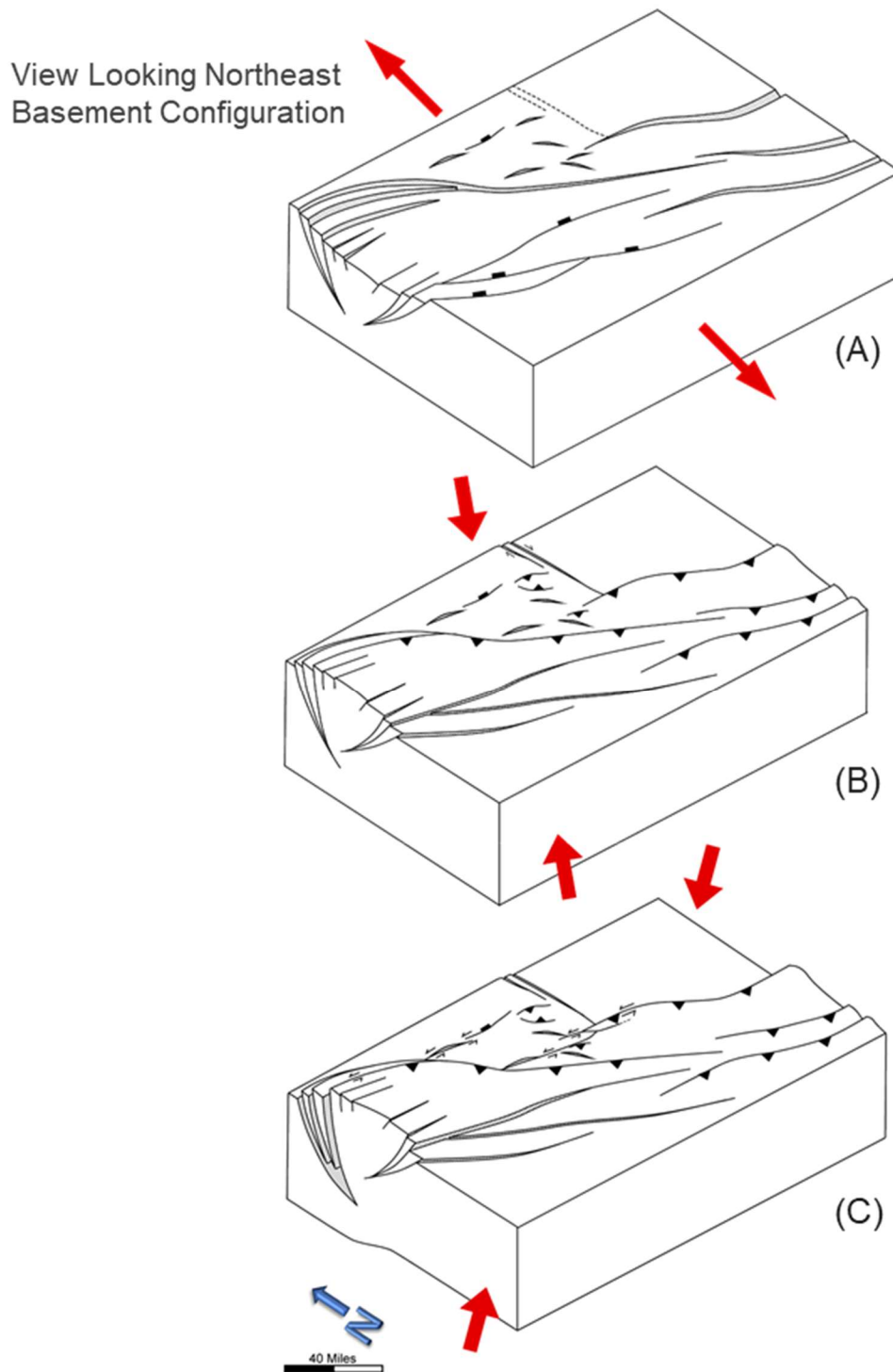


Figure 2.21 Schematic block diagram at the basement level. Red arrows represent stress orientations. (A) End of the rifting stage where extension was oriented N-S. (B) Contraction at the end of the Atokan, maximum horizontal stress is oriented NE-SW. (C) Contraction at the end of the Virgilian accompanied by strike-slip faulting along WNW-ESE faults, maximum horizontal stress has rotated to a ENE-WSW orientation.

9. Conclusions

A Precambrian-Cambrian failed rift laid the foundation for later Pennsylvanian age structures. Basement-rooted normal faults were either reactivated or controlled the location of Pennsylvanian age structures. These basement faults were predominantly oriented NW-SE and WNW-ESE. Contractional deformation occurred during the Early Pennsylvanian (Morrowan and Atokan) when maximum horizontal stress was likely oriented NE-SW causing the failed rift to become uplifted and inverted. During inversion, slip along the Wichita Mountain Fault and Mountain View Fault transferred slip into the Anadarko Basin along a detachment at the base of the Springer and at the base of the Arbuckle. As slip was transferred into the basin thin-skinned structures developed over the pre-existing rift faults. These thin-skinned structures are tight faulted-detachment folds cored by broader anticlines. Examples include Carter-Knox, Cement, Chickasha, and Cruce Anticlines. The faulted-detachments folds result from slip along the Springer detachment due to a forward-shear on the Wichita Uplift. The deeper folds are typically faulted from faults that sole out onto the Arbuckle detachment.

Contractional deformation continued throughout the Desmoinesian and Missourian but was more prominent on NW-SE oriented structures. By the Late Pennsylvanian (Virgilian), the NW-SE oriented structures continued to undergo contractional deformation, however the WNW-ESE oriented faults underwent strike-slip faulting accompanied by normal faulting. Examples include the Cement and Washita Valley Faults. Both faults are rooted to pre-existing normal faults that became reactivated when maximum horizontal stress rotated to an ENE-WSW direction. These faults experienced a small component of normal slip along with strike-slip. This resulted in the crest of the Cement anticline to be cut by oblique normal faults. Normal faulting is also observed along the Washita Valley Fault trend in the Anadarko Basin. Overall, the pre-

existing rift faults, changes in mechanical stratigraphy, and a progressive rotation in stress orientations resulted in the complex structural geology observed in southern Oklahoma.

References

- Allen, Robert W. 2000. Complex Structural Features of the Ardmore Basin. Oklahoma City Geological Society in the Shale Shaker 51.
- Amsden, T.W. 1975. Hunton Group in the Anadarko Basin of Oklahoma. Oklahoma Geological Survey Bulletin 121: 214.
- Axtmann, T.C. 1985. Structural Mechanisms and Oil Accumulation along the Mountain View-Wayne Fault, South-Central Oklahoma. Shale Shaker Digest 35: 17–45.
- Baker, Emma M, and Austin A Holland. 2013. Probabilistic Seismic Hazard Assessment of the Meers Fault, Southwestern Oklahoma: Modeling and Uncertainties SP2012-02.
- Beauchamp, Weldon. 1982. The Structural Geology of the Slick Hills. Master's thesis, Oklahoma State University, Stillwater, Oklahoma, 119 p.
- Behm, M., Andrew Cullen, A. Wallace, F. Cheng, P. Ratre, and A. Patterson. 2018. Integrated Seismic and Electrical Resistivity Imaging of the Meers Faults. In American Geophysical Union Annual Meeting, Abstract S13D-0499.
- Booth, S. L. 1982. Structural Analysis of Portions of the Washita Valley Fault Zone, Arbuckle Mountains, Oklahoma. Shale Shaker 31: 107–20.
- Bott, M. H. P. 1979. Subsidence Mechanisms at Passive Continental Margins. In Geological and Geophysical Investigations of Continental Margins: AAPG Memoir 29, 3–9.
- Brewer, J. A., L. D. Brown, D. Steiner, J. E. Oliver, S. Kaufman, and R. E. Denison. 1981. Proterozoic Basin in the Southern Midcontinent of the United States Revealed by COCORP Deep Seismic Reflection Profiling. *Geology* 9 (12): 569–75.
- Brewer, J. A., R. Good, J. E. Oliver, L. D. Brown, and S. Kaufman. 1983. COCORP Profiling across the Southern Oklahoma Aulacogen: Overthrusting of the Wichita Mountains and Compression within the Anadarko Basin. *Geology* 11: 109–14.
- Brown, W. G. 1984. Washita Valley Fault-A New Look at an Old Fault. Technical Proceedings of the 1981 AAPG Mid-Continent Regional Meeting, 68–80.
- Brueseke, Matthew E., Casey L. Bulen, and Stanley A. Mertzman. 2014. Major- and Trace-Element Constraints on Cambrian Basalt Volcanics in the Southern Oklahoma Aulacogen from Well Cuttings in the Arbuckle Mountains Region, Oklahoma U.S.A. In *Igneous and Tectonic History of the Southern Oklahoma Aulacogen*, Oklahoma Geological Survey Guidebook 38, edited by Neil H Suneson, 95–104.

- Brune, Sascha, Simon E Williams, and R Dietmar Müller. 2018. Oblique Rifting: The Rule, Not the Exception. *Solid Earth* 9: 1187–1206.
- Budnik, Roy T. 1986. Left-Lateral Intraplate Deformation along the Ancestral Rocky Mountains: Implications for Late Paleozoic Plate Motions. *Tectonophysics* 132 (1–3): 195–214. [https://doi.org/10.1016/0040-1951\(86\)90032-6](https://doi.org/10.1016/0040-1951(86)90032-6).
- Carpenter, M., and B. Tapp. 2014. Structural Analysis of Sho-Vel-Tum Using Balanced Cross sections. In *Igneous and Tectonic History of the Southern Oklahoma Aulacogen*, Oklahoma Geological Survey Guidebook 38, edited by Neil H Suneson, 327–340.
- Carter, Darryl Wayne. 1979. A Study of the Strike-Slip Movement Along the Washita Valley Fault Arbuckle Mountains, Oklahoma. *The Shale Shaker Digest* 30–32: 85–115.
- Casas, A. M., D. Gapais, T. Nalpas, K. Besnard, and T. Román-Berdiel. 2001. Analogue Models of Transpressive Systems. *Journal of Structural Geology* 23 (5): 733–43. [https://doi.org/10.1016/S0191-8141\(00\)00153-X](https://doi.org/10.1016/S0191-8141(00)00153-X).
- Chase, Brandon. 2019. High Resolution Geophysical Imaging Reveals Major Faults in the Southern Oklahoma Aulacogen: Implications for Mid-Continent Seismic Hazards and Ancestral Rocky Mountain Tectonics. Master's thesis, Oklahoma State University Stillwater, Oklahoma, 41 p.
- Chopra, Satinder, Kurt J. Marfurt, Folarin Kolawole, and Brett M. Carpenter. 2018. Nemaha Strike-Slip Expression on 3D Data in SCOOP Trend. *AAPG Explorer* June.
- Collins, D. S. 1992. A Petrographic Study of Igneous Rock from Three Drill Holes near the Meers Fault, Oklahoma, USGS Open File Report 92-411, 25p.
- Cooper, J. Calvin. 1995. Geological Evolution of the Criner Hills Trend, Ardmore Basin, Oklahoma. In *Structural Styles in the Midcontinent, 1992 Symposium*, Oklahoma Geological Survey Circular 97, edited by Kenneth S. Johnson, 144–60.
- Crone, A. J., and K. V. Luza. 1986. Holocene Deformation Associated with the Meers Fault, Southwestern Oklahoma. *The Slick Hills of Southwestern Oklahoma-Fragments of an Aulacogen?* OGS Guidebook 24: 68-72
- Cullen, Andrew. 2016. Seismic Risk of the Meers Fault, SW Oklahoma: A Hoary Giant or Great Imposter. *AAPG Mid-Continent Section Meeting, Search and Discovery #51239(2016)* 21p.
- Cullen, Andrew. 2018. An Imposter Exposed? A Meers Fault Outcrop in the Slick Hills. *Shale Shaker* 69 (6): 330–43.
- Cullen, Andrew. 2019. The Kimbell Ranch 32-1: Implications of a Deep Wildcat Well Drilled near the Meers Fault in the Slick Hills of Southwestern Oklahoma, USA. *Shale Shaker* 70 (5): 204–20.

- Denison, R. E. 1995. Significance of Air-Photograph Linears in Basement Rocks of the Arbuckle Mountains. In *Structural Styles in the Midcontinent, 1992 Symposium*, Oklahoma Geological Survey Circular 97, edited by Kenneth S. Johnson, 119–31.
- Denison, Roger E. 1989. Foreland Structure Adjacent to the Ouachita Foldbelt. In *The Geology of North America*, v. F-2, *The Appalachian-Ouachita Orogen in the United States*, edited by R. D. Jr Hatcher, William A. Thomas, and G. W. Viele, 681–88. The Geological Society of America.
- Dewey, J. F., R.E. Holdsworth, and R.A. Strachan. 1998. *Transpression and Transtension Zones*. Special Publications, Geological Society, London 135: 1–14.
- Domeier, Mathew, and Trond H. Torsvik. 2014. Plate Tectonics in the Late Paleozoic. *Geoscience Frontiers* 5 (3): 303–50. <https://doi.org/10.1016/j.gsf.2014.01.002>.
- Donovan, R Nowell. 1995. The Slick Hills of Oklahoma and Their Regional Tectonic Setting. Oklahoma Geological Survey Circular 97, 178–86.
- Donovan, R Nowell, M. C. Gilbert, Luza Keneth, David Marchini, and David Sanderson. 1983. Possible Quaternary Movement on the Meers Fault, Southwestern Oklahoma. *OGS Oklahoma Geology Notes* 43 (5): 124–33.
- Donovan, R Nowell, W. R. D. Marchini, David A. McConnell, Weldon Beauchamp, and David J. Sanderson. 1989. Structural Imprint on the Slick Hills, Southern Oklahoma. In *Anadarko Basin Symposium: Oklahoma Geological Survey Circular 90*, edited by Kenneth S. Johnson, 78–84.
- Dott, R. H. 1933. Presidential Address: Structural History of the Arbuckle Mountains. *Tulsa Geological Society Digest* 1: 37–40.
- Dunham, R. J. 1955. Pennsylvanian Conglomerates, Structure, and Orogenic History of the Lake Classen Area, Arbuckle Mountains, Oklahoma. *AAPG Bulletin* 39: 1–30.
- Erslev, Eric A. 1991. Trishear Fault-Propagation. *Geology* 19 (6): 617–20.
- Feinstein, Shimon. 1981. Subsidence and Thermal History of Southern Oklahoma Aulacogen-Implication for Petroleum Exploration. *AAPG Bulletin* 65 (2): 2521-33.
- Ferebee, C. D. 1991. Subsidence and Basin Development in the Southern Oklahoma Aulacogen. Master's thesis, University of Tulsa, Tulsa, Oklahoma, 121p.
- Friess, John P. 2005. The Southern Terminus of the Nemaha Tectonic Zone, Garvin County, Oklahoma. *Shale Shaker Digest* September- (October): 1–13.

- Gay, S Parker. 2014. Some Observations on the Amarillo/Wichita Mountains Thrust-Fold Belt and Its Extensions Southeast into East Texas and Northwest into New Mexico. *Shale Shaker* 65 (5): 338–67.
- Ghosh, Sayantan. 2017. Integrated Studies on Woodford Shale Natural Fracture Attributes, Origin, and Their Relation to Hydraulic Fracturing. PhD dissertation, University of Oklahoma, Norman, Oklahoma, 282 p.
- Gilbert, M Charles. 1983. Timing and Chemistry of Igneous Events Associated with the Southern Oklahoma Aulacogen. *Tectonophysics* 94: 439–55.
- Granath, James W. 1989. Structural Evolution of the Ardmore Basin, Oklahoma: Progressive Deformation in the Foreland of the Ouachita Collision. *Tectonophysics* 8 (5): 1015-1036.
- Ham, William E. 1951. Structural Geology of the Southern Arbuckle Mountains. *Tulsa Geological Society Digest* 19: 68–71.
- Ham, William E. 1950. Geology and Petrology of the Arbuckle Limestone in the Southern Arbuckle Mountains. PhD dissertation, Yale University, New Haven, Connecticut, 159p.
- Ham, William E., Roger E. Denison, and Clifford A. Merrit. 1964. Basement Rocks and Structural Evolution of Southern Oklahoma *Bulletin* 9.
- Hanson, Richard E., Robert E. Puckett, G. Randy Keller, Matthew E. Brueseke, Casey L. Bulen, Stanley A. Mertzman, Shane A. Finegan, and David A. McCleery. 2012. Intraplate Magmatism Related to Opening of the Southern Iapetus Ocean: Cambrian Wichita Igneous Province in the Southern Oklahoma Rift Zone. *Lithos* 174: 57–70.
<https://doi.org/10.1016/j.lithos.2012.06.003>.
- Harlton, Bruce. 1956. The Harrisburg Trough, Stephens and Carter Counties, Oklahoma. In *Petroleum Geology of Southern Oklahoma*, v. I, 135–43.
- Harlton, Bruce H. 1951. Faults in the Sedimentary Part of Wichita Mountains of Oklahoma. *AAPG Bulletin* 35 (5): 988–99.
- Harlton, Bruce H. 1960. Stratigraphy of Cement Pool and Adjacent Area, Caddo and Grady Counties, Oklahoma. *AAPG Bulletin* 44 (2): 210–26.
- Harlton, Bruce H. 1963. Frontal Wichita Fault System of Southwestern Oklahoma. *AAPG Bulletin* 47 (8): 1552–80.
- Heran, W. D., Green, G. N., and Stoeser, D. B., 2003, A Digital Geologic Map Database for the State of Oklahoma: USGS Open-File Report OF-2003-247
- Herrmann, Leo A. 1961. Structural Geology of Cement-Chickasha Area, Caddo and Grady Counties, Oklahoma. *AAPG Bulletin* 45 (12): 1971–93.

- Hilley, George, Ramon Arrowsmith, and Lee Amorso. 2001. Interaction between Normal Faults and Fractures and Fault Scarp Morphology. *Geophysical Research Letters* 28 (19): 3777–80.
- Hoffman, P., J. F. Dewey, and K. Burke. 1974. Aulacogens and Their Genetic Relations to Geosynclines, with a Proterozoic Example from Great Slave Lake, Canada. In *Modern and Ancient Geosynclinal Sedimentation: Society of Economic Paleontologists and Mineralogists Special Publication 19*, edited by R. J. Jr Dott and R. H. Shaver, 38–55.
- Hornblow, S, M Quigley, A Nicol, R Van Dissen, and N Wang. 2014. Paleoseismology of the 2010 M-W 7.1 Darfield (Canterbury) Earthquake Source, Greendale Fault, New Zealand. *Tectonophysics* 637 (10): 178–90. <https://doi.org/10.1016/j.tecto.2014.10.004>.
- Houseknecht, D. W. 1983. Tectonic-Sedimentary Evolution of the Arkoma Basin. *Society of Economic Paleontologists and Mineralogists* 1: 3–33.
- Jacobson, Mark I. 1984. The Harrisburg Trough, Stephens County, Oklahoma. In *Technical Proceedings of the 1981 Mid-Continent Regional Meeting*, 127–37.
- Jones-Cecil, M. 1995. Structural Framework of the Meers Fault and Slick Hills Area, Southwestern Oklahoma. *Oklahoma Geological Survey Circular* 97, 187–207.
- Keller, G Randy. 2014. The Southern Oklahoma Aulacogen: It’s a Classic. *Oklahoma Geological Survey Guidebook* 38, 389–91.
- Keller, G. R., and R.A. Stephenson. 2007. The Southern Oklahoma and Dnieper-Donets Aulacogens: A Comparative Analysis. In *The 4D Framework of Continental Crust: Geological Society of America Memoir 200*, edited by R. D. Jr. Hatcher, M. P. Carlson, J. H. McBride, and J. R. Martinez Catalan, 127–43.
- Keller, G. Randy. 2012. A Regional Overview of Southern Oklahoma Structures. *Oklahoma Geological Survey Presentation*
http://www.ogs.ou.edu/MEETINGS/Presentations/OilGasMar2012/Keller_Southern_OK.pdf
- Kilic, D., and B. Tapp. 2014. Structural Analysis of the Eola-Robberson Field using Balanced Cross Sections, Garvin County, Oklahoma. In *Igneous and Tectonic History of the Southern Oklahoma Aulacogen, Oklahoma Geological Survey Guidebook* 38, edited by Neil H Suneson, 341-356.
- Kluth, C. F. 1986. Plate Tectonics of the Ancestral Rocky Mountains. In *Paleotectonics and Sedimentation in the Rocky Mountains Region, United States*, edited by J. A. Peterson, 353–69.
- Kluth, C. F., and P. J. Coney. 1981. Plate Tectonics of the Ancestral Rocky Mountains. *Geology* 9: 10–15.

- Leary, Ryan J., Paul Umhoefer, M. Elliot Smith, and Nancy Riggs. 2017. A Three-Sided Orogen: A New Tectonic Model for Ancestral Rocky Mountain Uplift and Basin Development. *Geology* 45 (8): 735–38. <https://doi.org/10.1130/G39041.1>.
- Marsh, S., and Austin A. Holland. 2015. Comprehensive Fault Database and Interpretive Fault Map of Oklahoma: Oklahoma Geological Survey Open-File Report OF2-2016.
- McBee, William. 1995. Tectonic and Stratigraphic Synthesis of Events in the Region of the Intersection of the Arbuckle and Ouachita Structural Systems, Oklahoma. In *Structural Styles in the Midcontinent, 1992 Symposium*, Oklahoma Geological Survey Circular 97, edited by Kenneth S. Johnson, 45–81.
- McBee, William. 2003. The Nemaha and Other Strike-Slip Faults in the Midcontinent U.S.A. In *Midcontinent Section Meeting*, 1–23.
- McCaskill Jr., Jerry Glen. 1998. Multiple Stratigraphic Indicators of Major Strike-Slip Movement Along the Eola Fault, Subsurface Arbuckle Mountains, Oklahoma, Part I. *The Shale Shaker Digest* 48 (4): 93-109
- McCaskill Jr., Jerry Glen. 2015. A Palinspastic Restoration of Southern Oklahoma: A Necessary Framework for Regional Pre-Deformation Structural, Depositional and Diagenetic Studies. AAPG Mid-Continent Section Meeting, Search and Discovery #20418(2018) 88p.
- McClay, K., and T. Dooley. 1995. Analogue Models of Pull-Apart Basins. *Geology* 23 (8): 711–14.
- McConnell, D. A. 1989. Determination of Offset across the Northern Margin of the Wichita Uplift, Southwest Oklahoma. *GSA Bulletin* 101 (10): 1317–32.
- McConnell, David A. 1987. Paleozoic Structural Evolution of the Wichita Uplift, Southwest Oklahoma. PhD dissertation, Texas A&M University, College Station, Texas, 219p.
- McCoss, Angus M. 1986. Simple Constructions for Deformation in Transpression/Transtension Zones. *Journal of Structural Geology* 8 (6): 715–18.
- Meyers, B, K.P. Furlong, G.P. Hayes, M.W. Herman, and M Quigley. 2012. Surface and Subsurface Fault Displacements from the September 2010 Darfield (Canterbury) Earthquake. In *American Geophysical Union Fall Meeting*, T33A-2645.
- Miller, R. D., D. W. Steeples, and P. B. Myers. 1990. Shallow Seismic Reflection Survey of the Meers Fault, Oklahoma. *Geological Society of America Bulletin* 102 (January): 1328–31. <https://doi.org/10.1190/1.1892527>.
- Miser, H. D. 1954. Geologic Map of Oklahoma: Oklahoma Geological Survey and U.S. Geological Survey, Scale 1:500,000.

- Mitra, Shankar. 2002. Fold-Accommodation Faults. AAPG Bulletin 86 (4): 671–693.
- Mitra, Shankar. 2002. Structural Models of Faulted-detachment folds. AAPG Bulletin 9 (9): 1673–94.
- Moody, J. A., and M. J Hill. 1956. Wrench-Fault Tectonics. Apeiron 67 (9): 1207–46.
<http://www.degruyter.com/view/j/apeiron>.
- Naruk, S. J. 1994. Geometric Analysis and Balanced Cross sections of the Arbuckle Mountains and Washita Valley Fault. The Shale Shaker Digest 13 (40-45): 158-162.
- Perry, W. J. 1989. Tectonic Evolution of the Anadarko Basin Region, Oklahoma. US Geological Survey Bulletin 1866-A, A1–19.
- Petersen, F A. 1983. Foreland Detachment Structures. In Rocky Mountain Foreland Basins and Uplifts: Rocky Mountain Association of Geologists, edited by James D Lowell and R. R. Gries, 65–77.
- Puckett, Robert E. 2011. A Thick Sequence of Rift Related Basalts in the Arbuckle Mountains, Oklahoma as Revealed by Deep Drilling. Shale Shaker 61: 207–16.
- Puckett, Robert E., Richard E. Hanson, Amy M. Eschberger, Matthew E. Brueseke, Casey L. Bulen, and Jonathan D Price. 2014. New Insights into the Early Cambrian Igneous and Sedimentary History of the Arbuckle Mountains Area of the Southern Oklahoma Aulacogen from Basement Well Penetrations. In Igneous and Tectonic History of the Southern Oklahoma Aulacogen, Oklahoma Geological Survey Guidebook 38, edited by Neil H Suneson, 61–94.
- Quigley, M, R. Van Dissen, N. Litchfield, P. Villamor, and B. Duffy. 2011. Surface Rupture during the 2010 M (Sub w) 7.1 Darfield (Canterbury) Earthquake; Implications for Fault Rupture Dynamics and Seismic Hazard Analysis. Geology 40 (1): 55–58.
- Ramelli, A. R., and D. B. Slemmons. 1986. Neotectonic Activity of the Meers Fault. In The Slick Hills of Southwestern Oklahoma-Fragments of an Aulacogen? OGS Guidebook 24, 45–54.
- Reedy, H. J., and H. A. Sykes. 1959. Carter Knox Oil and Gas Field. In Petroleum Geology of Southern Oklahoma, v. II, 198–219. AAPG.
- Richard, P., and R. W. Krantz. 1991. Experiments on Fault Reactivation in Strike-Slip Mode. Tectonophysics 188: 117–31.
- Sanderson, David J., and W. R. D. Marchini. 1984. Transpression. Journal of Structural Geology 6 (5): 449–58.

- Saxon, Christopher Paul. 1998. Structural Style of the Wichita and Arbuckle Orogenies, Southern Oklahoma. PhD dissertation, University of Oklahoma, Norman, Oklahoma, 313p.
- Saxon, Christopher Paul. 1994. Surface to Subsurface Structural Analysis, Northwest Arbuckle Mountains, Southern Oklahoma. Master's thesis, Baylor University, Waco, Texas, 205p.
- Shah, A. K., and C. A. Finn. 2018. Airborne Magnetic Surveys over Oklahoma, 2017: U.S. Geological Survey Data Release. <https://doi.org/10.5066/F7ZG6RJP%0A>.
- Shatski, N.S. 1946. The Great Donets Basin and the Wichita System; Comparative Tectonics of Ancient Platforms. *Akademiya Nauk SSSR Izvestiya, Seriya Geologicheskaya* 6: 57–90.
- Skulski, T., D. Francis, and J. Ludden. 1991. Arc-Transform Magmatism in the Wrangell Volcanic Belt. *Geology* 19: 11–14.
- Skulski, T., D. Francis, and J. Ludden. 1992. Volcanism in Arc-Transform Transition Zone: The Stratigraphy of the St. Clare Creek Volcanic Field, Wrangler Volcanic Belt, Yukon, Canada. *Canadian Journal of Earth Sciences* 29: 44–461.
- Streig, A. R., S. E. Bennet, T. K. Hornsby, J. C. Chang, and S. Mahan. 2018. Recent Paleoseismic and Tectonic Geomorphic Studies of the Meers Fault, Oklahoma Reveal Longer Rupture Lengths and More Surface Deforming Earthquakes in the Last 6,000 Years. In American Geophysical Union Annual Meeting Abstract.
- Taff, J. A. 1904. Preliminary Report on the Geology of the Arbuckle and Wichita Mountains. USGS Professional Papers 31.
- Tanner, J. H. 1967. Wrench Fault Movements along Washita Valley Fault, Arbuckle Mountain Area, Oklahoma. *AAPG Bulletin* 51: 126–41.
- Tanner, W. F. 1963. Tectonic Patterns in the Appalachian-Ouachita-Oklahoma Mountain Complex. *Shale Shaker Digest* 14 (3): 2–6.
- Tapp, B. 1995. Inversion Model for the Structural Style of the Arbuckle Region. In *Structural Styles in the Midcontinent, 1992 Symposium*, Oklahoma Geological Survey Circular 97, edited by Kenneth S. Johnson, 113–18.
- Thomas, William A. 2011. The Iapetan Rifted Margin of Southern Laurentia. *Geosphere* 7 (1): 97–120. <https://doi.org/10.1130/ges00574.1>.
- Thomas, William A. 2014. The Southern Oklahoma Transform-Parallel Intracratonic Fault System. In *Igneous and Tectonic History of the Southern Oklahoma Aulacogen*, Oklahoma Geological Survey Guidebook 38, edited by Neil H. Suneson, 375–87.

- Tikoff, Basil, and Christian Teyssier. 1994. Strain Modeling of Displacement-Field Partitioning in Transpressional Orogens. *Journal of Structural Geology* 16 (11): 1575–88. [https://doi.org/10.1016/0191-8141\(94\)90034-5](https://doi.org/10.1016/0191-8141(94)90034-5).
- Tomlinson, C. W., and William Jr. McBee. 1959. Pennsylvanian Sediments and Orogenies of Ardmore District, Oklahoma. *SP 19: Petroleum Geology of Southern Oklahoma* 2: 461–500.
- Torsvik, Trond H., B. Steinberger, I. R. M. Cocks, and K. Burke. 2008. Longitude: Linking Earth's Ancient Surface to Its Deep Interior. *Earth and Planetary Science Letters* 276 (3–4): 273–82.
- Tripplehorn, Tyler. 2014. Structural Characterization and Elastic Flexure Modeling of Basement Geometry in Southern Central Oklahoma. Master's thesis, University of Tulsa, Tulsa, Oklahoma, 118p.
- Walker, W. M. 2006. Structural Analysis of the Criner Hills, South-Central Oklahoma. Master's thesis, Baylor University, Waco, Texas, 73p.
- Walper, J. L. 1982. The Geotectonic Evolution of the Oklahoma Aulacogen, Oklahoma. *North Texas Geological Society, Basins of the Southwest-Phase 2*, 192–211.
- Ye, Hongzhuan, Leigh Royden, Clark Burchfield, and Martin Schuepbach. 1996. Late Paleozoic Deformation of Interior North America: The Greater Ancestral Rocky Mountains. *AAPG Bulletin* 80 (9): 1397–1432.

Appendix 2.1 Well Information from Cross Sections

Cross Section	Well #	API	Well Name and Number
A	1	35137000920000	S J PINSON 1
A	2	35137240310000	WOOLEVER GEORGE A 1
A	3	35137265880000	HINES 1-9
A	4	35137252690000	HOWARD 1
A	5	35137227790000	DEBBY-SUE 1-36
A	6	35137236900000	SUMNER GARY 1
A	7	35137253890000	LAMAR 1-21
A	8	35137255150000	KILGO 3-21
A	9	35051365150000	LEONA HAYES 1
A	10	35051227710000	J KAYE 3-33
A	11	35051227140000	JULES 1-34
A	12	35051227410000	BLOCH 1-34
A	13	35051226150000	CALEB 1-27
B	1	35137264190000	PEARSON 1-8
B	2	35137265090000	BEXAR 3-27
B	3	35137006710000	HOUSE 1
B	4	35137214490000	CALLAWAY 23-1
B	5	35137256300000	COTTONWOOD 1-11
B	6	35137260600000	BONNER 1-12
C	1	35031020510001	FT STILL NW 1
C	2	35031021840000	SCHOOL LAND 1-A
C	3	35031201900000	CHOENS 1
C	4	35031201500001	GENEVA 1
C	5	35031204570000	MCFARLAND 1
C	6	35031214280000	ELGIN 31-1
C	7	35031214040000	CIRCLE 'H' 1
C	8	35031208670000	BROCK 1-20
C	9	35031020620000	CRANE 1
C	10	35031209180000	FLETCHER 1
C	11	35031208990000	WHITE HORSE 1
C	12	35031208930000	CRAWFORD 1
C	13	35051200480001	CEMENT /ORDVCN UN/ 1-A
C	14	35051227630000	FLYNN 1-18
C	15	35051228520000	BENTLEY 1-8
C	16	35051224420000	BENTLEY 1-8

C	17	35051205580000	WILLIAMS 1
C	18	35051212770000	HILLSBORO 1
C	19	35051212510000	THOMAS MARTIN 1
D	1	35015230100000	KIMBELL 32 1
D	2	35015227270000	GOODMAN 14 1
D	3	35015212870000	CECIL KIEFER 1
D	4	35015220990000	ESTHER 1-15
D	5	35015213020000	WEIDEMAIER 1-15
D	6	35015000270000	WEIDEMAIER 1
D	7	35015231250000	ORRELL 1-1
E	1	35075203770000	GEIMAUSSADDLE GRACE 1
E	2	35075003630000	LONEWOLF UNIT 1
E	3	35075219150000	EDWARDS 1-19
E	4	35075219360000	RUSSELL 1-20
E	5	35075200420000	L L HOLSTED 1
F	1	35075004080000	SMITH 1
F	2	35075005860000	WATTENBARGER 1
F	3	35149000490000	H K BISHOP 1
F	4	35149207620000	MCRAE 2
F	5	35149200950000	DUNCAN 1
F	6	35149203920000	KING 1
F	7	35149212990000	THUNDER RIDGE 1-11
F	8	35149203050000	ANNA TREDER 1-13
F	9	35149203790000	STATE OF OKLAHOMA 1
F	10	35039200450000	DUKE 1-35
F	11	35039222890000	DEER CREEK MONSTER 2-26
G	1	4208700370000	COOK 1
G	2	42087003070000	ALEXANDER E G 1
G	3	42087003720000	WISCHKAEMPER 1
G	4	42087004910000	WISCHKAEMPER -F- 1
H	1	35065200900000	STATE 1-13
H		35065201300000	HYSINGER 9-27
H	3	35055205690000	DUFFER 2-32
I	1	35141004700000	COLYER 2
I	2	35141002760000	LOCKE 1
I	3	35141000230000	BREWSTER 1
1	1	35051200120000	CARTER J W UNIT 1
1	2	35051367020000	DUKE 1
1	3	35051207270000	BILLY J BENNET ETAL 1

1	4	35051221740000	DUKE 1-35
2	1	35051234240000	IRENE 1-11
2	2	35051213710000	KAHLE 1
2	3	35051203550000	FARWELL UNIT 1
3	1	35051218050000	FLORENE 1-33
3	2	35051227880000	MARSHALL-CRADDOCK 1-22
4	1	35137251450000	MAXWELL 1-16
4	2	35137210360001	GOLDFEDER DAN 1-9
4	3	35137088830000	WESTFALL 1
4	4	35137307810000	HARRELL H 'B' 1
4	5	35137250810000	DAVIS 1-3
4	6	35137236600000	BELDON 1
4	7	35137139260000	STEWART ART 2
4	8	35137252970000	DUNCAN 1-26
4	9	35137252800000	HPC 1-14
4	10	35137255730000	TED 1-14
5	1	35137255190000	GANT 1-19
5	2	35137226620000	KELLY 1
5	3	35137006490000	ALMA GLOVER 1

Appendix 2.2 Additional Cross Sections

Two additional cross sections were constructed over the eastern trace of the Washita Valley Fault in the southeast Anadarko Basin. These cross sections emphasize the late timing of strike-slip/normal faulting. Cross section 4 (Figure 2.23) extends over the Doyle Field into the southeast part of the Carter-Knox structure. The Doyle structure consists of a large WNW-ESE oriented faulted fold that developed prior to being truncated by the unconformity at the base of the Desmoinesian. The faults cutting this fold extend from the detachment at the base of the Arbuckle. Two south-verging out-of-syncline thrust faults (Mitra, 2002) extend from the Springer detachment cutting the Springer through Atokan units but do not extend into the Desmoinesian. The Desmoinesian units onlap the Doyle structure and are gently folded before being truncated by another unconformity at the base of the Missourian. Both Missourian and Virgilian units are relatively flat over the structure suggesting the contractional deformation had ceased. Evolution of the Carter-Knox structure is similar to what was discussed for regional cross section A, however the back-limb of the anticline is cut by a normal fault based on seismic reflectors and missing-section in well number eight. This normal fault likely has a component of left-lateral strike-slip and merges with the near-vertical Washita Valley Fault at depth. The Washita Valley Fault cuts the basement up through the Virgilian. Accommodation space created along this fault was filled with Virgilian age sediments indicating the late timing on the strike-slip motion.

Cross section 5 (Figure 2.24) is located three miles east of cross section 4 and shows the architecture of the strike-slip/normal faulting outside of the Doyle Field which was impacted by earlier contraction. The same two strike-slip/normal faults continue to the east. The normal fault that cut the southeast part of Carter-Knox has increased its offset. This fault dies out towards the

west, but towards the east it extends into the Eola-Robberson Field, a structurally complex field cut by strike-slip faulting (McCaskill, 1998; Kilic and Tapp, 2014; McCaskill, 2015). Based on the trace of these faults in map-view, along with the large graben formed between them, these faults likely represent a strike-slip pull-apart. Studies have shown that a left-step along a left-lateral strike-slip fault will result in a pull-apart basin (McClay and Dooley, 1995). The timing of this pull-apart is Virgilian based on syn-depositional fill in the graben. Cross sections 4 and 5 validate a change in structural style by the Late Pennsylvanian.

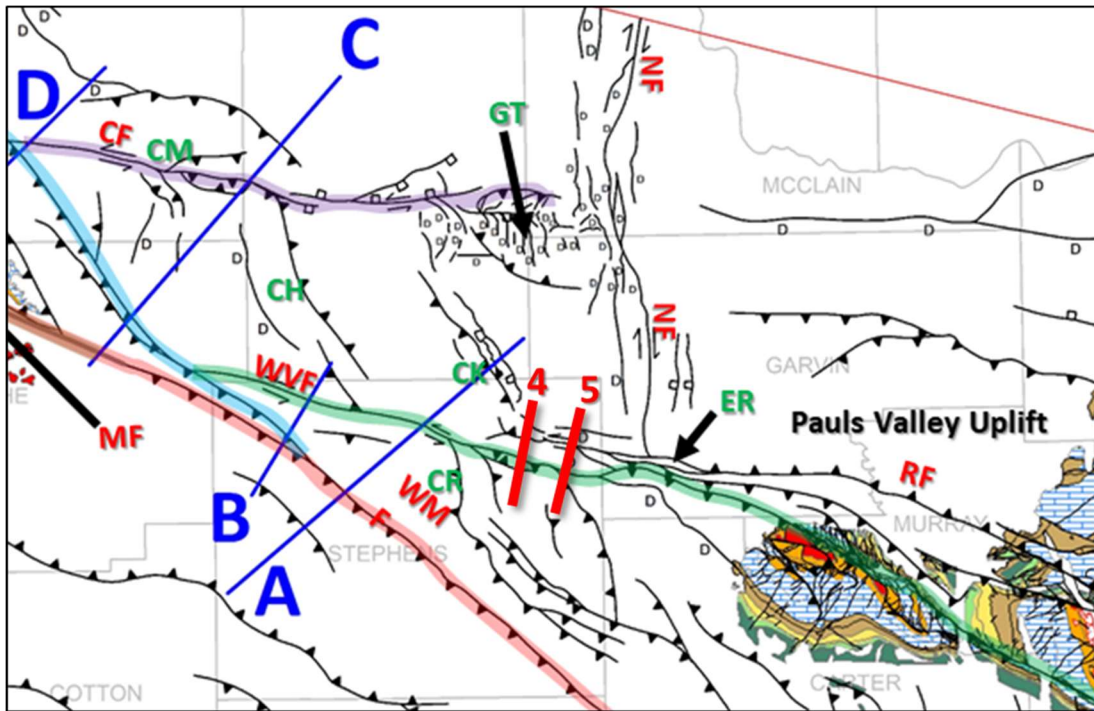


Figure 2.22 Location map for supplementary cross sections 4 and 5 (in red) superimposed on a cropped version of the regional fault map from Figure 2.1. The trace of the Washita Valley Fault is highlighted in green. ER is the Eola-Robberson Field just east of the cross sections. See Figure 2.1 for legend and key to named structures.

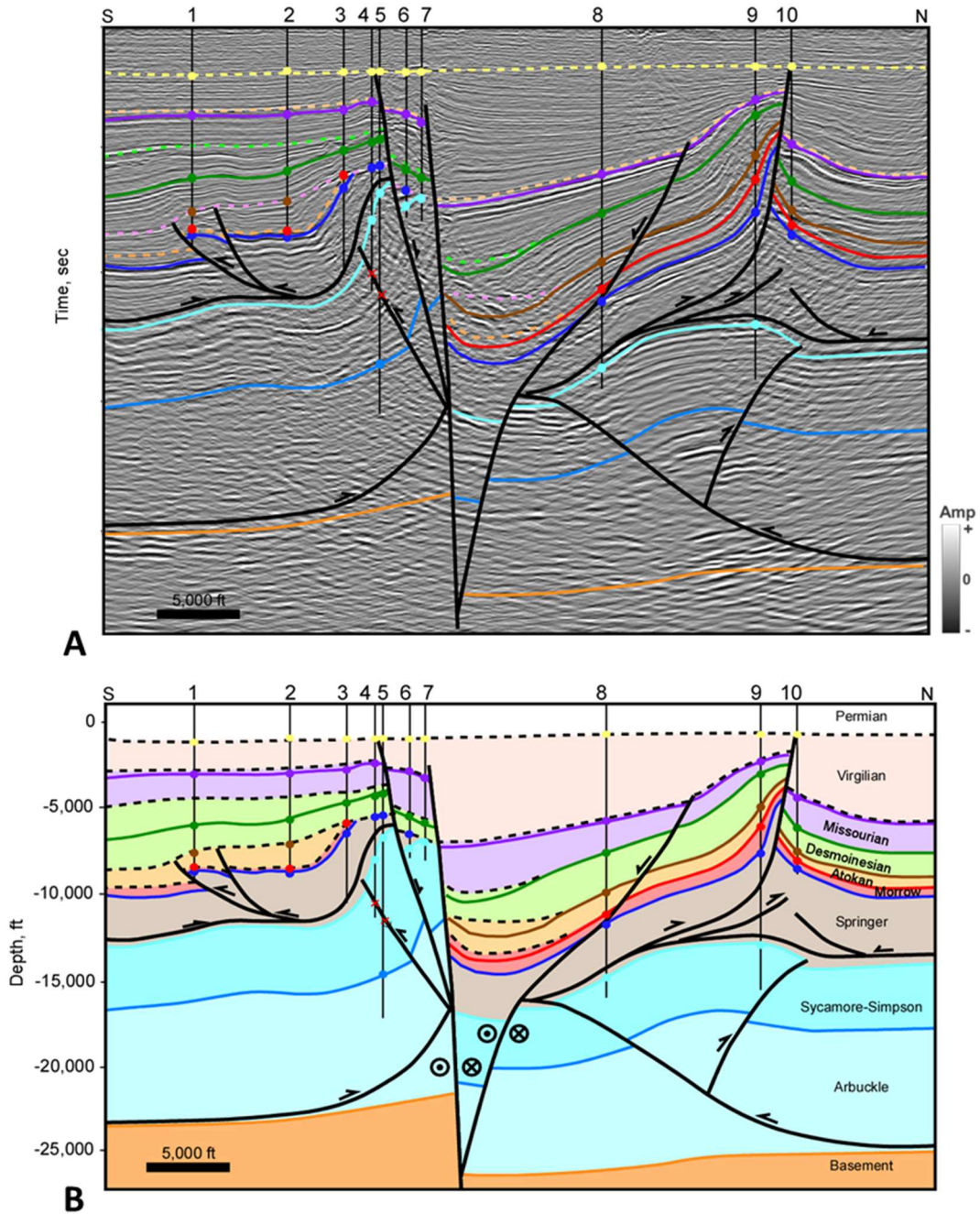


Figure 2.23 Cross section 4. (A) Interpreted seismic section in time. Time scale has been removed for proprietary data. Horizon colors are shown in Figure 2.3. (B) Depth cross section. Well information is listed in appendix 1. Well tops (colored circles), dip data (brown check mark), and fault picks (red x) are shown where available. Seismic Data Courtesy of SEI, Interpretation is that of Molly Turko.

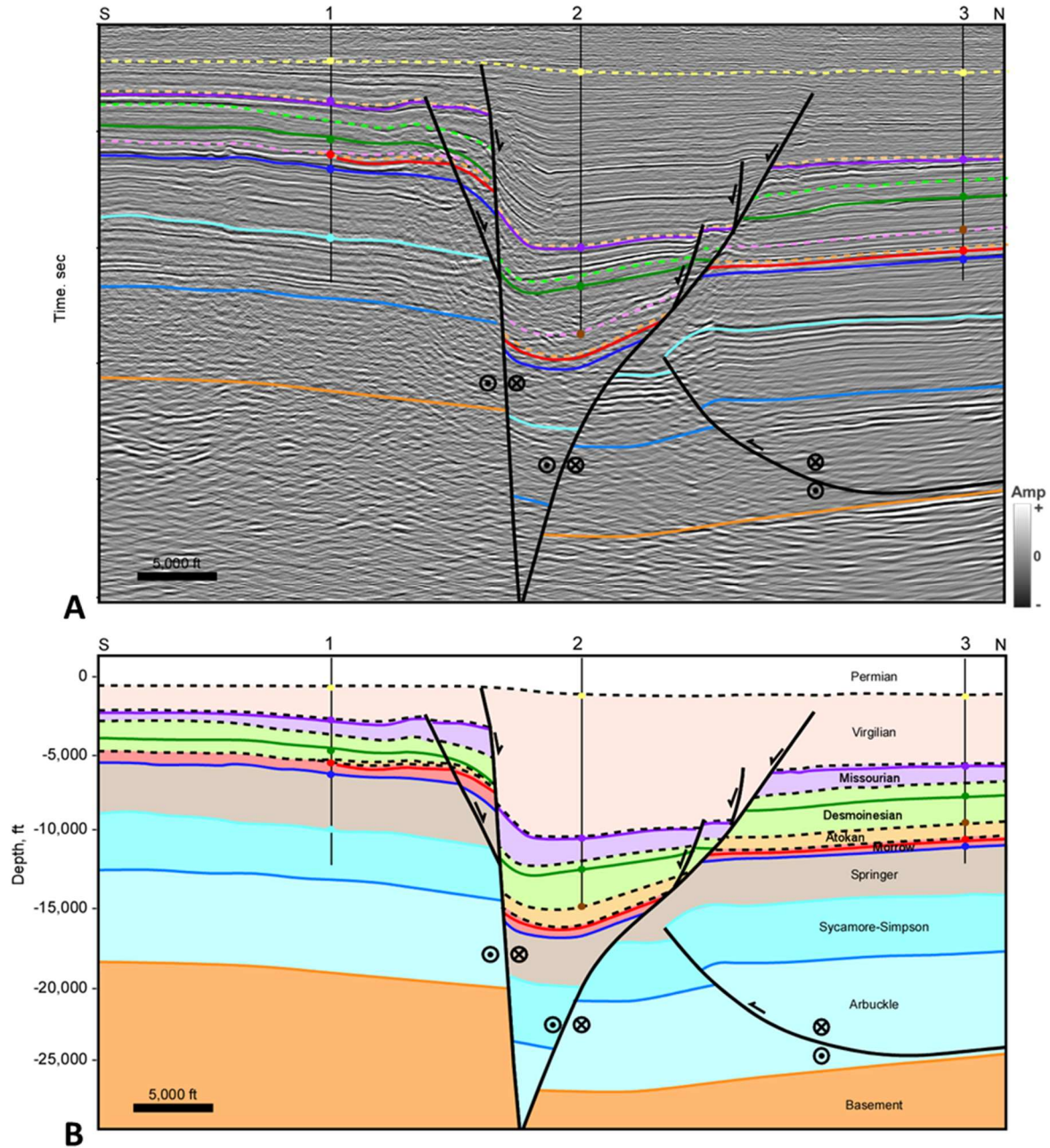


Figure 2.24 Cross section 5. (A) Interpreted seismic section in time. Time scale has been removed for proprietary data. Horizon colors are shown in Figure 2.3. (B) Depth cross section. Thrust fault cutting the Arbuckle-Sycamore is shows out-of-the-plane movement. Well information is listed in appendix 1. Well tops (colored circles), dip data (brown check mark), and fault picks (red x) are shown where available. Seismic Data Courtesy of SEI, Interpretation is that of Molly Turko.

Chapter 3: Macroscopic Structural Styles in the Southeastern Anadarko Basin, Southern Oklahoma

Abstract

The Anadarko Basin in south-central Oklahoma contains a number of oil and gas fields located on anticlinal structures formed during the Pennsylvanian orogeny. New 2-D and 3D seismic and well data was used to interpret the structural geometry and kinematic evolution of the Carter-Knox, Cruce, Chickasha, and Cement structures. The structures consist of tight faulted-detachment folds within the Pennsylvanian units related to slip along a detachment at the base of the Springer Shale, cored by deeper low amplitude faulted folds within the pre-Pennsylvanian thick carbonate units detaching at the base of the Arbuckle Group. Slip on these detachments was derived from the Wichita Uplift, which was a Precambrian-Cambrian failed rift that became inverted during the Pennsylvanian Orogeny. A greater amount of slip occurred along the Springer detachment than the Arbuckle detachment, resulting in a forward-shear motion on the frontal faults. The trend and location of these structures was likely controlled by discontinuities related to pre-existing rift-related basement normal faults. Some of the structures were cut by Virgilian strike-slip and associated normal faults as a result of a rotation of the maximum compressive stress from an earlier NE-SW to an ENE-WSW direction in the Late Pennsylvanian. In summary, the geometry, trend, and evolution of the structures were influenced by the mechanical stratigraphy, pre-existing basement structures, and a rotation in stresses during their formation.

1. Introduction

The Anadarko and Ardmore Basins in south-central Oklahoma contain a number of large oil and gas fields located on anticlinal structures. The subsurface geology is complex due to

intense faulting and folding which has led to various interpretations on the structural styles of the area. Previous studies in this area were conducted prior to the availability of modern 3D seismic data.

The objective of this study is to utilize well data and 3D seismic data to understand the structural geometry and evolution of macroscopic or field-scale structures. We focus specifically on the structural styles of some key structures in the southeastern Anadarko Basin in front of the Wichita Mountains, where it meets the northwestern end of the Ardmore Basin (Figure 3.1). These include the Carter-Knox, Cruce, Chickasha, and Cement structures, all of which contain major fields.

The tectonic evolution of the area based on regional transects and reconstructions play a key role in deciphering the structural geometry. This includes the role of contractional tectonics associated with the transfer of slip from the Wichita Uplift into the Anadarko Basin, as well as the effects of late stage strike-slip and extension along some key WNW-ESE trending faults. The regional transects are combined with more detailed cross sections through individual structures to determine their structural geometry. Multiple unconformities in the Pennsylvanian are used to understand the episodic nature of their evolution. The results of the study will be useful in interpreting other structures in the Anadarko and adjacent basins.

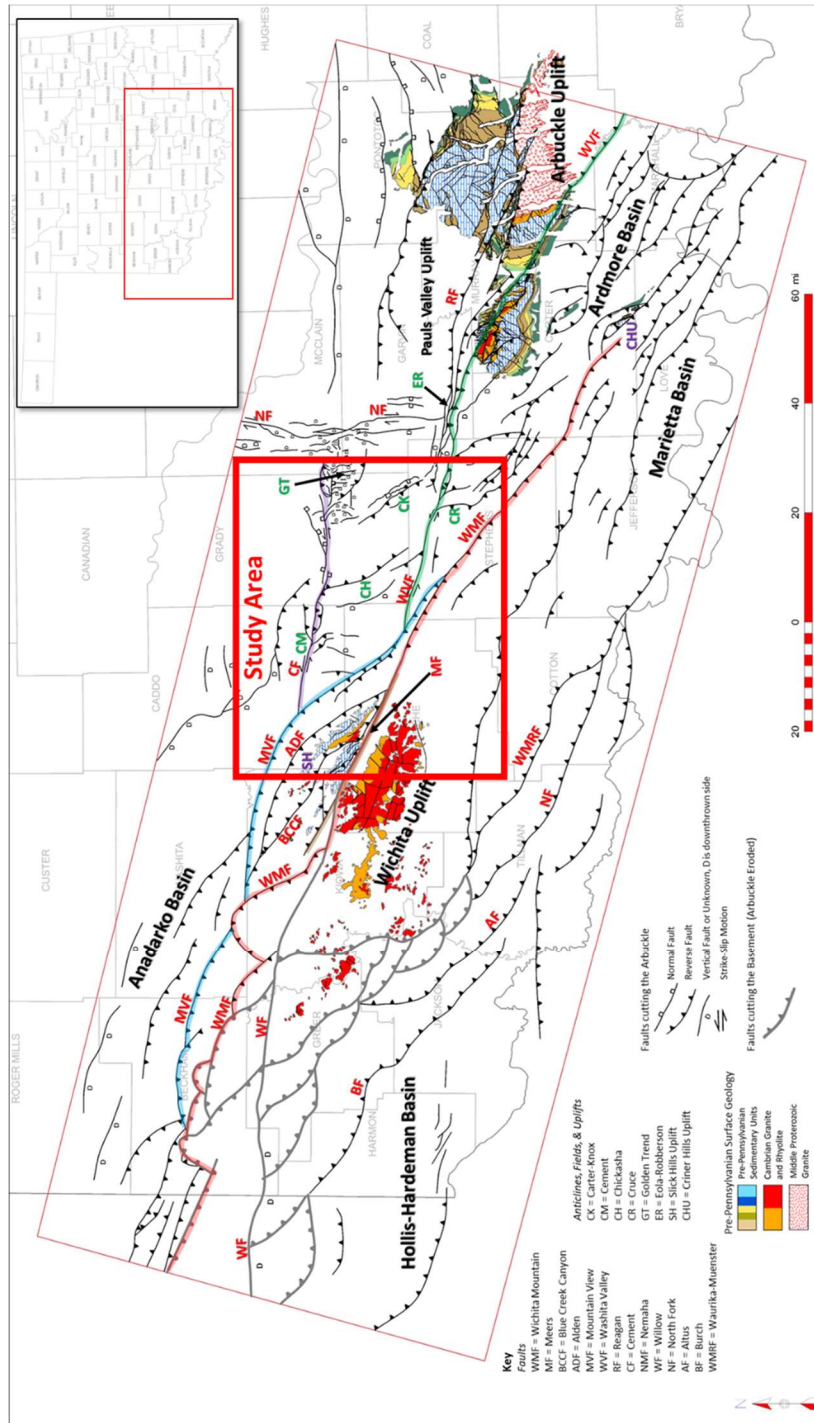


Figure 3.1 Regional map showing faults mapped at the Arbuckle level (black), and at the basement where Arbuckle is eroded on the Wichita Uplift (bold gray). The Mountain View Fault is highlighted in blue; Washita Valley Fault in green; Cement Fault in purple; and Wichita Mountain Fault in red. The study area is within the red rectangle. Pre-Pennsylvanian surface geology is derived from USGS (Heran et al., 2003). Significant uplifts, basins, fields and structures are labeled with a key on the map.

2. Geologic Background

The tectonic history of the region involves three significant events: (1) development of an aulacogen, or failed rift, that initiated in the Late Precambrian through the Middle Cambrian (Shatski, 1946; Hoffman et al., 1974; Walper, 1982; Perry, 1989; Keller and Stephenson, 2007; Keller, 2014). Understanding the Precambrian-Cambrian tectonic framework is important since it laid the foundation for later Pennsylvanian structures; (2) thermally controlled isostatic subsidence from cooling from the Middle Cambrian through the end of the Ordovician (Feinstein, 1981; Perry, 1989); and (3) the Pennsylvanian Orogeny, during which the aulacogen was uplifted, or inverted, resulting in intense faulting and folding in the Anadarko and Ardmore Basins. The effects of this orogeny are also evident in the surface geology of the Wichita and Arbuckle Mountains.

The Pennsylvanian Orogeny can be divided into three tectonic events (Granath, 1989). The first and second Wichita Orogenies occurred during the Morrowan and Atokan, when the Wichita block underwent significant inversion and uplift. These Wichita Orogenies culminated in the early Atokan but uplift likely initiated in the late Mississippian as indicated by onlapping of Chesterian age (Springer) units onto the Criner Uplift (Tomlinson and McBee, 1959; Granath, 1989; Perry, 1989; Cooper, 1995). Unconformities exist at the top of both the Morrowan and Atokan with as much as 8,000-13,000 feet of sediment eroded prior to the Desmoinesian time (Tomlinson and McBee, 1959). The third event is the Arbuckle Orogeny and occurred from the Late Desmoinesian time through Virgilian (Granath, 1989) and resulted in the uplift of the Arbuckle Mountains. The structural styles that resulted from these orogenies have been variously attributed to compression (Taff, 1904; Dott, 1933; Brown, 1984; Naruk, 1994; Saxon, 1998),

strike-slip (Ham, 1951; Tanner, 1963; Carter, 1979; Tomlinson and McBee, 1987) and/or transpression through inversion (Granath, 1989; Ferebee, 1991; Tapp, 1995).

3. Stratigraphy

Figure 3.2 shows the stratigraphic column. The stratigraphic units can be divided into three mechanical packages; the basement, a deeper carbonate section, and shallower clastic section. The basement rock that underlies much of the study area consists of Cambrian-age layered rhyolite that formed during the rifting stage. Overlying the basement is a relatively thin transgressive sandstone that varies in thickness throughout the region (Donovan et al., 1989). Ordovician through mid-Mississippian age stratigraphy is dominated by a thick carbonate package including the Arbuckle, Viola, Hunton, and Sycamore Limestone Groups. It also includes the Simpson, Woodford, Sylvan clastic Groups. The Mississippian Caney Shale and Springer Shale cap the deeper carbonate package. These shales act as a regional detachment surface and separate mechanical units with different structural styles.

Formations above the Springer detachment are primarily syn-depositional with the Pennsylvanian Orogeny and are dominantly clastic sand/shale packages with some thin limestone intervals. The tectonic events listed to the right of the stratigraphic chart are adapted from Granath (1989). The events show which formations are synchronous with the orogenies. These formations are important for determining the timing of structures. The region was relatively quiet during post-Pennsylvanian time, with only some structures being mildly reactivated.

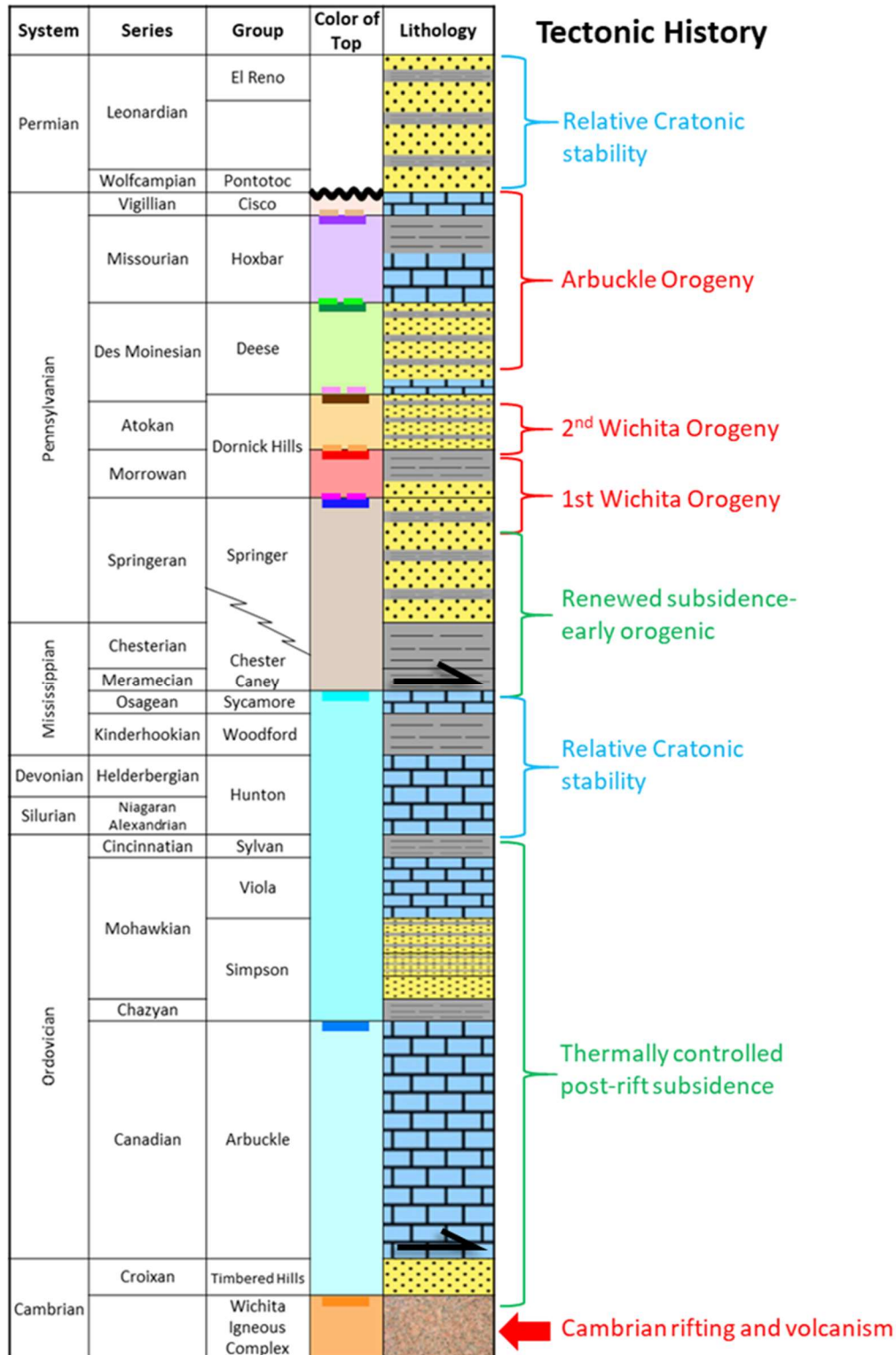


Figure 3.2 Modified from Granath (1989). Color of top refers to horizons interpreted in the cross sections. Dashed lines represent the top of an age, which in some parts of the cross sections represents an unconformity. The solid lines represent a marker within the different ages to help constrain structure in the cross sections.

4. Previous Studies

Several significant structures extend over the study area including the Carter-Knox Anticline, Cruce Anticline, Chickasha Anticline, Cement Fault Zone and Anticline (Figure 3.1). Previous studies and conclusions for each of these structures are discussed below.

4.1 Carter-Knox Anticline

Early analyses of the Carter-Knox anticline based on well data depicted the structure as a steeply-dipping faulted and asymmetric NW-SE oriented anticline consisting of Springer and younger units overlying a more gentle anticline in the pre-Pennsylvanian units (Reedy and Sykes, 1959). Several unconformities were observed with two important ones occurring at the top of the Desmoinesian and top of Morrowan (Reedy and Sykes, 1959). Movement on the anticline occurred post-Morrowan creating a gentle anticline, with the structure continuing to grow during the Desmoinesian with the largest movement occurring post-Missourian.

Some workers have described the structure as a foreland detachment structure that occurred from contractional deformation of the Wichita Uplift extending into the Anadarko Basin (Petersen, 1983; Saxon, 1998). These authors recognized a detachment within the thick Springer Shale as well as the Arbuckle Group. Saxon (1988, 1998) suggested that differences in mechanical stratigraphy above and below the Springer detachment caused the different styles of folding, which he classified as a concentric deeper fold (pre-Pennsylvanian units) overlain by a fault-propagation fold (Pennsylvanian units). Other workers have interpreted the Carter-Knox structure as a positive flower structure related to left-lateral strike-slip faulting along the Washita Valley Fault (Perkins, 1997; Hoffman, 1996).

4.2 Cruce Anticline

Studies on the NW-SE oriented Cruce Anticline suggest that the structure is very similar to Carter-Knox. Saxon (1998) grouped this structure as part of the Fox-Milroy-Velma-Cruce trend, which is a series of long, tight, doubly-plunging, NW-SE oriented subsurface uplifts in the footwall of the eastern flank of the Wichita Uplift (Saxon, 1998). He suggested that the Cruce Anticline is separated from the NW-SE trend by a series of tear faults that strike northeast (Saxon, 1998), resulting in its more north-northwest trend compared to the Fox-Milroy-Velma trending structures. The Cruce Anticline has a detachment in both the Arbuckle Group and the Springer Shale which results in a similar geometry to Carter-Knox with a tight faulted fold above a more concentric faulted fold (Saxon, 1998). Saxon described the shallow structure as a fault-propagation fold that plunges at very high rates to the northwest. Throw on this fault is unknown but appears to exceed 5,000 feet based on Saxon's cross section. The deeper fold is slightly more concentric but is also faulted by an east-northeast verging thrust fault extending from the Arbuckle detachment. Although his focus area was just to the east of the Cruce Anticline near the Velma trend, Jacobson (1984) described the syn-depositional history of the Harrisburg Trough indicating structural movement and timing along this trend. The Harrisburg Trough was a paleo valley originally described by Harlton (1956) that may have had a topographic relief of more than 5,000 feet (Jacobson, 1984). Atokan age units form a thick wedge in the trough suggesting the Cruce Anticline structures started to grow during that time (Jacobson, 1984). Saxon (1998) also shows a growth wedge of Atokan sediment on his cross section over the Cruce Anticline. Desmoinesian age units are also shown to thin onto the structure while Missourian age units show less thinning suggesting the Wichita Uplift had become submerged and buried by Missourian sediment (Jacobson, 1989; Saxon, 1998). Virgilian age units form a wedge of growth

sediments indicating that the present-day structure was likely formed during the Arbuckle Orogeny (Jacobson, 1984; Saxon, 1998). A major unconformity exists at the base of the Permian and experienced only mild compression (Jacobson, 1984).

4.3 Chickasha Anticline

The Chickasha Anticline is a NW-SE oriented structure that bends sharply to form the Cement structure. Early cross sections over the field show a northeast verging faulted anticline that is detached from a deeper more concentric fold below the Springer detachment (Herrmann, 1961). The throw on the reverse fault is approximately 3,700 feet (Herrmann, 1961). The Morrowan shows slight thinning over the structure, but the main growth began in the Atokan and continued into the Permian (Herrmann, 1961). The greatest amount of structural growth occurred in the Missourian and Virgilian, followed by truncation from the Permian Unconformity with only minor reactivation (Herrmann, 1961).

4.4 Cement Fault Zone and Anticline

The Cement Fault is oriented approximately E-W and extends from the Cement Field to the east where it makes up the northern boundary of the Golden Trend before abutting against the N-S oriented Nemaha Fault. The Cement structure comprises two major culminations which contain the West Cement Field and the East Cement Field. Early analyses on the Cement Field show cross sections similar to Carter-Knox, Cruce, and Chickasha Anticlines, with a tight faulted anticline above the Springer detachment and a more concentric fold in deeper pre-Pennsylvanian units (Harlton, 1960; Herrmann, 1961). The crest of the Cement Anticline was interpreted to be cut by several normal faults that are sub-parallel to the structure (Harlton, 1960; Herrmann, 1961). The throw on one of these normal faults was estimated to be up to 2,800 feet in West Cement at the Hoxbar level and less than 100 feet in East Cement (Herrmann, 1961). The major

reverse fault cutting the structure was shown to have a throw of about 1,000 feet in West Cement and 2,800 feet in East Cement (Herrmann, 1961). Although the Morrowan units are relatively uniform over the Cement structure, East Cement was depicted to show some thinning near the crest, suggesting it could have been active during that time (Herrmann, 1961). The structure began its main growth during the Atokan and continued with little to no interruption into the Permian as indicated by continuous thinning of Desmoinesian, Missourian, and Virgilian age units onto the structure which were then peneplaned by the Permian Unconformity (Herrmann, 1961).

Alternatively, Saxon (1998) described the Cement Anticline as a foreland detachment structure and showed multiple detachment levels including some in the Springer, Desmoinesian, and Arbuckle. His cross sections show that the detachments branch into complex imbricates as they die upward into the fold with some even breaking the forelimb of the fold. A southwest-verging thrust fault also detaches in the Springer creating a triangle zone above the forelimb syncline of a deep fault-propagation fold in pre-Pennsylvanian units (Saxon, 1998). His depiction of the Cement Anticline is similar to the Carter-Knox or Cruce Anticlines in that they are thin-skinned and do not involve the basement nor strike-slip movement. Timing of the structure is similar to previous interpretations that suggest there was early rapid growth during the Morrowan and Atokan as evident by thinning on the crest, and that this structure was active till the Permian with only minor folding occurring post-Permian (Saxon, 1998).

5. Data and Methods

The dataset includes several 3D seismic surveys along with wells and well log data. The 3D seismic surveys cover the eastern Wichita Mountain front and the Washita Valley Fault as well as the Carter-Knox, Cruce, Chickasha, and Cement structures in the study area (Figure 3.3).

Interpretations were initially made in seismic time profiles. Sonic logs were used to make well ties to the seismic data and to determine appropriate time-depth charts for wells without sonic data. Well logs were used to interpret formation tops and fault picks. Dip-meter data was used when available. When dip-meter data was not available, relationships between true thickness and apparent thickness were used to calculate bed dip angle. This information was projected onto the seismic time profiles. Seismic time interpretations were converted to depth. Both regional and local sections were constructed to interpret individual structures and their relationship to regional tectonics.

A number of the cross sections were restored to illustrate the evolution and timing of major structures. The sections were restored using both line-length and area-balancing methods. Several cross sections were also supplemented by structure maps and time slices to study variations in structural styles and fault geometries along trend.

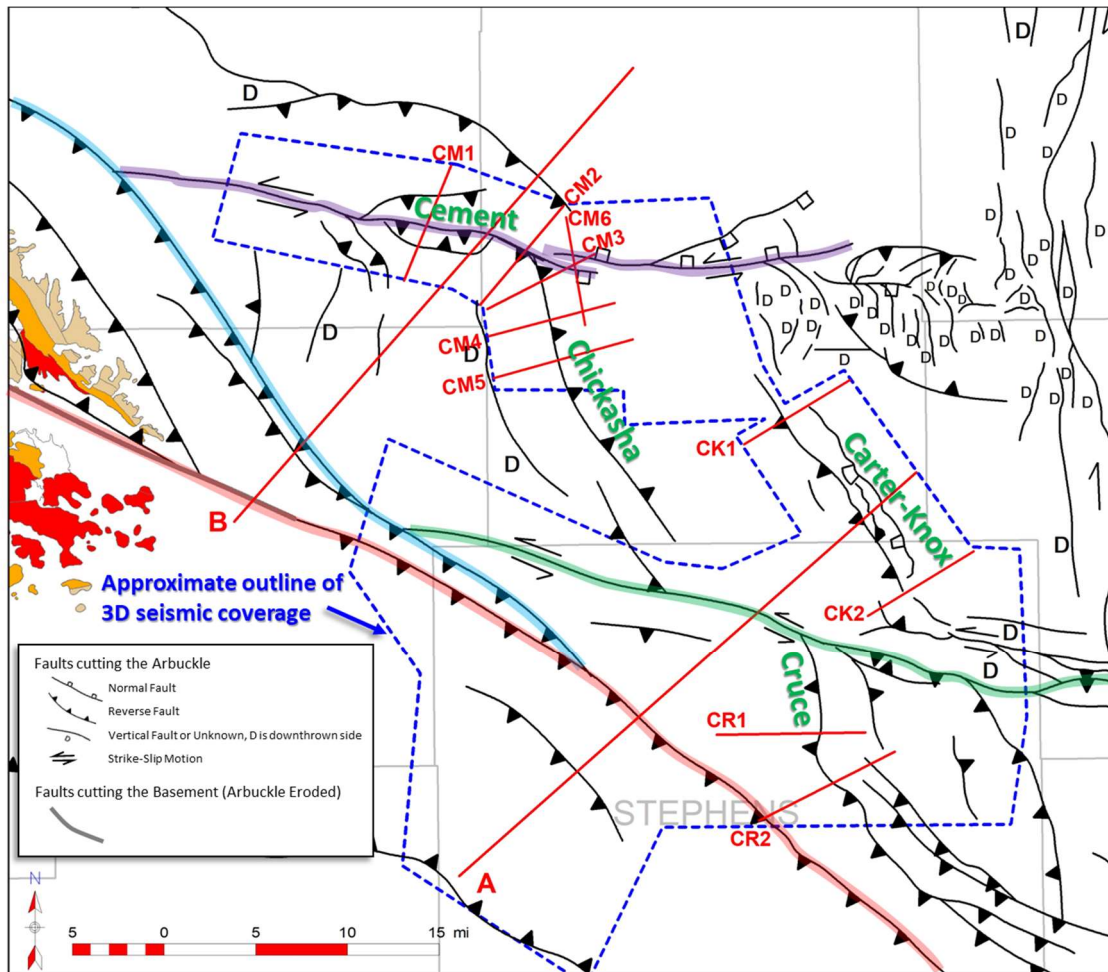


Figure 3.3 Map showing locations of cross sections (red), field names (green), and approximate outline of 3D seismic coverage (blue dashed line). Trace of the Washita Valley Fault is highlighted in green, Cement Fault in purple, Mountain View Fault in blue, and Wichita Mountain Fault in red. Faults are mapped at the Arbuckle level, except a small part of the Wichita Mountain Fault is mapped on the basement near the Slick Hills where the Arbuckle is eroded. Pre-Pennsylvanian surface geology on the southeast end of the Wichita Uplift is from USGS (Heran et al., 2003).

6. Results

6.1 Structure Map

Twelve cross sections were constructed over the southeastern Anadarko Basin and are shown on the Mississippian Sycamore structure map in Figure 3.4. The map was constructed using formation tops from well logs as well as seismic data. The cross sections extend over the Carter-Knox, Cruce, Chickasha, and Cement structures along with two regional cross sections that extend over the Wichita Uplift. The Sycamore Group is eroded off the Wichita Uplift but extends over parts of the Slick Hills Block making up anticlinal structures representing the Fort Sill, Apache, Alden, Carnegie, and Gotebo Fields. The Wichita Mountain Fault and the Carter-Knox, Cruce, and Chickasha Anticlines trend NW-SE. These structures are cut by thrust faults. A southwest-dipping normal fault has been mapped along the east side of the Carter-Knox structure that cuts up into the Sycamore Formation. Other normal faults can be mapped along the Nemaha trend and Cement Fault trend. The Cement Fault and the Washita Valley Fault trends are oriented more E-W and marked by left-lateral strike-slip symbols. The Cement Fault trend east of the Chickasha Anticline consists of a north-dipping normal fault leading into the Golden Trend. The Golden Trend is a west-plunging structural nose that consists of an array of small-offset high-angle normal faults. These faults primarily drop down-to-the-west. The southern boundary of the Golden Trend is marked by a south-verging reverse fault while the eastern boundary is the N-S trending Nemaha Fault zone. This fault zone consists of several high-angle N-S faults that drop down towards the west. It has historically been interpreted as a pre-existing structure reactivated in right-lateral strike-slip during the Pennsylvanian (Amsden, 1975; Budnik, 1986; McBee, 2003; Friess, 2005). Along the Nemaha Trend, and eastward, the Sycamore becomes eroded due to uplift of the Pauls Valley. South of this uplift is the very western extent

of the Arbuckle Anticline where the Sycamore has been eroded. South of this area, the Cruce Anticline curves to become more parallel with the Wichita Mountain Fault and splits into a series of large faulted anticlines. This area is known as the Velma trend and continues into the Ardmore Basin. The north end of the Cruce Anticline abuts up against the Washita Valley Fault. Cross sections have been constructed over the Carter-Knox, Cruce, Chickasha, and Cement structures to show how they are inter-related. Two regional cross sections have also been constructed to illustrate the relationship to the Wichita Uplift. Together these cross sections provide insight to the tectonic evolution of the study area.

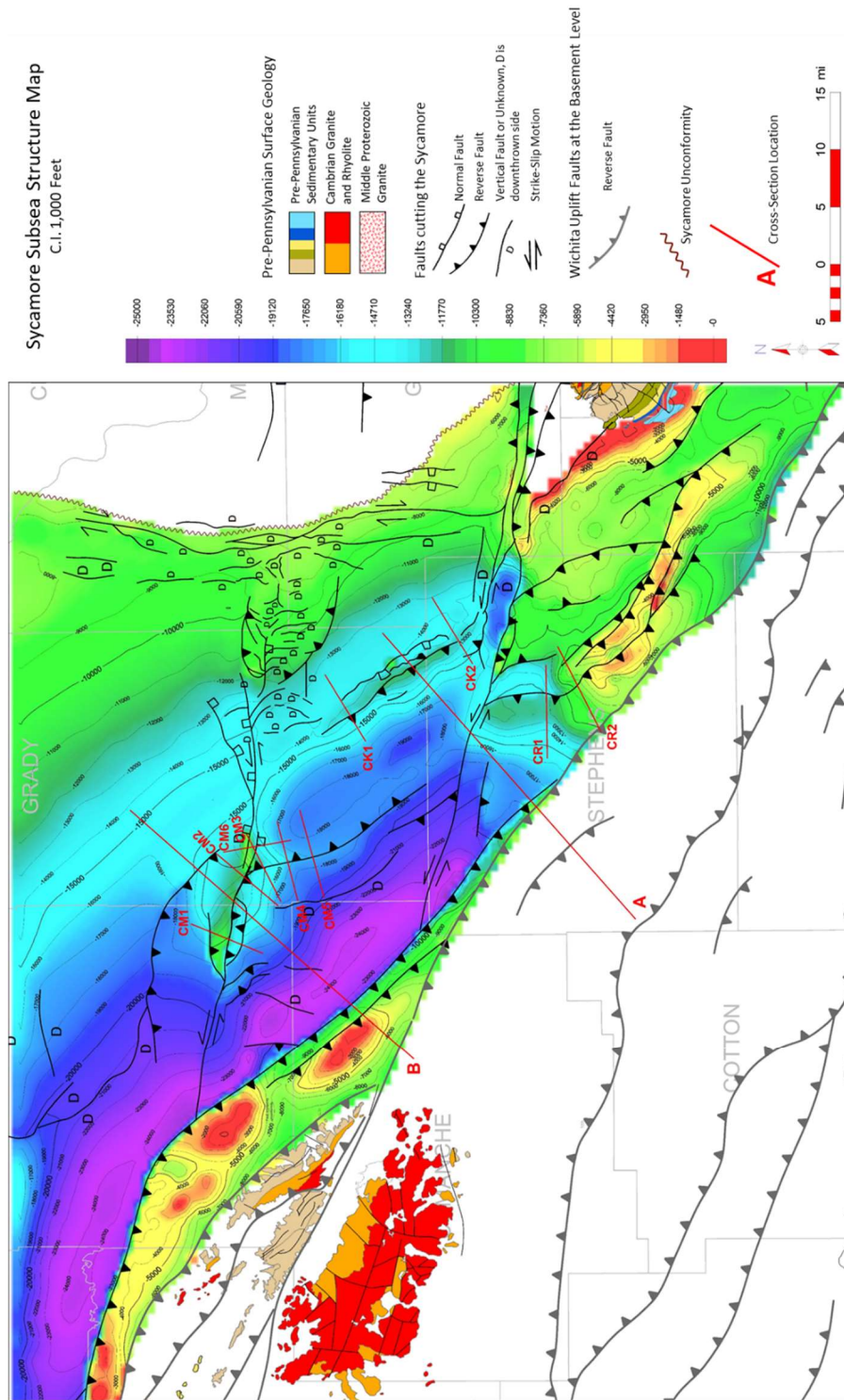


Figure 3.4 Subsea structure map on top of the Mississippian Sycamore Formation, contour interval is 1,000 feet. Cross section locations are shown in red. Faults on the Wichita Uplift shown in bold gray are at the basement level. Sycamore is eroded off of the Pauls Valley Uplift in the east. Pre-Pennsylvanian surface geology on uplifts is from USGS (Heran et al., 2003).

6.2 Carter-Knox Structure

Regional cross section A shows the link between the Wichita Uplift and the Carter-Knox structure (Figure 3.5). It extends over the Wichita Uplift towards the northeast into the Carter-Knox Field and highlights the significant unconformities, the impact of mechanical stratigraphy, and changes in structural styles. The Wichita Mountain Fault brings up the core of Wichita Uplift and is also responsible for much of the slip along the Springer detachment. Slip on the Springer detachment is dissipated along a number of forward-propagating imbricates, culminating in the Carter-Knox structure. Movement on these imbricates is episodic as indicated by the truncation and reactivation of some of the faults at multiple unconformities. Footwall imbricates underlying the Wichita Mountain Fault transfer slip to a detachment at the base of the Arbuckle Group, which is transferred into the Carter-Knox structure.

A significant amount of slip is transferred into the Carter-Knox structure. This structure is interpreted to be a faulted-detachment fold (Mitra, 2002) generated from slip along the Springer detachment with a steep to vertical front limb. Offset of the main thrust fault is close to 4,500 feet along this cross section. Flowage of the Springer Shale causes thickening in the core of the fold and the formation of two imbricate thrust faults. The faulted-detachment fold is limited to the Pennsylvanian units, consisting primarily of thin-bedded clastics. Pre-Pennsylvanian units below the Springer detachment consist of several thicker carbonate packages and show a different structural style than the clastic units above. Slip along a detachment at the base of the Arbuckle formed a broad faulted fold below the tight faulted-detachment fold. Two normal faults extend along the base the Carter-Knox structure and may have acted as a buttress to slip along the Arbuckle detachment causing the structure to form where it did.

Growth units of the Carter-Knox structure show that it was active from the Atokan through Virgilian prior to truncation by the Permian Unconformity. Morrowan units are relatively uniform over the structure while Atokan through Virgilian units thin and onlap the structure. In the seismic data (Figure 3.5A), the Missourian units can be seen onlapping the Desmoinesian units, while the Virgilian units can be seen onlapping the Missourian units. As the structure grew, a hinge in the basement developed due to sedimentary loading resulting in the thickened growth units along the southwestern flank of the structure. This hinge can be observed in the cross sections between the second normal fault at Carter-Knox and the Washita Valley Fault.

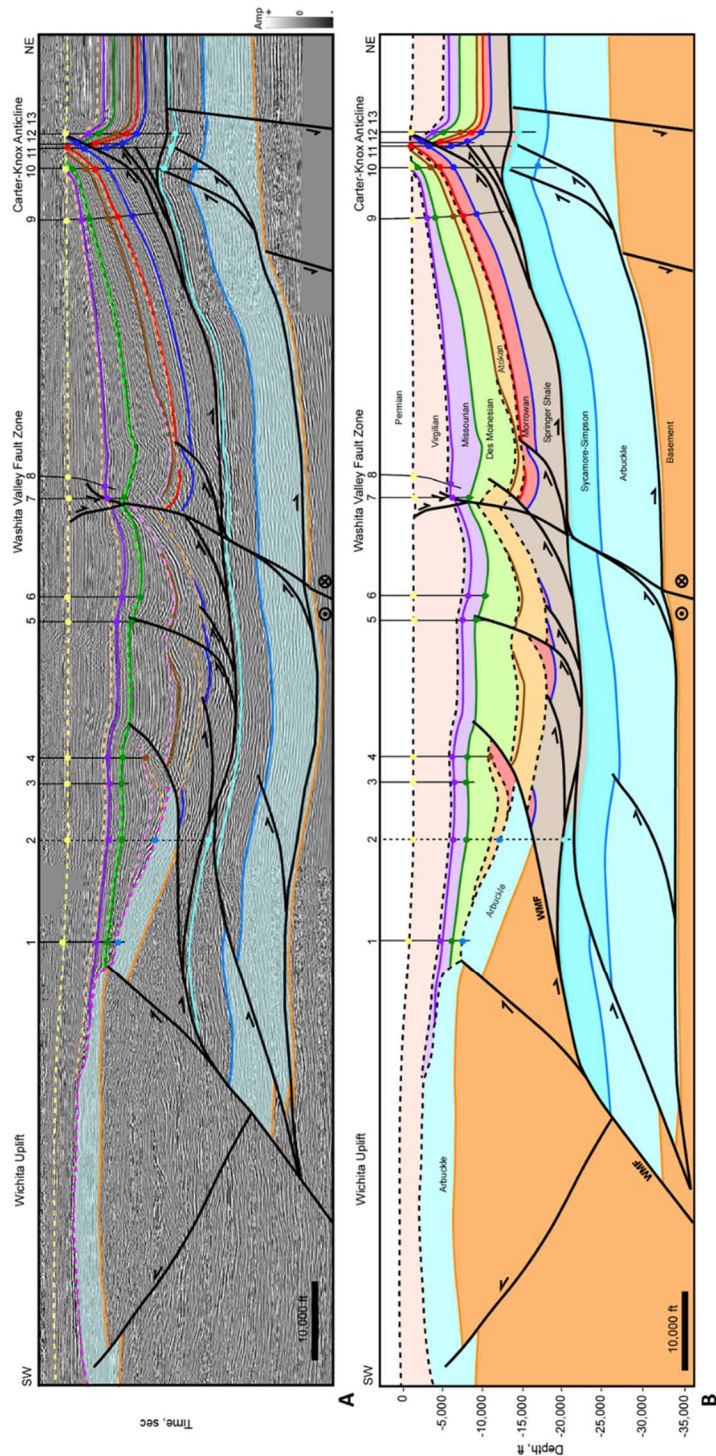


Figure 3.5 Regional cross section A. (A) Interpreted seismic section in time. Time scale removed from proprietary data. Horizon colors are shown in Figure 3.2. (B) Depth cross section. Well information is listed in appendix 1. Well tops (colored circles), dip data (brown check mark), and fault picks (red x) are shown where available. Dashed well is projected 9 miles. Seismic Data Courtesy of Chesapeake Energy & SEI.

Regional cross section A extends through central the central part of Carter-Knox. A more detailed cross section CK1 extends through the northwest end of the structure (Figure 3.6). The structural style of this cross section is similar to cross section A except that the displacement along the main thrust fault is less preserving some of the details of the structure, especially in the Late Pennsylvanian units. The structure is defined by two structural units, a deeper unit made up dominantly of thick carbonates from the Arbuckle to Sycamore and a shallower unit made up of thin-bedded Pennsylvanian clastics. These two packages are separated by the Springer Shale that acts as a detachment. A second detachment is observed at the base of the Arbuckle. Slip along the Arbuckle detachment allowed a northeast-verging thrust fault and backthrust to cut the deeper section resulting in a gentle faulted fold. The basement under the structure is not involved in the folding but does show a change in dip under the crest of the structure. This change in dip represents a flexural hinge that developed as sediments were deposited resulting in the stratigraphic changes of the Atokan to Virgilian growth section. All these units show an increase in thickness on the southwestern flank of the structure from sedimentary loading.

Figure 3.7 shows the kinematic reconstruction of cross section CK1 showing the structural evolution of Carter-Knox. The steps in the reconstruction include (1) restoration of the faulting (Figure 3.7B) enabling an understanding of the fold geometry; (2) restoration to the end of Missourian (Figure 3.7C) showing the relative lengths of the mapped growth units; and (3) restoration of the Morrowan and older units to their undeformed state to compare the shortening of different structural units (Figure 3.7D).

Because the Springer Shale shows significant flowage, restoration to the undeformed stage uses area restoration, in two steps (Figure 3.8). Line-length restoration results in a shorter line length of the basal unit of the detachment compared to the top of the detachment (Springer),

resulting in a negative shear in the restored state (Figure 3.8B). To area restore the package the area was divided by the original thickness (t) to obtain the average restored length (l_0) (Figure 3.8C). The Morrowan to Springer package shows a larger restored length so that the Springer detachment between the two sequences separates simultaneous but different amounts of contractional deformation (Figure 3.7D). The units between the Morrowan and the Permian Unconformity show progressively shorter lengths of stratigraphically higher units (Figure 3.7C), which is typical of growth packages in contractional settings. Furthermore, the growth units thicken progressively down-dip on the southwest flank suggesting growth of the Carter-Knox structure was accompanied by a downwarp associated with sedimentary loading due to thrusting and uplift of the Wichita front. This down-warping likely occurred along a flexural hinge located below the crest of the Carter-Knox structure which can be seen in both cross sections. Both the regional cross section and CK1 illustrate the impact of mechanical stratigraphy on structure as well as the impact of the forward-shear motion from the Wichita Mountain Fault.

Section CK2 (Figure 3.9) is on the southern segment of the structure with significantly lower relief and displacements on the Carter-Knox thrust (less than 500 feet). The structure is cut by an oblique E-W dipping normal fault that drops down or cuts through the Permian displacement, suggesting that the fault formed after the formation of the main Carter-Knox structure. This fault appears to detach in the Springer detachment and carry slip back towards the southwest. The post-Hoxbar stratigraphy is thickened (growth section) in the large dropped-down block along this fault indicating the timing. The lower structural package is also marked by a southwest verging structure with a back thrust showing the change in vergence from previous cross sections. A detailed structural analysis of Carter-Knox is discussed further in Chapter 4.

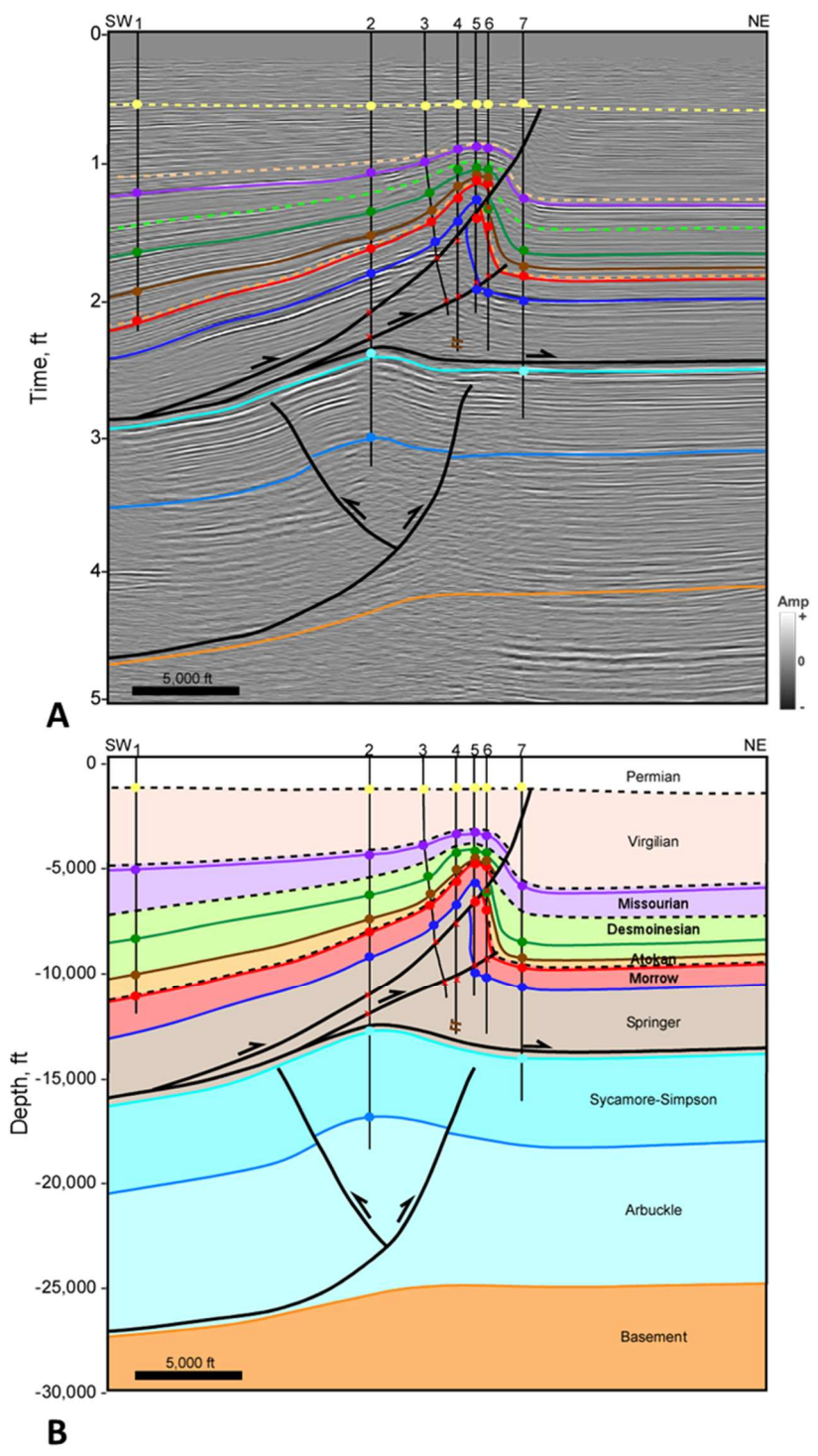


Figure 3.6 Cross section CK1 over the Carter-Knox structure (A) Interpreted seismic section in time. Horizon colors are shown in Figure 3.2. (B) Depth cross section. Well information is listed in appendix 1. Well tops (colored circles), dip data (brown check mark), and fault picks (red x) are shown where available. Seismic Data Courtesy of Chesapeake Energy.

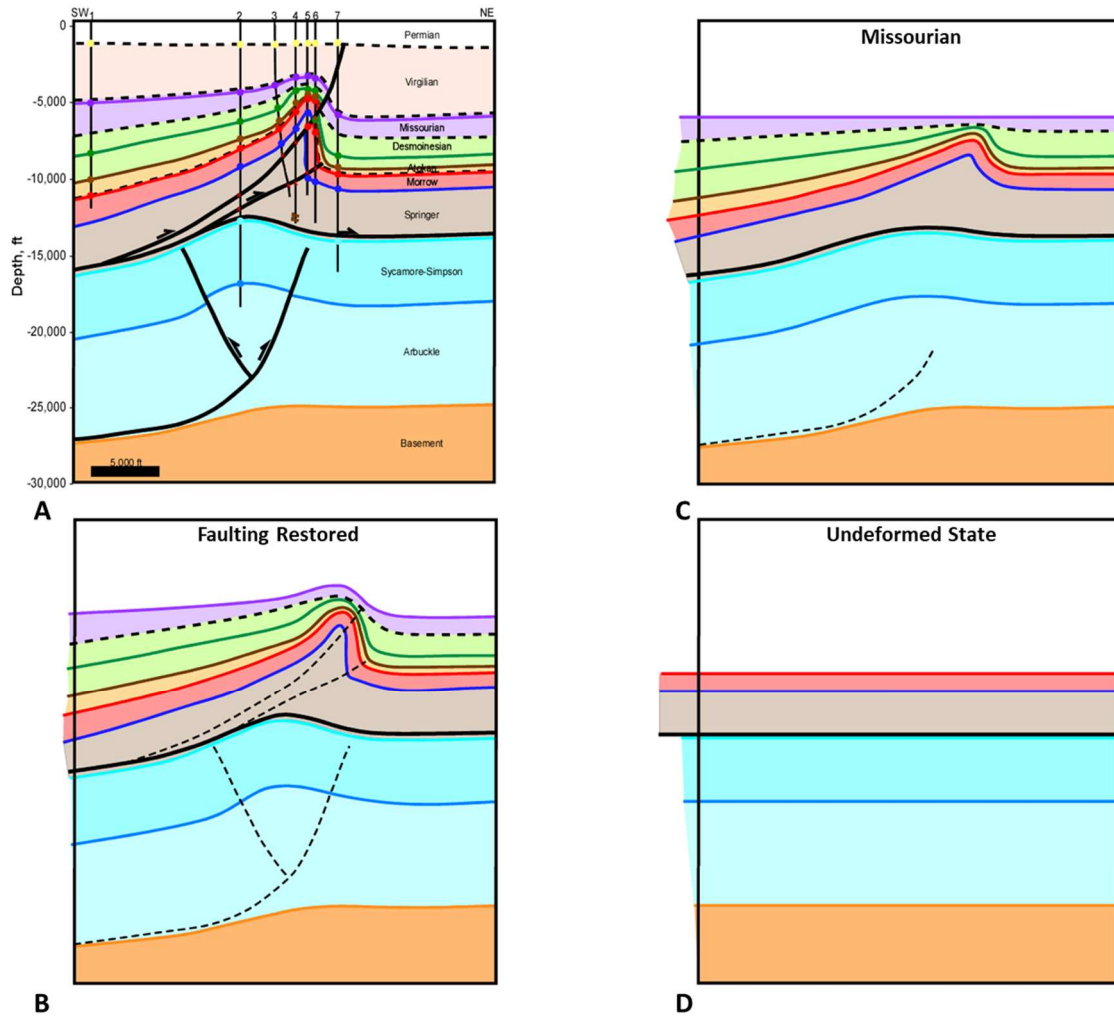


Figure 3.7 Kinematic reconstruction and structural evolution of section CK1 (A) Depth cross section. (B) Faulting is restored and dashed to illustrate fold geometries. (C) Structure is restored to Missourian time with the Hoxbar horizon flattened. (D) Morrow and older units are restored to their undeformed state. Initial dips of these units are not known, so units are shown as horizontal.

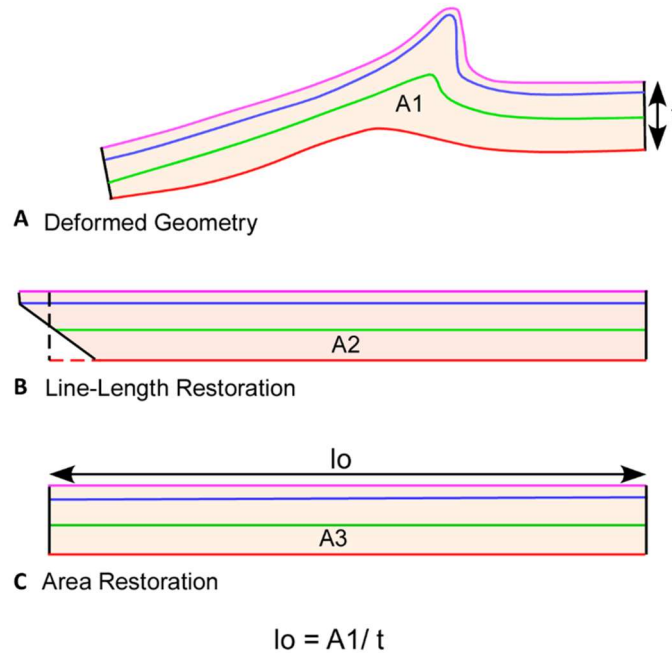


Figure 3.8 Method of area restoration applied to the units between the Springer detachment and the top of the Morrow/Springer Formation. (A) Final cross section. (B) Line-length restoration showing a wedge-shaped geometry resulting from differential strain of individual units. (C).

Restoration with the area balanced into a rectangle shape. The height of the rectangle is determined by the average thickness (t), and the average restored length (l_o) is determined by dividing the area (A) by t .

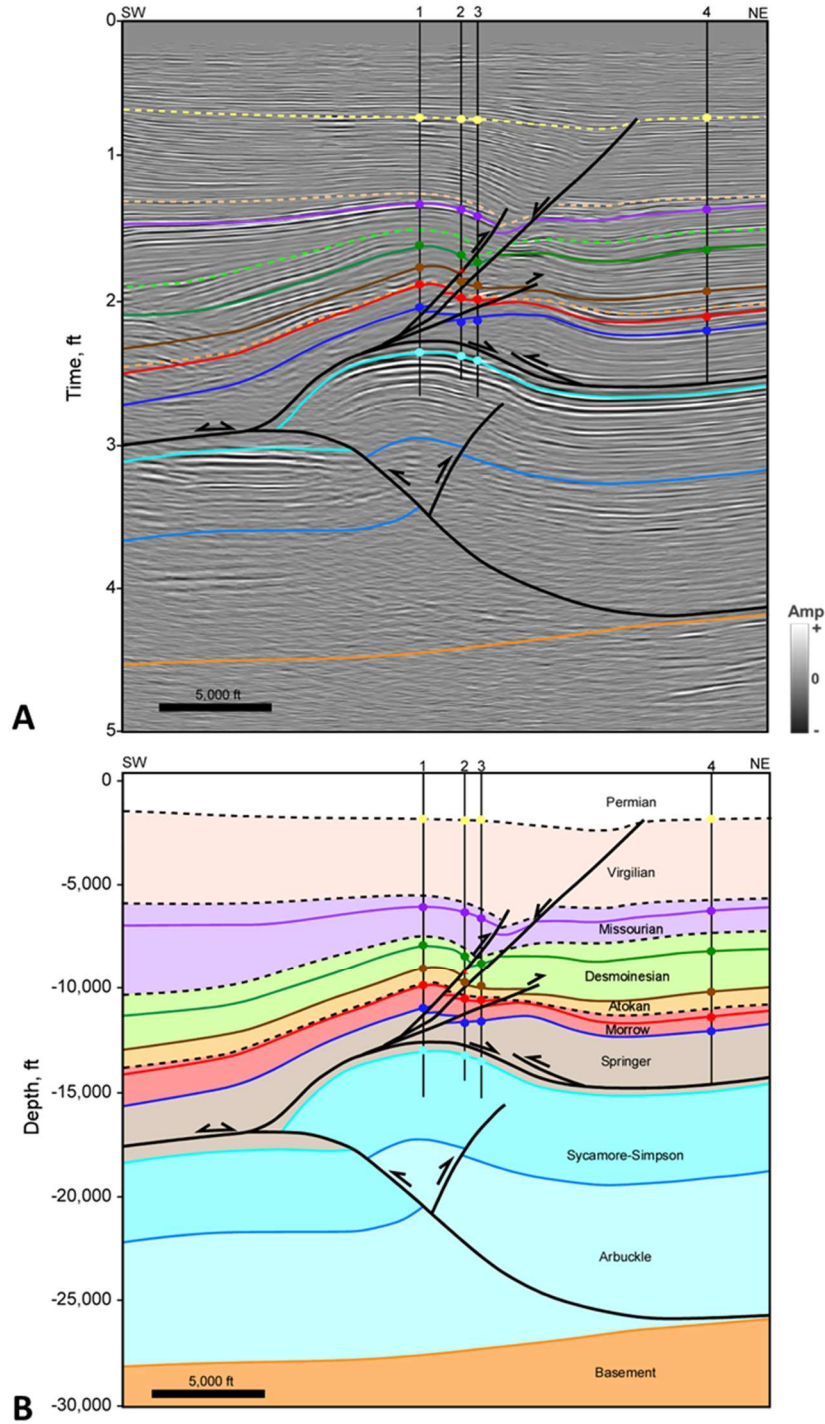


Figure 3.9 Cross section CK1 over the Carter-Knox structure (A) Interpreted seismic section in time. Horizon colors are shown in Figure 3.2. (B) Depth cross section. Well information is listed in appendix 1. Well tops (colored circles), dip data (brown check mark), and fault picks (red x) are shown where available. Seismic Data Courtesy of Chesapeake Energy.

6.3 Cruce Structure

The Cruce structure has a similar geometry to Carter-Knox. Its trend varies between NNW-SSE and NW-SE along trend. The northern termination of the structure is marked by an E-W trending fault. The Cruce structure is significantly oblique to the Wichita front compared to the other structures discussed in this study. This may be due to the oblique orientation of the pre-existing basement fault which controlled the trend of the structure. As in Carter-Knox, two structural packages with different structural styles are separated by the Springer detachment (Figures 3.10 and 3.11). Above the Springer detachment, the Cruce Anticline is a tight, asymmetrical faulted-detachment fold with a steep to vertical front limb and a large through-going thrust fault that soles out onto the Springer detachment. In cross section CR1, the offset on the large thrust fault is unknown due to erosion but is estimated to be greater than 8,000 feet, almost twice as much as the 4,500 feet estimated at Carter-Knox. In cross section CR2 the offset is close to 6,000 feet suggesting decreasing displacement toward the southeast. A southwest verging thrust fault near the core of the detachment fold results in a small triangle zone. A lower amplitude fold makes up the deeper structure of the Cruce Anticline. Northeast-verging thrust faults cut this fold and sole out onto the Arbuckle detachment. Offset on these faults is small, likely less than 100 feet. A southwest dipping normal fault is interpreted to cut the basement below this structure based on changes observed in the seismic reflectors. This basement-rooted normal fault is a pre-existing rift fault.

Cross section CR2 is closer to the Wichita Uplift and shows the relationship between the Wichita Mountain Fault and structures in the basin. The Wichita Mountain Fault flattens along the Springer detachment allowing slip to be transferred into the basin resulting in a greater amount of slip along the upper section compared to the deeper section. An unconformity at the

base of the Atokan that truncates the Wichita Mountain Fault shows that a significant amount of slip occurred during the Morrowan, while another unconformity at the base of Desmoinesian suggests the reactivated fault continued to remain active during the Atokan. Desmoinesian and Missourian units are folded over the tip of the Wichita Mountain Fault but showing thinning and significant offset over the Cruce Anticline. During this time much of the slip on the Wichita Mountain Fault was transferred into the basin along the Springer detachment resulting in the growth of the Cruce structure.

The growth history of the Cruce Anticline is shown in the kinematic restoration of cross section CR1 (Figure 3.12). This cross section was restored in the same manner as cross section CK1 using both line-length and area-balancing methods. In the first step (Figure 3.12B), the crest of the anticline was restored prior to erosion based on the offset and thickness of footwall units. An unconformity at the base of Desmoinesian truncated almost all the Atokan sediments towards the east. This is more apparent in Figures 3.12C and D. In Figure 3.12C the faulting has been restored on the Missourian and Desmoinesian units, while a small amount of faulting remains across the lower Pennsylvanian units. Although faulting and folding likely occurred simultaneously, this step illustrates the geometry of the Cruce anticline without the faulting.

In Figure 3.12D, the structure is restored to the end of the Missourian. The Missourian and Desmoinesian units are both nearly conformable, whereas the Springer through Atokan units show a higher dip. The length of the Morrowan units and higher decreases up-section, highlighting that these are growth units. The discrepancy between the lengths of the top and bottom of the Springer Shale is due to the flow of this unit into the core of the anticline. This was addressed by area balancing the units in the final restoration step. The unconformity at the base of the Desmoinesian suggests the basin was dipping prior to deposition allowing the preservation

of down-dip units and erosion of up-dip Atokan and Morrowan units. Down-warping likely occurred along a flexural hinge located below the crest of structure due to sedimentary loading and thrusting of the Wichita front. That hinge was likely focused around the pre-existing normal fault in the basement.

In the last step (Figure 3.12E), the Springer and older units were restored to their undeformed state to compare simultaneous but different amounts of shortening. The Springer unit is significantly longer than the deeper units. This suggests a forward-shear motion on the Wichita Mountain Fault, which also impacted the Carter-Knox structure, but to a lesser extent. While the Virgilian units were not incorporated into the reconstruction, the seismic horizons are seen onlapping the Missourian units. Therefore, the growth of this structure occurred from the Morrowan to Virgilian before being truncated by the Permian Unconformity. Minor folding of the Permian Unconformity in cross section CR1 suggests a mild reactivation.

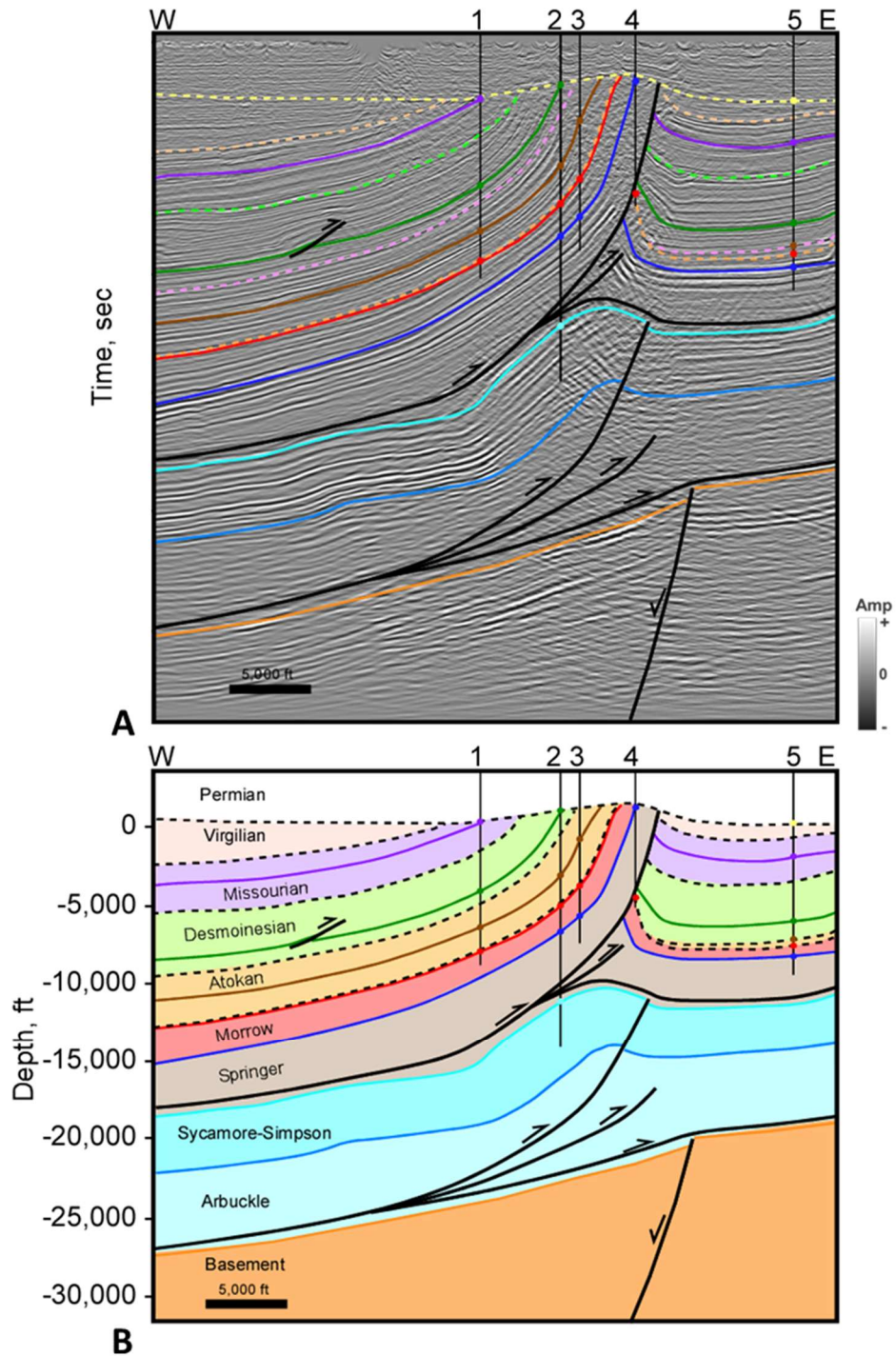


Figure 3.10 Cross section CR1 over the Cruce structure (A) Interpreted seismic section in time. Time scale removed from proprietary data. Horizon colors are shown in Figure 3.2. (B) Depth cross section. Well information is listed in appendix 1. Well tops (colored circles), dip data (brown check mark), and fault picks (red x) are shown where available. Seismic Data Courtesy of SEI.

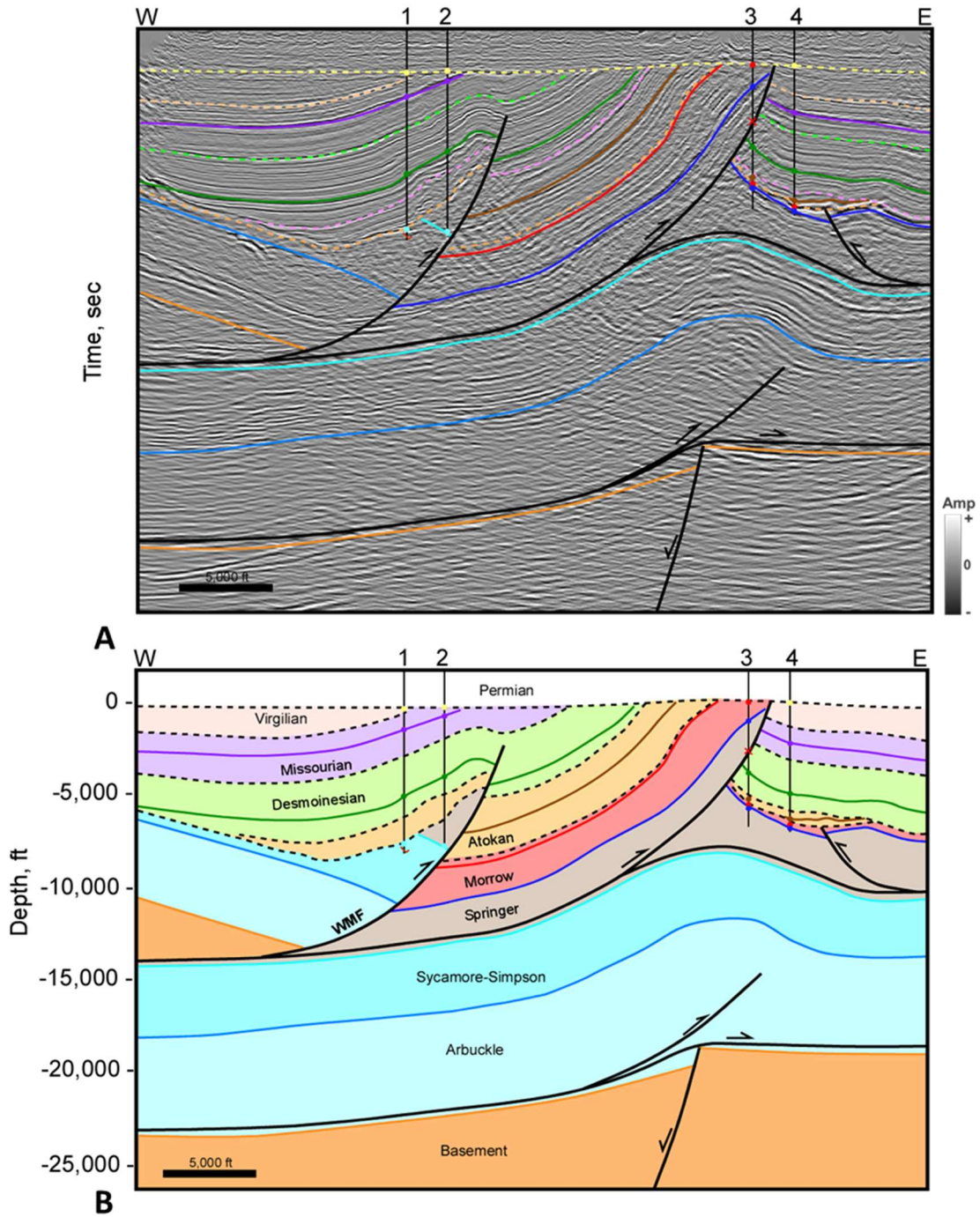


Figure 3.11 Cross section CR2 over the Cruce structure (A) Interpreted seismic section in time. Time scale removed from proprietary data. Horizon colors are shown in Figure 3.2. (B) Depth cross section. Well information is listed in appendix 1. Well tops (colored circles), dip data (brown check mark), and fault picks (red x) are shown where available. Seismic Data Courtesy of SEI.

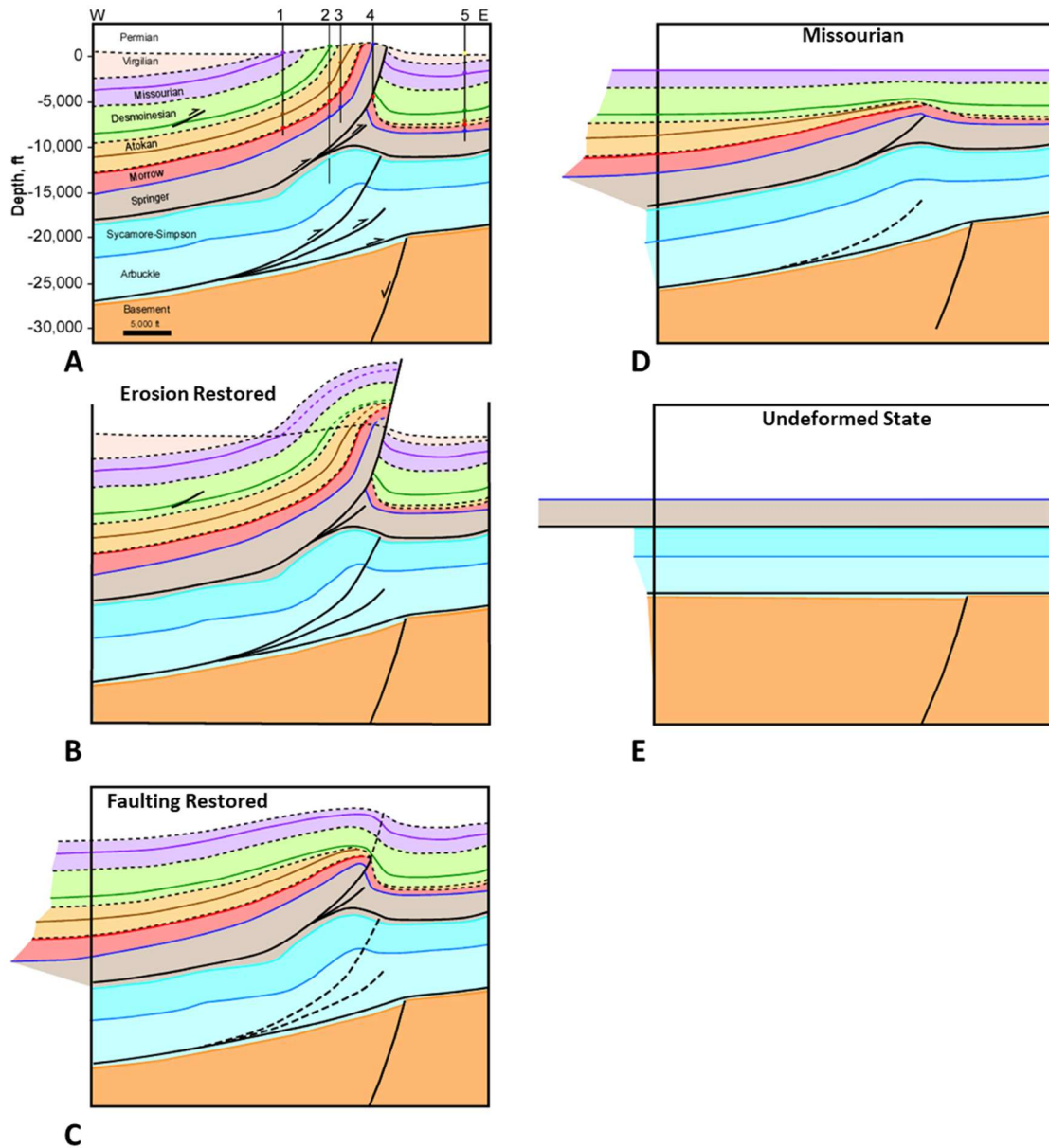


Figure 3.12 Kinematic reconstruction and structural evolution of section CR1 (A) Depth cross section. (B) Faulting is restored and dashed to illustrate fold geometries. (C) Structure is restored to Missourian time with the Hoxbar horizon flattened. (D) Springer and older units are restored to their undeformed state. Initial dips of these units are not known, so units are shown as horizontal.

6.4 Chickasha Structure

The Chickasha structure is a NW-SE oriented anticline which bends sharply to the west-northwest to form the Cement structure. Figure 3.13 shows a structure map over the Cement-Chickasha trend constructed on the Missourian Hoxbar horizon and shows the location of cross sections that traverse this structure.

Cross sections CM4 and CM5 over the Chickasha structure (Figures 3.14 and 3.15) exhibit a broad faulted-detachment fold above the Springer detachment cored by a gentle structure below. The main thrust fault creating the faulted-detachment fold verges to the northeast and is accompanied by a small backthrust. A second imbricate on the Springer detachment verges to the southwest in the core of the fold creating a small triangle zone. The offset of the main thrust fault is similar in both cross sections, CM4 and CM5, with about 2,000 feet on the Springer and only 1,300 feet on the Hoxbar, much less than on the Carter-Knox (4,500 feet) and Cruce (+8,000 feet) thrust faults. The deeper structure consists of a southwest verging thrust fault that soles out in the Arbuckle detachment. The offset on this fault is small and creates a minor fold in the Arbuckle through Sycamore units. The basement is relatively flat under the structure.

The growth history is similar to both Carter-Knox and Cruce and can be seen in the kinematic reconstruction of cross section CM4 in Figure 3.16. This cross section was restored in the same manner as cross sections CK1 and CR1 using both line-length and area-balancing methods. In Figure 3.15B the faulting has been restored to illustrate the fold geometry. Restoration to the Missourian (Figure 3.16C) shows a gentle faulted fold, marked by thinning of Atokan and Desmoinesian units onto the crest of the structure. Although the Virgilian is not shown in the restoration, the Virgilian seismic reflectors appear to onlap and become folded over

the structure indicating the structure was active from the Atokan through Virgilian. In Figure 3.16D, the Morrowan and older units were restored to their undeformed state to compare simultaneous but different amounts of shortening. The restored Morrow-Springer package has a greater length than the deeper units but, the difference is significantly smaller than for the Carter-Knox and Cruce structures.

In summary, the Carter-Knox, Cruce, and Chickasha structures show similar structural styles as well as similar growth histories. However, the Chickasha structure is associated with much less shortening than the Cruce and Carter-Knox structures. These three anticlines make up the NE-SW oriented structures in the southeast Anadarko Basin.

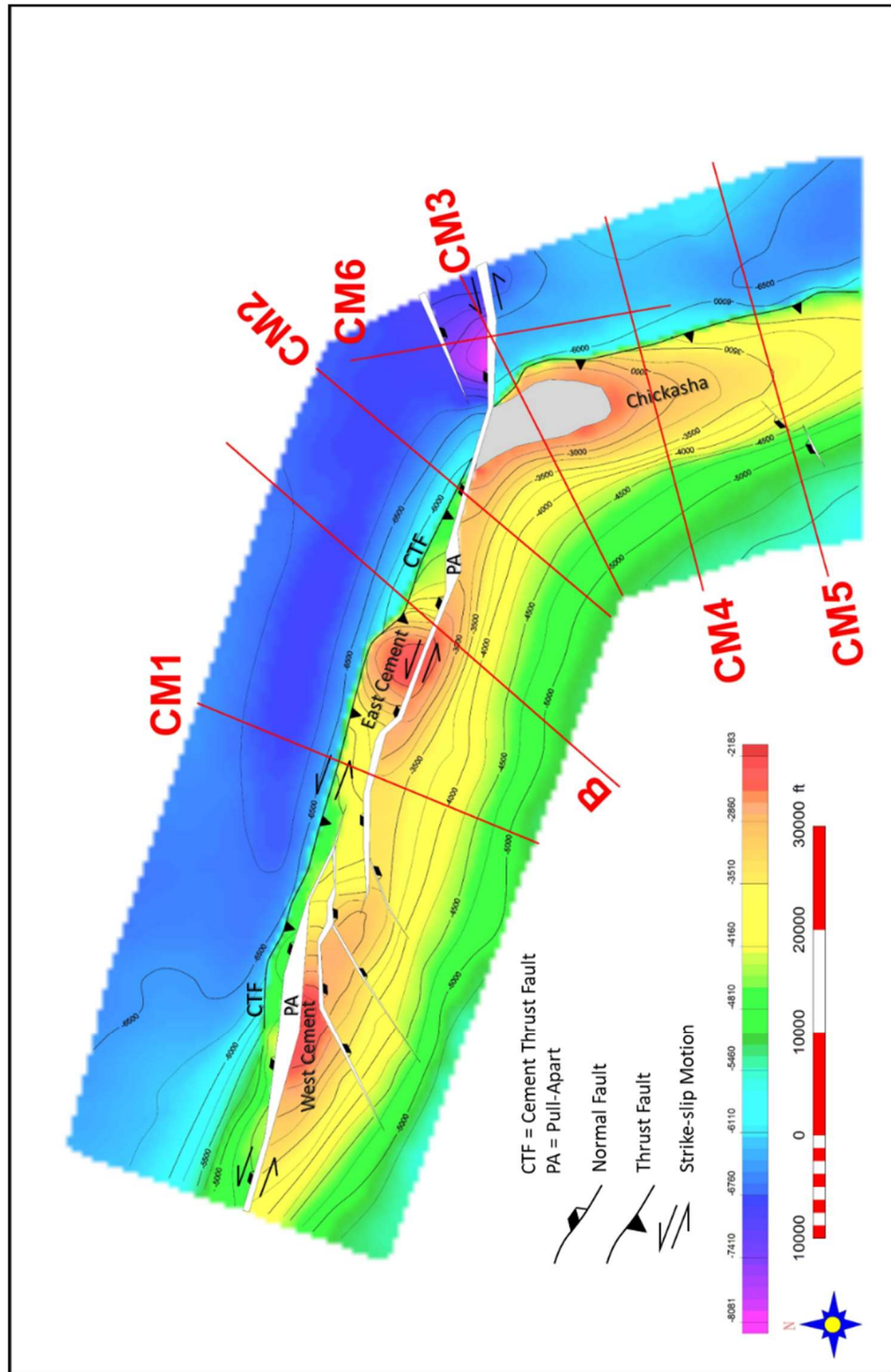


Figure 3.13 Missourian age Hoxbar subsea structure map over the Cement-Chickasha structure. Contour interval is 500 feet. West Cement, East Cement, and Chickasha Fields are labeled. Part of the Hoxbar is eroded on the Chickasha structure in gray. Cement-Chickasha cross section locations are shown in red.

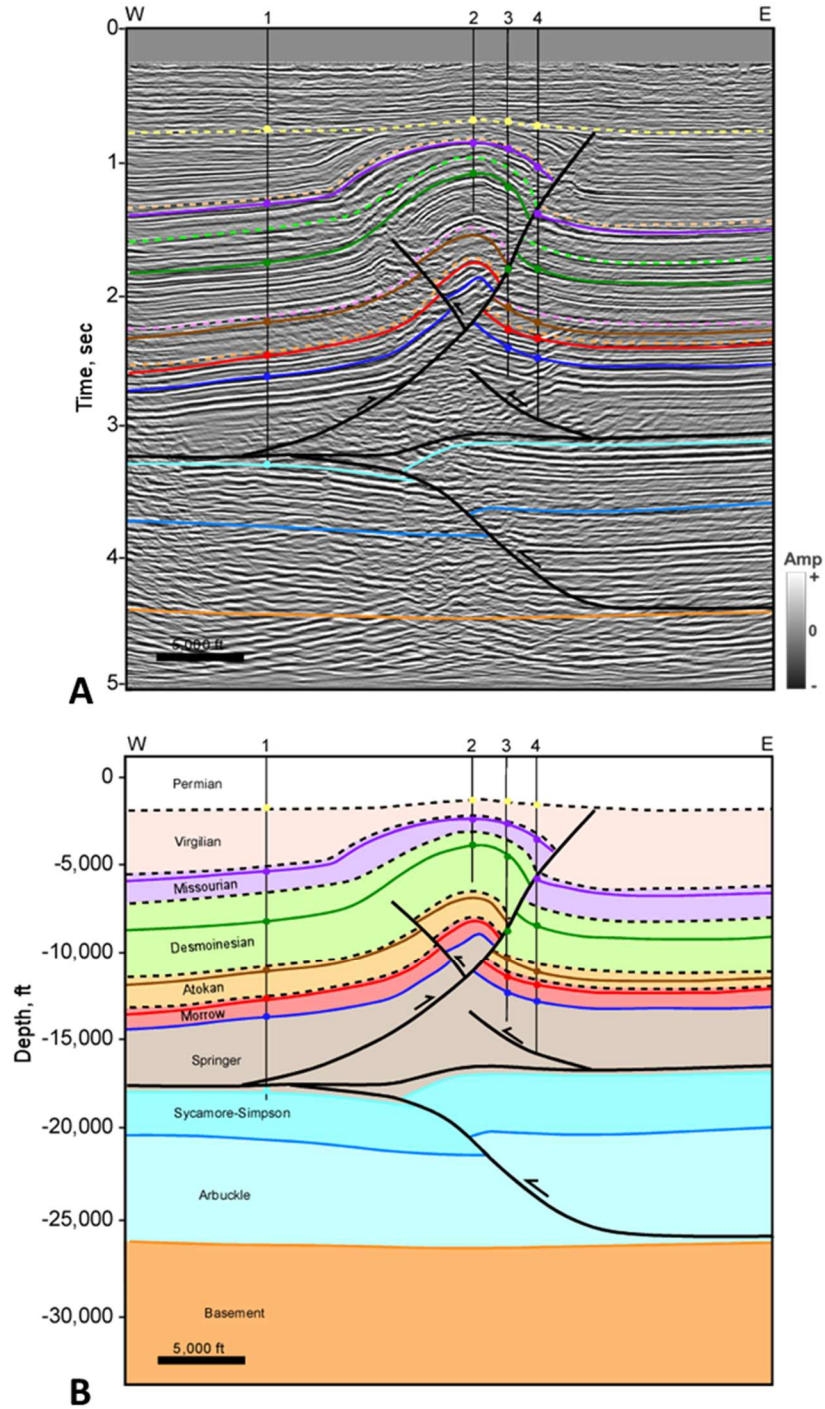


Figure 3.14 Cross section CM4 over the Chickasha structure (A) Interpreted seismic section in time. Horizon colors are shown in Figure 3.2. (B) Depth cross section. Well information is listed in appendix 1. Well tops (colored circles), dip data (brown check mark), and fault picks (red x) are shown where available. Seismic Data Courtesy of Chesapeake Energy.

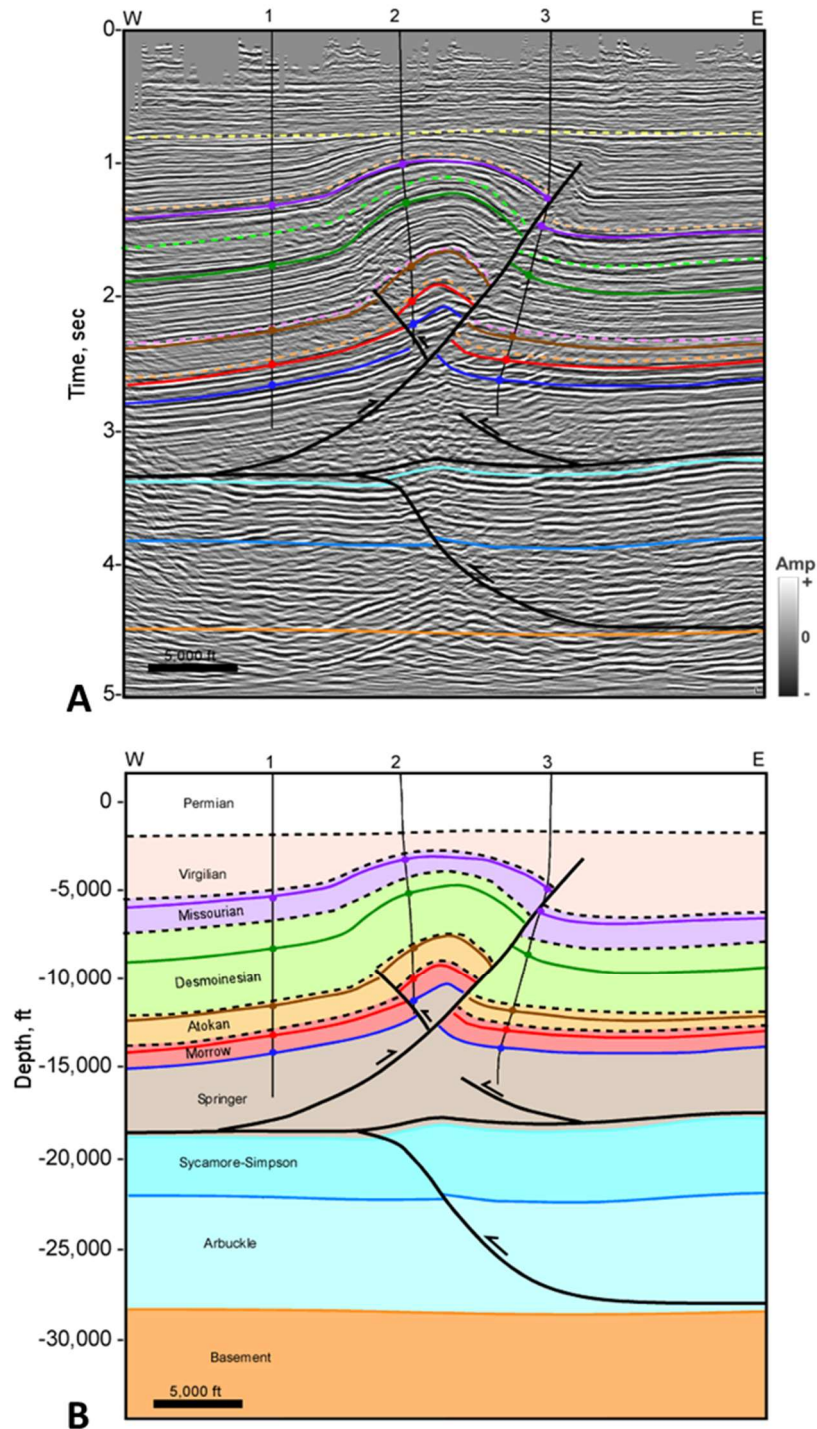


Figure 3.15 Cross section CM5 over the Chickasha structure (A) Interpreted seismic section in time. Horizon colors are shown in Figure 3.2. (B) Depth cross section. Well information is listed in appendix 1. Well tops (colored circles), dip data (brown check mark), and fault picks (red x) are shown where available. Seismic Data Courtesy of Chesapeake Energy.

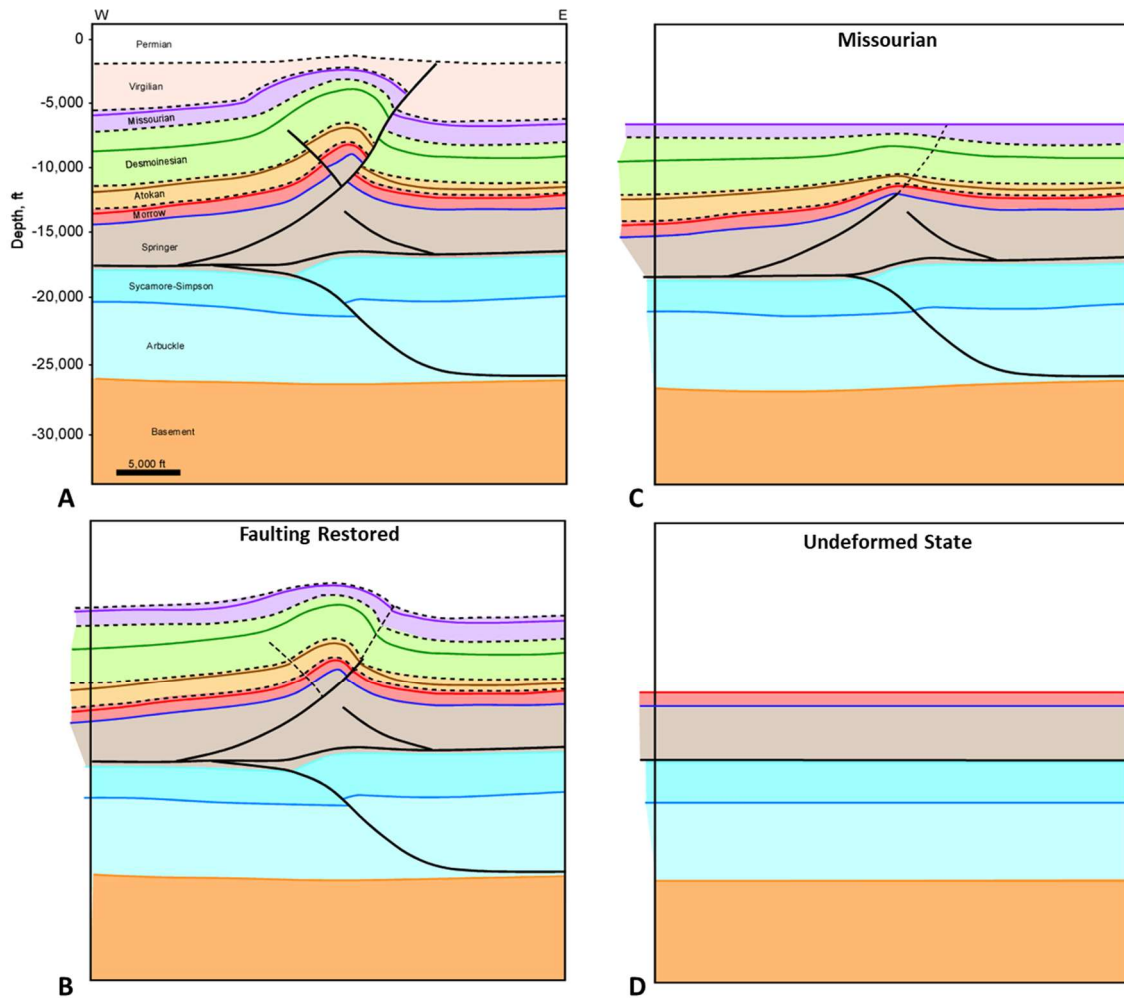


Figure 3.16 Kinematic reconstruction and structural evolution of section CM4 (A) Depth cross section. (B) Faulting is restored and dashed to illustrate fold geometries. (C) Structure is restored to Missourian time with the Hoxbar horizon flattened. (D) Morrow and older units are restored to their undeformed state. Initial dips of these units are not known, so units are shown as horizontal.

6.5 Cement Structure and Fault

The northwestern termination of the Chickasha structure is marked by a sharp bend, with the structure assuming an approximate E-W trend and referred to as the Cement structure. This structure contains two major fields, the West Cement and East Cement. We studied the Cement structure by first using a regional line (cross section B) to study its relationship with the Wichita Uplift. Two additional local lines CM1 and CM2 were used to study the detailed geometry of the structure. A third line, CM3 was used to study the transition from the Chickasha to the Cement structure. Finally, CM6 to the East of the Cement structure was used to define the geometry of late stage normal faulting affecting the Cement structure.

Regional cross section B extends from the Wichita Uplift to the Cement Anticline in the Anadarko Basin (Figure 3.17). The section traverses the southeast end of the Slick Hills Block including the Mountain View Fault system. The trend of the Wichita Uplift is NW-SE while the trend of the Cement Anticline is more E-W. This cross section shows the relationship between the uplift and structures in the basin. Along the mountain front, two splays of the Wichita Mountain Fault can be observed on the southwest end of the cross section while the Mountain View Fault system brings up the southeast end of the Slick Hills Block. These faults developed with a tri-shear geometry allowing intense folding to occur above the fault tips. They also cut the Virgilian suggesting they were active until the Late Pennsylvanian.

Slip is transferred into the basin along a detachment at the base of the Springer and results in a tight faulted-detachment fold to develop at Cement that is underlain by a deeper structure. A pre-existing basement normal fault below the Cement structure may have acted as a buttress defining the location of the structure. Slip along the Arbuckle detachment caused a faulted fold to develop within the Arbuckle to Sycamore units at Cement. This structure is

separated from the faulted-detachment fold above that was generated from slip along the Springer detachment. The faulted-detachment fold is cut by a north-verging thrust. It is estimated that slip on this fault is close to 4,500 feet. In the cross section, the structure is cut by a late-stage antithetic normal fault, which develops during negative inversion on the main fault. The antithetic fault and possibly the main normal fault are also marked by a component of left-lateral strike-slip faulting as indicated by lateral offset of seismic reflectors on time slices, and the presence of rhomb-shaped pull-apart structures. The system of late-stage E-W faults with strike-slip/normal components of movement is referred to as the Cement Fault system.

The late-stage normal faulting, which can be significant, is at least partially brought back along the Springer detachment. Two models can be used to explain the transfer of late-stage strike-slip/normal faulting. Figure 3.18A represents pre-strike-slip motion and shows a gentle faulted fold overlain by a tight faulted-detachment fold. These structures are underlain by a pre-existing normal fault. In Figure 3.18B, the basement-rooted normal fault becomes reactivated in strike-slip with a small component of normal displacement. Some slip is also transferred back along the Springer detachment. In Figure 3.18C, all the normal and strike-slip motion is occurring along the Springer detachment resulting in oblique slip, while the deeper structures remain in place. The crestal normal faults were filled with Virgilian age sediments, indicating the timing of movement. Although the basement-involved model shown in Figure 3.17B is favored, it is likely that the Cement structure experienced a component of both models.

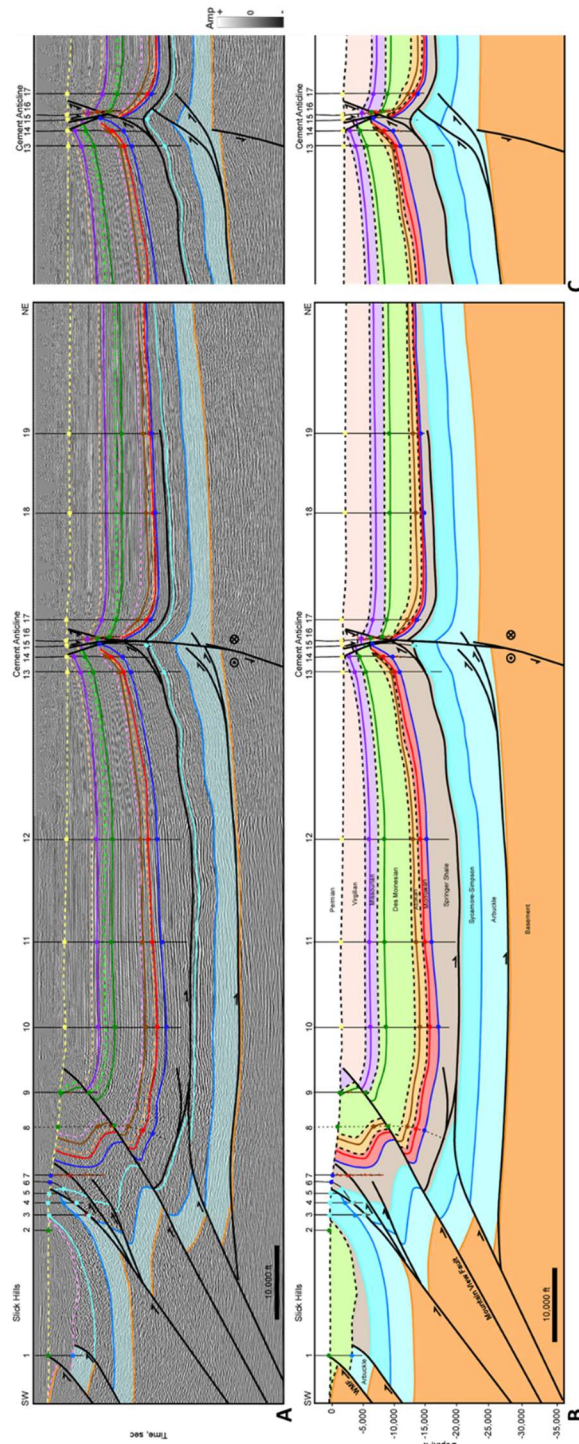


Figure 3.17 Regional cross section B. (A) Interpreted seismic section in time. Time scale removed from proprietary data. Horizon colors are shown in Figure 3.2. (B) Depth cross section. (C) Alternative interpretation of the Cement structure. Well information is listed in appendix 1. Well tops (colored circles), dip data (brown check mark), and fault picks (red x) are shown where available. Dashed well is projected from 1.5 miles. Seismic Data Courtesy of SEI & Seitel.

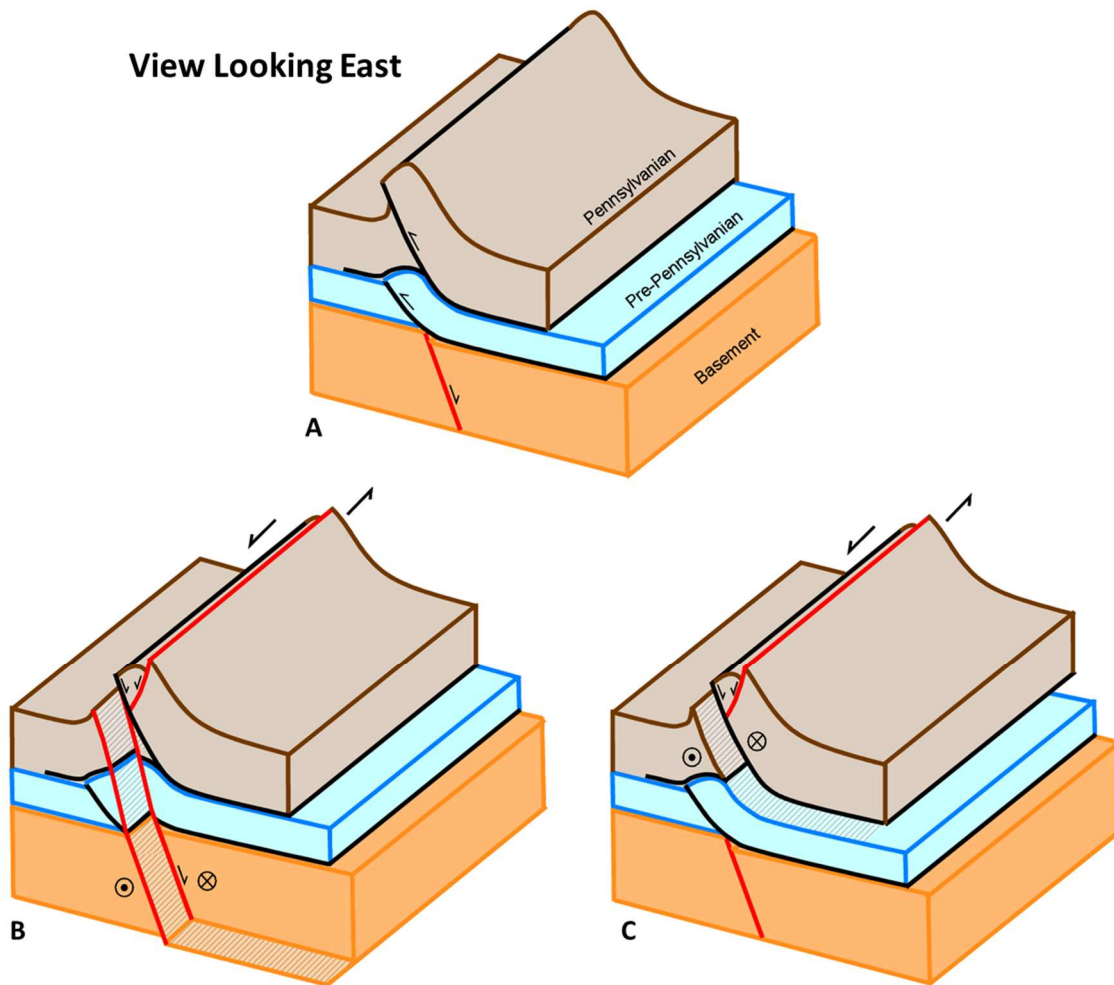


Figure 3.18 Block diagram of the Cement structure looking east. (A) Configuration prior to strike-slip movement. (B) Left-lateral strike-slip occurs along a pre-existing basement fault. A small amount of normal slip on the Springer detachment allows for the normal fault to cut the crest of the structure. (C) Alternative interpretation, left-lateral strike-slip occurs along the Springer detachment, a small amount of normal slip allows for the normal fault to cut the crest of the structure.

A second cross section through the Cement structure, CM1 (Figure 3.19), is approximately three miles west of the regional cross section and shows more detail. The seismic survey only extends to 4 seconds but an interpretation of the structure below that interval was derived from the regional cross section. Figures 3.19A-B shows the preferred interpretation where the strike-slip motion is linked to a pre-existing basement-rooted normal fault, whereas Figures 3.19C-D show an alternative interpretation where the strike-slip motion occurs along the Springer detachment. The overall structure in each interpretation is very similar. Slip along the Springer detachment has resulted in two splays to develop. The first splay (furthest southwest) developed prior to deposition of the Desmoinesian where folding and fault offset is limited to Springer through Atokan units. The second splay makes up the large thrust fault responsible for the Cement structure. This fault cuts Springer through Virgilian units. Fault symbols show that this fault experienced a component of negative inversion during late stage strike-slip movement as the structure moved backwards along the Springer detachment. The main fault and the antithetic normal fault transfer slip into the strike-slip fault (Cement Fault) and contain Virgilian age syn-depositional units indicating the timing of normal fault movement was Late Pennsylvanian.

The structure above the Springer detachment overlies a deeper faulted fold that resulted from slip along the Arbuckle detachment. A north verging thrust fault and backthrust cut the deeper Sycamore through Arbuckle units. The structure is underlain by a basement-rooted normal fault that likely acted as a buttress controlling the location and trend of the structure.

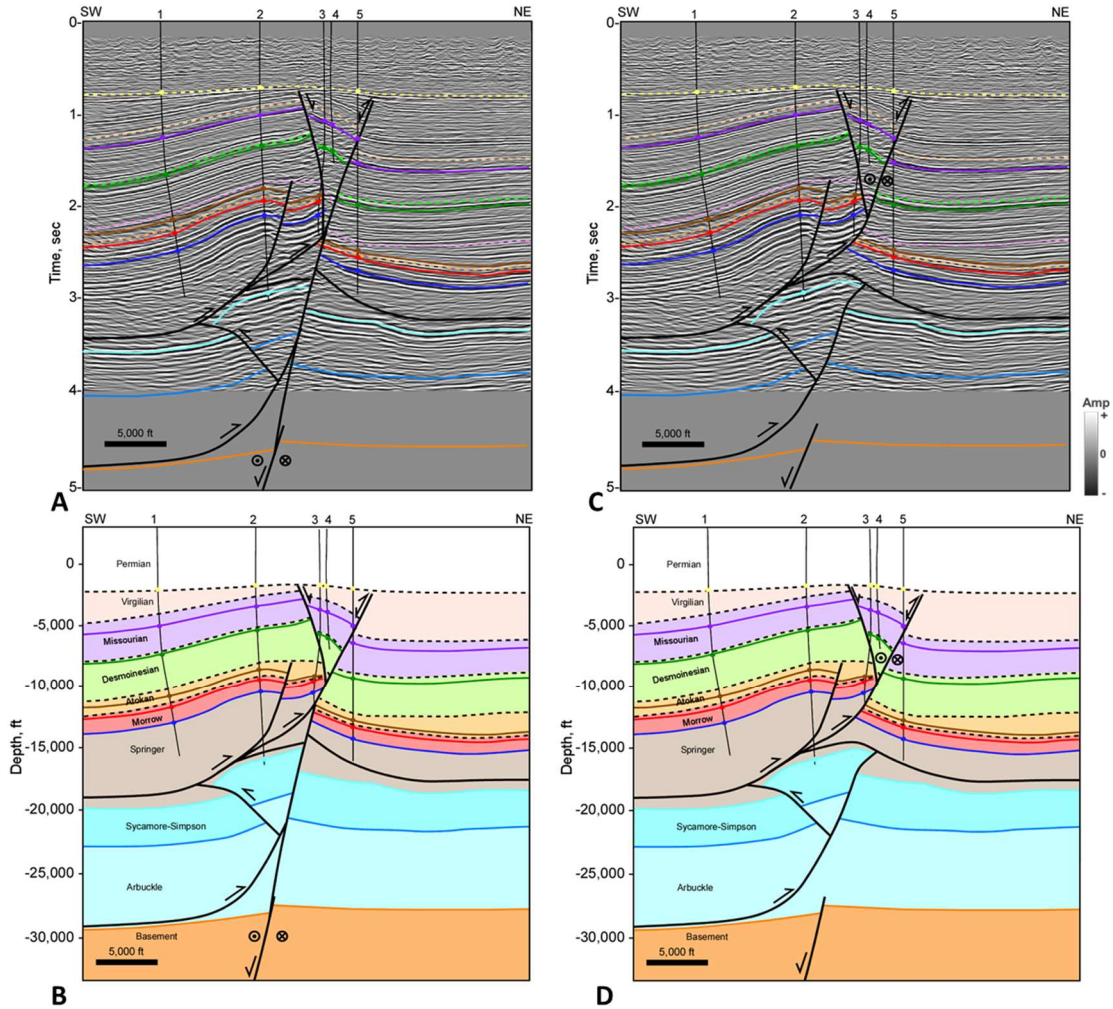


Figure 3.19 Cross section CM1 over the Cement structure (A) Interpreted seismic section in time. Horizon colors are shown in Figure 3.2. (B) Depth cross section. (C) Alternative seismic interpretation in time. (D) Alternative interpretation of depth cross section. Well information is listed in appendix 1. Well tops (colored circles), dip data (brown check mark), and fault picks (red x) are shown where available. Seismic Data Courtesy of Chesapeake Energy.

The Cement structure trends approximately E-W, in contrast to the Cruce, Carter-Knox, and Chickasha structures, which have more NW-SE trends. Figure 3.13 shows a structure map

on the Missourian age Hoxbar formation over the Cement-Chickasha structure constructed from a 3D seismic survey and then converted to subsea depth and cross-checked with well data. The Cement structure consists of the West and East Cement Anticlines (fields) which are oriented E-W. The structure makes an abrupt bend to the southeast into the Chickasha Anticline (Field). The Chickasha Anticline is cut by a southwest-dipping thrust fault and plunges to the south-southeast. Two small NE-SW oriented normal faults were observed on the hanging wall of this structure.

The Cement Anticline is cut by a south-dipping thrust fault (Cement Thrust Fault) that was reactivated as a left-lateral strike-slip fault with a component of normal faulting during the late stages of deformation. The crest of the Cement Anticline is also cut by a major north-dipping antithetic normal fault, and additional imbricate faults. Three of these normal faults just south of the West Cement Field are oriented NE-SW and drop down to the southeast. The antithetic normal fault that traverses the crest of the structure drops down to the north and is accompanied by left-lateral strike-slip motion resulting in small rhombohedral pull-aparts. The pull-apart cutting West Cement is larger than the one near East Cement. Axtmann (1985) mentioned that Thorman (1965) estimated about five miles of left-slip along West Cement in an unpublished study. He notes that Thorman used the Missourian age Marchand and Medrano sands to estimate the strike-slip and that the offsets decreased towards the east. A similar relationship can be observed in the structure map. Based on the shape of the rhombohedral pull-apart, strike-slip offset at West Cement is close to 13,300 feet (2.5 miles) while at East Cement it is 3,000 feet (0.5 miles).

The occurrence of left-lateral strike slip is consistent with the rotation of the maximum horizontal stress to an ENE-WSW trend from an earlier NE-SW trend during the late stages of

deformation. The NE-SW trend of some of the secondary normal faults that formed during the late stages of deformation are also consistent with this model.

A shallow time slice over the Cement-Chickasha structure is shown in Figure 3.20. The seismic data here shows the abrupt bend in the structure as it transitions from the Cement to the Chickasha structure. The purple trace in the time slice is where it cuts the Hoxbar horizon. Several NE-SW normal faults are shown by the yellow arrows. The red arrows indicate locations where the antithetic normal fault trend cuts the crest of the structure. These normal faults continue to the east of the Chickasha structure and can be observed on the time slice (blue arrows) as well as on the structure map. Although the strike-slip faulting cuts through the crest of the Cement structure, the amount of strike-slip faulting is relatively minor, as indicated by the lack of noticeable offset on the time slice. The preferred interpretation is that the strike-slip fault occurs along a basement-rooted fault based on observations just east of Chickasha along the Cement Fault trend that shows Pennsylvanian age basement faulting.

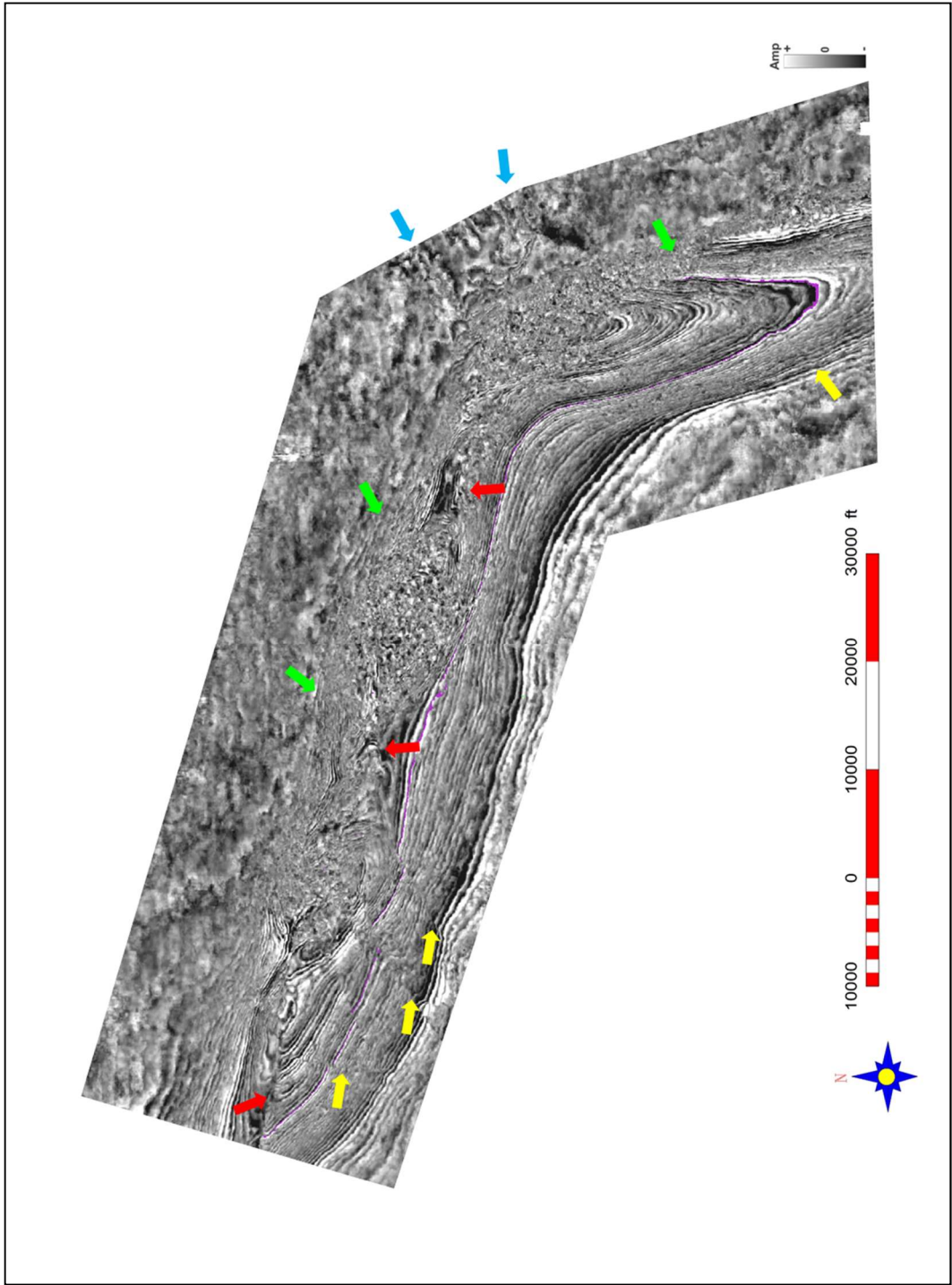


Figure 3.20 Shallow time slice over the Cement-Chickasha trend. Green arrows indicate the main thrust fault cutting the slice. Yellow arrows indicate normal faults oriented NE-SW. Red arrows show where the Cement normal/strike-slip fault cuts the slice. Blue arrows show the continuation of that fault trend east of the main structure. Seismic data courtesy of Chesapeake Energy.

The transition in style from the Cement to Chickasha structure is documented in cross sections CM2 and CM3 (Figures 3.21 and 3.22). The shallow structure in these cross sections have similarities to both Cement and Chickasha. At Chickasha, a backthrust extended from the main thrust fault (see cross sections CM4 and CM5) and can be seen in both these cross sections. The normal fault on the crest of the Cement structure also cuts cross section CM2 but was not observed in CM3. In cross section CM2 the north-verging thrust fault that cuts the deeper structure can still be observed. However, the amplitude and fault offsets are smaller suggesting that the structure is dying out towards the east. In cross section CM2, the strike-slip fault still cuts through the crest of the structure, but in cross section CM3 the strike-slip fault zone is now in front of the structure. An alternative interpretation is shown in Figure 3.21C-D. The main difference is that the strike-slip is occurring along the Springer detachment.

In cross section CM3 the strike-slip fault zone consists of two basement-rooted normal faults. These normal faults cut through a southwest verging thrust fault along the Arbuckle detachment. The normal fault that drops down to the southwest is likely the same basement-rooted normal fault extending along the base of the Cement structure in other cross sections. This fault is likely reactivated with left-lateral strike-slip/normal faulting. The second normal fault that is down-to-the-north is not observed in other cross sections towards the west suggesting that fault likely dies out in that direction. Both normal faults have a component of left-lateral slip resulting in the high-angle normal faults cutting up-section into the Virgilian. These two cross sections through the bend show that the folding follows the Cement-Chickasha trend, but that the strike-slip/normal faults maintain an E-W orientation towards the east.

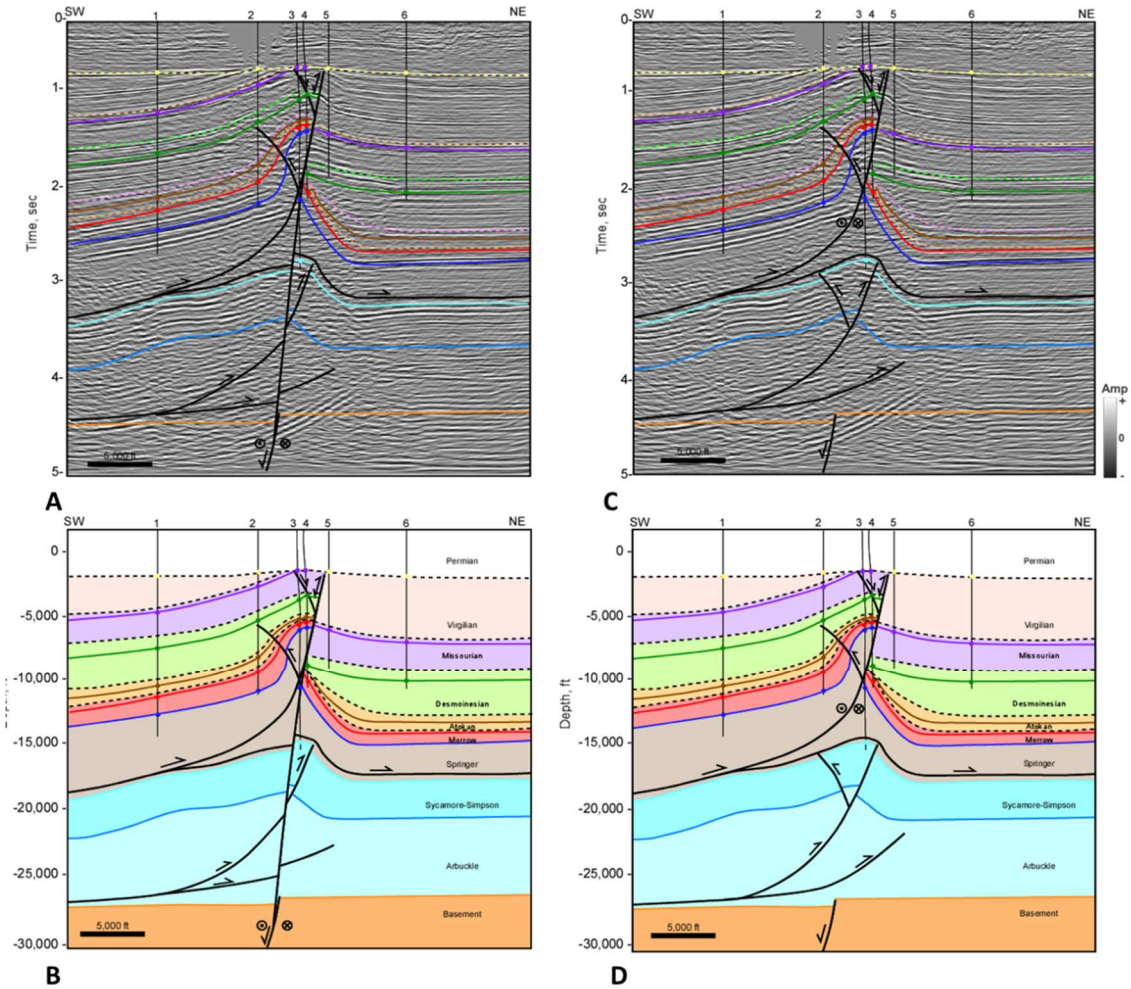


Figure 3.21 Cross section CM2 over the Cement-Chickasha transition (A) Interpreted seismic section in time. Horizon colors are shown in Figure 3.2. (B) Depth cross section. (C) Alternative seismic interpretation in time. (D) Alternative interpretation of depth cross section. Well information is listed in appendix 1. Well tops (colored circles), dip data (brown check mark), and fault picks (red x) are shown where available. Seismic Data Courtesy of Chesapeake Energy.

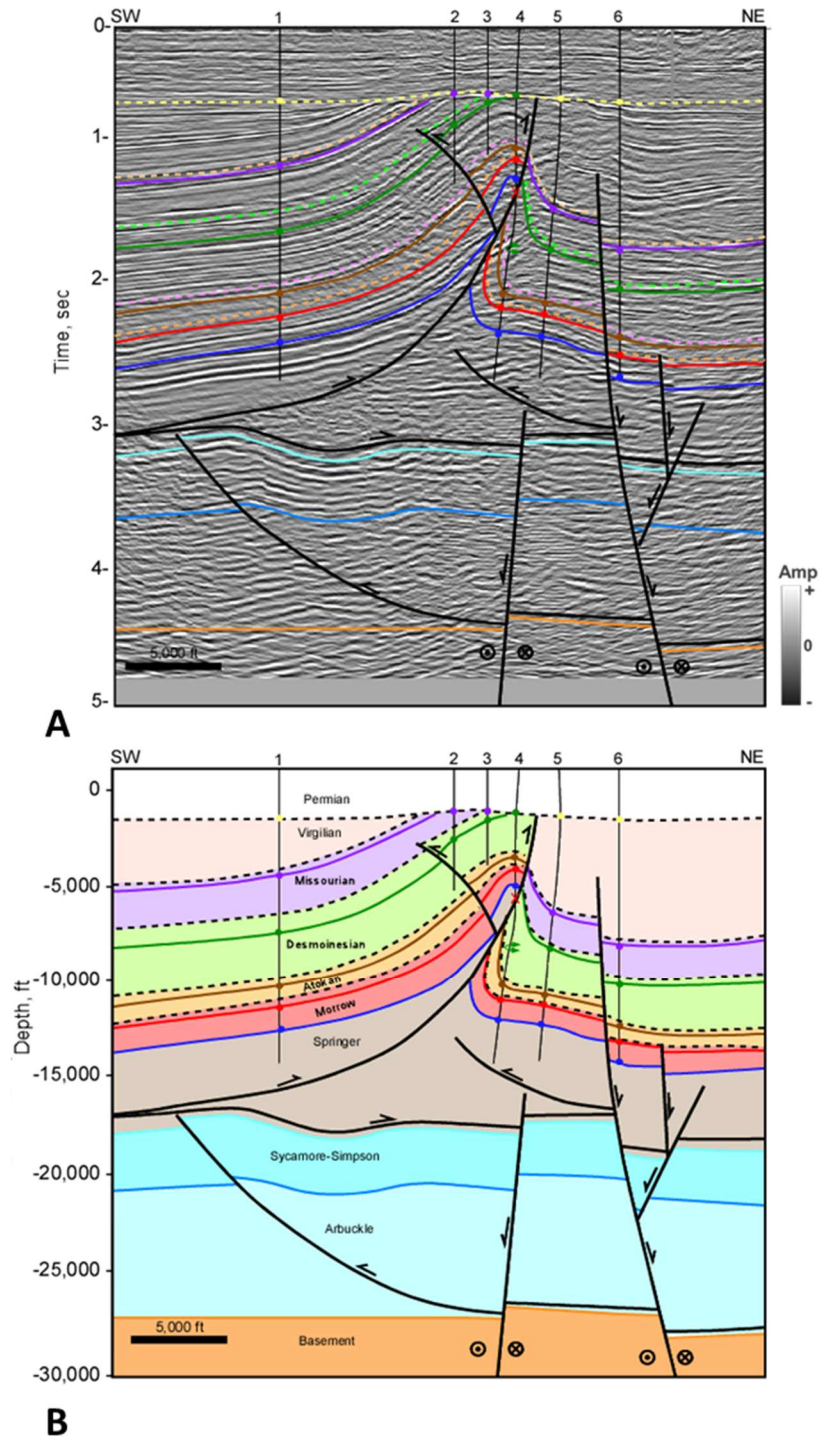


Figure 3.22 Cross section CM3 over the Cement-Chickasha transition (A) Interpreted seismic section in time. Horizon colors are shown in Figure 3.2. (B) Depth cross section. Well information is listed in appendix 1. Well tops (colored circles), dip data (brown check mark), and fault picks (red x) are shown where available. Seismic Data Courtesy of Chesapeake Energy.

Cross section CM6 (Figure 3.23) extends over the strike-slip normal fault trend outside of the folding and contains the two basement-rooted normal faults seen in CM3. Offset on the south-dipping normal fault has nearly diminished suggesting this fault has almost reached its tip point. However, the north-dipping normal faults has nearly 2,100 feet of offset on the Hoxbar horizon and is associated with two antithetic normal faults. Although these faults likely have a component of left-lateral strike-slip, the dip is closer to 60°-70° suggesting that the strike-slip component is diminishing, and that normal faulting is the dominant mechanism. Stratigraphic thickness of all the units are relatively uniform across the structure except for the Virgilian units. The Permian Unconformity is also nearly flat across the structure suggesting that the timing of normal faulting is limited to the Virgilian. Virgilian age seismic reflectors appear to onlap the hanging wall of the north-dipping normal fault in a fan-like geometry representing syn-depositional growth strata (Figure 3.23A). Cross section CM6 validates that the strike-slip faulting that cut the crest of the Cement Anticline occurred during the Virgilian.

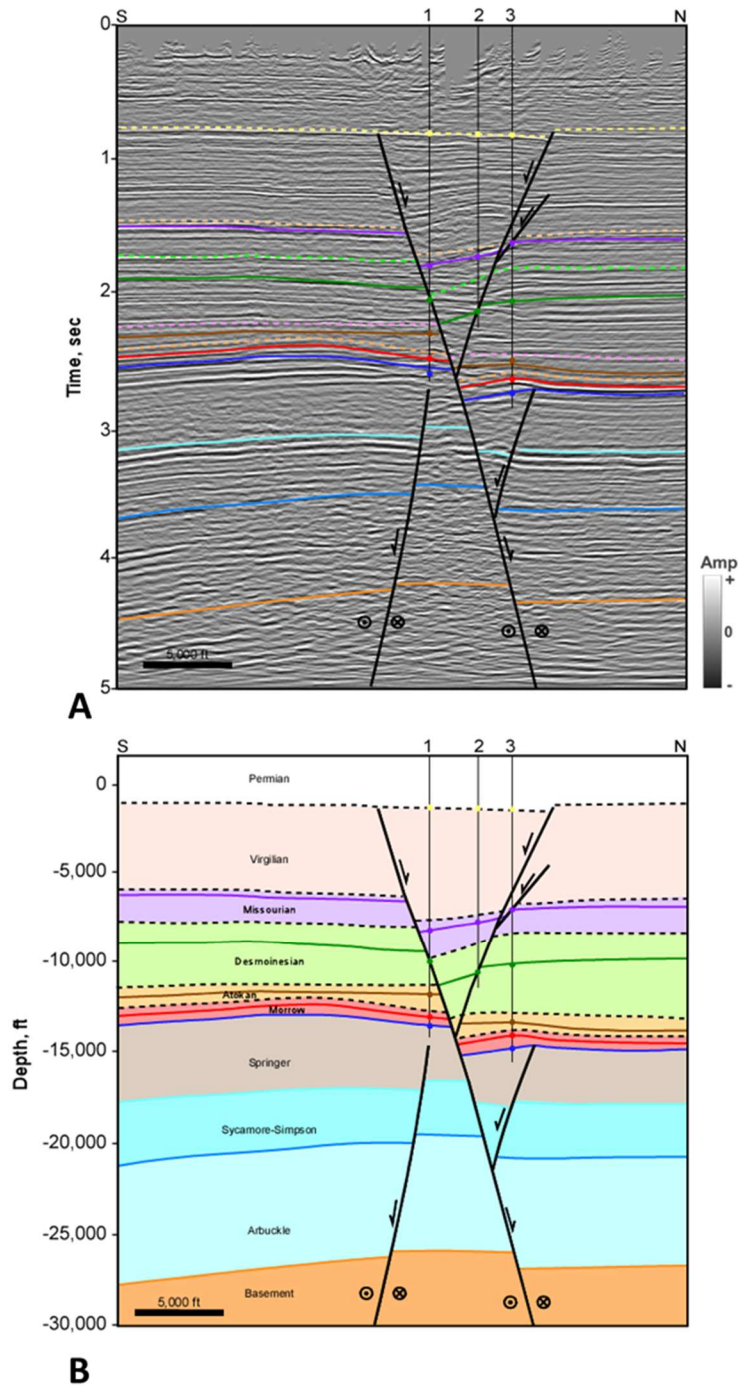


Figure 3.23 Cross section CM6 over the Cement Fault zone (A) Interpreted seismic section in time. Horizon colors are shown in Figure 3.2. (B) Depth cross section. Well information is listed in appendix 1. Well tops (colored circles), dip data (brown check mark), and fault picks (red x) are shown where available. Seismic Data Courtesy of Chesapeake Energy.

7. Discussion and Conclusions

Major anticlinal structures that make up the southeastern Anadarko Basin include the Carter-Knox, Cruce, Chickasha, and Cement structures. All these structures are faulted-detachment folds forming within the thin-bedded Pennsylvanian clastic units, above a detachment at the base of the thick Springer Shale. The fold geometries range from moderately open (Chickasha) to tight, with steep to vertical front limbs (Cruce and Carter -Knox), depending on the amount of shortening. The steep dips of the main faults forming the structures are due their passive rotation with increased shortening. This is evident from the fact that the Chickasha structure, which is more open, shows a shallower dipping main fault than the tighter Carter-Knox and Cruce structures, which show much steeper dipping main faults. The structures formed primarily as a result of NE-SW directed compressional stresses. The variation in trends of the structures from NW-SE to E-W are possibly related to the trends of pre-existing basement faults. Below the Springer detachment, thick-bedded Pre-Pennsylvanian carbonate units are folded into low-amplitude faulted folds above a detachment at the base of the Arbuckle Group.

Slip along the Springer and Arbuckle detachments are derived from basement-involved thrusts in the Wichita Uplift. The uplift resulted from inversion of a Precambrian-Cambrian failed rift during the Pennsylvanian Orogeny and transferred slip from the Wichita Mountain front into the Anadarko Basin along these detachments. A forward-shear motion along the Wichita Mountain Fault and Mountain View Fault allowed more slip to be transferred along the Springer detachment compared to the Arbuckle detachment. Reconstructions of cross sections show that the two levels of folding developed simultaneously, but a greater amount of shortening occurred higher in the section due to the forward-shear motion.

Growth strata and the presence of multiple unconformities suggest that the structures were active throughout most of the Pennsylvanian, but their growth was also episodic. The most prominent unconformity in each of the restorations is at the base of the Desmoinesian suggesting that significant movement had occurred along the Wichita Uplift during the Morrowan and Atokan. The structures resulted primarily from contractional deformation which continued into the Virgilian and were truncated by the Permian Unconformity.

A component of strike-slip and associated normal faulting affected some of these structures along E-W trending faults. The faults are associated with Virgilian age syn-depositional units, indicating the timing of movement. The Cement Fault trend and the Washita Valley Fault are two of the through-going strike-slip fault systems in the southeastern Anadarko Basin, and both are oriented approximately E-W. The normal fault component of the late stage deformation is either completely transferred back along preexisting thrust related detachments as in the case of Carter-Knox, or partially transferred back along these detachments, with the remaining component transferred into basement involved faults, as in the case of Cement. The strike-slip and associated normal faults are linked to reactivation of pre-existing basement-rooted normal faults. This may have occurred as a result of late stage reorientation of regional compressive stresses to an approximately ENE-WSW orientation.

References

- Amsden, T.W. 1975. Hunton Group in the Anadarko Basin of Oklahoma. *Oklahoma Geological Survey Bulletin* 121: 214.
- Axtmann, T.C. 1985. Structural Mechanisms and Oil Accumulation along the Mountain View-Wayne Fault, South-Central Oklahoma. *Shale Shaker Digest* 35: 17–45.
- Beauchamp, Weldon. 1982. The Structural Geology of the Slick Hills. Master's thesis, Oklahoma State University, Stillwater, Oklahoma, 119 p.
- Bott, M. H. P. 1979. Subsidence Mechanisms at Passive Continental Margins. In *Geological and Geophysical Investigations of Continental Margins: AAPG Memoir* 29, 3–9.
- Brewer, J. A., R. Good, J. E. Oliver, L. D. Brown, and S. Kaufman. 1983. COCORP Profiling across the Southern Oklahoma Aulacogen: Overthrusting of the Wichita Mountains and Compression within the Anadarko Basin. *Geology* 11: 109–114.
- Brown, W. G. 1984. Washita Valley Fault-A New Look at an Old Fault. *Technical Proceedings of the 1981 AAPG Mid-Continent Regional Meeting*, 68–80.
- Brueseke, Matthew E., Casey L. Bulen, and Stanley A. Mertzman. 2014. Major- and Trace-Element Constraints on Cambrian Basalt Volcanics in the Southern Oklahoma Aulacogen from Well Cuttings in the Arbuckle Mountains Region, Oklahoma U.S.A. In *Igneous and Tectonic History of the Southern Oklahoma Aulacogen, Oklahoma Geological Survey Guidebook* 38, edited by Neil H Suneson, 95–104.
- Budnik, Roy T. 1986. Left-Lateral Intraplate Deformation along the Ancestral Rocky Mountains: Implications for Late Paleozoic Plate Motions. *Tectonophysics* 132 (1–3): 195–214. [https://doi.org/10.1016/0040-1951\(86\)90032-6](https://doi.org/10.1016/0040-1951(86)90032-6).
- Carter, Darryl Wayne. 1979. A Study of the Strike-Slip Movement Along the Washita Valley Fault Arbuckle Mountains, Oklahoma. *The Shale Shaker Digest* 30–32: 85–115.
- Casas, A. M., D. Gapais, T. Nalpas, K. Besnard, and T. Román-Berdiel. 2001. Analogue Models of Transpressive Systems. *Journal of Structural Geology* 23 (5): 733–43. [https://doi.org/10.1016/S0191-8141\(00\)00153-X](https://doi.org/10.1016/S0191-8141(00)00153-X).
- Cooper, J. Calvin. 1995. Geological Evolution of the Criner Hills Trend, Ardmore Basin, Oklahoma. In *Structural Styles in the Midcontinent, 1992 Symposium*, Oklahoma Geological Survey Circular 97, edited by Kenneth S. Johnson, 144–60.
- Denison, Roger E. 1989. Foreland Structure Adjacent to the Ouachita Foldbelt. In *The Geology of North America*, v. F-2, The Appalachian-Ouachita Orogen in the United States, edited by

- R. D. Jr Hatcher, William A. Thomas, and G. W. Viele, 681–88. The Geological Society of America.
- Dewey, J. F., R.E. Holdsworth, and R.A. Strachan. 1998. Transpression and Transtension Zones. Special Publications, Geological Society, London 135: 1–14.
- Donovan, R Nowell. 1995. The Slick Hills of Oklahoma and Their Regional Tectonic Setting. Oklahoma Geological Survey Circular 97, 178–86.
- Donovan, R Nowell, W. R. D. Marchini, David A. McConnell, Weldon Beauchamp, and David J. Sanderson. 1989. Structural Imprint on the Slick Hills, Southern Oklahoma. In Anadarko Basin Symposium: Oklahoma Geological Survey Circular 90, edited by Kenneth S. Johnson, 78–84.
- Dott, R. H. 1933. Presidential Address: Structural History of the Arbuckle Mountains. Tulsa Geological Society Digest 1: 37–40.
- Feinstein, Shimon. 1981. Subsidence and Thermal History of Southern Oklahoma Aulacogen. AAPG Bulletin 65 (2): 2521–2533.
- Ferebee, C. D. 1991. Subsidence and Basin Development in the Southern Oklahoma Aulacogen. Master's thesis, University of Tulsa, Tulsa Oklahoma, 121 p.
- Friess, John P. 2005. The Southern Terminus of the Nemaha Tectonic Zone, Garvin County, Oklahoma. Shale Shaker Digest September- (October): 1–13.
- Gilbert, M Charles. 1983. "Timing and Chemistry of Igneous Events Associated with the Southern Oklahoma Aulacogen." *Tectonophysics* 94: 439–55.
- Granath, James W. 1989. Structural Evolution of the Ardmore Basin, Oklahoma: Progressive Deformation in the Foreland of the Ouachita Collision. *Tectonophysics* 8 (5).
- Ham, William E. 1951. Structural Geology of the Southern Arbuckle Mountains. Tulsa Geological Society Digest 19: 68–71.
- Hanson, Richard E., Robert E. Puckett, G. Randy Keller, Matthew E. Brueseke, Casey L. Bulen, Stanley A. Mertzman, Shane A. Finegan, and David A. McCleery. 2012. Intraplate Magmatism Related to Opening of the Southern Iapetus Ocean: Cambrian Wichita Igneous Province in the Southern Oklahoma Rift Zone. *Lithos* 174: 57–70.
- Harlton, Bruce. 1956. The Harrisburg Trough, Stephens and Carter Counties, Oklahoma. In *Petroleum Geology of Southern Oklahoma*, v. I, 135–43. AAPG.
- Harlton, Bruce. 1960. Stratigraphy of Cement Pool and Adjacent Area, Caddo and Grady Counties, Oklahoma. AAPG Bulletin 44 (2): 210–26.

- Heran, W. D., Green, G. N., and Stoesser, D. B., 2003, A Digital Geologic Map Database for the State of Oklahoma: USGS Open-File Report OF-2003-247
- Herrmann, Leo A. 1961. Structural Geology of Cement-Chickasha Area, Caddo and Grady Counties, Oklahoma. AAPG Bulletin 45 (12): 1971–93.
- Hoffman, Brian P. 1996. Geometry of the Northern Carter-Knox Structure, Anadarko Basin, Grady County, Oklahoma. Master's thesis, Oklahoma State University, Stillwater, Oklahoma, 81 p.
- Hoffman, P., J. F. Dewey, and K. Burke. 1974. Aulacogens and Their Genetic Relations to Geosynclines, with a Proterozoic Example from Great Slave Lake, Canada. In *Modern and Ancient Geosynclinal Sedimentation: Society of Economic Paleontologists and Mineralogists Special Publication 19*, edited by R. J. Jr Dott and R. H. Shaver, 38–55.
- Jacobson, Mark I. 1984. The Harrisburg Trough, Stephens County, Oklahoma, An Update. In *Technical Proceedings of the 1981 Mid-Continent Regional Meeting*, 127–37.
- Jones-Cecil, M. 1995. Structural Framework of the Meers Fault and Slick Hills Area, Southwestern Oklahoma. *Oklahoma Geological Survey Circular 97*, 187–207.
- Keller, G Randy. 2014. The Southern Oklahoma Aulacogen : It ' s a Classic. *Oklahoma Geological Survey Guidebook 38*, 389–91.
- Keller, G. R., and R.A. Stephenson. 2007. The Southern Oklahoma and Dnieper-Donets Aulacogens: A Comparative Analysis. In *The 4D Framework of Continental Crust: Geological Society of America Memoir 200*, edited by R. D. Jr. Hatcher, M. P. Carlson, J. H. McBride, and J. R. Martinez Catalan, 127–43.
- Kluth, C. F., and P. J. Coney. 1981. Plate Tectonics of the Ancestral Rocky Mountains. *Geology* 9: 10–15.
- McBee, William. 1995. Tectonic and Stratigraphic Synthesis of Events in the Region of the Intersection of the Arbuckle and Ouachita Structural Systems, Oklahoma. In *Structural Styles in the Midcontinent, 1992 Symposium*, Oklahoma Geological Survey Circular 97, edited by Kenneth S. Johnson, 45–81.
- McBee, William. 2003. The Nemaha and Other Strike-Slip Faults in the Midcontinent U.S.A. In *Midcontinent Section Meeting*, 1–23.
- McConnell, David A. 1987. Paleozoic Structural Evolution of the Wichita Uplift, Southwest Oklahoma. PhD dissertation, Texas A&M University, College Station, Texas, 219p.
- McCoss, Angus M. 1986. Simple Constructions for Deformation in Transpression/Transtension Zones. *Journal of Structural Geology* 8 (6): 715–18.

- Mitra, Shankar. 2002. Structural Models of Faulted-detachment Folds. *AAPG Bulletin* 9 (9): 1673–94.
- Naruk, S. J. 1989. Geometric Analysis and Balanced Cross sections of the Arbuckle Mountains and Washita Valley Fault. *The Shale Shaker Digest* 13: 40–45.
- Perkins, Tony. 1994. Geometry of the Southern Part of the Carter-Knox Structure, Anadarko Basin, Southern Oklahoma. Master's thesis, Oklahoma State University, Stillwater, Oklahoma, 92.
- Perry, W. J. 1989. Tectonic Evolution of the Anadarko Basin Region, Oklahoma. *US Geological Survey Bulletin* 1866-A, A1–19.
- Petersen, F A. 1983. Foreland Detachment Structures. In *Rocky Mountain Foreland Basins and Uplifts: Rocky Mountain Association of Geologists*, edited by James D Lowell and R. R. Gries, 65–77.
- Puckett, Robert E. 2011. A Thick Sequence of Rift Related Basalts in the Arbuckle Mountains, Oklahoma as Revealed by Deep Drilling. *Shale Shaker* 61: 207–16.
- Puckett, Robert E., Richard E. Hanson, Amy M. Eschberger, Matthew E. Brueseke, Casey L. Bulen, and Jonathan D Price. 2014. New Insights into the Early Cambrian Igneous and Sedimentary History of the Arbuckle Mountains Area of the Southern Oklahoma Aulacogen from Basement Well Penetrations. In *Igneous and Tectonic History of the Southern Oklahoma Aulacogen*, Oklahoma Geological Survey Guidebook 38, edited by Neil H Suneson.
- Reedy, H. J., and H. A. Sykes. 1959. Carter Knox Oil and Gas Field. In *Petroleum Geology of Southern Oklahoma*, v. II, 198–219. AAPG.
- Richard, P., and R. W. Krantz. 1991. Experiments on Fault Reactivation in Strike-Slip Mode. *Tectonophysics* 188: 117–31.
- Sanderson, David J., and W. R. D. Marchini. 1984. Transpression. *Journal of Structural Geology* 6 (5): 449–58.
- Saxon, Christopher Paul. 1998. Structural Style of the Wichita and Arbuckle Orogenies, Southern Oklahoma. University of Oklahoma.
- Shatski, N.S. 1946. The Great Donets Basin and the Wichita System; Comparative Tectonics of Ancient Platforms. *Akademiya Nauk SSSR Izvestiya, Seriya Geologicheskaya* 6: 57–90.
- Skulski, T., D. Francis, and J. Ludden. 1991. Arc-Transform Magmatism in the Wrangell Volcanic Belt. *Geology* 19: 11–14.

- Skulski, T., D. Francis, and J. Ludden. 1992. Volcanism in Arc-Transform Transition Zone: The Stratigraphy of the St. Clare Creek Volcanic Field, Wrangler Volcanic Belt, Yukon, Canada. *Canadian Journal of Earth Sciences* 29: 44–461.
- Taff, J. A. 1904. Preliminary Report on the Geology of the Arbuckle and Wichita Mountains. USGS Professional Papers 31.
- Tanner, J. H. 1967. Wrench Fault Movements along Washita Valley Fault, Arbuckle Mountain Area, Oklahoma. *AAPG Bulletin* 51: 126–41.
- Tapp, B. 1995. Inversion Model for the Structural Style of the Arbuckle Region. In *Structural Styles in the Midcontinent, 1992 Symposium*, Oklahoma Geological Survey Circular 97, edited by Kenneth S. Johnson, 113–18.
- Thomas, William A. 2014. The Southern Oklahoma Transform-Parallel Intracratonic Fault System. In *Igneous and Tectonic History of the Southern Oklahoma Aulacogen*, Oklahoma Geological Survey Guidebook 38, edited by Neil H. Suneson, 375–87.
- Thomas, William A. 2011. The Iapetan Rifted Margin of Southern Laurentia. *Geosphere* 7 (1): 97–120. <https://doi.org/10.1130/ges00574.1>.
- Thorman, C. H. 1965. Cement Field Study. Mentioned in Axtmann, 1985.
- Tikoff, Basil, and Christian Teyssier. 1994. Strain Modeling of Displacement-Field Partitioning in Transpressional Orogens. *Journal of Structural Geology* 16 (11): 1575–88. [https://doi.org/10.1016/0191-8141\(94\)90034-5](https://doi.org/10.1016/0191-8141(94)90034-5).
- Tomlinson, C. W., and William Jr. McBee. 1959. Pennsylvanian Sediments and Orogenies of Ardmore District, Oklahoma. *SP 19: Petroleum Geology of Southern Oklahoma* 2: 461–500.
- Turko, Molly J., and Shankar Mitra. 2019. Structural Geometry and Evolution of the Carter-Knox Structure, Anadarko Basin, Oklahoma. *AAPG Bulletin*.
- Walper, Jack L. 1982. The Geotectonic Evolution of the Oklahoma Aulacogen, Oklahoma. *North Texas Geological Society, Basins of the Southwest-Phase 2*, 192–211.
- Appendix 3.1 Well Information from Cross Sections

Regional Cross Sections

Cross Section	Well #	API	Well Name and Number
A	1	35137000920000	S J PINSON 1
A	2	35137240310000	WOOLEVER GEORGE A 1
A	3	35137265880000	HINES 1-9
A	4	35137252690000	HOWARD 1
A	5	35137227790000	DEBBY-SUE 1-36
A	6	35137236900000	SUMNER GARY 1
A	7	35137253890000	LAMAR 1-21
A	8	35137255150000	KILGO 3-21
A	9	35051365150000	LEONA HAYES 1
A	10	35051227710000	J KAYE 3-33
A	11	35051227140000	JULES 1-34
A	12	35051227410000	BLOCH 1-34
A	13	35051226150000	CALEB 1-27
B	1	35031020510001	FT STILL NW 1
B	2	35031021840000	SCHOOL LAND 1-A
B	3	35031201900000	CHOENS 1
B	4	35031201500001	GENEVA 1
B	5	35031204570000	MCFARLAND 1
B	6	35031214280000	ELGIN 31-1
B	7	35031214040000	CIRCLE `H` 1
B	8	35031208670000	BROCK 1-20
B	9	35031020620000	CRANE 1
B	10	35031209180000	FLETCHER 1
B	11	35031208990000	WHITE HORSE 1
B	12	35031208930000	CRAWFORD 1
B	13	35051200480001	CEMENT /ORDVCN UN/ 1-A
B	14	35051227630000	FLYNN 1-18
B	15	35051228520000	BENTLEY 1-8
B	16	35051224420000	BENTLEY 1-8
B	17	35051205580000	WILLIAMS 1
B	18	35051212770000	HILLSBORO 1
B	19	35051212510000	THOMAS MARTIN 1

Carter-Knox and Cruce Cross Sections

Cross Section	Well #	API	Well Name and Number
CK1	1	35051200760000	BERNARD 1-4
CK1	2	35051209160000	BRAY 1
CK1	3	35051219230000	BRAY 2-25
CK1	4	35051216900000	BRAY 1-25
CK1	5	35051220850000	FISHER 1-25
CK1	6	35051207770000	NEVIUS 1-25
CK1	7	35051212820000	CLEARY 1A
CK2	1	35137083600000	GRAHAM 1
CK2	2	35137255310000	DIANE P 3
CK2	3	35137259070000	GOODRICH 1-30
CK2	4	35137268460000	BRANCH 1H-16
CR1	1	35137214930000	RUSSELL 1-26
CR1	2	35137006860000	CRUCE UNIT O/A 1
CR1	3	35137253490000	JONES L E 1
CR1	4	35137253360000	EGGLESON 30-1
CR1	5	35137300420000	KETCHUM 1-28
CR2	1	35137241430000	SLEDGE 1-14
CR2	2	35137210420000	CLESTON BROWN 1
CR2	3	35137211350000	BEAVERS UNIT 1
CR2	4	35137032240000	F M GENTRY 1

Cement and Chickasha Cross Sections

Cross Section	Well #	API	Well Name and Number
CM1	1	35015226590000	ESTES 1-15
CM1	2	35015226020000	BUCKMASTER 1-11
CM1	3	35015230640000	CENTER CITY 1-3
CM1	4	35015222490000	GRAND DEWEY 1-3
CM1	5	35015220350000	7601 JV-P DAY 2-Y
CM2	1	35051200200000	ELLA ELLIOT UNT 1
CM2	2	35051209070000	BUSS 1
CM2	3	35051229850000	MICHELLE LORI 1-16
CM2	4	35051230070000	DAWN 1-16
CM2	5	35051221570000	TIVIS 2
CM2	6	35051213990000	CARL 1
CM3	1	35051210200000	BAXTER 1
CM3	2	35051351910000	DAHL 2
CM3	3	35051351920000	POOLER A 6
CM3	4	35051231530000	POOLER 1-22
CM3	5	35051229080000	BERRY 2-23
CM3	6	35051203550000	FARWELL UNIT 1
CM4	1	35051200120000	CARTER J W UNIT 1
CM4	2	35051367020000	DUKE 1
CM4	3	35051207270000	BILLY J BENNET ETAL 1
CM4	4	35051221740000	DUKE 1-35
CM5	1	35051200190000	PRUITT 1
CM5	2	35051234820000	DELK 1-10
CM5	3	35051219920000	WILLIAMS JIMMY UNIT 1
CM6	1	35051234240000	IRENE 1-11
CM6	2	35051213710000	KAHLE 1
CM6	3	35051203550000	FARWELL UNIT 1

Chapter 4: Structural Geometry and Evolution of the Carter-Knox Structure, Anadarko Basin, Oklahoma

Abstract

The Carter-Knox field is located on a NW-SE trending faulted anticline in the southeastern part of the Anadarko Basin. 3D seismic and well data is used to develop a model for the geometry and evolution of the structure. The Carter-Knox structure formed during contractional deformation associated with the Wichita Uplift in Pennsylvanian time. It is characterized by different structural styles in the two main structural units. The lower unit which includes the Arbuckle to Sycamore Groups is folded into a broad anticline associated with one or more frontal faults and back thrusts, with a change in the vergence along trend. The upper unit which includes the Springer Shale to the Primrose Formation and the overlying Pennsylvanian growth units is marked by a tight faulted-detachment fold with a steep to vertical front limb, associated with multiple thrust faults which detach within the Springer shales. The tightness of the structure and the dip of the front limb increase with increasing fault slip in the central part of the structure. The southern portion of the structure is cut by several Late Pennsylvanian E-W normal faults that merge into the Springer detachment. Kinematic reconstruction shows differential shortening between the two main structural packages. The evolution of the structure was episodic resulting in two major angular unconformities within the Pennsylvanian, and a major Permian Unconformity which truncates the crest of the structure. The southwest flank of the structure was rotated along a flexural hinge in the basement due to sedimentary loading, resulting in thickening of growth units on this flank.

1. Introduction

The Carter-Knox structure is a NW-SE trending faulted anticline located in the southeastern part of the Anadarko Basin, close to its boundary with the Ardmore basin (Figure 4.1). It is one of several complex structures in the Anadarko Basin marked by a tight structural geometry, multiple detachments, and a complex growth history. The Carter-Knox Field located on the crest of the structure is one of the largest producing oil and gas fields in Oklahoma. It produces oil and associated gas from shallow Permian units, and Pennsylvanian units of the Springer, Morrowan, Deese and Hoxbar Formations, as well as gas and condensate from deeper units within the Woodford Shale and Simpson Group. Cumulative production from the field is greater than 270 MMBOE with reserves estimated to be around 385 MMBOE (IHS).

In order to understand the structural geometry and evolution of this and other structures in the Anadarko Basin, a detailed structural analysis, including the structural style and timing, was conducted using proprietary 3D seismic data combined with well log and dipmeter data. The approach used in the study included (1) integration of the 3D seismic data with well log and dipmeter data, (2) interpretation of a series of dip lines and related strike lines across the structure, (3) construction of a series of balanced structural cross sections and (4) kinematic reconstruction of key sections to decipher the structural evolution of different stratigraphic packages. The resulting structural framework will be beneficial for future production plans in both the Carter-Knox Field and similar structures in the Anadarko Basin.

2. Regional Structure and Stratigraphy

2.1 Basin History

The tectonic history of southern Oklahoma is marked by the inversion of a Precambrian-Cambrian failed rift during multiple episodes of Pennsylvanian deformation. Rifting was active

from Late Precambrian through Middle Cambrian (Perry, 1989), followed by subsidence from the Middle Cambrian through the end of the Ordovician (post-Hunton) (Feinstein, 1981).

Intrusive rocks within the failed rift are evident on gravity and magnetic data and show a general NW-SE trend. Contractional deformation associated with the uplift and inversion of the failed rift resulted in the formation of the basement-cored Wichita and Arbuckle Uplifts. Transfer of slip from the Wichita Uplift to the Anadarko Basin led to the formation of a number of contractional structures including Carter-Knox.

2.2 Regional Structure

Figure 4.1 shows the locations of major uplifts, basins, and fault trends of the Wichita Uplift and Anadarko Basin. Pre-Cambrian basement and related igneous intrusions of the Wichita Uplift crop out approximately 50 miles (80 km) directly west of the Carter-Knox structure. The Wichita front changes trend between NW-SE and WNW-ESE along trend. The NW-SE trend of the Carter-Knox structure is almost parallel to the trend of the Wichita front directly behind it. Fault slip associated with the Wichita Uplift was transferred along detachments to the Carter-Knox, Chickasha, Cruce, and other contractional structures in the Anadarko Basin.

The area north and northeast of Carter-Knox is known as the Golden Trend. The structures in this trend consist of high angle thrust/reverse faults with two dominant trends, N-S to NW-SE and E-W. The eastern side of the Golden Trend is bounded by the regional N-S trending Nemaha Fault, whereas the north side is bounded by the Cement Fault.

A number of major east west trending faults affect both the Wichita Mountain front and the Anadarko Basin. The most important of these is the complex Washita Valley Fault zone,

which is traditionally interpreted as a left-lateral strike-slip fault. Estimates of the total slip range from 1 to 40 miles (1.6-64 km) (Ham, 1950; Dunham, 1955; Tanner, 1967; Carter, 1984; McCaskill, 1997). The wide range in estimates is due to different methods for measuring the slip which include looking at pre-Pennsylvanian stratigraphic changes across the fault (Tanner, 1967, Carter, 1984, and McCaskill, 1998) to observing the offset of anticlinal axes in the Arbuckle Uplift, as well as offsets in Pennsylvanian age conglomerates (Ham, 1950; Dunham, 1955).

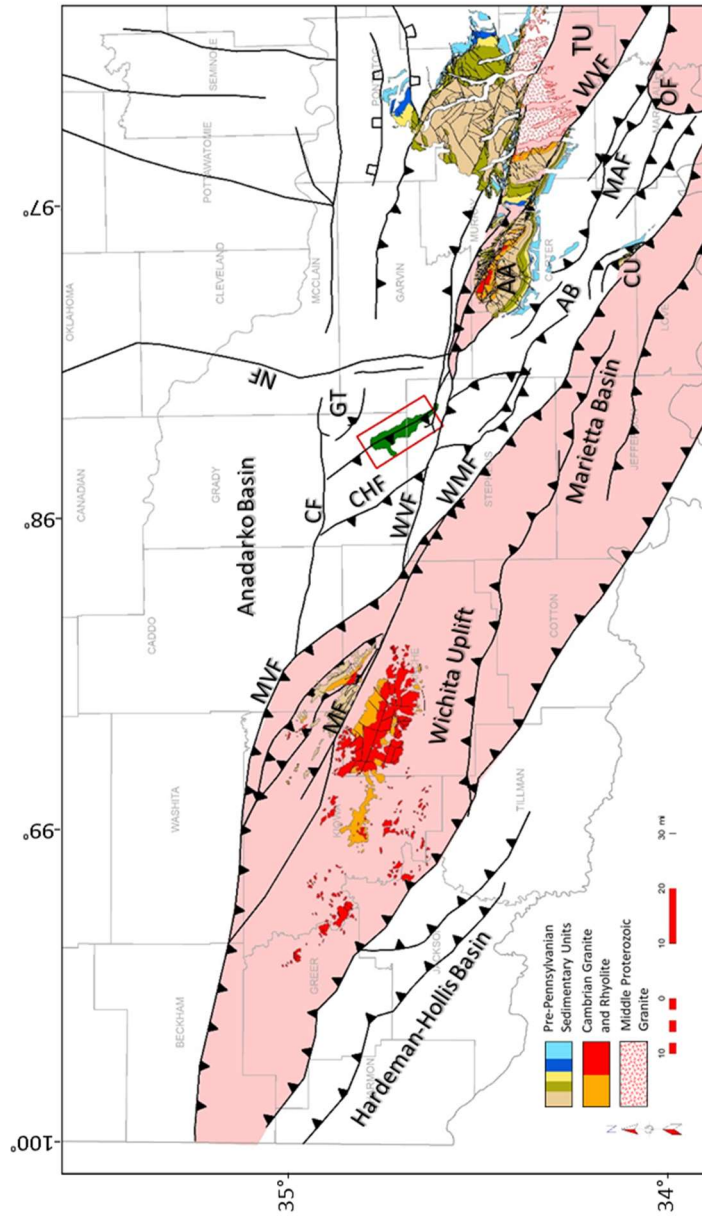


Figure 4.1 Regional map showing uplifts, basins, and regional fault trends. Pre-Pennsylvanian surface geology is shown in uplifted areas. Red triangle is the location of the 3D seismic study area. Carter-Knox Field is the green polygon. Uplifted areas are highlighted in light red. AA = Arbuckle Anticline; AB = Ardmore Basin; CF = Cement Fault; CHF = Chickasha Fault; CU = Criner Hills Uplift; GT = Golden Trend; MAF = Madill-Aylesworth Fault; MF = Meers Fault; MVF = Mountain View Fault; OF = Ouachita Frontal Thrust Fault; TU = Tishomingo Uplift; WMF = Wichita Mtn Fault. Faults are modified from Marsh and Holland, 2015, Axtmann 1985, and proprietary data. Surface data and Carter-Knox Field outline are from USGS and Oklahoma Geological Survey (Boyd, 2002; Heran et al., 2003).

2.3 Stratigraphy

Figure 4.2 shows the stratigraphic column in the Carter-Knox Field. Several detachment surfaces are also highlighted in the table. Pre-Pennsylvanian units consist of thicker carbonate packages including the Arbuckle, Viola, Hunton, and Sycamore Groups, whereas Pennsylvanian age and younger units are dominantly clastic and include some thinner limestone units. The Springer Shale, locally referred to as the Goddard Shale, separates these mechanical packages. The base of the Springer Shale is a detachment surface both regionally and locally at Carter-Knox. Different styles of deformation occur above and below this detachment due to the variations in mechanical stratigraphy.

The stratigraphic units from the Upper Dornick Hills to the Hoxbar show growth on the structure. They are significantly thicker on the southwestern flank than on the crest, suggesting that the main deformation occurred during this time. Multiple intermediate unconformities have been documented within this interval. The crest of the structure is truncated by the Permian Unconformity, so that most deformation ceased at this unconformity, with the Permian units exhibiting broad folding.

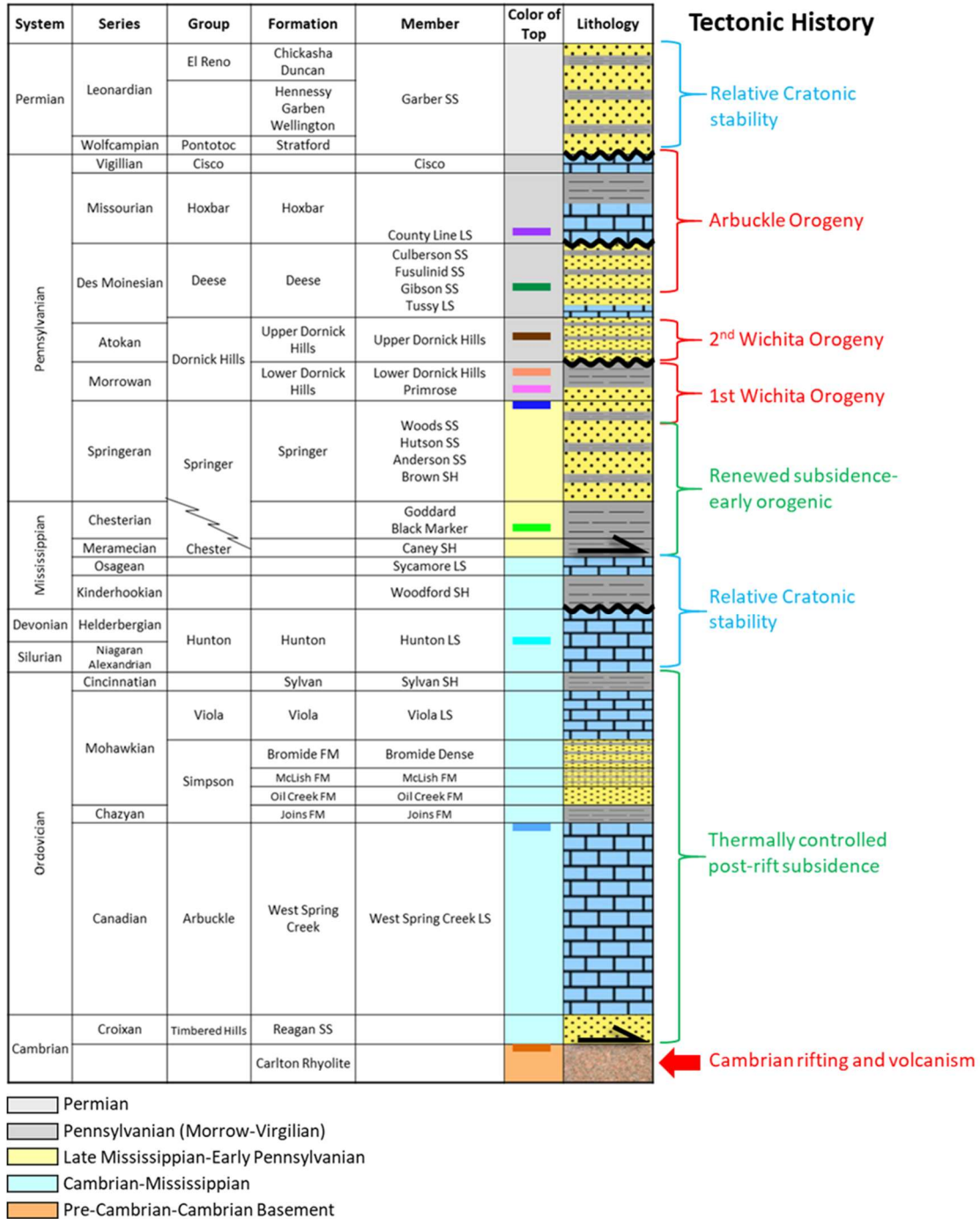


Figure 4.2 Stratigraphic Chart for the Carter-Knox Field modified from Reedy and Sykes, 1958. Tectonic History is modified from Granath (1989). Legend shows colors for tops of formations. Black arrows represent detachment locations near basal Springer and basal Arbuckle/Reagan ss.

3. Previous Studies

Seismic and well data through the Carter-Knox structure have been available for some time, so that a number of structural interpretations have been made. Many of these are in internal proprietary files of oil and gas companies that have worked on the field. Published sections described below are restricted to single sections across the structure.

Reedy and Sykes (1959) described Carter-Knox as a steeply dipping faulted anticline producing oil and gas from the Permian, Hoxbar, Deese, Springer and Simpson Groups. They interpreted a number of unconformities including two important ones at the top of Deese and Lower Dornick Hills Formations. Several structural movements were interpreted, with the first occurring post-Hunton and pre-Woodford and truncating part of the Hunton in section 3 of T2N and R5W. This was followed by a post-Lower Dornick Hills and pre-Upper Dornick Hills movement, forming a gentle anticline at Carter-Knox. The anticline continued to grow during Deese time with the largest movement occurring post-Hoxbar time, when folding and faulting became significant (Reedy and Sykes, 1958). The anticline was then truncated by an unconformity prior to Permian deposition. Reedy and Sykes estimated that the slip on the main thrust fault exceeded 5,000 ft (1,524m). They also interpreted a number of small cross faults on the structure with throws of 100-200 ft (30-61 m) (Figure 4.3A).

Petersen (1983) suggested that the Carter-Knox Field is a classic foreland detachment structure and described it as a second-order anticline. The faults that sole out in the basal Springer Shale were active throughout the Pennsylvanian with the greatest movement in the Missourian through Virgilian time as well as early Permian. He noted that the deeper structure is detached within the Arbuckle Group, whereas basement is undeformed (Figure 4.3B).

Saxon (1998) described the anticline as a foreland detachment structure where the fold geometry is controlled by two main detachments, with the lower detachment rooted in the Arbuckle Group and the upper detachment rooted in the Springer shales. The Springer detachment is several thousand feet higher in the section. He suggested that upward tightening of the Wichita Mountain front flank syncline creates a greater amount of out-of-syncline thrusting on the Springer detachment than on the Arbuckle detachment resulting in a greater amount of shortening higher in the section (Saxon, 1998). He described the folds above both detachments as fault-propagation folds with different structural styles due to mechanical and lithological differences between pre-Pennsylvanian and Pennsylvanian sections, resulting in a characteristically concentric deeper fold and more complex shallow fold (Figure 4.3C).

Contrary to the above interpretations, which primarily invoked contractional fold-thrust tectonics for the formation of the structure, Perkins (1997) and Hoffman (1996) described the structure as a positive flower structure related to left-lateral strike-slip faulting along the Washita Valley Fault zone, and suggested that it fits into a predictable pattern of the location and trend of anticlines associated with strike-slip faulting. Their cross sections depict several vertical faults cutting through the entire stratigraphic section and basement (Figure 4.3D).

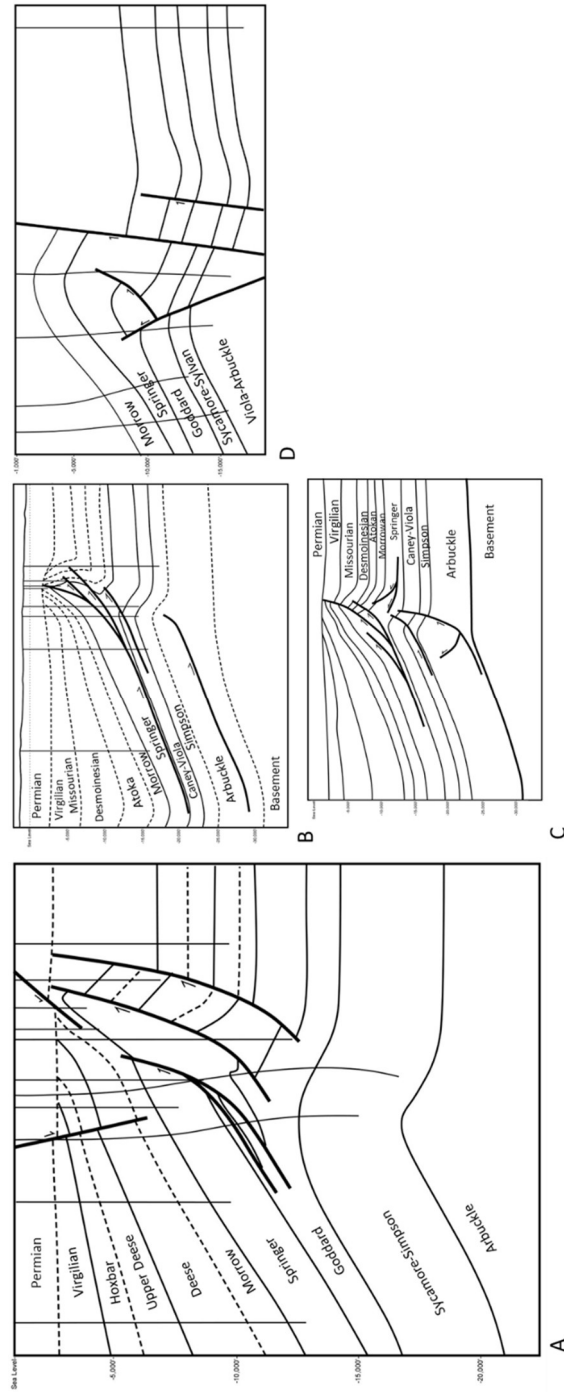


Figure 4.3 Cross sections showing previous interpretations of the Carter-Knox structure. (A) Cross section modified from Reedy and Sykes (1959) showing three to four thrust faults and two shallower normal faults. (B) Cross section from Petersen (1983), showing detachment surface within Middle Arbuckle (C) Cross section from Saxon (1998), showing triangle zone in core of fold (D) Cross section modified from Perkins (1997) showing near vertical strike-slip faults.

4. Structural Interpretation and Approach

Structural interpretation of Carter-Knox was conducted by integrating a 3D seismic volume through the structure with well log and dipmeter data (Figure 4.4). The approach involved (1) the construction of structural maps at key horizons; (2) a series of seven balanced cross sections based on seismic time interpretations of dip lines from the 3D survey and their conversion to depth; and (3) kinematic reconstruction of three key sections to understand the evolution of the structure.

5. Structural Maps

Structural maps in two-way time for the top of the Pennsylvanian (Atokan) Upper Dornick Hills, Pennsylvanian (Morrowan) Primrose, and the Silurian-Devonian Hunton horizons are shown in Figure 4.5. These are representative of the two important structural packages with different structural styles and shortening. The Upper Dornick Hills (Figure 4.5A) and Primrose (Figure 4.5B) show structures forming above a detachment in the Springer (Goddard) shales, whereas the Hunton (Figure 4.5C) shows the structures forming above a lower detachment at the base of the Arbuckle. All three maps show a NW-SE faulted anticline related primarily to thrust faults. The crest of the anticline shifts toward the southwest with depth, most notably on the Hunton structure map which is below the Springer detachment.

The structure above the Springer detachment is a tight anticline with a steep to vertical front limb related to one or more steep southwest-dipping thrust faults. Additional secondary thrust faults cut the structure, but not all of these propagate to the top of the Primrose or Upper Dornick Hills Formations. The crest of the structure is truncated by the Permian Unconformity at its culmination for the Upper Dornick Hills, and only in the central culmination, where the slip and uplift are greatest, for the Primrose Formation.

A series of transverse to oblique low-displacement normal faults exist on the hanging wall in the shallower formations. These are interpreted to be faults related to the lateral expansion of the anticline, parallel to the fold axis.

Two anticlinal closures occur at the Hunton level, both of which have a larger wavelength and a smaller amplitude than the structure above the Springer detachment. The southeastern closure is smaller whereas the northwestern closure has a linear crest that extends over most of the field. Cross sections show a change in fault vergence for these two faulted anticlines. The fault in the southeastern anticline verges to the southwest while the fault in the northwestern anticline verges to the northeast. Back thrusts are associated with both faults.

A steep NW-SE trending low displacement basement-involved normal fault occurs to the northeast of the structure. This normal fault probably developed early and provided a buttressing effect for the formation of the Carter-Knox structure.

The southeastern part of the structure is marked by a large E-W trending and south-dipping normal fault, dropping down the southern portion of the structure, and possibly connecting to the E-W trending Washita Valley Fault zone.

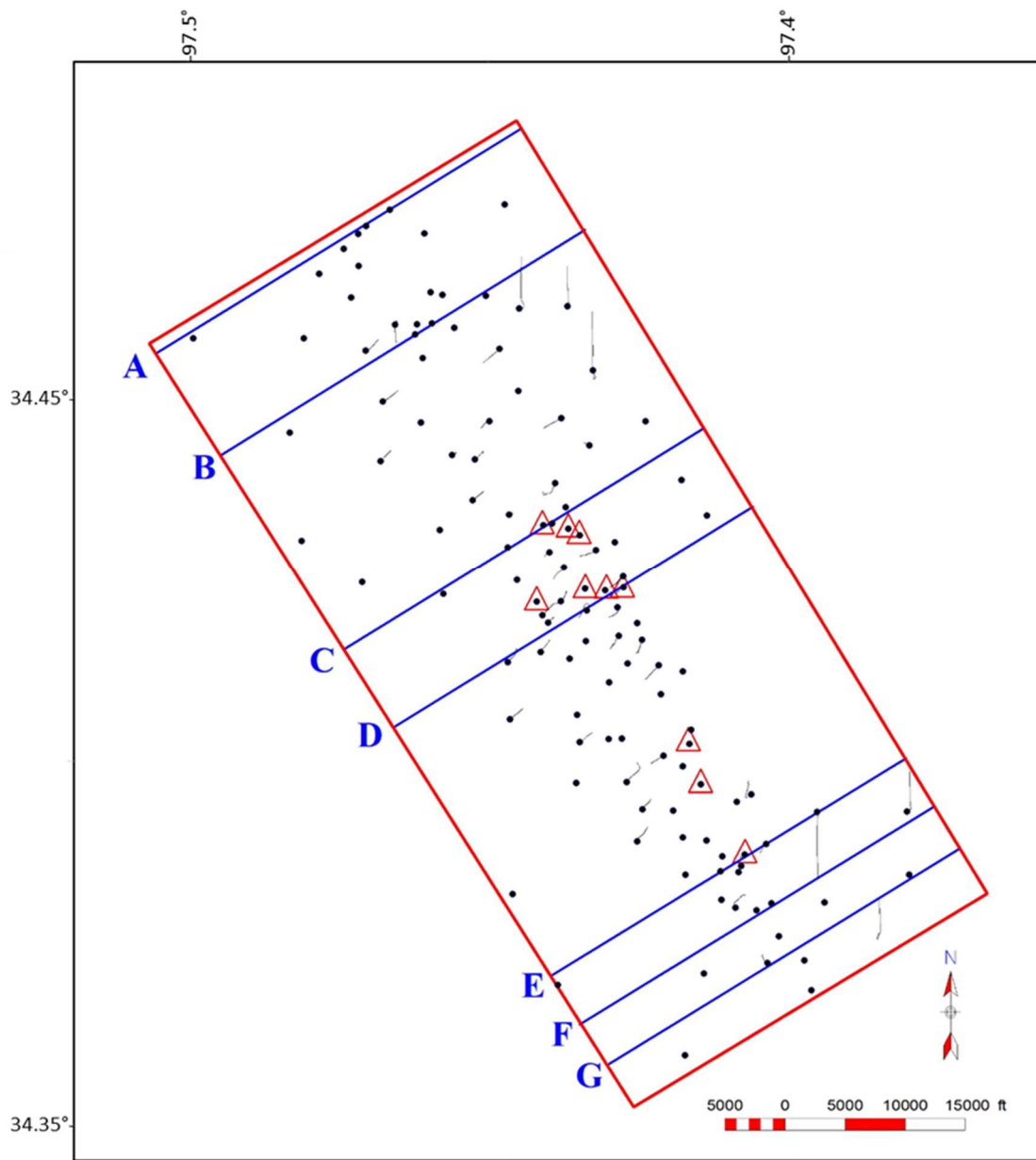


Figure 4.4. Map of the study area showing data used. Area of 3D seismic is located in red rectangle. Surface locations of selected wells are shown by black dots and deviated tracks. Wells with dipmeter data are shown by red triangles. Locations of cross sections are shown by blue lines.

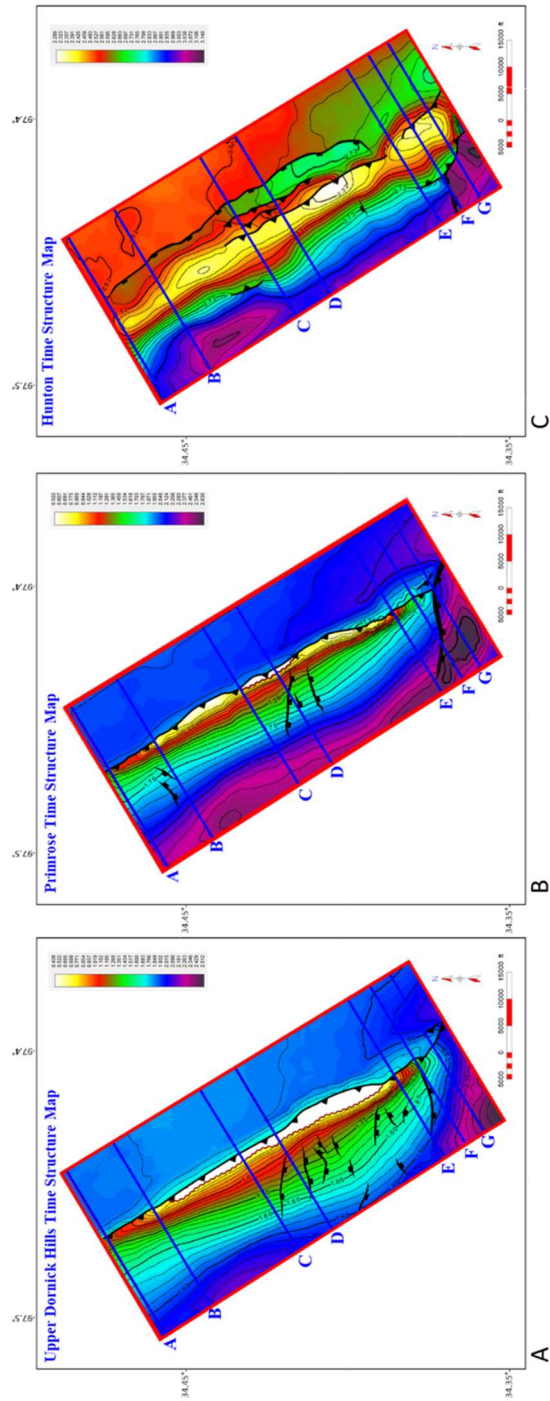


Figure 4.5. Time structure maps on (A) Upper Dornick Hills (B) Primrose (C) Hunton. Cross sections are shown by blue lines. A portion of the Upper Dornick Hills and Primrose are truncated by the Permian Unconformity near the crest of the structure. Note the significant change in structure between the two shallower horizons (A) & (B), and the deeper Hunton horizon c. which are separated by the Springer detachment.

6. Structural Cross Sections

A series of seven structural cross sections were constructed through the Carter-Knox structure, by integrating 3D seismic data, formation tops, and dipmeter data from key wells. Sections AA' and BB' are located on the northwestern plunging segment of the structure, CC' and DD' are located in the central area with the maximum relief and fault displacement, and EE', FF' and GG' are located on the southeastern segment, where the structure is affected by late-stage E-W trending normal faults. The main components of the structural style are discussed for section AA', where the structure is relatively simple. Discussion of the remaining sections is restricted to variations from the basic style observed in AA'. For each section both the interpreted seismic time section and the related depth cross sections are shown.

In section AA' (Figure 4.6), the basic structural style is defined by two structural units: a lower unit made up dominantly of the carbonates of the Ordovician Arbuckle to the Mississippian Sycamore Groups, and detaching near the base of the Arbuckle, and an upper unit ranging from the Mississippian Springer Shale to the Permian, and rooting within a detachment in the Springer shales. The Precambrian basement underlying the structure is not involved in the structure and shows a change in dip under the crest of the structure.

The deeper structure is a broad faulted anticline related to a major fault and an associated back thrust that terminates below the top of the Hunton Limestone. On the other hand, the upper unit is deformed into a tight northeast verging faulted-detachment fold (Mitra,2002), with a steep front limb related to two major faults and a number of smaller imbricates rooting in the Springer shales. The largest fault is referred to in this paper as the Carter-Knox Fault, and shows displacement of the top of the Springer of approximately 1000 ft (305 m). The Caney-Goddard to Lower Dornick Hills sections shows little change in stratigraphic thickness, although the

Springer shales show significant structural thickness due to shale flowage from the flanks to the core of the structure. The Upper Dornick Hills to Hoxbar section is a growth section, showing changes in stratigraphic thickness with all of the units showing increases in thickness down the southwestern flank of the structure. In addition to the Permian Unconformity, which truncates the crest of the structure and represents the termination of most of the uplift, two additional unconformities, at the base of the Upper Dornick Hills and the Hoxbar, are also present, suggesting that the structural evolution was episodic. These are more prominent on some of the central sections with larger displacements and uplift. The Hoxbar unconformity results in truncation and thinning of the Deese from the southeastern flank to the crest of the structure. The Permian Unconformity is folded on the crest of the structure, indicating some reactivation of the structure during Permian time.

Section BB' (Figure 4.7) shows a similar style to section AA', with a larger displacement on the main Carter-Knox Fault of approximately 2,500 ft (762 m) for the top of the Springer. However, all units up to the Hoxbar are essentially preserved under the Permian Unconformity. The lower structural package is marked by a steep normal fault that extends into the Precambrian basement, with displacement of the top of the Arbuckle of less than 500 ft (152 m). This early normal fault is located northwest of the crest of the structure and may have provided a buttress for the development of the Carter-Knox structure.

Section CC' (Figure 4.8) traverses the crestral area of the structure and shows significant structural relief. Displacement of the top of the Springer is approximately 4,000 ft (1,219 m). All units from the Primrose to the Hoxbar are eroded along the crest of the structure. Dipmeter data from four wells on the front limb show that the beds have a maximum dip of 80 degrees. A shallow normal fault cuts this cross section at an oblique angle on the southwest flank. This fault

and others like it are shown on the Upper Dornick Hills time structure map (Figure 4.4A) and are related to late stage extension parallel or oblique to the fold axis. Offset on these faults die out with depth and usually end in or above the Springer Shale.

Section DD' (Figure 4.9) shows the largest displacement on the Carter-Knox Fault with the top of the Springer offset by more than 4,500 ft (1372 m), resulting in all units in the upper package truncated by the Permian Unconformity at the crest. The front limb is very steep with dips approaching 80 degrees in the steepest areas. The steep basement involved normal fault in sections BB' and CC' is also seen in this section.

Section EE' (Figure 4.10) is located southeast of the crest and shows less structural relief and smaller displacement (3,500 ft (1,067 m)) on the main Carter-Knox thrust fault. The Springer Shale shows two smaller southeast dipping faults as well as a northeast dipping back thrust forming a triangle zone in the core of the structure in the upper units. The lower structural package shows a change in vergence from previous sections, with the main fault dipping to the northeast and having a larger displacement than on the back thrust.

Sections FF' (Figure 4.11) and GG' (Figure 4.12) are on the southern segment of the structure with significantly lower relief and displacements on the Carter-Knox Thrust Fault (less than 500 ft (152 m)). Both sections are affected by an oblique east-west dipping normal fault that drops down or cuts through the Permian displacement, suggesting that the fault formed after the formation of the main Carter-Knox structure. These faults appear to detach in the Springer detachment. The post-Hoxbar stratigraphy is significantly thickened (growth section) in the large dropped-down block along this fault. The lower structural package is also marked by a southwest verging structure with a back thrust, as in section EE'.

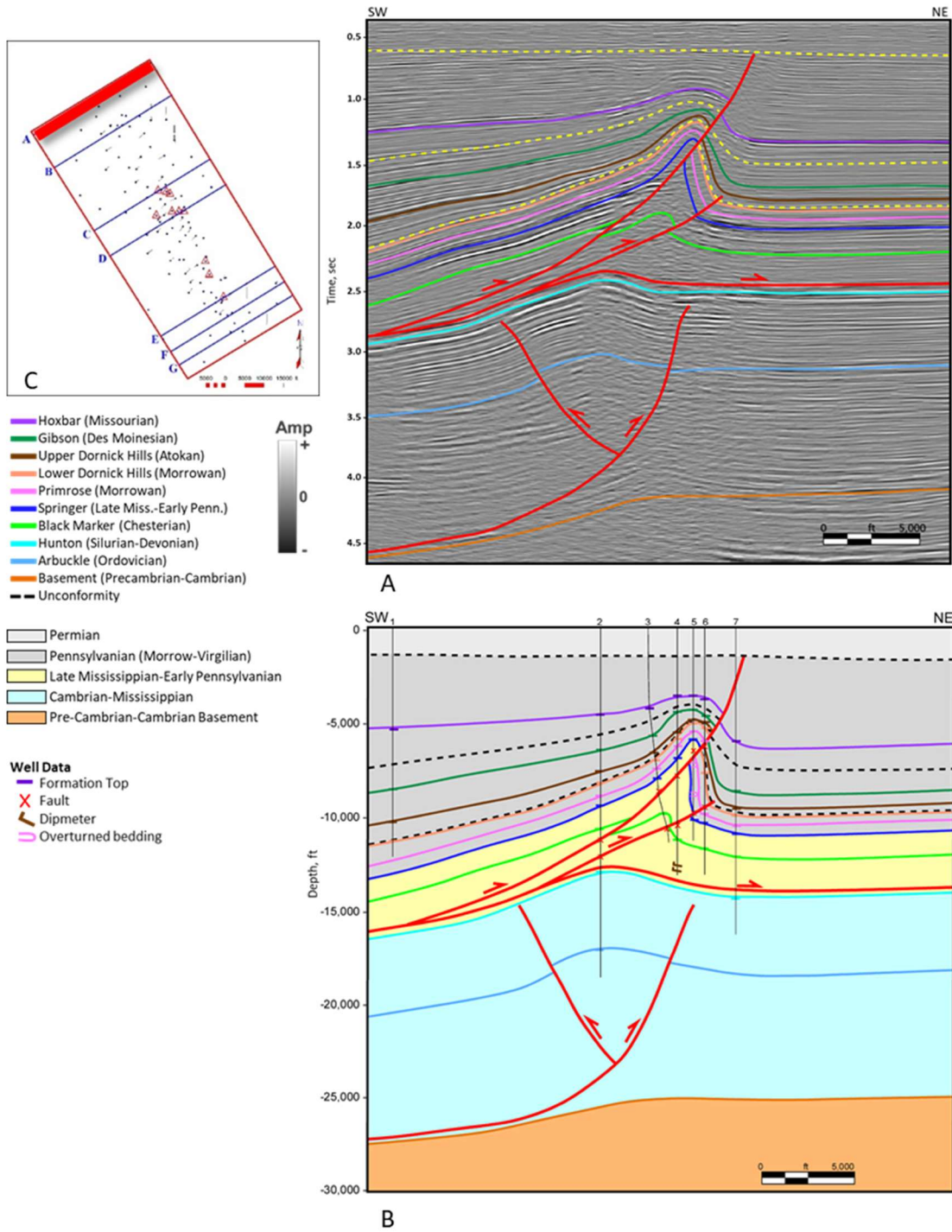


Figure 4.6 Cross section AA' (A) Interpreted seismic section in time (B) Depth cross section (C) location map. Wells on sections are 1 = BERNARD 1-4; 2 = BRAY 1; 3 = BRAY 2-25; 4 = BRAY 1-25; 5 = FISHER 1-25; 6 = NEVIUS 1-25; 7 = CLEARY 1A.

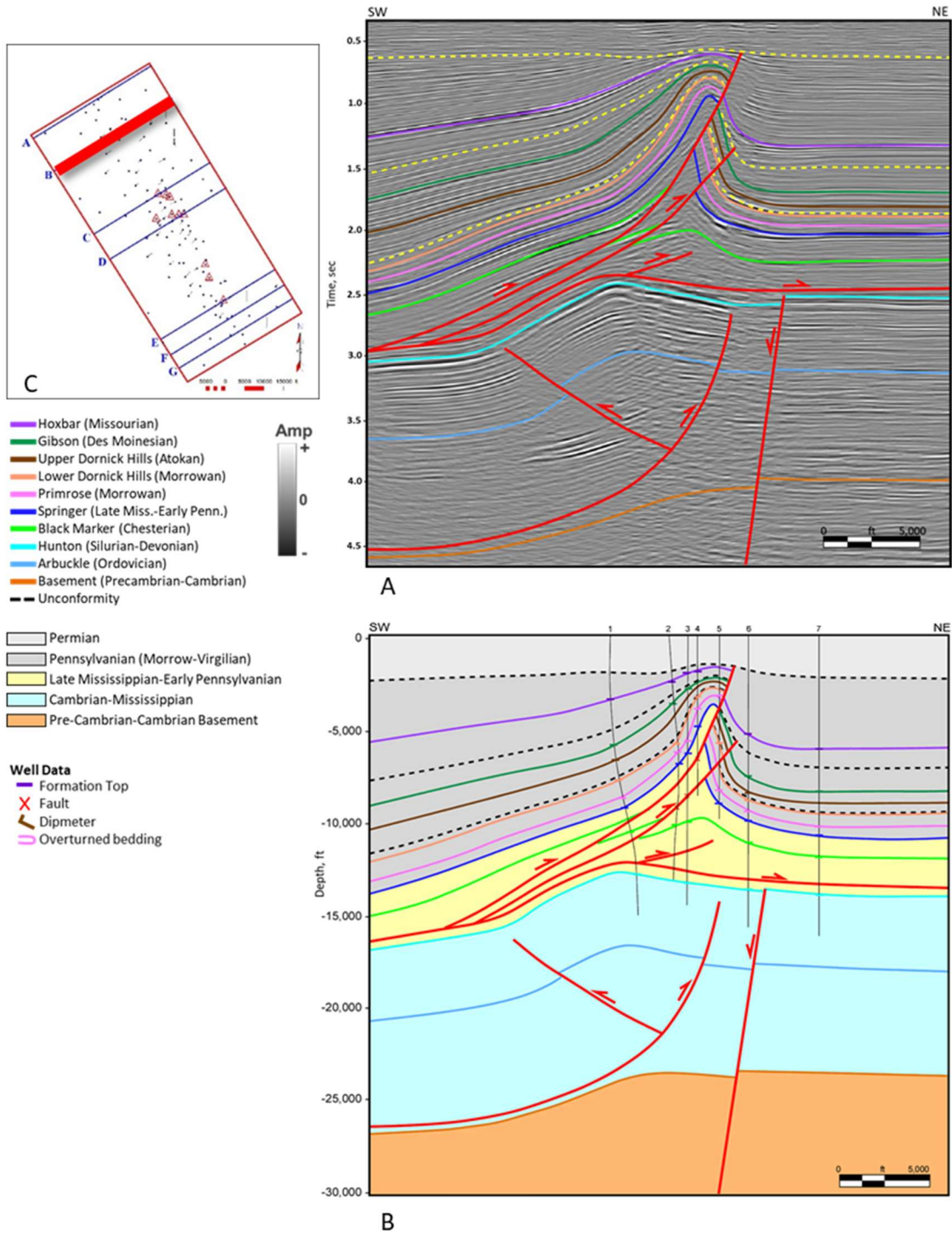


Figure 4.7 Cross section BB' (A) Interpreted seismic section in time (B) Depth cross section (C) location map. Wells on sections are 1 = SIZEMORE-PHIPPS 1; 2 = LYNDELL 1-1; 3 = PRESIDIO 1-6; 4 = JOHNSON 1-6; 5 = PRESIDIO 2-6; 6 = HEFNER 1-6; 7 = BETSY RUTH 1-32

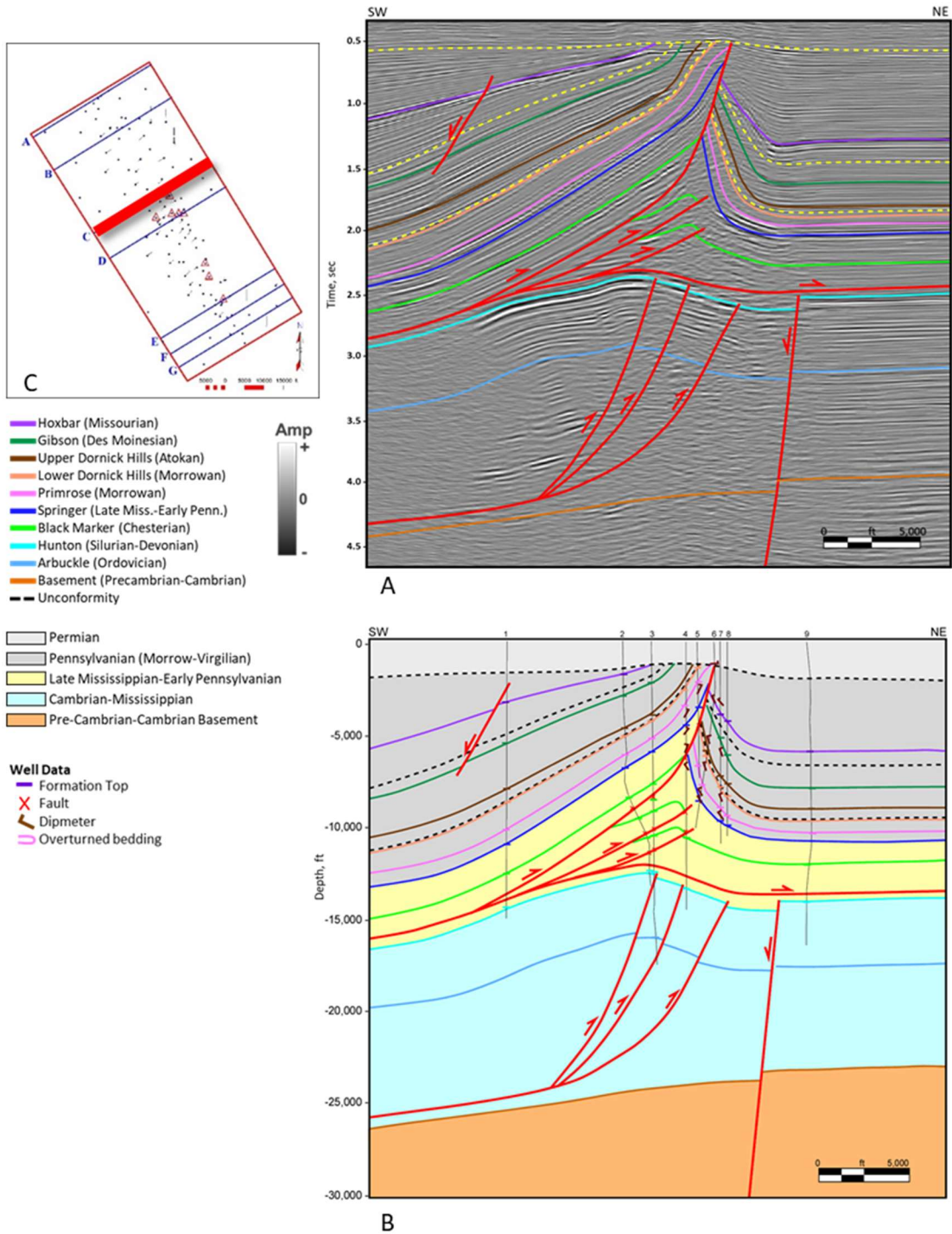


Figure 4.8 Cross section CC' (A) Interpreted seismic section in time (B) Depth cross section (C) location map. Wells on sections are 1 = MARY DAN 1-30; 2 = JAELYN 1; 3 = SIERRA K 4-20; 4 = PHILMORE 1-21; 5 = CAROLINE 1; 6 = BY 'G' MERCER 1-21; 7 = EASON-KNOX 1; 8 = SLEDGE DEEP 1; 9 = GOFF 1-16

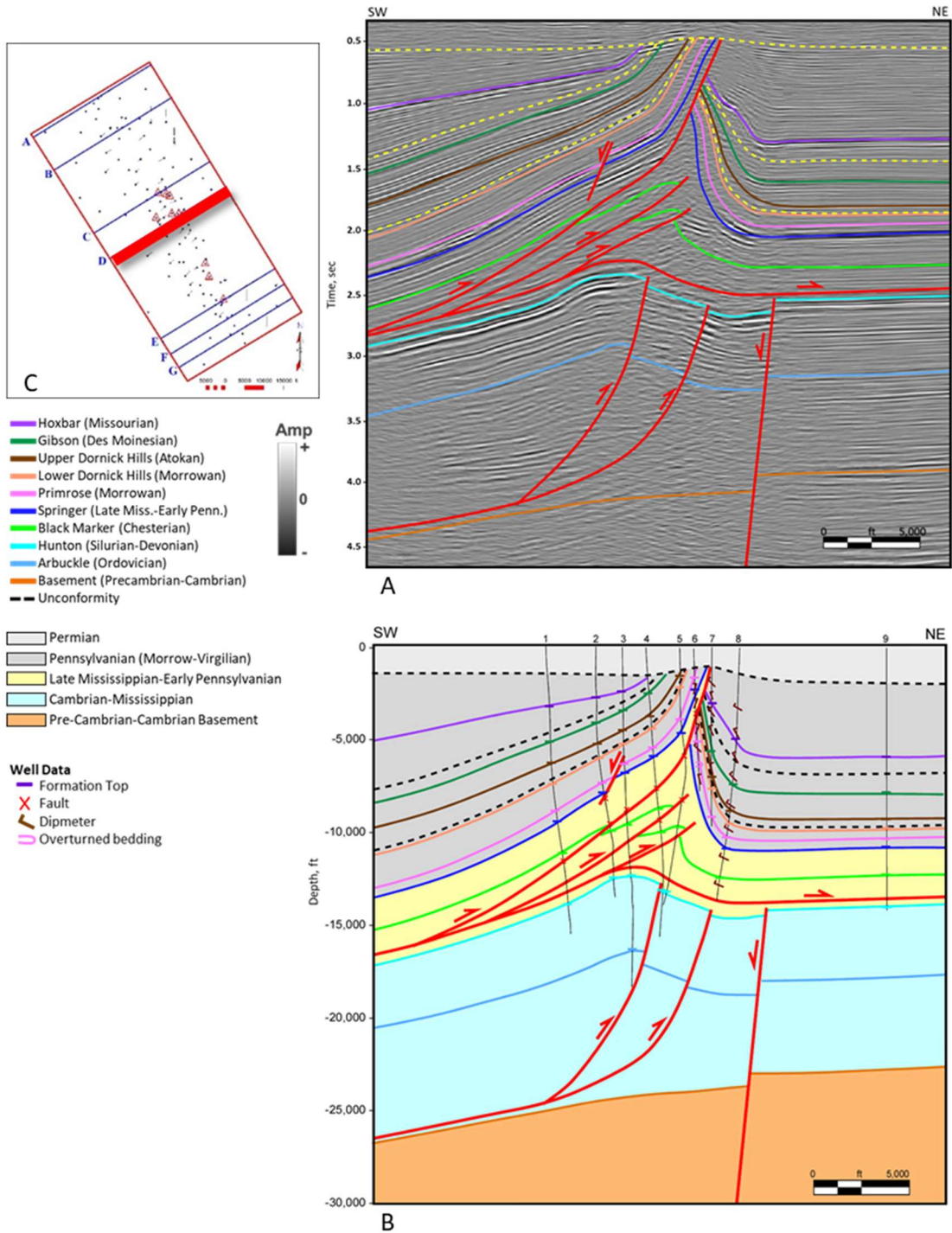


Figure 4.9 Cross section DD' (A) Interpreted seismic section in time (B) Depth cross section (C) location map. Wells on sections are 1 = LEONA HAYES 1; 2 = KAYE J 2; 3 = JENNA NICOLE 1-28; 4 = W D HARRISON B 1; 5 = JULES 1-34; 6 = MONICA 1-28; 7 = MAGNOLIA 1-27; 8 = CUNNINGHAM 1-27; 9 = CUNNINGHAM 23-A

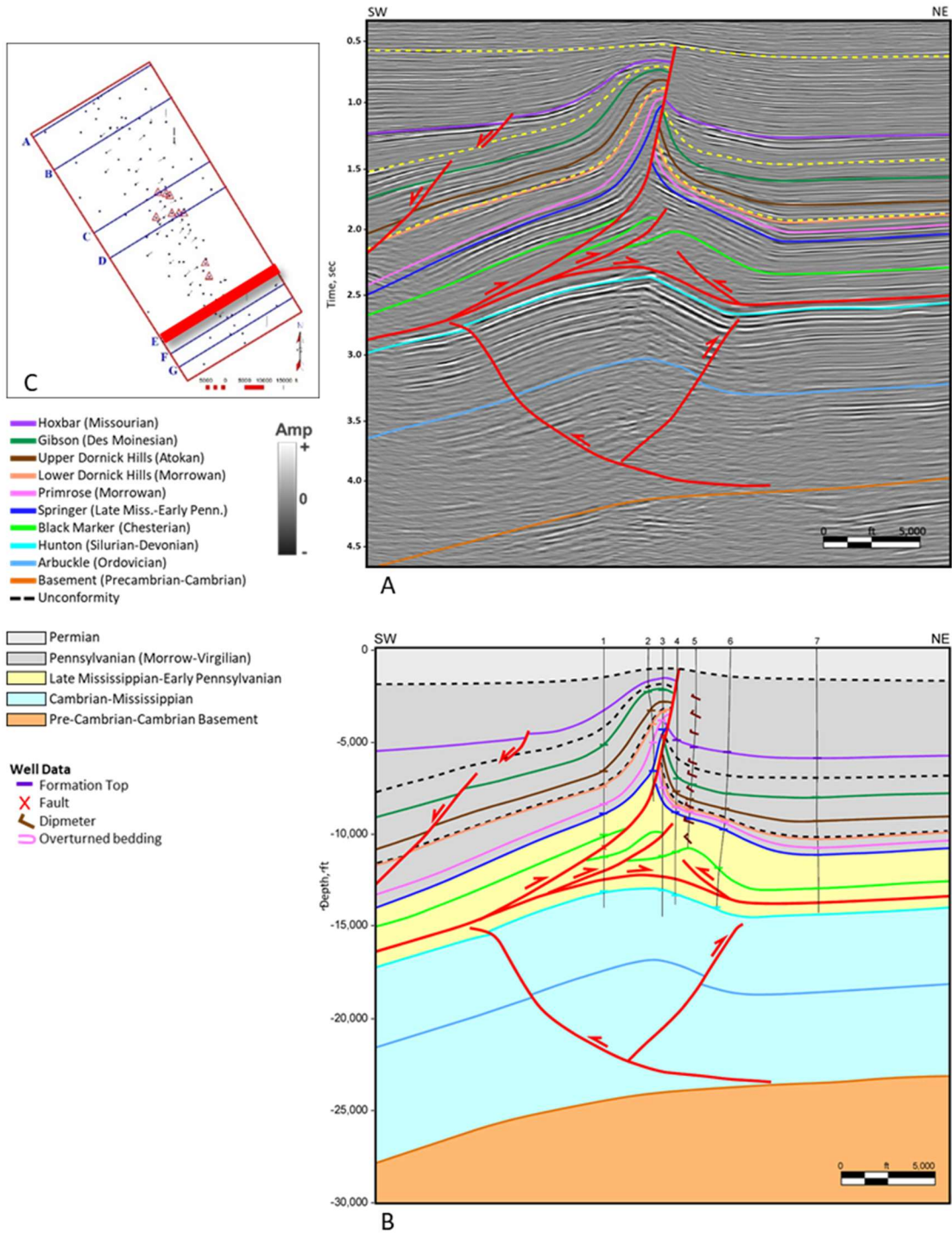


Figure 4.10 Cross section EE' (A) Interpreted seismic section in time (B) Depth cross section (C) location map. Wells on sections are 1 = BOYD 1-14; 2 = ROMAN 1-14; 3 = HPC 1-14; 4 = ANDERSON 1-13; 5 = ARCANGUES 1-13; 6 = SNODGRASS 1-13; 7 = JO ANN 1H-18

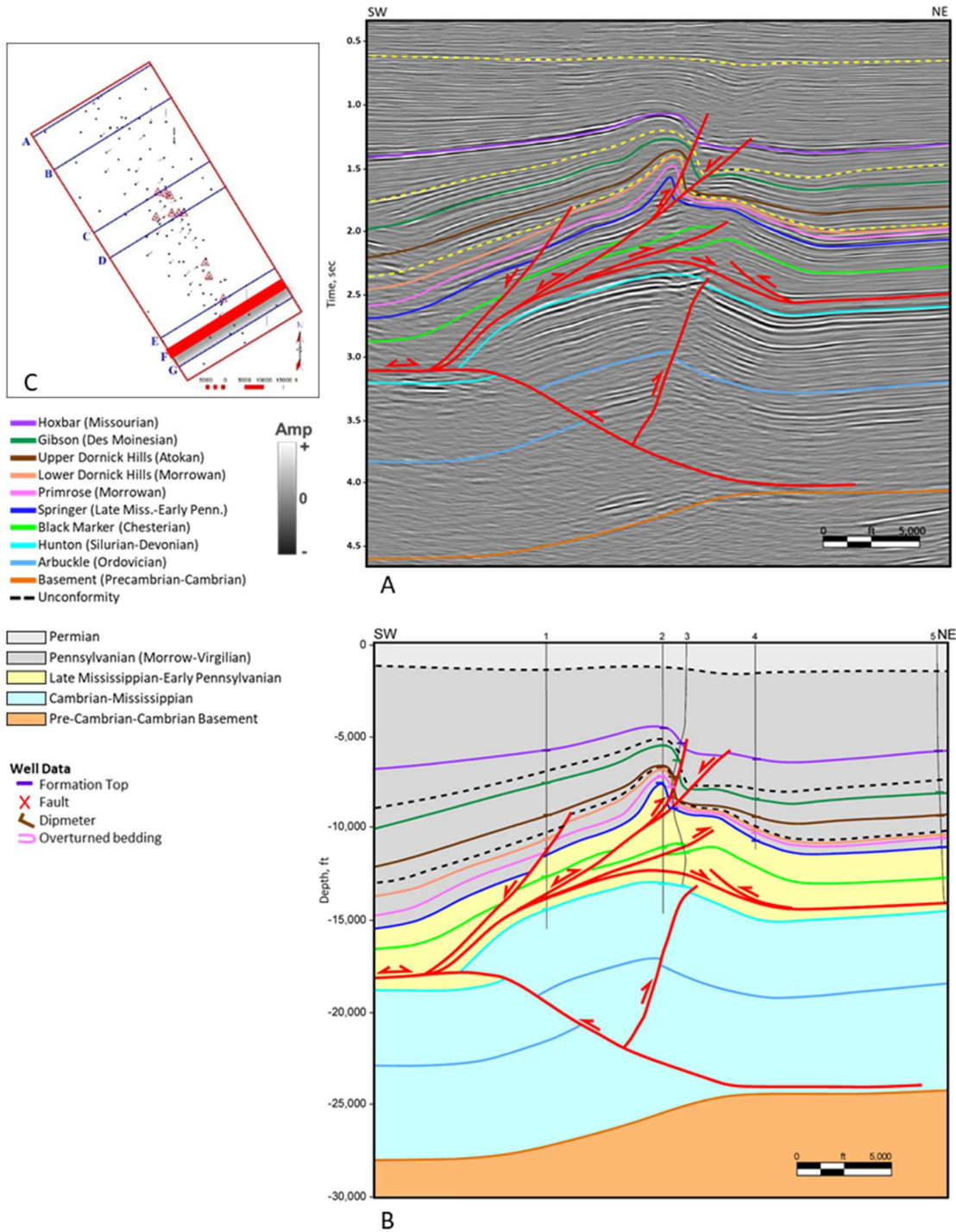


Figure 4.11 Cross section FF' (A) Interpreted seismic section in time (B) Depth cross section (C) location map. Wells on sections are 1 = DUNCAN 1-26; 2 = DAISY MCKINNEY 1; 3 = DIANE P 4; 4 = GRAHAM 1-19; 5 = FORREST 1-8H

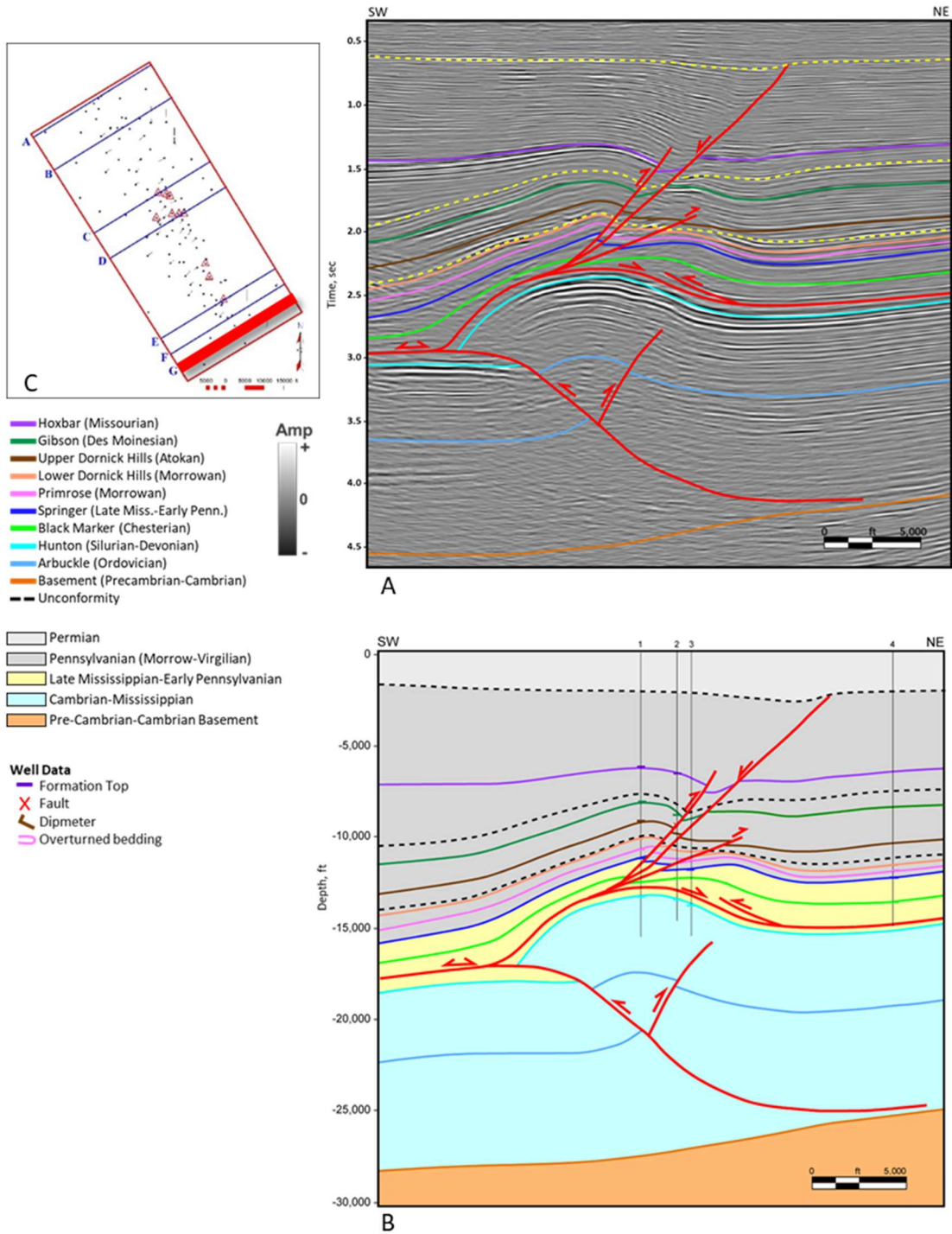


Figure 4.12 Cross section GG' (A) Interpreted seismic section in time (B) Depth cross section (C) location map. Wells on sections are 1 = GRAHAM 1; 2 = DIANE P 3; 3 = GOODRICH 1-30; 4 = BRANCH 1H-16

7. Kinematic Reconstruction and Structural Evolution

Kinematic reconstruction was conducted of three representative sections AA', DD', and FF' (Figures 4.13, 4.15, and 4.16) to understand the structural evolution of the Carter-Knox structure. The fault slip was first restored in both structural packages (Figures 4.13B, 4.15B, and 4.16B). Although folding and faulting occurs simultaneously during the later stages of development of faulted-detachment folds, this step enables an understanding of the geometry of the folds. The structure was then restored to Missourian time with the top of the Hoxbar Formation flattened (Figures 4.13C, 4.15C, and 4.16C). This essentially restores the highest stratigraphic unit involved in most of the deformation and shows the relative lengths of the mapped growth units. Finally, the Primrose and older units are restored to their undeformed state to compare the shortening of different structural units.

Reconstruction of section AA' is shown in Figure 4.13. Because the Springer to Primrose package shows significant flowage of the shale units, restoration to the undeformed stage uses area restoration, in two steps (Figure 4.14). Line-length restoration results in a shorter line length of the basal unit above the detachment compared to the top of the Primrose, resulting in a negative shear in the restored state. To area restore the package the area was divided by the original thickness (t) to obtain the average restored length (l_0). This procedure was used for restoration of all cross sections.

Restored stages (C) and (D) provide an understanding of the evolution of the structure. Five main structural packages show different amounts of shortening. In (D) the top of the basement is not involved in the contractional deformation and has a shorter restored length than the Arbuckle-Sycamore package. The Goddard to Primrose package shows a larger restored length so that the detachment between the two sequences separates simultaneous but different

amounts of contractional deformation. The units between the Primrose and the Permian Unconformity show progressively shorter length of stratigraphically higher units typical of growth packages in contractional settings. The units above the Permian units are essentially undeformed, except for a small amount of warping due to minor reactivation above the crest of the structure.

Although there was likely a small southwestward slope of the basement prior to deformation, the actual slope is unknown, so the units are restored to a horizontal geometry. Most of the slope of the present-day top of the basement and overlying units was acquired during the development of the Carter-Knox structure. This is indicated by the fact that the pre-growth Arbuckle to Primrose units are essentially parallel to the basement on the southwest flank of the structure, whereas the overlying growth units show progressively decreasing dips. Furthermore, the growth units typically thicken progressively down dip on the southwest flank. This suggests that growth of the Carter-Knox structure was accompanied by a downwarp of the southwest flank associated with sedimentary loading due to thrusting and uplift of the Wichita front. This down-warping likely occurred along a flexural hinge located below the crest of the Carter-Knox structure.

Section DD' (Figure 4.15) through the central part of the structure is characterized by much greater uplift and shortening in the upper (Goddard to Primrose) package, so that most units are truncated by the Permian Unconformity at the crest of the structure. Restoration of the fault slip (Figure 4.15B) shows the tight geometry of the structure at this stage almost resembling a lift-off fold (Mitra and Namson, 1989; Mitra, 2003). Because the underlying Arbuckle-Sycamore section shows about the same shortening as the previous section, the final restored geometry (Figure 4.15D), shows a larger difference in restored lengths of the upper and lower

packages than in section AA'. The growth units overlying the Primrose show a pattern of decreasing lengths of stratigraphically higher units (Figure 4.15C).

Section FF' (Figure 4.16) through the southeastern nose of the structure shows much smaller shortening relief and associated fault slip and relief in the Springer-Primrose package resulting in a more open fold. Also, late stage oblique normal faults that terminate within the Springer detachment cause a component of extension of the upper units. The Arbuckle-Sycamore section is marked by an opposite vergence to section DD', and greater slip on the main thrust fault. Restoration of the fault slip on this section shows a disharmonic detachment fold (Mitra, 2002), and an offset between the crests of the structure in the upper and lower stratigraphic packages. Restoration to the undeformed section shows a slightly smaller restored length of the Goddard- Primrose package than the Arbuckle-Sycamore package.

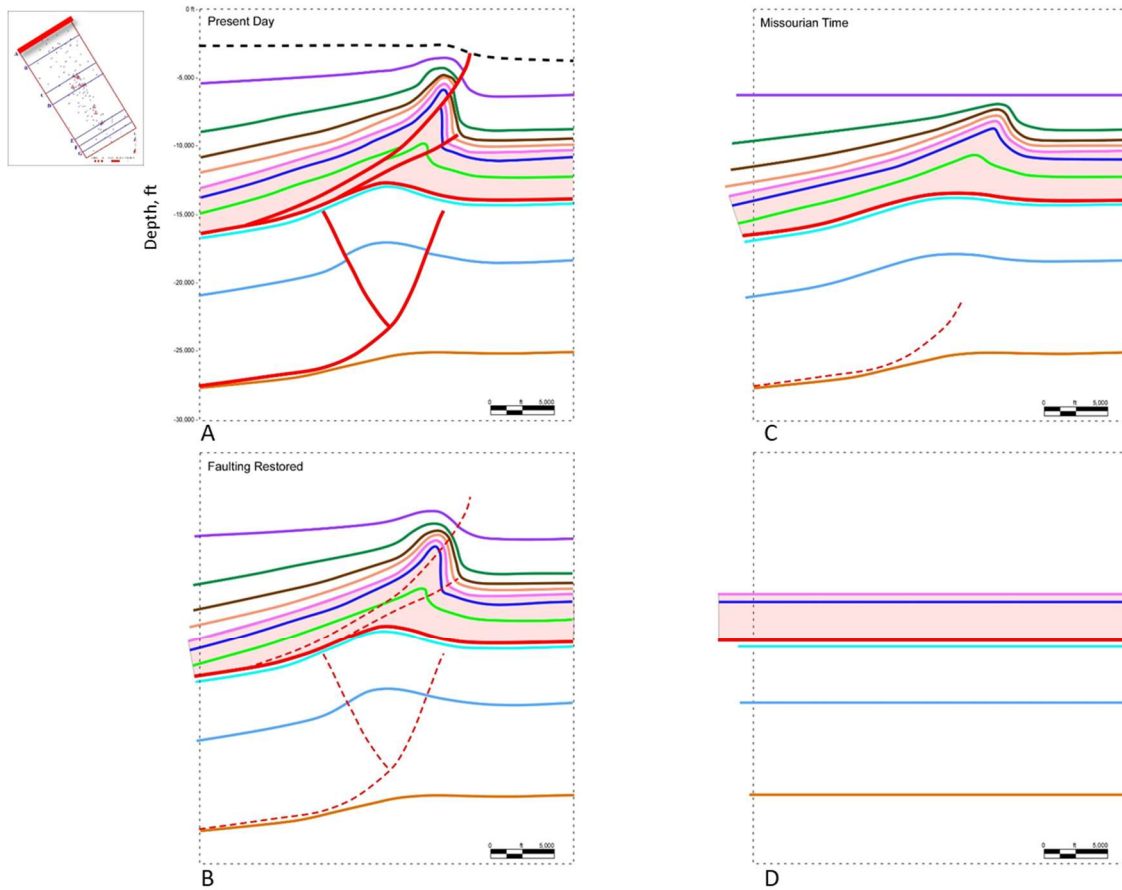
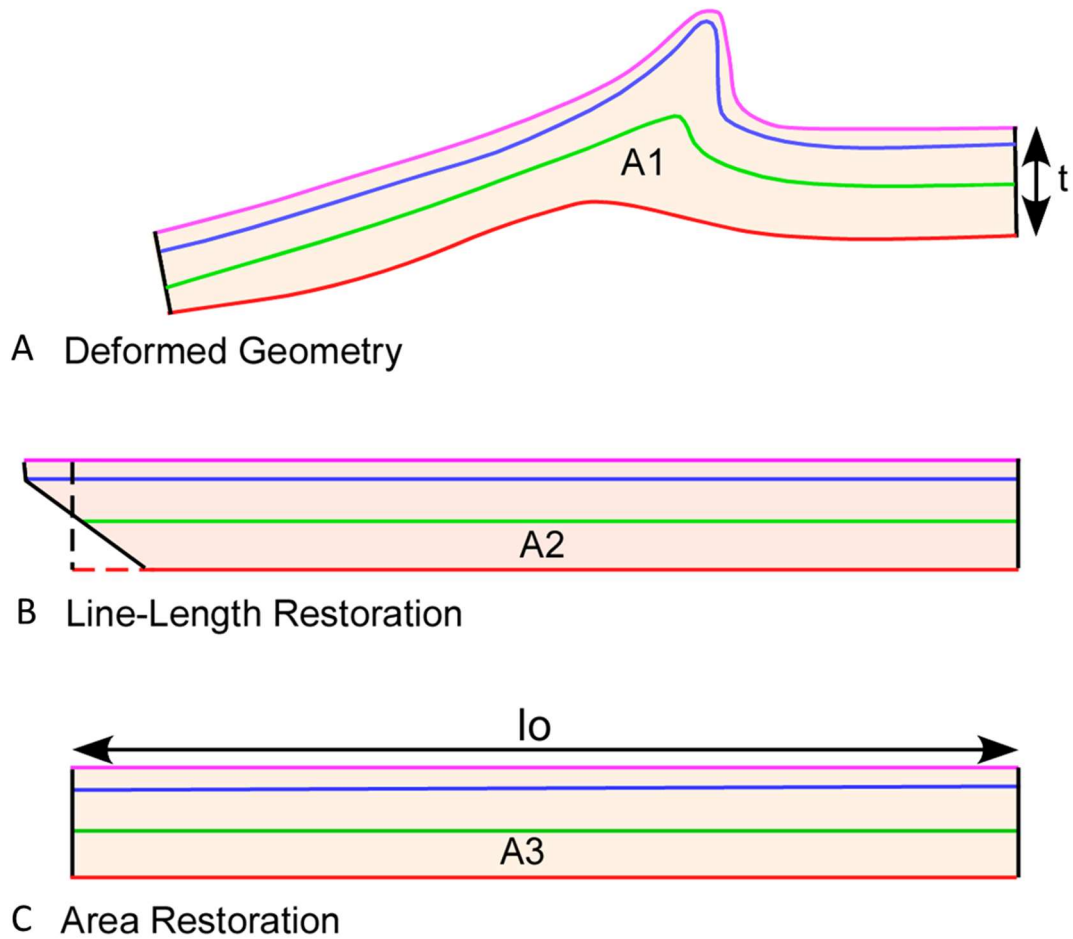


Figure 4.13 Kinematic reconstruction and structural evolution of section AA' (A) Depth cross section. (B) Faulting is restored and dashed in red to illustrate fold geometries. (C) Structure is restored to Missourian time with the Hoxbar horizon flattened. (D) Primrose and older units are restored to their undeformed state. Initial dips of these units are not known, so units are shown as horizontal.



$$l_o = A1 / t$$

Figure 4.14 Method of area restoration applied to the units between the Springer detachment and the top of the Primrose Formation in all restorations. (A) Final cross section. (B) Line-length restoration showing a wedge-shaped geometry resulting from differential strain of individual units. (C) Restoration with the area balanced into a rectangle shape. The height of the rectangle is determined by the average thickness (t), and the average restored length (l_o) is determined by dividing the area (A) by t .

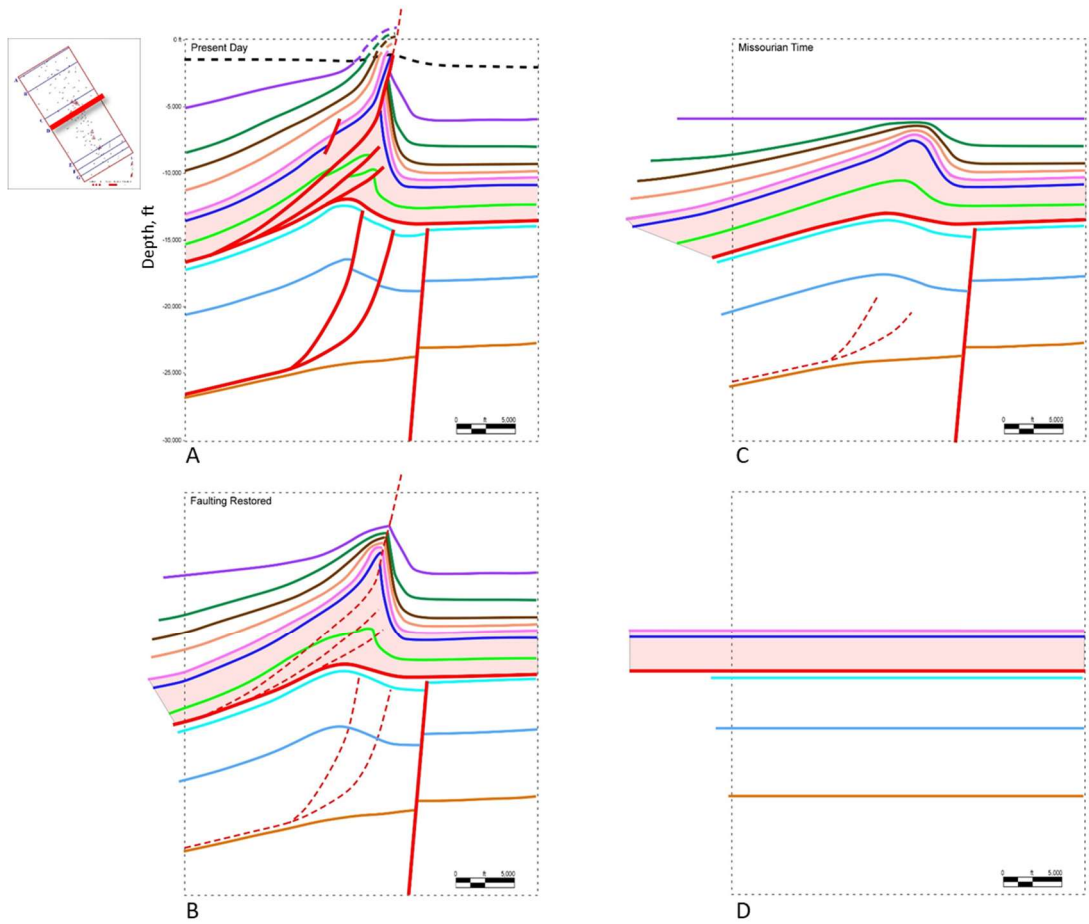


Figure 4.15 Kinematic reconstruction and structural evolution of section DD'. (A) Depth cross section. (B) Faulting is restored and dashed in red to illustrate fold geometries. (C) Structure is restored to Missourian time with the Hoxbar horizon flattened. (D) Primrose and older units are restored to their undeformed state.

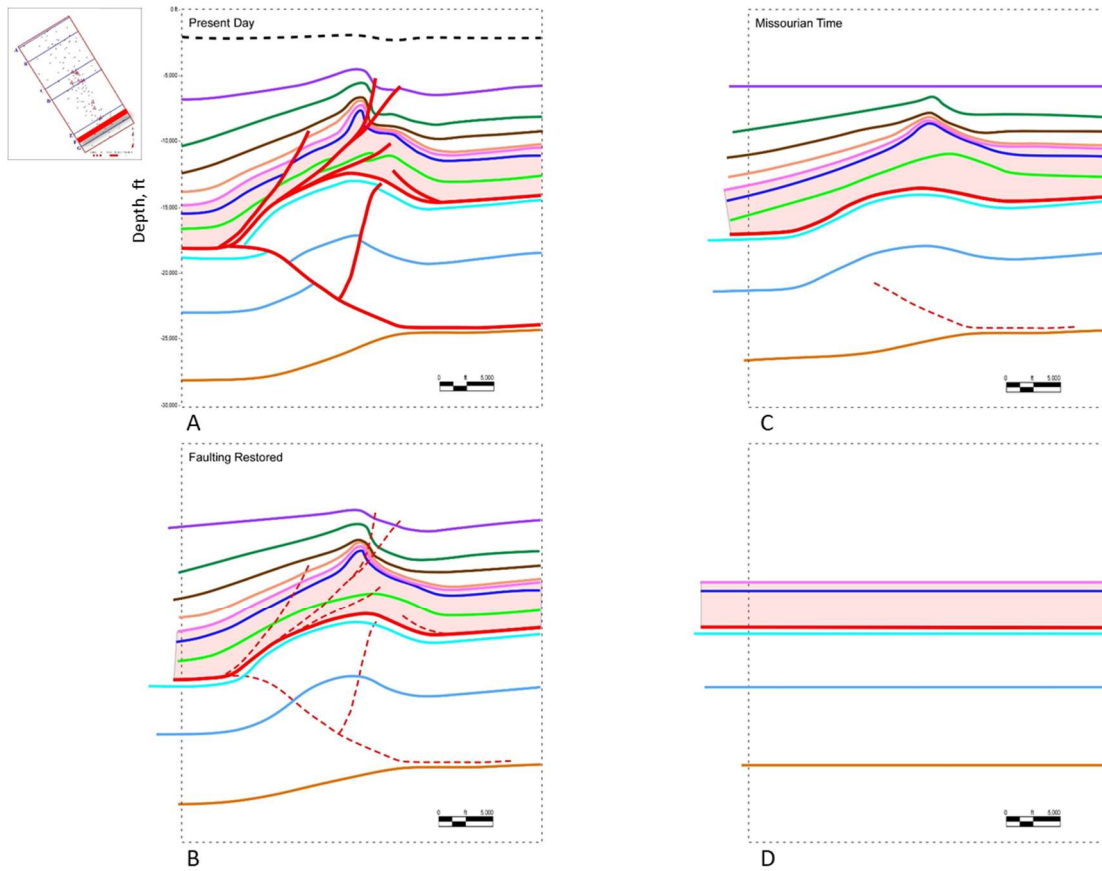


Figure 4.16 Kinematic reconstruction and structural evolution of section FF'. (A) Depth section. (B) Faulting is restored and dashed in red to illustrate fold geometries. (C) Structure is restored to Missourian time with the Hoxbar horizon flattened. (D) Primrose and older units are restored to their undeformed state.

8. Regional Structural Evolution

Evolution of the Carter-Knox structure can be related to the regional tectonics associated with the Wichita Uplift. Figure 4.17 shows an interpreted time profile and related depth cross section from the uplift to the Carter-Knox structure. The main thrust fault responsible for most of the slip flattens within the Springer Shale before ramping through the Morrowan section to form the Wichita Mountain Fault. Movement on this fault is episodic, as indicated by the erosion of the hanging wall by the Atokan Unconformity and subsequent reactivation through the Atokan and Desmoinesian section before termination beneath the Permian Unconformity. A secondary steeper imbricate, a backthrust, and one or more footwall imbricates also develop with the main Wichita Mountain Fault. We propose that slip on the fault is dissipated not only on the Wichita Mountain Fault but transferred along two main detachments, one within the Springer Shale, and the other at the base of the Arbuckle section. Slip on the upper Springer detachment is dissipated along multiple imbricate faults and related structures in front of the Wichita Mountain Fault, including the Carter-Knox structure. These structures formed later than the early Wichita Mountain Fault movement and involve sediments deposited from the rising Wichita thrust front. The slip on the lower detachment at the base of the Arbuckle section is also dissipated in structures within the Arbuckle-Sycamore section. This slip is significantly less, explaining the difference in the shortening between the Arbuckle-Sycamore and the Goddard-Primrose sections. A forward-shear on the Wichita thrust is necessary to compensate for this difference in slip between the two sections. Most of the deformation in the two structural packages occurred simultaneously within the Carter-Knox structure.

Updated

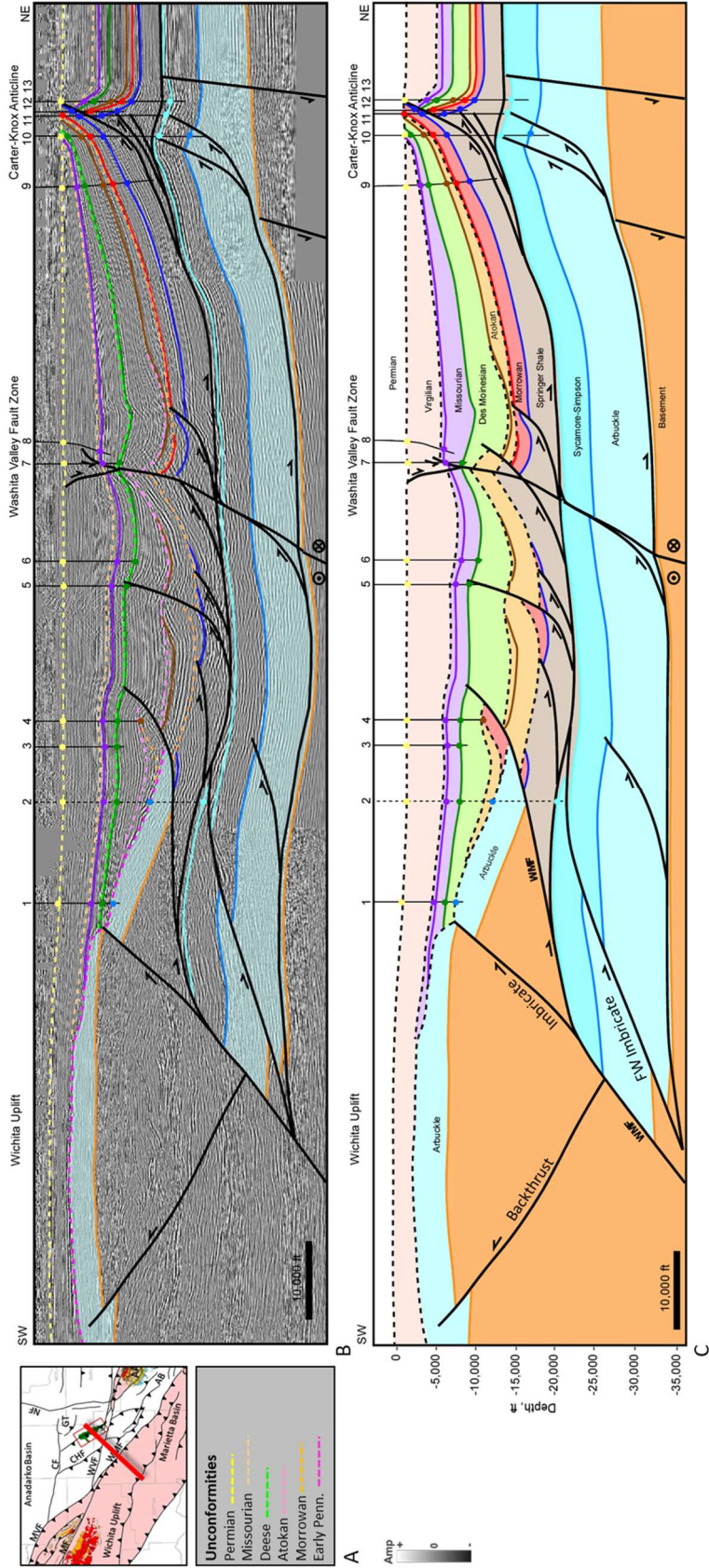


Figure 4.17. Regional section from the Wichita Uplift to the Carter-Knox structure showing the interpreted seismic interpretation in time, (B) and depth cross section (C). Location map and unconformity legend shown in (A). Faults related to the Wichita Mountain Fault (WMF) are labeled. Dashed lines represent unconformities. This section crosses a portion of the Washita Valley Fault where there may be some out-of-plane movement (black dashed fault). Wells on the depth section include 1 = S J PINSON 1; 2 = WOOLEVER GEORGE A 1 and is projected from 9 miles to the northwest, this well penetrates the Arbuckle, crosses the WMF and then goes into Mississippian and older units; 3 = HINES 1-9; 4 = HOWARD 1; 5 = DEBBY-SUE 1-36; 6 = SUMNER GARY 1; 7 = LAMAR 1-21; 8 = KILGO 3-21; 9 = LEONA HAYES 1; 10 = J KAYE 3-33; 11 = JULES 1-34; 12 = BLOCH 1-34; 13 = CALEB 1-271. Seismic Data Courtesy of Chesapeake Energy & SEI. Interpretation is that of Molly Turko.

9. Conclusions

The Carter-Knox structure is a NW-SE trending structure located in the southeastern part of the Anadarko Basin. The Carter-Knox field located on the crest of the structure produces oil and associated gas from the shallow Permian units, and Pennsylvanian units of the Springer, Morrowan, Deese and Hoxbar Formations, as well as gas and condensate from deeper units within the Woodford Shale and Simpson Group.

The structure formed primarily during contractional deformation in the Pennsylvanian (Atokan to Missourian) time. Slip associated with the Wichita Uplift was transferred primarily along an upper detachment in the Springer shales, a large part of which was consumed along the Wichita Mountain frontal fault. The remaining slip was transferred to the Carter-Knox and other structures in the Anadarko Basin. Some slip was also transferred to a secondary detachment at the base of the Arbuckle Group. The Carter-Knox structure was formed by the simultaneous deformation above these two main detachments, resulting in differential shortening of the two structural packages.

Different stratigraphic packages show different amounts of deformation. The Pre-Cambrian basement and associated intrusive and volcanic rocks are largely undeformed, except

for the development of a flexural hinge underlying the structural crest and an early steep normal fault in the central part of the structure, which may have provided a buttress for the formation of the structure. The deeper pre-Pennsylvanian units are folded into of a broad faulted anticline associated with one or more frontal thrust faults and associated back thrusts. The structure verges to the northeast for most of the structural trend but switches vergence to the southwest in the southeastern segment of the structure. The Pennsylvanian units are folded into a tight faulted-detachment fold with a steep front limb and considerable flowage of the Springer shales into the core of the structure. The fold tightness and fault dip increase in the central culmination, where the fault slip is also the greatest. The section between the Lower Dornick Hills and the Permian units are growth units and show progressive thickening down dip on the southwest flank. This section is also marked by at least two unconformities at the base of the Upper Dornick Hills and Hoxbar units, suggesting episodic growth of the structure.

Kinematic reconstruction of key units shows that the structure developed primarily between Atokan and Virgilian (Pennsylvanian) time, with a minor reactivation during the Permian. Structural evolution was episodic with important unconformities at the base of the Upper Dornick Hills and Hoxbar Formations. Differential strain between different structural packages results in different restored lengths of the units. Loading of sediments resulted in the development of a flexural hinge in the basement below the crest of the structure.

References

- Axtmann, T. C., 1985, Structural Mechanisms and Oil Accumulation Along the Mountain View-Wayne Fault, South-Central Oklahoma: *The Shale Shaker Digest*, v. 11, no. 33-35, p. 17-45
- Boyd, D. T., 2002, Map of Oklahoma Oil and Gas Fields: Oklahoma Geological Survey Map GM-36
- Carter, D. W., 1984, A Study of Strike-Slip Movement along the Washita Valley Fault Arbuckle Mountains, Oklahoma: *The Shale Shaker Digest*, v. 20, no. 30-32, p. 85-115
- Dunham, R. J., 1955, Pennsylvanian Conglomerates, Structure, and Orogenic History of the Lake Classen Area, Arbuckle Mountains, Oklahoma: *AAPG Bulletin*, v. 39, no. 1, p. 1-30
- Feinstein, s., 1981, Subsidence and Thermal History of Southern Oklahoma Aulacogen: Implications for Petroleum Exploration: *AAPG Bulletin*, v. 65, no. 12, p. 2521-2533
- Granath, J. W., 1989, Structural Evolution of the Ardmore Basin, Oklahoma: Progressive Deformation in the Foreland of the Ouachita Collision: *Tectonophysics*, v. 8, no. 5, p. 1015-1036
- Ham, W. E., 1950, Geology and Petrology of the Arbuckle Limestone in the southern Arbuckle Mountains, Oklahoma: PhD thesis, Yale University, New Haven, Connecticut, 159 p.
- Heran, W. D., Green, G. N., and Stoeser, D. B., 2003, A Digital Geologic Map Database for the State of Oklahoma: USGS Open-File Report OF-2003-247
- Hoffman, B. P., 1996, Geometry of the Northern Part of the Carter-Knox Structure, Anadarko Basin, Oklahoma: Master's Thesis, Oklahoma State University, Stillwater, Oklahoma, 65 p.
- Marsh, S. and A. Holland, 2015, Comprehensive Fault Database and Interpretive Fault Map of Oklahoma: Oklahoma Geological Survey Open-File Report OF2-2016
- McCaskill, J. G., 1998, Multiple Stratigraphic Indicators of Major Strike-Slip Movement Along the Eola Fault, Subsurface Arbuckle Mountains, Oklahoma: *The Shale Shaker*, v. 48, no. 4, p. 93-109
- Mitra, Shankar. 2002. Structural Models of Faulted-detachment folds. *AAPG Bulletin* 9 (9): 1673-94.
- Mitra, S., 2003, A Unified Kinematic Model for the Evolution of Detachment Folds: *Journal of Structural Geology*, v. 25, no. 10, p. 1659-1673
- Mitra, S. and J. S. Namson, 1989, Equal-Area Balancing: *American Journal of Science*, v. 289, no. 5, p. 563-599
- Perkins, T., 1997, Geometry of the Southern Part of the Carter-Knox Structure, Anadarko Basin, Oklahoma: Master's Thesis, Oklahoma State University, Stillwater, Oklahoma, 79 p.

- Perry, W. J., 1989, Tectonic Evolution of the Anadarko Basin Region, Oklahoma: USGS Bulletin 1866
- Petersen, F. A., 1983, Foreland Detachment Structures, in Lowell, J. D., and Gries, R. R., Rocky Mountain Foreland Basins and Uplifts: Rocky Mountain Association of Geologists, p. 65-77
- Reedy, H. J. and H. A. Sykes, 1959, Carter-Knox Oil Field, Grady and Stephens Counties, Oklahoma, in Mayes, J. W., Westheimer, J., Tomlinson, C. W. and D. M. Putman, SP 19: Petroleum Geology of Southern Oklahoma: AAPG Special Volumes, v. 2, p. 198-219
- Saxon, C. P., 1998, Structural Styles of the Wichita and Arbuckle Orogenies, Southern Oklahoma: PhD Thesis, University of Oklahoma, Norman, Oklahoma, 248 p.
- Tanner, J. H., 1967, Wrench Fault Movement along Washita Valley Fault, Arbuckle Mountain Area, Oklahoma: AAPG Bulletin, v. 51, no. 1, p. 126-141